Investigating two AHSV non-structural proteins: tubule-forming protein NS1 and novel protein NS4.

by

Lizahn Zwart

Submitted in partial fulfilment of the requirements for the degree

Magister Scientiae

In the Faculty of Natural and Agricultural Science

University of Pretoria

Pretoria

December 2013

Under the supervision of Dr. V. van Staden and Dr. C.A. Potgieter

The financial assistance of the National Research Foundation (NRF) towards this research is hereby acknowledged. Opinions expressed and conclusions arrived at, are those of the author and are not necessarily to be attributed to the NRF.

Declaration

I, Lizahn Zwart, declare that the thesis/dissertation, which I hereby submit for the degree *Magister Scientiae* at the University of Pretoria, is my own work and has not previously been submitted by me for a degree at this or any other tertiary institution.

SIGNATURE: …….. DATE: …….

Contents

Research outputs

The following aspects of this study were presented and published:

L. Zwart, C.F. van der Merwe, A.N. Hall, V. van Staden and H. Huismans, 2012 Investigating the localisation and interaction dynamics of AHSV non-structural protein NS1. Presented at the Microscopy Society of Southern Africa 50th Annual Conference, 2012.

L. Zwart, A.N. Hall, C. A. Potgieter, H. Huismans and V. van Staden, 2013 Investigating the intracellular distribution of novel AHSV non-structural protein NS4. Presented at the Microscopy Society of Southern Africa 51st Annual Conference, 2013, and the 11th Annual Genetics Postgraduate Symposium, 2013 (Best MSc Student Presentation Award).

Summary

Thesis title: Investigating two AHSV non-structural proteins: tubule-forming protein NS1 and novel protein NS4.

Full name: Lizahn Zwart

Supervisor: Dr. V. van Staden

Co-supervisor: Dr. C.A. Potgieter

Department: Department of Genetics, University of Pretoria

Degree: *Magister Scientiae*

African horse sickness is an equid disease caused by African horse sickness virus (AHSV). AHSV produces seven structural proteins that form the virion and four non-structural proteins with various roles during replication. The first part of this study investigated the intracellular distribution and co-localisations of NS1 with other AHSV proteins to facilitate its eventual functional characterisation. Confocal microscopy revealed that NS1 formed small cytoplasmic foci early after infection that gradually converged into large fluorescent NS1 tubule bundles. Tubule bundles were more organised in AHSV-infected cells than in cells expressing NS1 alone, suggesting that tubule bundle formation requires the presence of other AHSV proteins or regulation of NS1 expression rates. NS1 occasionally co-localised with VP7 crystalline structures, independently of other AHSV proteins. However, when NS1-eGFP, a modified NS1 protein that contains enhanced green fluorescent protein (eGFP) near the C-terminus, was co-expressed with VP7, co-localisation between these proteins occurred in most co-infected cells. It is not clear how the addition of eGFP to NS1 induces this co-localisation and further investigation will be required to determine the function of NS1 during viral replication.

The second part of the study focused on characterising the novel non-structural AHSV protein NS4. The NS4 open reading frame (ORF) occurs on segment 9, overlapping the VP6 ORF in a different reading frame. *In silico* analysis of segment 9 nucleotide and NS4 predicted amino acid sequences revealed a large amount of variation between serotypes, and two main types of NS4 were identified based on these analyses. These proteins differed in length and amino acid sequence and were named NS4-I and NS4-II. Immunoblotting confirmed that AHSV NS4 is translated in AHSV infected insect and mammalian cells, and also in Sf9 insect cells infected with recombinant baculoviruses that overexpress the genome segment 9 proteins, VP6 and NS4. Confocal microscopy showed that NS4 localised to both the cytoplasm and nucleus, but not the nucleolus, in AHSV-infected cells and recombinant baculovirus infected Sf9 cells. Nucleic acid protection assays using bacterially expressed purified NS4 showed that both types of NS4 bind dsDNA, but not dsRNA. This was the first study to focus on AHSV NS4. Future work will focus on determining the role of non-structural proteins in viral pathogenesis, and will involve the use of a reverse genetics system for AHSV.

List of abbreviations

°C	Degrees Celcius
AHSV	African horse sickness virus
bp	base pairs
BCA	Bicinchoninic acid
Bis-Tris	Bis(2-hydroxyethyl)amino-tris(hydroxymethyl)methane
BTV	Bluetongue virus
CLP	Core-like particle
CPE	Cytopathic effect
DAPI	4',6-diamidino-2-phenylindone
dpi	days post infection
dsDNA	Double stranded deoxyribonucleic acid
dsRNA	Double stranded ribonucleic acid
E. coli	*Escherichia coli*
EDTA	Ethylenediaminetetraacetic acid
eGFP	Enhanced green fluorescent protein
EtBr	Ethidium bromide
EMEM	Eagle's Minimal Essential Medium
FITC	Fluorescein isothiocyanate
FCS	Foetal calf serum
G	Gauge
GIV	Great Island virus
HPF-FS	High-pressure freezing and freeze substitution
hpi	hours post infection
IgG	Immunoglobulin G
IPTG	Isopropyl β-D-1-thiogalactopyranoside
hpin	Hours post induction
kDa	Kilodalton
LB	Luria Bertani (medium)
LEW	Lysis-Equilibration-Wash (buffer)
MAFFT	Multiple alignment using fast Fourier transform
µg	Micrograms
µL	Microliters
µm	micrometres
mA	Milliamperes
mg	Milligrams

mL	Millilitres
mM	Millimoles
MOI	Multiplicity of infection
MOPS	3-(N-morpholino)propanesulfonic acid
NEAA	Non-essential amino acids
ng	Nanograms
NLS	Nuclear localisation signal
nm	Nanometres
OD	Optical density
ORF	Open reading frame
PAGE	Polyacrylamide gel electrophoresis
PBS	Phosphate buffered saline
PCA	Paracrystalline array
PCR	Polymerase chain reaction
PFA	Paraformaldehyde
PSB	Protein solvent buffer
rpm	Revolutions per minute
SDS	Sodium dodecyl sulphate
TEM	Transmission electron microscopy
TEMED	Tetramethylethylenediamine
Tris	tris(hydroxymethyl)aminomethane
U	Units
V	Volt
VIB	Viral inclusion body
VLP	Virus-like particle
w/v	Weight per volume
X-Gal	5-bromo-4-chloro-3-indolyl-β-D-galactopyranoside

Chapter 1:
Literature Review

1.1 Introduction

Most viruses produce a set of structural proteins that are included in the mature virus particle, as well as one or more non-structural proteins, which perform various ancillary functions during the viral replication cycle, but are not part of the mature virion. These functions vary greatly depending on the dynamics of the viral infection in question, and include processes such as nucleic acid synthesis, intercellular transmission of infection and suppression of RNA silencing. In some cases, no clear function has been assigned to each of the viral non-structural proteins; this is the case for the orbivirus protein NS1, which forms the bundles of tubules characteristic of orbivirus infected cells, and the newly discovered protein NS4, which has been subjected to preliminary characterisation in Great Island virus (GIV) and bluetongue virus (BTV). Since NS1 tubules are produced in cells infected with all orbiviruses studied to date, and since it is unclear whether NS4 is produced in viruses other than GIV and BTV, findings pertaining to these proteins in African horse sickness virus (AHSV) could potentially be relevant to other viruses in the genus as well. To provide background information to describing the aims of this study, various aspects of the AHSV infection cycle will be reviewed briefly. These include the epidemiology and control of AHSV, the viral structure and replication cycle, and finally the information currently available about the two non-structural proteins, NS1 and NS4, with which this investigation is particularly concerned. It transpires from perusal of the literature that the interactions of NS1 with other AHSV proteins and its tubulisation dynamics have not yet been described; likewise, AHSV NS4 has yet to be characterised. Addressing these pertinent questions could lead to an enhanced understanding of the AHSV replication cycle, particularly with regard to the role of non-structural proteins in determining viral pathogenesis and virulence, which could lead to the development of improved disease prevention and control strategies.

1.1.2 African horse sickness

African horse sickness (AHS) is a serious disease of *Equidae* which is enzootic in sub-Saharan Africa and caused by African horse sickness virus (AHSV). AHS has a high mortality rate (up to 95%) among naive horses, and there is no cure or specific treatment for the disease (House 1993). Because of this, AHS is notifiable to the World Organisation for Animal Health (OIE). AHS significantly impedes the trade and movement of horses to and from South Africa, especially when AHS-free countries are involved. The virus has emerged several times in non-endemic regions, which has drawn focus to the epizootiology, molecular biology and control of the virus (MELLOR and BOORMAN 1995).

AHSV (*Reoviridae*: *Orbivirus*) resembles the orbivirus type species, bluetongue virus, in many respects. Viruses within the *Reoviridae* family infect vertebrates, arthropods and plants (ROY 2007). AHSV is an arbovirus transmitted primarily by *Culicoides imicola* (*Diptera: Ceratopogonidae*) biting midges (HOUSE 1993), although ticks (BOUWKNEGT *et al.* 2010) and mosquitoes have transmitted the virus to susceptible horses experimentally (MELLOR 1994). Other *Culicoides* species have been suspected of vectoring the virus as well, based on experimental susceptibility to AHSV and isolation of AHSV from field samples of these

insects, including *C. variipennis* (MELLOR *et al.* 1975), *C. bolitinos* (MEISWINKEL and PAWESKA 2003), and several others (VENTER *et al.* 2009).

Four forms of AHS exist, namely the peracute or pulmonary, subacute or cardiac, acute or mixed and horse sickness fever forms, in descending order of severity. Immunohistochemical analysis of tissue samples of AHSV infected horses shows targeting of the virus mainly to the heart and lungs, and to an extent the spleen. Microvascular endothelial cells and monocyte-macrophages are the main sites of viral replication. This is similar to the tissue and cell tropism of other orbiviruses and is consistent with the symptoms of infection (CLIFT and PENRITH 2010). Furthermore, conventional dendritic cells (cDCs) appear to be involved in spreading BTV from the skin of bitten ruminants to the draining lymph nodes, whence it spreads to the secondary organs. Productive BTV infection of cDCs enhances cell survival and certain serotypes can induce the expression of co-stimulatory molecules on the cell surface or cytokine mRNA synthesis, suggesting that BTV utilises the host immune system to optimise primary dissemination (HEMATI *et al.* 2009). Epidemiological studies of orbiviruses have contributed significantly to the development of strategies to control the spread of disease. Further research will be required for a more complete understanding of AHS pathogenesis.

1.1.3 Epidemiology

African horse sickness has a seasonal incidence, occurring most often in spring and summer. This is probably related to the vector life cycle; biting midges are most active during these periods. The presence of vector, host and virus is essential for AHS to occur (MELLOR 1994). This would imply that infectious virus must persist during periods of low vector activity, a phenomenon known as overwintering. The mechanism of AHSV overwintering in enzootic regions is unknown, although BTV may overwinter in *Culicoides sonorensis*. BTV RNA is found in the larvae of this species, suggesting that vertical transmission may occur with the viral RNA persisting without being translated until favourable conditions arise. It is not known, however, whether such persistently infected vectors are capable of transmitting the virus to susceptible vertebrate hosts (WHITE *et al.* 2005) or whether this is also the case for AHSV.

It is possible that a reservoir host may be responsible for sustaining populations of AHSV in enzootic regions, and the ability of several vertebrates to act as an AHSV (or BTV) reservoir has been investigated. Much evidence implicates the zebra as an important vertebrate reservoir host. AHSV-infected zebra are usually asymptomatic, and zebra very frequently have AHSV-specific antibodies (BARNARD 1998; BINEPAL *et al.* 1992). Carnivores can occasionally become seropositive for AHSV, probably as a result of consuming contaminated equid meat or prey species, but are unlikely to be of epidemiological importance in the long term. The effect of AHSV infection on wild carnivores is unclear (ALEXANDER *et al.* 1995; BINEPAL *et al.* 1992). Although AHSV can be transmitted from dogs to horses and vice versa via insect vectors, it appears to occur only rarely in nature (BRAVERMAN and CHIZOV-GINZBURG 1996). Dogs are therefore unlikely to be of epizootiological importance in the spread of AHSV via insect vectors, although more recent evidence

suggests that BTV may be transmitted to domestic dogs via the bites of *Culicoides* midges (OURA and EL HARRAK 2011). Whether this is also the case for AHSV is unknown. Donkeys, although susceptible to AHSV infection, are also unlikely to be important reservoir hosts in the long term (HAMBLIN *et al.* 1998).

Climate change may affect the distribution of temperature sensitive arthropod vectors of AHSV and BTV, and could therefore alter the geographic distribution of these diseases, with important implications for their emergence into previously unaffected regions (GUIS *et al.* 2012). Other factors may also be involved, but are in need of further analysis (MACLACHLAN and GUTHRIE 2010). The various epidemiological factors are closely interrelated to the evolution of the virus, and these factors can place mutual constraints upon one another.

1.1.4 Evolution

The phylogenetic relationships between various orbiviruses are shown in Figure 1.1. Several factors influence the evolution of the virus. It must adapt to several different environments and maintain the ability to infect and replicate in different cell types. It must be transmitted to and replicate in *Culicoides* by being present in the blood or skin of the vertebrate host, migrate to the salivary glands of the midge and be reintroduced into the vertebrate upon feeding. It must evade host immunity whilst maintaining the ability to infect cells (WILSON *et al.* 2009). The presence of a segmented genome yields the possibility of reassortment, which also has important implications for the evolution of the virus.

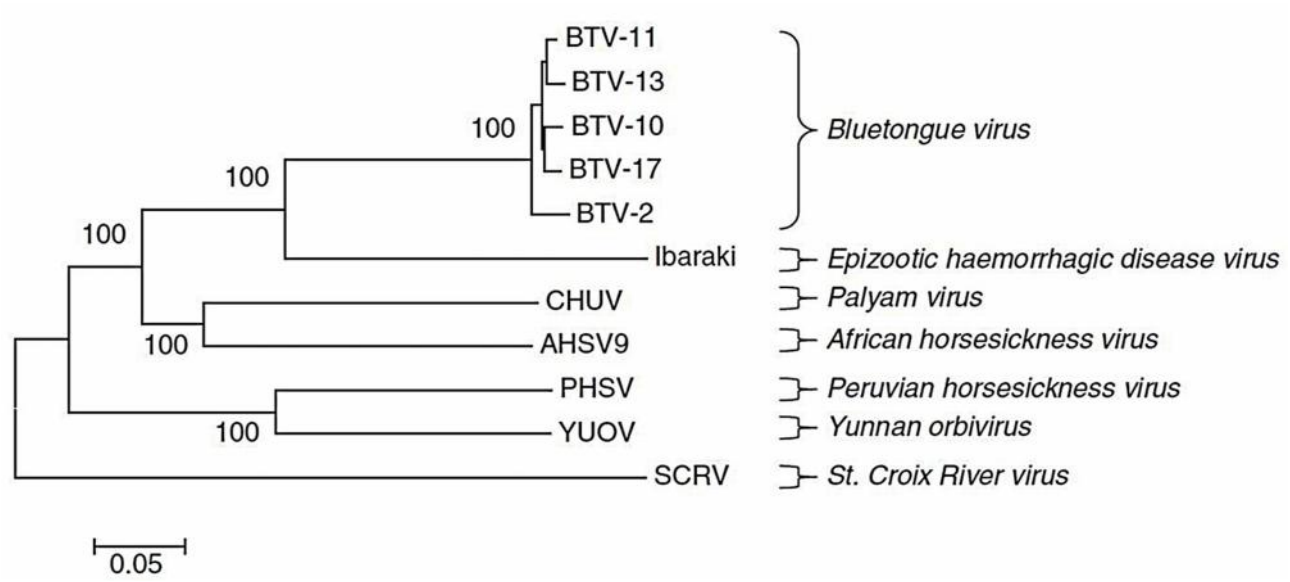

Figure 1.1. – A phylogenetic tree derived from polymerase amino acid sequences of viruses within the *Orbivirus* genus (ATTOUI *et al.* 2009). The bar shows the distance corresponding to 0.05 amino acid substitutions per site and the bootstrap values are indicated at the nodes.

Much lower levels of cytopathic effect (CPE) is seen in infected insect cells compared to mammalian cells. This difference may result from different selective pressures on the virus in different hosts. In mammals, virus transmission to the vector must be maximised, which could be enhanced by increased pathogenicity

in a number of ways (WILSON *et al.* 2009), whereas insect vectors must remain relatively unaffected to allow the spread of the virus to as many vertebrate hosts as possible. The collective features of AHSV epidemiology, evolution and pathogenicity present unique challenges to the control of AHSV infection; these are met primarily with vaccination strategies, although other auxiliary measures have been proposed.

1.1.5 Vaccination

Given the lack of a specific treatment, the most important measure for the control of AHS (LORD *et al.* 1997) and BTV (DUNGU *et al.* 2004) is vaccination. Indeed, following the emergence of BTV in Germany in 2006, a two-year vaccination strategy allowed the country to recover their BTV-free status by 2012 (BAETZA 2013). Information regarding the insect vectors was an important aspect of the six-year eradication process; *C. obsoletus* was found to be the main vector in this region and it was shown that there was no vector-free period (HOFFMANN *et al.* 2009; MEHLHORN *et al.* 2009a; MEHLHORN *et al.* 2009b).

The first AHSV vaccination in 1933 made use of a bivalent live virus. Two years later, field trials were being conducted with a quadrivalent vaccine, and polyvalent live-attenuated vaccines were in use by 1958. Some strains were poorly immunogenic and had serious side-effects in vaccinated animals, which led to the production of tissue culture attenuated vaccines by the 1960's (MACLACHLAN *et al.* 2007). These live-attenuated vaccines were more immunogenic than killed or subunit vaccines and somewhat safer than their antecedents, but posed a risk of reversion to virulence. The authors enumerate the various pitfalls of current vaccination strategies and discuss new approaches to vaccine design to overcome them. The current AHSV vaccines are live-attenuated vaccines (modified-live virus, MLV), administered in two vaccinations that collectively protect against all 9 serotypes (cross protection is expected to occur for serotypes 5 and 9, which are not included in the cocktails).

Although the AHS situation has been ameliorated by the vaccination strategy, outbreaks still occur and the vaccine is liable to various objections, including the potential for reversion to virulence, inadequate attenuation, spread of the vaccine strain by vaccinated immunocompromised hosts and the requirement for repeated vaccinations in some cases due to low immunogenicity. In one study, field collected *C. imicola* and *C. bolitinos* were shown to be susceptible to experimental infection with AHSV vaccine strains, although the virus replication rate was reduced within the insect hosts and may not be sufficient for transmission to vertebrate hosts in the field. If transmission is possible, however, vaccination with certain live attenuated strains may potentially result in AHS outbreaks (PAWESKA *et al.* 2003). For example, a virus strain (serotype 9), that was probably derived from the reference live attenuated vaccine strain, was isolated in the Gambia enforcing the notion that vaccine strains may spread amongst susceptible hosts or revert to virulence by means of reassortment (OURA *et al.* 2011). A recent study in South Africa showed that 16% of ponies immunised with a live-attenuated polyvalent vaccine became naturally infected with AHSV within two years. Half of these animals were sub-clinically infected (WEYER *et al.* 2013).

New promising vaccination strategies include the use of reverse genetic engineered viruses lacking, or with mutations in, essential genes, subunit vaccines displaying immunogenic neutralising epitopes, and DNA vaccines expressing the immunogenic protein at the injection site. These strategies could result in safer, more effective vaccines and can be designed to differentiate infected from vaccinated animals (DIVA). In one study, a BTV vaccine strain could be differentiated from wild type BTV strains with panBTV PCR tests was produced with reverse genetics (VAN RIJN *et al.* 2013). Although early attempts to produce subunit vaccines were fraught with obstacles, including problems with the insolubility and immunogenicity of purified antigen (DU PLESSIS *et al.* 1998), it was later shown that subunit vaccination strategies could provide full protection against lethal virus challenge in vaccinated horses (SCANLEN *et al.* 2002). A subunit vaccine against BTV was recently tested in cattle and had the potential to differentiate infected from vaccinated cattle serologically (ANDERSON *et al.* 2013). These vaccines have not yet been implemented. Metz and Pijlman (2011) review the potential for the use of the baculovirus expression system in the production of arbovirus vaccines.

Since AHSV shares many epidemiological features with BTV, an effective vaccination strategy against the latter may be adapted to the former. Noad and Roy (2009a) review several BTV vaccination strategies. Several approaches have been explored to develop safer vaccines that address the requirement for a DIVA system (BOONE *et al.* 2007; LOUDON and ROY 1991). Several display systems have shown promising results, including the incorporation of target epitopes in viral proteins that form insoluble particles (GHOSH *et al.* 2002; LARKE *et al.* 2005; MURPHY and ROY 2008; RUTKOWSKA *et al.* 2011). More recently, it was demonstrated that reassortants using the avirulent vaccine strain BTV6/net08 as a backbone could potentially be used for the rapid production of safe serotype-specific vaccines, which is important during the incursion of a new BTV serotype (VAN GENNIP *et al.* 2012a). Disabled infectious single cycle (DISC) vaccines, which have a deleted or mutated gene that is essential for replication, are especially promising; only a single vaccination is required, a DIVA design can be incorporated, and various safety concerns are eliminated (CELMA *et al.* 2013; MATSUO *et al.* 2011). The speed with which these vaccines can be produced is of great value in controlling emerging BTV serotypes specifically. The control of BTV following its emergence in Europe in 2006, which entailed a vaccination strategy, has also been reviewed (ZIENTARA and SANCHEZ-VIZCAINO 2013). In addition to vaccination, a number of alternative control measures have been attempted, with varying success.

1.1.6 Other control measures

Alternative control measures that have been implemented are primarily aimed at the insect vector. Stabling as a means to protect horses from biting midges at night may be relatively effective for *C. imicola*, which is exophilic, but not for another AHSV vector species, *C. bolitinos*. This distinction may be especially important in regions where *C. bolitinos* is the more abundant vector species (MEISWINKEL *et al.* 2000).

Housing may also protect cattle against bites from *Culicoides obsoletus,* and could therefore ameliorate the spread of BTV (BAYLIS *et al.* 2010).

Pharmacological agents, including antihelminthics and insect repellents, could supplement vaccination in the control of BTV infection. Treatment of sheep with the antihelminthic agent avermectin may be protective against BTV by reducing the affinity of *Culicoides* midges for sheep. Avermectins appear to reduce the olfactory sensitivity of midges for animal attractants; hence their reduced propensity to bite treated sheep (SOLLAI *et al.* 2007). Flectron® ear tags appear to repel biting midges and could be an effective aid in controlling the spread of BTV (LIEBISCH and LIEBISCH 2008). Insecticides are probably of little use as a vector control strategy in the field (VENAIL *et al.* 2011). In addition, preliminary data regarding the use of entomopathogenic fungi as bio-control agents of the biting midge *C. nubeculosus* shows promise (ANSARI *et al.* 2011). Recently, the potential for the development of virostatic agents against BTV has been explored. Li *et al.* (2009) performed high-throughput screening of a large number of small molecules to identify six sets of related compounds with putative protective properties. Gu *et al.* (2012) determined that two aminothiophenecarboxylic acid derivatives were protective against BTV-induced cytopathic effect (CPE) *in vitro,* possibly by preventing BTV-induced host cell autophagy. MacLachlin and Mayo (2013) review bluetongue virus control strategies and suggest that holistic approaches are likely to be the most effective at eradicating the disease and limiting its spread. They also highlight the importance of preventive control in addition to reactive control. The molecular biology of AHSV and BTV infection has been studied extensively, partly with the purpose of identifying targets for the control and prediction of disease progression, and new approaches to disease control are likely to emerge.

1.2. Orbivirus structure and replication cycle

1.2.1 Orbivirus structure

The AHSV virion is a non-enveloped, icosahedral particle with a ± 70nm diameter, consisting of three layers: the subcore, core, and outer capsid. The virion is composed of seven structural proteins and the segmented dsRNA genome (Fig. 1.2). The core consists of five proteins (VP1, VP3, VP4, VP6, and VP7) and contains the group specific epitopes. The subcore is formed by the VP3 layer which contains the transcriptase complex proteins VP1, VP4 and VP6 and the 10 double stranded RNA (dsRNA) genome segments. The outer capsid layer is formed by VP2 and VP5 and contains the type specific epitopes. There are nine AHSV serotypes, and the serotypic determinants occur on the two capsid proteins of the virion, VP2 (mainly) and VP5 (MERTENS *et al.* 1989; NOAD and ROY 2009b). The relationships between the genome segments and the proteins they encode are summarised in Table 1.1.

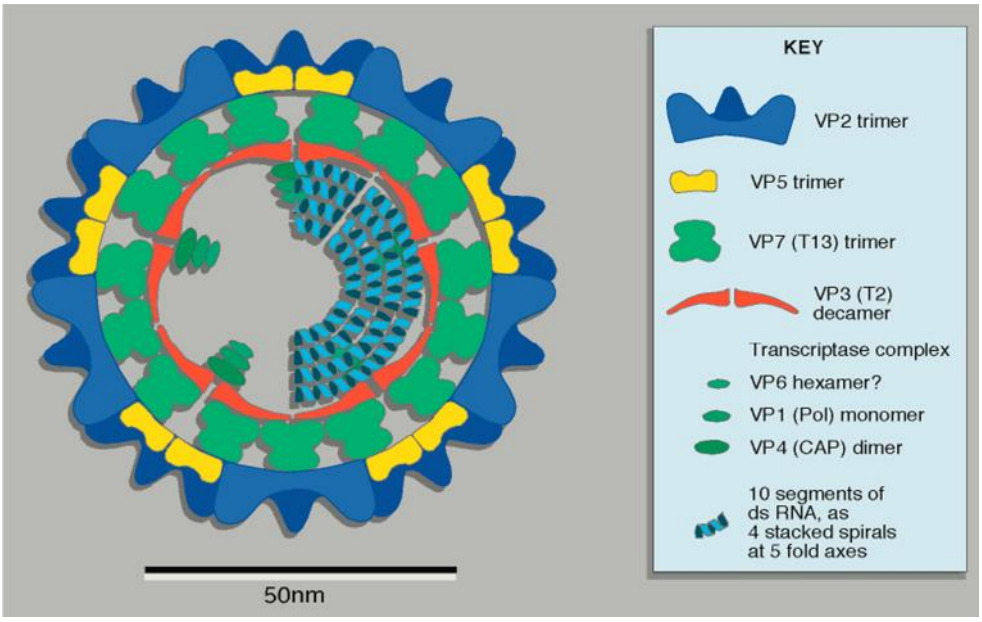

Figure 1.2. – Diagram of the structure of the BTV particle (MERTENS *et al.* 2009).

Table 1.1. – Orbivirus genome segments and the proteins they encode. BTV data adapted from Roy (1996).

	BTV			AHSV		
Genome segment	Size (bp)	Protein	Size (kDa)	Size (bp)	Size (kDa)	Reference
1	3954	VP1	150	3965	150	Vreede and Huismans (1998)
2	2926	VP2	111	3205	123	Venter (2000)
3	2770	VP3	103	2792	103	Iwata (1992)
4	1981	VP4	76	1978	76	Mizukoshi (1993)
5	1769	NS1	64	1748	63	Nel, L.H. (GenBank U01069)
6	1638	VP5	59	1566	57	Du Plessis and Nel (1997)
7	1156	VP7	38	1167	38	Maree *et al.* (1998)
8	1124	NS2	41	1166	41	van Staden *et al.* (1991)
9	1046	VP6/NS4	36/17-20	1169	38/17	Firth (2008); Turnbull *et al.* (1996)
10	822	NS3/NS3A	25.5/24	756	23.6/22.5	van Staden and Huismans (1991); Zientara,S. and Sailleau,C. (GenBank AF116461)

The structure of the BTV capsid has been determined by means of cryo-electron microscopic (cryo-EM) reconstruction. VP2 is the outermost capsid protein, forming triskelion-shaped structures on the surface of the virion. Each VP2 trimer contains 3 putative sialic acid binding domains which could be involved in virus entry into host cells. VP5 trimers, which form the inner layer of the capsid, have a globular shape. The VP5 trimers bear structural similarity to the fusion proteins of enveloped viruses and the VP5 layer has some weak interactions with the VP2 and VP7 layers, which may facilitate uncoating (ZHANG *et al.* 2010).

The three-dimensional structure of the BTV core has also been determined by cryo-electron microscopy (PRASAD *et al.* 1992), and the atomic structure of the BTV core by X-ray crystallography (GRIMES *et al.* 1998). The structure of the AHSV virion as analysed with electron cryomicroscopy and three-dimensional image reconstruction is very similar to that of BTV (MANOLE *et al.* 2012). The subcore layer of the virion is composed of VP3 multimers. VP3 shows substantial amino acid conservation among orbiviruses and several residues essential for core-like particle formation have been identified by means of site-directed mutagenesis (TANAKA and ROY 1994). The assembly of the BTV VP3 subcore has been investigated by means of various mutant VP3 constructs; the core assembly intermediates appear to be VP3 oligomers (KAR *et al.* 2004). VP7 is also highly conserved (OLDFIELD *et al.* 1990) and similar functional studies have been conducted on VP7 to identify residues required for trimerisation and core assembly (LE BLOIS and ROY 1993; LIMN *et al.* 2000; MONASTYRSKAYA *et al.* 1997). In addition, the crystal structure of BTV VP7 has been resolved (GRIMES *et al.* 1995).

Co-expression of AHSV VP3 and VP7 in recombinant baculovirus-infected insect cells results in the formation of core-like particles (CLPs) which structurally resemble cores produced during infection (MAREE *et al.* 1998). The presence of dsRNA, NS1, NS2 or NS3 is not required for the formation of BTV core-like particles when VP3 and VP7 are co-expressed in insect cells (FRENCH and ROY 1990), suggesting that these proteins have the inherent ability to assemble into CLPs *in vivo*. Similarly, co-expression of VP3, VP7, VP2 and VP5 results in the formation of virus-like particles (VLPs) (FRENCH *et al.* 1990).

The ten dsRNA genome segments occur within the core and are associated with the 10-12 transcriptase complexes containing the minor structural proteins VP1, VP4 and VP6. A model for the organisation of the 10 dsRNA genome segments within the BTV core has been proposed, based on X-ray crystallographic examination of a transcriptionally active virus particle (GOUET *et al.* 1999). According to this model, VP4 and VP1 interact with the VP3 layer (decamers) and form flower-like structures beneath the 5 fold axes of the core. VP4 has more direct contact with VP3 than does VP1. The location of VP6 has not been confirmed, but it is probably found near the VP1-VP4 complexes (NASON *et al.* 2004; NOAD and ROY 2009b). How the virus structure relates to the viral replication cycle will be examined in the following sections.

1.2.2 Orbivirus replication

The economically important bluetongue virus (BTV) has been more extensively studied than AHSV, but many similarities exist between these viruses regarding structure and replication cycle, which is depicted in Figure 1.3. Reference will therefore be made primarily to BTV in the following sections, although AHSV will be included where the literature permits. The first barrier to infection of either the vertebrate host or the vector following consumption of a blood meal is virus entry into the cell. The virus must then generate multiple infective copies of itself, some of which are released to infect surrounding naive cells.

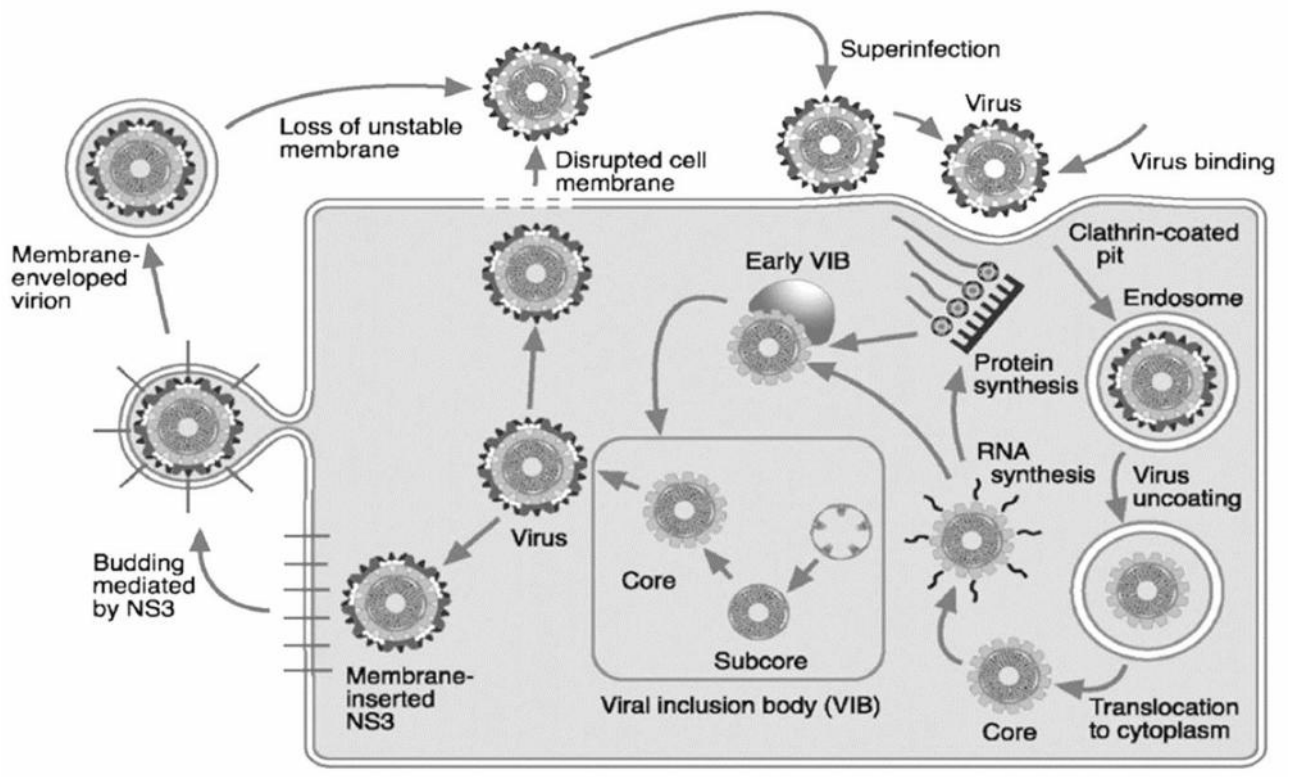

Figure 1.3. – An overview of the BTV replication cycle (ROSS-SMITH *et al.* 2009).

1.2.2.1 Entry

The proteins forming the outer capsid layer of the virus particle, VP2 and VP5, are responsible for virus entry into the host cell cytoplasm. VP2 is the most variable AHSV protein. It contains neutralising epitopes and mediates virus attachment to host cells (HASSAN and ROY 1999), possibly via three putative sialic acid binding domains (ZHANG *et al.* 2010). Studies with baculovirus-expressed and purified BTV VP2 showed that VP2 alone mediates virus cell attachment and entry and attaches to the same surface molecule as the virion. VP2 has an affinity for glycophorin A, which is found on red blood cells, and this could mediate transmission of the virus from the insect vector to the vertebrate host during consumption of a blood meal (HASSAN and ROY 1999). Subtle differences appear to exist between mammalian and insect cells regarding virus entry. BTV entry into mammalian cells involves the clathrin-dependent endocytic pathway. However, at least one BTV serotype can infect cells independently of the clathrin-mediated endocytosis pathway,

suggesting that this model is not universally applicable to BTV infection. In the alternative scenario, cell entry may resemble macropinocytosis and requires dynamin (GOLD *et al.* 2010).

Following VP2-mediated entry into the endosome, the virus particle penetrates the host cell cytoplasm, seemingly through the involvement of two amphipathic alpha helices which occur on VP5. Assays with purified recombinant BTV VP5 showed that the protein causes cell permeabilisation of both insect and mammalian cells, but is not involved in receptor-mediated endocytosis. The function of the amphipathic alpha helices on VP5 was confirmed with mutagenesis assays and expression of the helix peptides alone, which abolished and conferred cytotoxicity, respectively. Purified VP5 trimerises, which is a common feature amongst cell penetration proteins. The data collectively suggest that VP5 is involved in virus penetration into the cell following endocytosis (HASSAN *et al.* 2001). Cryo-EM analysis of the outer coat structure of BTV shows that the VP5 trimers bear structural similarity to the fusion proteins of enveloped viruses and the VP5 layer forms few, weak interactions with the VP2 and VP7 layers, which may facilitate uncoating. The authors suggest that VP5 could "unfurl like an umbrella" prior to release of the core particle (ZHANG *et al.* 2010), so that the amphipathic helices no longer interact with VP7 trimers, but are exposed on the surface and interact with the endosome membrane once VP2 is removed, leading to permeabilisation (NOAD and ROY 2009b).

Experimental vacuolar H^+- ATPase inhibition, which causes alkalinisation of acidic organelles, inhibits virus replication, suggesting that productive infection requires low endosomal pH. A model for BTV entry into cells has been proposed based on this evidence: the virus undergoes clathrin-mediated endocytosis from the plasma membrane, with BTV enclosed in clathrin vesicles. Low pH-induced penetration then occurs in early endosomes: following loss of the VP2 outer capsid layer, VP5 destabilises the endosomal membrane to form pores through which cores are released into the cytoplasm and the VP5 remains associated with the endosomal membrane (FORZAN *et al.* 2007). AHSV VP5 also contains two amphipathic alpha helical domains which plausibly cause endosomal membrane permeabilisation (STASSEN *et al.* 2011b).

A different mode of cell attachment may occur during infection of insect cells. BTV VP7 appears to bind a cell-membrane receptor of *C. variipennis* and KC cells; core particles bind more efficiently to these cells compared to whole virus (XU *et al.* 1997). BTV cores are also more infective in insect (KC and C6/36) cells than in mammalian (BHK21) cells (MERTENS *et al.* 1996). A VP7 RGD motif, which is exposed on the surface of core particles, appears to mediate core particle attachment to insect cells (TAN *et al.* 2001). The presence of different proteases within the sera of vertebrate hosts could be responsible for differences in infectivity of AHSV in *Culicoides* midges. These species-specific proteases can cleave VP2, possibly yielding particles with enhanced infectivity (MARCHI *et al.* 1995). *In vitro* protease treatment of BTV particles results in cleavage of VP2 and the formation of infectious subviral particles (ISVP), which show enhanced infectivity in insect, but not mammalian, cells. *C. sonorensis* saliva contains a trypsin-like protease which is absent from the saliva of the less efficient vector species *C. nubeculosis*. Treatment of purified virus with *C.*

sonorensis saliva proteins also yields ISVP with enhanced infectivity in KC cells and reduced infectivity in mammalian cells, suggesting that insect vector saliva could enhance BTV infectivity by altering the structure of the virus particle. This was the first demonstration of enhanced infectivity through direct modification of the viral structure by substances in host saliva (DARPEL *et al.* 2011). Following virus entry into the cell and release of the core from the endosomal compartment into the cytoplasm, expression of viral genes can take place.

1.2.2.2 Core release and transcription

Once the VP2 and VP5 layers are removed and the endosomal membrane has been permeabilised by VP5, the exposed transcriptionally active viral cores are released into the cytoplasm. Upon release from the endosome, the core undergoes a conformational change. VP3 and VP7 move outward, resulting in the formation of pores within the subcore layer at the 5-fold axis of the core through which capped mRNA transcripts are extruded into the cytoplasm. The transcriptase complexes are located near these pores. Transcription is fully conservative and involves two steps. Positive strand mRNA is first synthesised from the negative strand template, some of which is translated after extrusion from the core. This positive strand RNA is also used for synthesis of the negative strand at a later stage of replication to yield dsRNA, which is packaged into nascent virions at an unknown point during replication. All 10 segments are transcribed simultaneously within the core. This presents certain logistical problems regarding substrate availability and space, and possible solutions to these problems have been proposed based on X-ray crystallographic data (DIPROSE *et al.* 2001).

Transcription of viral mRNA from cytoplasmic cores prevents dsRNA from entering the cytoplasm, which might prevent the induction of host cell apoptosis that is normally mediated by the presence of free dsRNA within the cell. Additionally, dsRNA can bind to BTV cores, which could allow further evasion of the host dsRNA surveillance system by sequestering any dsRNA that might be present within the cytoplasm (DIPROSE *et al.* 2002).

The transcriptase complex consists of VP1, VP4 and VP6. *In vitro* studies of baculovirus-expressed and purified BTV VP1 (BOYCE *et al.* 2004), along with bio-informatic and mutagenesis analyses (WEHRFRITZ *et al.* 2007) suggest that VP1 is the BTV RNA-dependent RNA polymerase. BTV VP1 can produce dsRNA from ssRNA templates derived from several members of the *Reoviridae* family, but not from distantly related sequences. This suggests the presence of conserved sequences or structural elements on the RNA of members of the *Reoviridae* family that are recognised by VP1, resulting in preferential production of viral dsRNA (MATSUO and ROY 2011).

BTV VP4 covalently binds guanosine triphosphate (GTP) or guanosine monophosphate (GMP), and catalyses all the steps of the ssRNA capping (guanylyl transferase) reaction, possessing guanylyltransferase, Type I and Type II methyltransferase activities (MARTINEZ-COSTAS *et al.* 1998; RAMADEVI *et al.* 1998). The 5' cap

stabilises the mRNA and is involved in translation initiation. BTV VP6 contains a number of helicase-associated motifs, has *in vitro* RNA-dependent ATPase and helicase activities and can act upon blunt ended dsRNA in addition to dsRNA with 3' or 5' overhangs (STAUBER *et al.* 1997). Site directed mutagenesis, baculovirus expression and binding assays were performed to confirm the functions of the putative VP6 helicase domains. Critical residues for adenosine triphosphate (ATP) binding, RNA binding and helicase activity were identified, and it was demonstrated with electron microscopy that purified VP6 mixed with RNA forms oligomeric ring-like structures, which is characteristic of helicases (KAR and ROY 2003). Although the nucleic acid binding sites identified in BTV VP6 do not occur on ASHV VP6, it also exhibits nucleic acid binding activity, which requires the presence of a crucial amino acid region, (DE WAAL and HUISMANS 2005). The transcribed viral ssRNA can serve as templates for translation of viral proteins and for negative strand synthesis to form dsRNA genome segments.

1.2.2.3 Replication and virus assembly

During assembly, the synthesised dsRNA genome segments are packaged into viral particles composed of the newly translated viral structural proteins. The processes of virus assembly, trafficking and release are mediated by a combination of viral and host molecules.

Within infected cells, new core particles are assembled within viral inclusion bodies (VIBs). VIBs are large granular cytoplasmic bodies formed by NS2, independently of other viral proteins. Initially, VIBs occur near the nucleus of an infected cell, but become progressively larger, more numerous and widely distributed (BROOKES *et al.* 1993). VIBs are also the sites of negative strand RNA synthesis. All BTV core structural proteins localise to VIBs in the absence of other viral proteins, except VP7, which only localises to VIBs in the presence of VP3 (KAR *et al.* 2007).

Baculovirus-expressed AHSV, BTV and EHDV (epizootic haemorrhagic disease virus) NS2 proteins are phosphorylated *in vitro,* probably by a cellular protein kinase (THERON *et al.* 1994). NS2 binds ssRNA *in vitro* with varying efficiency and non-specifically. Binding ability may be related to alpha-helix content (UITENWEERDE *et al.* 1995). NS2 binds BTV ssRNA preferentially to non-specific RNA *in vitro*, by recognising hairpin-loop secondary structures on BTV mRNA (MARKOTTER *et al.* 2004). These data suggest that NS2 may recruit ssRNA for replication or genome assembly. Phosphorylation of NS2 is required for the formation of VIBs, but not for its association with ssRNA or VP1, as shown by mutational analysis of putative phosphorylation sites (MODROF *et al.* 2005). Core particles may be released from the VIB when NS2 becomes dephosphorylated (NOAD and ROY 2009b).

Immuno-electron microscopic analyses suggest that VP7 is incorporated into nascent virions within VIBs, and that VP2 is added during or after egress from the VIB (HYATT and EATON 1988). Virus cores are found within VIBs, and mature virus particles at the periphery, which suggests that viral assembly and release from VIBs occur at the periphery rather than from the matrix (BROOKES *et al.* 1993). The fact that assembly

of cores and genome packaging occur within VIBs prevents the addition of the outer capsid proteins, so that the cores are transcriptionally active for longer. Vimentin intermediate filaments of the host cytoskeleton appear to be involved in assembly of the outer capsid (EATON *et al.* 1987b).

Another feature of AHSV infection is the formation of flat hexagonal (S. Bekker, unpublished) or rod-shaped VP7 crystals within infected cells (VENTER *et al.* 2012). These crystals are also seen upon electron microscopic examination of baculovirus-expressed and purified AHSV VP7, and they have a 2-D crystalline lattice structure (BURROUGHS *et al.* 1994). AHSV VP7 is less soluble than BTV VP7, which could account for the absence of VP7 crystals from BTV-infected cells. Bioinformatic analyses revealed that AHSV VP7 contains an immunoreceptor tyrosine-based activation motif (ITAM), which occurs in B- and T-cell receptors (BCRs and TCRs) and several other virus-specified proteins and is involved in signal transduction. The VP7 proteins of several orbiviruses, including AHSV, Broadhaven virus (BRDV) and EHDV, also contain a proline rich sequence of unknown function upstream of the ITAM. The current data suggest that the AHSV VP7 ITAM (perhaps in concert with the proline-rich sequence) may affect signal transduction during infection by interacting with components of the host intracellular signalling pathways (CANTOR 1996).

Non-structural protein NS3 (see section 1.2.2.4) interacts with BTV VP5 (BEATON *et al.* 2002). Site directed mutagenesis, in conjunction with flotation assays to investigate lipid raft association and confocal microscopy, shows that VP5 contains a SNARE domain which is responsible for its localisation to cell membrane lipid rafts. VP5 also co-purifies with lipid raft domains when baculovirus expressed or in infected cells, and the disruption of lipid rafts revealed their involvement in BTV assembly. Therefore, the VP5-NS3 interaction may be involved in virus assembly (BHATTACHARYA and ROY 2008). The final stage of the viral replication cycle, critical for the spread of infection both within and between hosts, involves the release of newly assembled mature virus particles into the environs of the infected cell.

1.2.2.4 Egress

Mature virions are released from the infected cell by either cell lysis through localised disruptions in the cell membrane, or by budding. Virus release from insect cells is expected to follow the non-lytic path (budding), whereas release from mammalian cells involves lysis, although most viruses remain associated with the cell. These cell type specific differences regarding virus release is associated with a discrepancy in the degree of cytopathic effect (CPE) observed between infected mammalian and insect cells. AHSV appears to induce apoptosis in mammalian but not insect cells, which could account for this disparity in CPE (STASSEN *et al.* 2011a).

Genome segment 10 encodes two proteins, NS3 and its truncated counterpart, NS3A, which are synthesised in equimolar amounts in infected mammalian cells. Baculovirus-expressed AHSV NS3 localises to and permeabilises the cell membrane, causing cell death (VAN STADEN *et al.* 1995). The non-structural protein NS3 appears to play a critical role in BTV egress and virus yield (HYATT *et al.* 1993). Similarly, AHSV

NS3 localises to regions of the membrane within infected cells where virions are being released via either pathway (STOLTZ *et al.* 1996). When larger quantities of NS3 are present, which is the case in insect cells, virus release by budding is favoured, whilst lytic release predominates when less NS3 is present. BTV NS3 shares certain properties with viroporins, a group of virus-encoded small hydrophobic transmembrane proteins that form pores within the bilipid membranes of infected cells and affect virus release, protein trafficking and membrane permeability (VAN NIEKERK *et al.* 2001).

Mature BTV virions appear to associate with the cytoskeleton, and both of the outer capsid proteins are required for the association of VLPs with the cytoskeleton (HYATT *et al.* 1993). It was later demonstrated that the association of mature virus particles with vimentin intermediate filaments is mediated by VP2 and is independent of other viral proteins. Disruption of the formation of intermediate filaments by acrylamide or colchicine treatment resulted in reduced virus release, suggesting that this association is involved in virus egress from infected cells (BHATTACHARYA *et al.* 2007).

Interactions between NS3 and certain host proteins have also been demonstrated. The N-terminal amphipathic helix domain interacts with the calpactin light chain (p11) of the cellular annexin II complex, which is involved in exocytosis and regulated secretory pathways. Although the exact function of this interaction is unclear, it could plausibly direct NS3 to sites where exocytosis is occurring. The C-terminus of NS3 interacts with VP2, suggesting that NS3 could mediate an association between mature virions and the host exocytosis machinery (BEATON *et al.* 2002). When only NS3A is expressed, or when the N-terminal amino acids that differ between NS3 and NS3A and are involved in the NS3-p11 interaction are mutated, virus growth is reduced. Growth was less severely reduced by these mutations in insect cells than in mammalian cells, and viruses were found throughout the cytoplasm rather than within cytoplasmic vesicles as in wild type BTV infected insect cells. These data suggest that both NS3 and NS3A must be present for optimal replication in insect cells and that the N-terminal region of NS3 appears to be involved in the late stages of the replication cycle within mammalian cells with probable involvement in viral egress (CELMA and ROY 2011). More recently, an interaction between phosphatidylinositol (4,5) bisphosphate [PI(4,5)P2], NS3 and VP5 has also been demonstrated with confocal and electron microscopy (BHATTACHARYA and ROY 2013). When the production of PI(4,5)P2 is reduced or its distribution changed, the localisation of BTV proteins also changes and virus morphogenesis is disturbed as measured with virus titration. Protein p11 interacts with annexin, which in turn interacts with PI(4,5)P2, which provides a possible explanation for the interaction between NS3 and p11.

NS3 also interacts with Tsg101, a member of the ESCRT-I family which is involved in intracellular trafficking, within infected mammalian cells. Inhibition of Tsg101 by RNAi reduces BTV or AHSV release from infected HeLa cells. ESCRT proteins are involved in the formation of multivesicular bodies, which involves budding of vesicles into late endosomal compartments. NS3 also contains a conserved late domain motif that is common among viral proteins that recruit Tsg101, but does not recruit other cellular proteins that enhance

budding activity with equal efficacy to other viruses, which could account for the low levels of virus release by budding within infected mammalian cells. This interaction is probably involved in virus release as well. The insect cellular proteins with which NS3 interacts remain to be identified (WIRBLICH *et al.* 2006). When the Tsg101 binding motif on NS3 was mutated within a reverse genetics engineered BTV strain, the amount of budding was reduced, with virions localising to the cell membrane without being released. Furthermore, mutations within the NS3 VP2 binding domain abolished virus release by budding. This corroborates the hypothesis that NS3 is involved in trafficking and links virus particles with the cellular components required for virus release (CELMA and ROY 2009). More recently, Chauveau *et al.* (2013) demonstrated that NS3 may also play a role in the interaction between the BTV and the host innate immune system by reducing activation of the IFN-β promoter, thus preventing the cell from achieving an antiviral state.

Interestingly, an additional non-structural protein, designated NS4, has recently been identified in BTV and GIV (BELHOUCHET *et al.* 2011; RATINIER *et al.* 2011) and is predicted to exist in all orbiviruses except St. Croix river virus (SCRV), including AHSV (FIRTH 2008). BTV NS4 occurs within the nucleolus of infected cells and may be involved in inhibiting the host innate immune response to viral infection (RATINIER *et al.* 2011), although its precise function during the viral replication cycle is unknown.

The non-structural protein NS1 forms an abundance of tubules of unknown function within orbivirus-infected cells. Evidence has been obtained that suggests a role for NS1 in virus trafficking and morphogenesis, although NS1 alone does not mediate the release of VLPs from the cell (HYATT *et al.* 1993). Inhibition of NS1 function in BTV infected cells by means of a mammalian cell line that expresses a scFv (single chain antibody fragment) specific for BTV NS1 showed that NS1 or BTV tubules could be involved in BTV cellular pathogenesis and virus morphogenesis. Within these cells, fewer, less stable tubules were produced, CPE was reduced, more virions were released into the medium, and budding occurred (OWENS *et al.* 2004). Furthermore, an interaction between NS1 and host protein SUMO-1, which induces modification of proteins involved in intracellular trafficking, has been observed, which implies that NS1 could control trafficking of virus particles (NOAD and ROY 2009b). NS1 is discussed in more detail in section 1.3. Much is still unknown about the viral replication cycle, but some of the more abstruse details concerning the molecular biology of AHSV or BTV infection might soon be clarified through the use of newly developed reverse genetics systems.

1.2.3 Reverse genetics systems

Since the first demonstration that BTV ssRNA transcribed *in vitro* from purified cores can be used to transfect cells and recover infectious virus without the use of a helper virus (BOYCE and ROY 2007), the development of a BTV reverse genetics system has met with considerable success. Boyce *et al.* (2008) showed that transfection of cells with ssRNA synthesised *in vitro* from T7 cDNA clones in the presence of a cap analogue can also yield infectious BTV. This system can be used for reverse genetics investigations. It was possible to replace one or more core transcript derived segments with those of a different serotype.

Matsuo and Roy (2009) discovered that double transfection with BTV transcripts results in higher titres compared to single transfections. Cells were first transfected with the transcripts that are probably involved in primary replication (VP1, VP3, VP4, VP6, NS1 and NS2) and thereafter with a full complement of BTV transcripts. It has also been demonstrated that cDNA synthesised from BTV genome sequence data could be used to generate virus strains phenotypically indistinguishable from the wild type strains *in vivo* (VAN GENNIP *et al.* 2012b). A reverse genetics system for AHSV was shown to be possible when infectious virus was recovered from cells transfected with AHSV ssRNA transcribed from purified cores or T7 plasmids containing AHSV genes (MATSUO *et al.* 2010). A reverse genetics system would be an invaluable resource in the study of AHSV molecular biology, and has already been implemented successfully in the study of BTV. A plasmid-based reverse genetics system is currently being developed at the University of Pretoria (J. Theron, personal communication).

The next two sections describe the focus of the current investigation in more detail: the properties and possible functions of the AHSV non-structural proteins NS1 and NS4.

1.3. NS1

1.3.1 Properties and tubulisation of the NS1 protein

The literature pertaining to the structure and constraints on assembly of NS1 tubules will be reviewed in this subsection. NS1 is encoded by genome segment 5. It is the most efficiently translated BTV protein *in vivo*, constituting up to 25% of BTV proteins (VAN DIJK and HUISMANS 1988). The NS1 protein sequence is highly conserved amongst orbiviruses and AHSV serotypes (MAREE and HUISMANS 1997). Interestingly, expression of the BTV NS1 gene *in vitro* or in bacterial cells yields NS1 and a minor polypeptide, NS1a, which has also been observed within BTV infected cells (GRUBMAN 1990). Whether this minor polypeptide is of any functional significance is unclear.

Within infected cells, NS1 self-assembles into tubular structures that can be seen from 2-4 hours post infection (hpi) and persist throughout infection (URAKAWA and ROY 1988; VAN STADEN *et al.* 1998). The presence of these tubules is characteristic of orbivirus infection and they often form bundles (Fig. 1.4) which resemble cytoskeletal intermediate filaments. Initially, tubules associate with virus particles and VIBs, but later become dispersed throughout the cytoplasm (HUISMANS and ELS 1979). The structure of baculovirus-expressed and purified BTV NS1 tubules has been determined by means of cryo-electron microscopy, and it has been postulated that NS1 forms dimers which coil helically with 21-22 dimers per helical turn to yield tubular structures (HEWAT *et al.* 1992). BTV and EHDV NS1 tubules are large (68 nm and 54nm in diameter, respectively) with a ladder-like surface structure, whereas AHSV tubules are narrower (18-23 nm diameter, with lengths of up to 4 μm and a lumen diameter of ± 7 nm) and less stable than BTV tubules under certain conditions. AHSV NS1 lacks the ladder-like surface structure of BTV NS1 tubules, but

has an internal structure described as a “fine reticular cross-weave”. Early studies found that the tubules are empty and do not appear to contain RNA (HUISMANS and ELS 1979; MAREE and HUISMANS 1997).

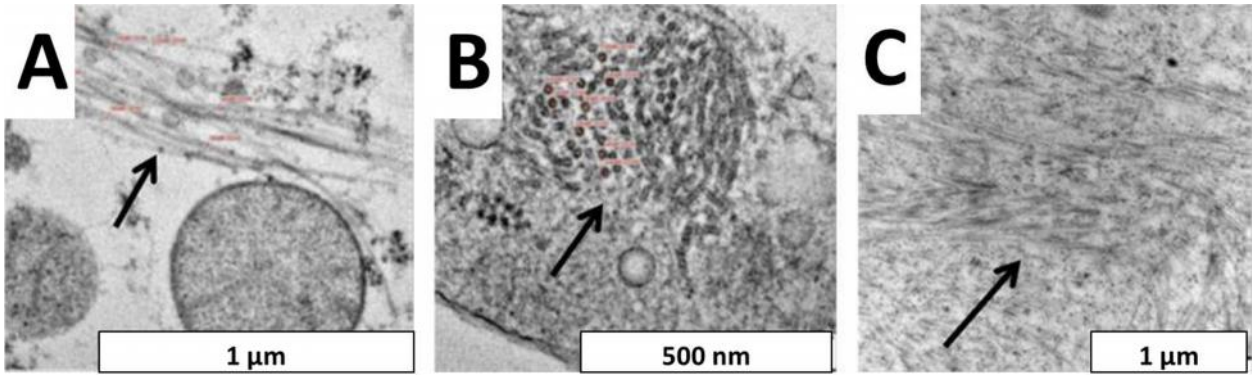

Figure 1.4. – Transmission electron micrographs of NS1 tubules (arrows) within AHSV-infected mammalian cells (E. Venter, unpublished) showing A and C: longitudinal sections and B: a cross-section of tubule bundles.

Studies investigating the process of BTV NS1 tubule formation have revealed several requirements for, and constraints on, tubulisation. Deletion and site-directed mutagenesis of BTV NS1, followed by electron microscopy of cells expressing mutant forms of NS1, revealed the importance of the NS1 N- and C-termini as well as two conserved cysteine residues at positions 337 and 340 for tubule formation. These mutant NS1 proteins formed ribbon-like aggregates in baculovirus-infected cells (MONASTYRSKAYA *et al.* 1994). Additional deletion mutation studies involving the C-terminus of BTV NS1 showed that the last five amino acids are not required for tubulisation, but that the penultimate set of five are. The addition of up to 16 amino acids to the C-terminus in the form of an antigenic sequence did not disrupt tubulisation, but extension by 19 amino acids did (MONASTYRSKAYA *et al.* 1995).

Furthermore, the potential for BTV NS1 tubules as an antigen display system has long since been recognised, and the development of such display systems has tested the robustness of tubule formation to certain mutations. The C-terminus is a frequently selected site of insertion for the development of display systems because it is exposed on the tubule surface and therefore simultaneously unlikely to disrupt tubulisation and aptly situated to encounter components of the immune system. C-terminal inserts of various lengths are generally well-tolerated. These inserts were mostly immunogenic epitopes, and NS1 tubules as a display system tend to induce full or partial protection against lethal challenge of immunised animals (MIKHAILOV *et al.* 1996). Interestingly, full-length green fluorescent protein (GFP), which is 238 amino acids long, can be inserted near the NS1 C-terminus without disrupting tubule formation or correct folding of GFP (GHOSH *et al.* 2002). The longest tolerated NS1 C-terminal insert reported to date contained 527 amino acids (LARKE *et al.* 2005). To date, similar studies of AHSV NS1 have not been published, although the high degree of NS1 conservation between orbiviruses suggests that at least some structural similarities with BTV NS1 should exist. Indeed, enhanced GFP (eGFP) has been inserted near the C-terminus of AHSV

NS1 without disrupting tubulisation (LACHEINER 2006). Future studies on orbivirus NS1, perhaps with the aid of reverse genetics, may enhance our current understanding of the process and function of NS1 tubule formation.

1.3.2 Distribution and interactions with host or viral proteins

Studies of the distribution and co-localisation of proteins can provide a basis for understanding protein function. Electron microscopic studies of the distribution of NS1 within BTV-infected cells showed that NS1 tubules are located near the nucleus during the early stages of infection and later become dispersed throughout the cytoplasm. BTV NS1 appears to associate with the cytoskeleton, specifically with cytoskeletal intermediate filaments, and also with virus particles and cores (BROOKES *et al.* 1993; EATON *et al.* 1987b). Fluorescence and immunogold labelling studies (Fig. 1.5) revealed a putative co-localisation between NS1 tubules and VP3 or VP7 in BTV infected cells (HYATT and EATON 1988).

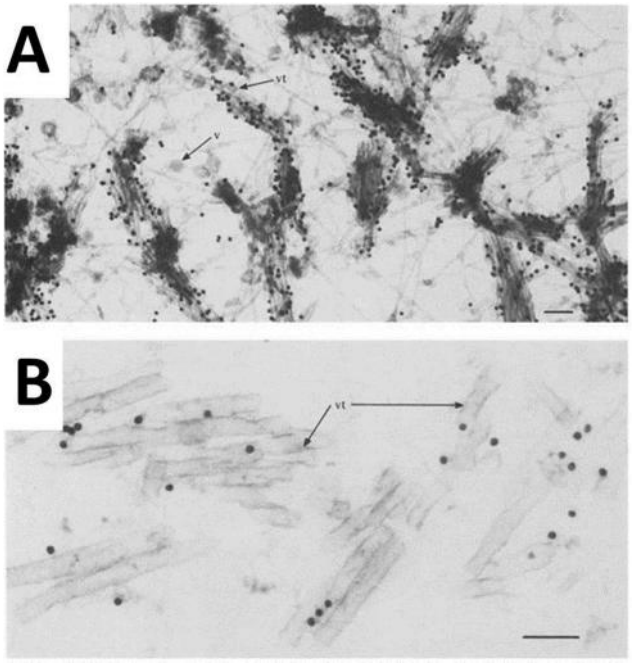

Figure 1.5. – Immunogold labelling with A: anti-VP3 or B: anti-VP7 indicates an association between both of these proteins and BTV tubules, which in turn are associated with purified cytoskeletons (HYATT and EATON 1988). Scale bars are 100 nm in length. Arrows indicate virus particles (v) and viral tubules (vt).

The association of NS1 with virus particles during all stages of assembly within the VIBs could denote a role for NS1 during early viral morphogenesis (BROOKES *et al.* 1993). Indeed, the inhibition of NS1 protein with a recombinant single-chain antibody fragment (scFv) expressed by the infected cell causes mammalian cell infection to resemble that seen in insect cells; in addition to disrupting tubule formation, lower cytopathic effect (CPE) was observed, more viruses were released and more often by budding. This suggests that NS1 could increase virus-cell association which results in lysis in mammalian cells, possibly related to the ratio of NS1 to NS3 within the cell. Based on these findings, the authors propose a role for NS1 during virus

pathogenesis and morphogenesis (OWENS *et al.* 2004). Co-localisation studies of NS1 with other AHSV proteins have not been published.

In addition to putative roles in pathogenesis and morphogenesis, another function has recently been proposed for BTV NS1. Viral protein synthesis predominates over cellular translation shortly after infection of mammalian cells with BTV (HUISMANS 1979). Boyce *et al.* (2012) recently showed that BTV NS1 is a major contributor to this up-regulation of viral protein synthesis at the expense of host translation. NS1 up-regulates the expression of mRNA containing viral 5' and 3' untranslated regions (UTRs), and variation in the relative amounts of each viral protein could be correlated to variation in UTR sequence between the different genome segments. This up-regulation was also apparent in the replicating virus, where the effect of different cellular levels of NS1 on viral protein synthesis was tested on a BTV strain lacking the NS1 gene. The precise mechanism by which NS1 enhances translation of viral proteins is still unclear.

1.3.3 Other virus-encoded tubules

Whilst possible roles for NS1 in orbivirus trafficking, morphogenesis, viral gene expression, pathogenesis, assembly or egress have been suggested, its precise function has yet to be defined. This subsection describes the properties and functions of several virus-specified tubules in other viruses, however distantly related to AHSV.

Plant viruses often produce movement proteins (MPs) that facilitate intercellular transport of viral RNA or virus particles. Some of these MPs also form tubular structures. The viral tubules found within infected plants or their arthropod vectors appear to mediate dissemination of the virus, both within the environs of each infected cell and to distal tissues of the plant. Two main mechanisms whereby these MP tubules facilitate the spread of infection have been identified: tubule-mediated intercellular transport of either mature virions or viral nucleic acid.

Cowpea mosaic virus (CPMV) is a relatively well-characterised example of tubule-mediated transport of virions. Infected plant cells contain virus-specified tubules within the plasmodesmata through which CPMV particles are presumably transmitted to neighbouring cells. The tubules contain the CPMV 58K/48K movement and capsid proteins (VAN LENT *et al.* 1991). Several other viruses produce tubules with a similar function with requirements for various host factors. Cauliflower mosaic virus (CaMV) intercellular virus trafficking requires an intact endomembrane system (HUANG *et al.* 2000). Grapevine fanleaf virus (GFLV) MP also forms tubules via which virions are transported to neighbouring cells. In this case, a functional secretory pathway, but not cytoskeleton, is needed for tubulisation (LAPORTE *et al.* 2003). Rice dwarf virus (RDV), also of the family *Reoviridae*, is an arbovirus that infects plants and viruliferous leafhoppers. In addition to its other functions, Pns10, a RDV non-structural protein, forms tubules 85nm in diameter, containing virus particles (Fig. 1.6) and surrounded by a layer of host cell membrane (Fig. 1.6 A). Transport of virions via membrane-enveloped tubules could provide a method for the virus to evade host immunity.

The movement of these tubules into neighbouring cells is dependent on an interaction with actin-based filopodia (WEI *et al.* 2006). The endomembrane system and myosin motors are essential for Pns10 tubule formation in RDV infected insect cells, although actin and microtubules are not. Actin is required for protrusion of Pns10 tubules from the cell membrane, but microtubules are not required for either tubule formation or protrusion (WEI *et al.* 2008). In addition to mediating intercellular virus movement, Pns10 is also a suppressor of RNA silencing (REN *et al.* 2010).

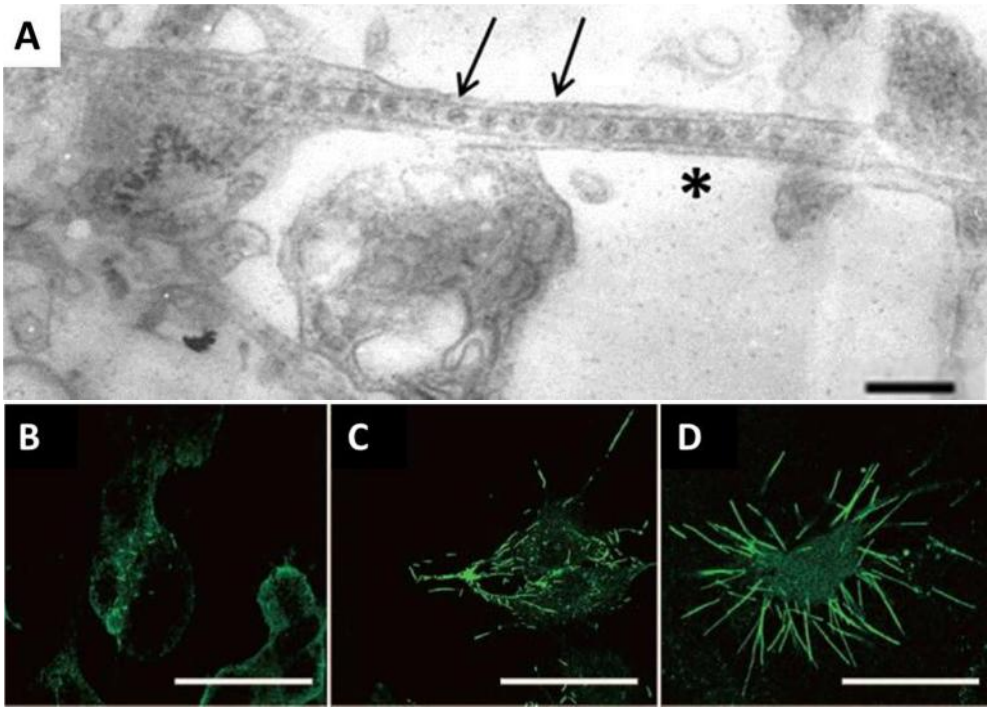

Figure 1.6. – A transmission electron micrograph of A: an RDV tubule (asterisk) transmitting virions to adjacent cells (WEI *et al.* 2006). Fluorescence micrographs depicting Pns10 distribution at B: 10 hpi, C: 14 hpi and D: 36 hpi, showing the progressive assembly and eventual protrusion of tubules from the cell surface (WEI *et al.* 2006). The scale bars are 300 nm in A and 25 µm in B-D.

The other type of transmission, which involves the spread of viral genetic material between adjacent cells, is a feature of tobacco mosaic virus (TMV) infection in plants. The TMV MP localises to plasmodesmata, where it increases their size exclusion limit to allow intercellular movement of the viral ssRNA genome (WOLF *et al.* 1989). The intercellular spread of infection appears to require intact filamentous actin and myosin, but is independent of microtubules (KAWAKAMI *et al.* 2004). The 35kDa MP of red clover necrotic mosaic virus (RCNMV) also traffics virus-specific RNA between cells via plasmodesmata, apparently by exploiting the putative macromolecule trafficking function of plasmodesmata (FUJIWARA *et al.* 1993).

Whether any functional similarity exists between plant virus tubules and NS1 tubules remains to be seen. The fact that the size of mature AHSV particles far exceeds the lumen diameter of AHSV NS1 tubules and the failure of NS1 to interact with nucleic acid (HUISMANS and ELS 1979) suggest that a role for NS1 tubules in mediating the intercellular spread of AHSV by similar mechanisms is unlikely.

1.4. NS4

Recent bio-informatic analysis of the genome segment of the members of the *Orbivirus* genus encoding the protein corresponding to AHSV VP6 (segment S9) revealed the presence of another AUG start codon in a generally strong Kozak context in all members but St Croix River Virus (SCRV). The predicted open reading frame (ORF) occurs in a different but overlapping reading frame with that of VP6. Amino acid conservation among serotypes was evident, suggesting functional constraints on the evolution of this ORF, which was initially named "ORFX". It was postulated that ORFX could be translated as a result of leaky scanning. The cognate peptide of BTV ORFX has a predicted size of approximately 9.5 kDa and perusal of past publications revealed several instances where this protein could conceivably have been present (FIRTH 2008).

It was recently shown that ORFX does in fact produce a previously unidentified protein upon infection with Great Island virus (GIV) or BTV, which was subsequently named NS4. Bioinformatic analysis of the NS4 sequences was undertaken to identify putative functional domains or analogues. The predicted proteins are rich in charged amino acids, mostly hydrophilic and range in size from 10-22.5 kDa. Amino acid conservation amongst orbivirus species ranges from 5-50%. Most orbivirus NS4 sequences showed similarity to dsRNA binding protein domains. SCRV lacks a putative NS4 due to the presence of a premature termination codon. This virus persistently infects ticks, but does not infect mammalian cells, which distinguishes SCRV from several other orbiviruses (BELHOUCHET *et al.* 2011).

BTV NS4 was predicted to be ± 10 kDa in size (BELHOUCHET *et al.* 2011) with a basic N-terminus and two predicted alpha helices and a conserved leucine zipper domain in the C-terminal alpha helix (RATINIER *et al.* 2011). BTV NS4 contains one putative nuclear localisation signal (NLS) with a cut-off score predictive of a dual nuclear and cytoplasmic localisation. It also contains regions reminiscent of a DUF (domain of unknown function) domain of the MetI/Arc repressor superfamily with a characteristic DNA-binding motif, although no dsRNA binding region was identified by bioninformatic analysis. BTV NS4 also resembles the fzo-mitofusin protein (putative transmembrane GTPase, coiled-coil) which mediates mitochondrial fusion, and protein family EMP24_GP25L, members of which are involved in transport from the ER and are related to the GOLD domain which is always observed along with lipid- or membrane-association domains. GIV NS4 resembles UTP20, a component of the U3 small nucleolar RNA (snoRNA) protein complex, which is involved in 18S rRNA processing (BELHOUCHET *et al.* 2011).

The predicted AHSV NS4 has a size of ± 17-20 kDa. AHSV NS4 shows homology to DUF domains that contain nucleic acid binding and/or modifying helical structures. Three potential overlapping NLSs with cut-off scores similar to that of the BTV NLS were identified in the predicted NS4 protein of AHSV (BELHOUCHET *et al.* 2011; FIRTH 2008).

Several experimental approaches were followed to determine whether NS4 of GIV and BTV possess the properties predicted by the bioinformatic analyses. Western blot analysis showed that NS4 is produced in

insect and mammalian cells infected with BTV, has a nuclear localisation pattern and is indeed non-structural since it does not form part of the virion (BELHOUCHET *et al.* 2011; RATINIER *et al.* 2011).

Confocal fluorescence microscopy of infected mammalian (BHK-21) cells showed that NS4 is already present from as early as 2-4 hpi. At 24 hpi, small cytoplasmic and nuclear aggregates are formed, and by 72 hpi, NS4 occurs less in the nucleus and more often near the cell membrane, suggesting a potential role in virus egress. An association with lipid droplets was confirmed with immunolabelling of NS4 and staining of cells with oil-red-O. The localisation of NS4 when expressed alone in mammalian cells approximates that observed within infected cells, although the lipid droplet association occurs more often. Furthermore, co-immunolabelling analyses showed a clear co-localisation of NS4 with the nucleolar markers fibrillarin (BELHOUCHET *et al.* 2011) and B23 (RATINIER *et al.* 2011), suggesting that NS4 localises to the nucleolus. Deletion mutagenesis of NS4-eGFP expressed in mammalian cells revealed the importance of the basic N-terminus for nuclear localisation (RATINIER *et al.* 2011). Nucleic acid protection assays showed that GIV NS4 binds dsRNA, but BTV NS4 does not. The NS4 proteins of both viruses bind dsDNA (BELHOUCHET *et al.* 2011). Overall, the experimental results were consistent with the properties predicted by bioinformatic analysis.

Ratinier *et al.* (2011) also used a reverse genetics system to investigate the role of NS4 during viral replication. NS4 null mutant BTV strains based on BTV-1 and BTV-8 were generated by means of a plasmid-based reverse genetics system. No difference in replication efficiency was observed between wild type and NS4 null mutant strains *in vitro* in BSR, C6/36, BFAE, CPT-Tert and KC (*Culicoides* cells) as assessed by virus titration assays of infected cell supernatants at various times post infection, which showed that BTV NS4 is not required for viral replication. To determine whether NS4 could play a role in viral replication in cells in an interferon-induced antiviral state, CPT-Tert cells were treated with two types of interferon (IFNT and UIFN) before being infected with BTV-1, BTV-8 or the NS4 deletion mutant BTV strains. In BTV-8, the presence of NS4 increased the yield of virus and cell death as analysed with titration and crystal violet staining, respectively. This effect was not observed in BTV-1 and was specific to the BTV-8 genetic background. The virulence of BTV-1, BTV-8 and NS4 deletion mutants was proven in a mouse model. The authors speculate that NS4 may be involved in the interaction between the virus and the host immune response.

1.5. Concluding remarks

The current evidence concerning the function of BTV NS1 during the viral replication cycle suggests that it could be of particular importance during viral morphogenesis, egress and pathogenesis. Therefore, identifying the exact function of NS1 could have profound implications for the understanding of orbivirus molecular biology as well as the development of measures to control the disease. Since very little comparable data regarding AHSV NS1 is available, an investigation of the intracellular distribution, dynamics of tubule bundle assembly and interactions of NS1 with other AHSV proteins was undertaken in

this study. This could provide a valuable intermediate step towards the eventual functional characterisation of AHSV NS1.

Analyses of the recently discovered non-structural protein NS4 in BTV showed that it localises to the nucleolus of infected cells and could be involved in modulating the host innate immune response to infection, although its exact function has not yet been determined. A closer examination of the putative AHSV homologue could advance the current understanding of the AHSV replication cycle substantially. The first step towards such characterisation of the putative AHSV NS4 protein would entail the determination of the expression status of NS4 in AHSV-infected cells and an experimental corroboration of its bio-informatically predicted properties. This is the other aim of the current study. Once this information is available, a more elaborate inquiry into the function of NS4 during viral replication may be justified.

1.6. Objectives

The aim of this study was to characterise the properties of AHSV NS1 tubules to facilitate the eventual determination of their function, and furthermore to preliminarily characterise the putative non-structural AHSV protein NS4, in order to justify more elaborate analysis of its function during viral replication. The following objectives were addressed:

- Describing the intracellular distribution of NS1 at different times after infection.
- Determining whether NS1 co-localises with other AHSV proteins during infection.
- Determining whether the putative NS4 protein of AHSV is translated during infection.
- Describing the intracellular distribution of AHSV NS4 at different times after infection.
- Determining whether AHSV NS4 possesses the predicted nucleic acid binding activity.

Chapter 2:
Intracellular distribution and co-localisations of AHSV non-structural protein NS1.

2.1 Introduction

The AHSV non-structural protein NS1 is highly conserved across all AHSV and BTV serotypes and its cognate mRNA is most efficiently transcribed relative to its length of all viral proteins within BTV infected cells. Although its function is still unclear, the overexpression and high degree of conservation of NS1 suggest that it performs an important function during the viral replication cycle.

NS1 spontaneously assembles into tubular structures that form groups or bundles, reminiscent of cytoskeleton intermediate filaments, that are characteristic of orbivirus infection, although their structural features differ among orbiviruses (MAREE and HUISMANS 1997; VAN STADEN *et al.* 1998). Certain critical regions and residues for tubulisation of BTV NS1 have been identified (Monastyrskaya *et al.* 1994; Monastyrskaya *et al.* 1995). Early in infection, BTV NS1 tubules occur near viral inclusion bodies (VIBs, where RNA synthesis and core assembly occur, are formed by NS2), core-like particles (CLPs) and virus-like particles (VLPs), either in groups of tubules or with no regular orientation. These co-localisations might suggest a role for NS1 in viral morphogenesis (Eaton *et al.* 1988). At later times after infection, the tubules occur throughout the cytoplasm in significant quantities (HUISMANS and ELS 1979). BTV NS1 tubules apparently also associate with the core structural proteins (VP3 and VP7) and cytoskeletal intermediate filaments (EATON *et al.* 1987a; HYATT and EATON 1988). More recently, an interaction between BTV NS1 and non-structural protein NS3/NS3A, has been reported. This suggests that NS1 may also be involved in virus transport or egress (OWENS *et al.* 2004), since NS3 plays an important role in controlling the mode of viral egress (VAN STADEN *et al.* 1998). Another recent study found that NS1 preferentially up-regulates the expression of viral proteins compared to cellular proteins (BOYCE *et al.* 2012).

The intracellular distribution and possibility of interactions between AHSV NS1, VP3 and VP7 have not yet been studied. Further characterization of AHSV NS1 regarding its intracellular localisation dynamics, as well as its interactions with other viral proteins, could assist the eventual elucidation of the function of NS1 during viral replication. The aim of this part of the study was to characterise the intracellular distribution of AHSV NS1 at various stages after infection, and to study its co-localisation with other AHSV proteins, with an initial focus on structural proteins VP3 and VP7. This was achieved by means of confocal- and transmission electron microscopic analyses of cells infected with AHSV and cells expressing recombinant NS1 in combination with VP3 or VP7.

2.2 Materials and methods

2.2.1 Cell culture and protein analysis

2.2.1.1 Antisera

The antisera used during this study are listed in Table 2.1. Polyclonal antisera against NS1 and VP3 (Complete Affinity-Purified Peptide pAb Package (Rabbit), catalogue number: SC1031) were produced by

the company GenScript USA (Inc). The peptide antigens for NS1 and VP3 were based on amino acid sequence analysis; a region conserved across all 9 serotypes with appropriate hydrophilic and antigenic properties was selected, synthesised, conjugated and used as immunogen in rabbits. Affinity purified antibody that was provided in lyophilised form by GenScript was resuspended in deionised water to the original concentration of the antiserum before lyophilisation, as per the supplier's instructions. All antibodies were diluted in blocking buffer comprising 1% (w/v) milk powder in 1 x PBS (phosphate buffered saline: 137 mM NaCl, 2.7 mM KCl, 10 mM Na_2HPO_4, 1.8 mM KH_2PO_4, pH 7.4).

To preabsorb polyclonal antisera in order to reduce background interaction with wild type baculovirus proteins, a monolayer of Sf9 cells (obtained from the American Type Culture Collection) grown in a 75 cm^2 flask was infected with wild type baculovirus at a multiplicity of infection (MOI) of 5, harvested and collected by centrifugation at 3500 rpm for 15 minutes at 4°C. Cells were resuspended in 0.5-1 mL of 1% blocking buffer and lysed by passage through a 29G needle. The antiserum was added to the lysate at a final dilution of 1:20 and incubated with agitation at room temperature for three hours. The mixture was centrifuged at 4000 rpm for 10 minutes at 4°C. The supernatant was retained for use as a preabsorbed antiserum and frozen at – 20°C for long term storage.

Table 2.1. – A summary of the antisera used, describing the animal of origin and antigens used. The peptide antigens are shown in the N-terminal to C-terminal orientiation.

Name	Origin	Description	Antigen
Anti-NS1	Rabbit	Affinity purified IgG	VLDGRDLTVLEDET, representing residues 489-502.
Anti-VP3	Rabbit	Affinity purified IgG	HMRKKIVRRVRAPD, representing residues 856-869.
Anti-VP7	Guinea pig	Anti-VP7-177-FMEpi	Soluble baculovirus expressed VP7-177-FMEpi (VP7 with a foot and mouth disease virus epitope inserted at amino acid residue 177), sarkosyl treated and removed.
Anti-AHSV	Rabbit	Clift and Penrith (2010)	Partially purified AHSV-9 virus particles.

2.2.1.2 Baculovirus stocks

The baculoviruses used during this study are described in Table 2.2. Sf9 cell monolayers in 75 cm^2 flasks were infected at a MOI of ± 0.1-1, harvested at 7-10 dpi and collected by centrifugation at 3500 rpm for 15 minutes at 4°C. The supernatant was filtered and retained for use as a virus stock solution. The cell pellet was resuspended in hypotonic buffer (10 mM Tris, 0.2 mM $MgCl_2$, pH 7.4) and lysed by passage through a 29G needle for use during SDS-PAGE (sodium dodecyl sulphate polyacrylamide gel electrophoresis) and Western blot analyses. All baculovirus stocks were titrated following the instructions for the viral plaque assay in the Bac-to-Bac® Baculovirus Expression Systems manual (Life Technologies). Briefly, Sf9 cells

seeded on 4% (w/v) agarose gel in 6-well plates were infected with eight-log serial dilutions of the baculovirus stock. The inoculum was replaced with plaquing overlay and the plates were incubated until plaques became visible (4-10 days). If necessary, the plaques were stained with a 0.1% (w/v) solution of Neutral Red. The titre in plaque forming units per mL (pfu/mL) was calculated with the following formula: pfu/ml (of original stock) = 1/dilution factor × number of plaques × 1/(ml of inoculum/plate). The Bac-VP3 virus was provided by Shani Bekker and Gideon de Jager (Department of Genetics, University of Pretoria).

Table 2.2. – A summary of the baculoviruses used during the study.

Name	Description
Bac-wt	Wild type baculovirus
Bac-NS1	Recombinant baculovirus containing the wild type AHSV-6 NS1 gene (LACHEINER 2006).
Bac-NS1-eGFP	Recombinant baculovirus containing the AHSV-6 NS1 gene with the eGFP gene inserted between amino acids 472 and 473 (LACHEINER 2006).
Bac-VP3	Recombinant baculovirus containing the wild type AHSV-4 VP3 gene.
Bac-VP7	Recombinant baculovirus containing the wild type AHSV-9 VP7 gene (MAREE *et al.* 1998).

2.2.1.3 Baculovirus plaque purification

Original baculovirus stock solutions were subjected to the viral plaque assay according to the manufacturer's instructions (Bac-to-Bac® Baculovirus Expression Systems manual, Life Technologies), but not stained with Neutral Red, and single plaques were picked and resuspended in serum-free TC100 Insect medium (Highveld Biological). The resuspended plaques were used to inoculate 6-wells of Sf9 cell monolayers, which were harvested at 7-10 dpi when significant cytopathic effect (CPE) was observed, centrifuged at 3500 rpm for 15 minutes at 4°C, lysed and analysed with SDS-PAGE or Western blotting as described in section 2.2.1.6. The supernatant of the selected plaque was then amplified for use as a baculovirus stock solution as described in section 2.2.1.2.

2.2.1.4 Protein expression with the baculovirus system

Sf9 cells were grown in monolayers in 24-wells, 6-wells, 25 cm^2 or 75 cm^2 flasks containing TC100 Insect medium with 10% foetal calf serum (FCS), 1% Pluronic F-68 (Sigma) and a mixture of antibiotic and antimycotic agents (100 U/ml penicillin, 0.1 mg/ml streptomycin and 2.4 µg/ml fungizone) was used. Cells were infected with baculovirus stock solutions at a MOI of 10 for Bac-VP3 and a MOI of 5 for all other baculoviruses and incubated for 24-72 hours at 28°C. Cells in wells were incubated with 90% humidity. Cells were harvested and concentrated by centrifugation at 3500 rpm for 15 minutes at 4°C, resuspended in hypotonic buffer and lysed by passage through a 29G needle. Samples were analysed with SDS-PAGE or Western blotting as described in section 2.2.1.6.

2.2.1.5 Infecting cells with AHSV

BSR mammalian cells (derived from baby hamster kidney cell line, BHK-21) were cultured in monolayers in 24-wells, 6-wells or 25 cm^2 flasks using Eagle's Minimal Essential Medium (EMEM, Lonza) containing 5% FCS, non-essential amino acids (NEAA) and antibiotics. Cells were infected by replacing the medium with serum-free EMEM and AHSV-3 (M322/97), AHSV-3 (13/63), AHSV-4 (Jane) #4 or AHSV-6 at a MOI of 0.1-3 and incubation for one hour at 37°C with 5% carbon dioxide (CO_2) and 90% humidity. The medium containing AHSV was replaced with serum-free EMEM containing NSAA and antibiotics and incubated under the same conditions for 2-48 hours at 37°C. Cells were harvested and centrifuged at 3500 rpm for 15 minutes at 4°C, resuspended in 1 x PBS or hypotonic buffer (10 mM Tris, 0.2 mM $MgCl_2$, pH 7.4) and lysed with a 29G needle for analysis with SDS-PAGE or Western blotting. KC (*Culicoides variipennis)* cell monolayers, grown in a mixture of 50% Insect-XPRESS medium with L-Glutamine (Lonza) and 50% TC100 Insect medium (Highveld Biological) containing 5% FCS, NEAA and antibiotics, were infected at a MOI of 0.1-1 without replacing the medium. Cells in well plates were incubated at 28°C in the presence of 5% CO_2 with 90% humidity.

2.2.1.6 SDS-PAGE and Western blot analysis

Polyacrylamide gels consisted of a layer of stacking gel containing 5% polyacrylamide (from a 30% acrylamide/0.8 % bisacrylamide solution) in stacking gel buffer (125 mM Tris, 0.1% sodium dodecyl sulphate (SDS), pH 6.8) and a layer of separating gel containing 8-15% polyacrylamide in separating gel buffer (375 mM Tris, 0.1% SDS, pH 8.8). The 30% acrylamide/0.8 % bisacrylamide was polymerised with 0.01% ammonium persulphate and 0.01% TEMED (tetramethylethylenediamine). Protein samples were electrophoresed in 1 x TGS buffer (25 mM Tris, 192 mM glycine, 0.1% SDS, pH 8.5) at 90-120 V and 250 mA for 1.5-4 hours. Protein samples from cell lysates were denatured at 94°C for 5-10 minutes in the presence of 1 x PSB (protein solvent buffer: 0.67 M Tris, 6.7% SDS, 10% glycerol and 5% 2-mercaptoethanol). PageRuler™ Prestained Protein Ladder (Fermentas), High Range Rainbow Molecular Weight Marker RPN755 (Amersham Biosciences) or Precision Plus Protein™ All Blue Standards were used as molecular weight markers. After electrophoresis, gels were incubated in Coomassie Brilliant Blue for 15 minutes, rinsed three times in water, submerged overnight in destain solution (5% methanol, 5% acetic acid) and visualised with the GelDoc™ XR+ Imaging System (Bio-Rad).

For Western blotting, the proteins were transferred from the gel after electrophoresis to a nitrocellulose membrane (Hybond™-C Extra, Amersham Biosciences) in transfer buffer (25 mM Tris, 192 mM glycine, 20% methanol, pH 8.3) for one hour at 100 V and 400 mA. The non-specific antibody binding sites were blocked by incubation of the membrane in blocking solution (1-2% milk powder in 1 x PBS) for 30-60 minutes. The membrane was incubated overnight with agitation in primary antibody in blocking solution at a 1:50 or 1:100 dilution. The primary antibody was detected colorimetrically with 4-chloro-1-naphthol (Sigma

Aldrich) and horseradish peroxidase (HRP)-conjugated protein A (1:10 000, Calbiochem®) and visualised with the GelDoc™ XR+ Imaging System (Bio-Rad).

2.2.2 Transmission electron microscopy

2.2.2.1 High-pressure freezing and freeze substitution

Infected cell monolayers in 25 cm^2 flasks were harvested by mechanically dislodging the adhered cells from the flask with a cell scraper and centrifuging the cell suspensions at 1000 rpm for 5 minutes. Approximately 0.5-1 µL of the wet cell pellet was placed on gold plated specimen carriers coated with phosphatidylcholine and frozen to -196°C in 10 ms (milliseconds) at 2 000 bar using methylcyclohexane as hydraulic fluid with the Leica EM PACT2 high pressure freezer as described by Studer *et al*. (2001). Samples were subjected to freeze substitution with 1% water in ethanol using the Leica AFS2 apparatus to increase the temperature of the samples logarithmically from -90°C to 0°C within a period of 72 hours. Following freeze substitution, the samples were washed three times with 100% ethanol.

2.2.2.2 Resin embedding and ultramicrotomy

Following high-pressure freezing and freeze-substitution (HPF-FS), washed cells were embedded in LR White resin (SPI Supplies) according to the manufacturer's instructions. Briefly, the frozen cells were dislodged from the sample carriers and submerged in a solution containing 50% ethanol and 50% resin for 0.5-1 hour at room temperature. The mixture of resin and ethanol was replaced with 100% resin and the cells were incubated at room temperature for 4 hours. The resin was replaced with fresh LR White and polymerised at 60°C for approximately 24 hours. Cells embedded in resin were sliced into 100 nm sections with a diamond knife (Diatome) using the Reichert Jung Ultracut E microtome and placed on 200 mesh copper grids.

2.2.2.3 Immunogold labelling

Sectioned cells on copper grids were placed on droplets of blocking buffer consisting of 1 x PBS with 5% FCS and 0.05% Tween® 20 (Sigma-Aldrich) for 1.5 – 2 hours and incubated on droplets of primary antibody diluted 1:100 to 1:200 in blocking buffer for 1.5 – 2 hours. The cells were washed by two 2 minute long incubations each on droplets of blocking solution and 1 x PBS before incubation on droplets of secondary antibody (10 nm gold particle conjugated goat anti-rabbit or anti-guinea pig affinity isolated IgG, Sigma-Aldrich®) diluted 1:20 or 1:30 in blocking buffer for one hour. Grids were washed again and dried before staining with 1% uranyl acetate and Reynolds lead citrate. Samples were visualised with a JEOL 2100F field emission transmission electron microscope.

2.2.3 Confocal microscopy

2.2.3.1 Fixing and immunolabelling cells

Cells were seeded on 22 mm^2 coverslips in 6-well plates or 12 mm round coverslips in 24-well plates. Sf9 cells that were not immunolabelled were washed once for 2-5 minutes in 1 x PBS, fixed in ice cold 50% methanol: 50% acetone for 2 minutes, washed again in 1 x PBS, mounted on microscope slides with VectaShield mounting medium (Vector Laboratories) before the edges of the coverslips were sealed with glue.

For immunolabelling, Sf9 cells were washed twice for 2-5 minutes in 1 x PBS, fixed as described above and washed again for 2-5 minutes. BSR cells were washed once for 2-5 minutes in 1 x PBS, fixed with 4% paraformaldehyde (PFA) for 40 minutes and permeabilised with 0.2% Triton® X-100 (Merck Millipore) in 1 x PBS for 10 minutes. Thereafter, both Sf9 and BSR cells were incubated in blocking solution (5% milk powder in 1 x PBS) for 30 minutes and incubated overnight in primary antibody diluted 1:50 or 1:100 in 1% blocking solution. Cells were washed three times for 2-5 minutes in wash buffer containing 0.05% Tween® 20 (Sigma-Aldrich) in 1 x PBS and incubated with secondary antibody tagged with Alexa Fluor® (Invitrogen) at a 1:100 or 1:250 dilution or fluorescein isothiocyanate (FITC, Sigma-Aldrich) at a 1:100 dilution in 1% blocking buffer for one hour. Cells were again washed two or three times in washing buffer and twice in 1 x PBS. If nuclei were stained with DAPI (4',6-diamidino-2-phenylindole, Life Technologies), the cells were incubated in 5 mg/mL DAPI diluted 1:1000 in 1% blocking buffer for 10 minutes and washed once with 1 x PBS. Coverslips were mounted on microscope slides in VectaShield mounting medium and the edges sealed with glue to prevent sample dessication. Samples were viewed with a Zeiss LSM510 Meta Laser Scanning Confocal Microscope.

2.3 Results

2.3.1 The intracellular localisation of NS1

The intracellular localisation of NS1 in AHSV-infected cells, or in cells expressing recombinant NS1, was investigated in order to obtain a clearer understanding of how NS1 is distributed within the cell throughout the infection cycle and to provide a basis for determining whether NS1 co-localises with other viral proteins.

2.3.1.1 Obtaining recombinant baculoviruses expressing NS1, NS1-eGFP and VP3

In order to study the intracellular localisation of NS1 and to determine whether NS1 co-localises with other AHSV proteins, recombinant baculoviruses expressing wild type NS1, NS1-eGFP and VP3 were required. Recombinant baculovirus stocks expressing NS1 and NS1-eGFP were available (LACHEINER 2006), but did not express large amounts of recombinant protein. In order to obtain pure stock solutions that expressed NS1 and NS1-eGFP more efficiently, these original virus stocks were subjected to plaque purification. The

original stock solutions were titrated to obtain single plaques, which were picked and used to infect Sf9 cells. Lysates of the infected Sf9 cells were analysed with SDS-PAGE to identify a suitable plaque for further amplification. Unique bands of the expected sizes could be seen in the samples infected with Bac-NS1 (62 kDa) and Bac-NS1-eGFP (90 kDa) plaques (Fig. 2.1, Fig. 2.2). The levels of recombinant NS1 expressed by the original stocks could not be detected with SDS-PAGE and Coomassie brilliant blue staining (Fig. 2.1, lane 4), which suggests that the original stock strains were genetically heterogeneous with respect to recombinant protein expression. Bac-NS1 Plaque 2 (Fig. 2.1, lane 6) and Bac-NS1-eGFP Plaque 4 (Fig. 2.2, lane 7) were selected for amplification to stock scale.

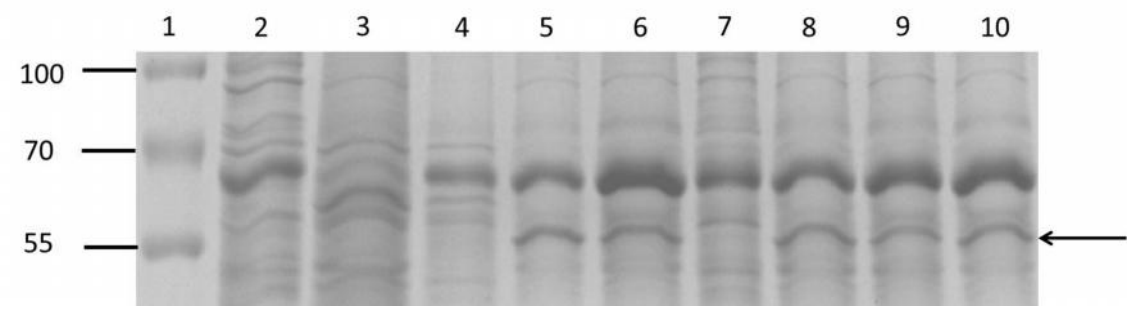

Figure 2.1. – SDS-PAGE analysis of Sf9 cells infected with individual plaques from a Bac-NS1 stock. Lane 1: Molecular marker (sizes in kDa). Lane 2: mock infected cells. Lane 3: wild type baculovirus infected cells. Lane 4: cells infected with the original Bac-NS1 stock. Lanes 5-10: cells infected with plaques 1 through 6. The position of NS1 is indicated (arrow).

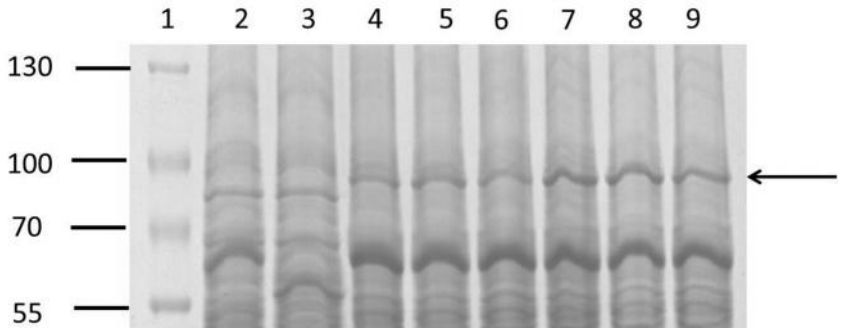

Figure 2.2. – SDS-PAGE of Sf9 cells infected with individual plaques from a Bac-NS1-eGFP stock. Lane 1: Molecular marker (sizes in kDa). Lane 2: mock infected cells. Lane 3: wild type baculovirus infected cells. Lanes 4-9: cells infected with plaques 1 through 6. The position of NS1-eGFP is indicated (arrow).

In order to confirm the identities of the proteins expressed by the amplified baculovirus strains, Sf9 cells infected with each baculovirus stock solution were subjected to Western blotting with anti-NS1 serum. Both NS1 and NS1-eGFP were detected with high specificity and sensitivity and a more intense band was present in the sample containing NS1-eGFP compared to NS1, suggesting that NS1-eGFP was expressed more efficiently than NS1 (Fig. 2.3).

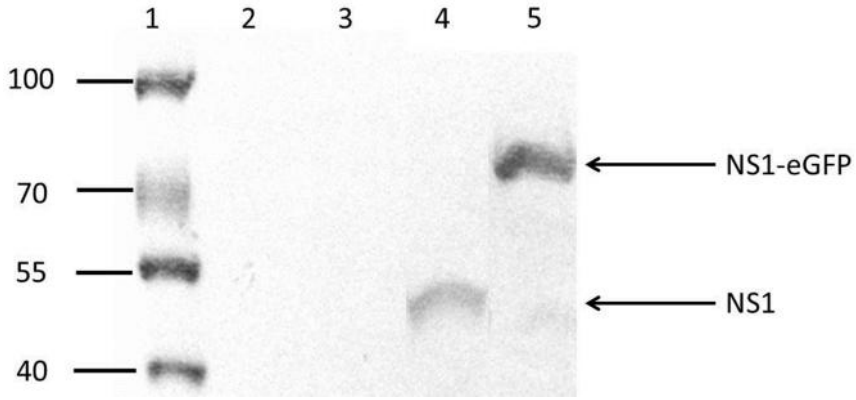

Figure 2.3. – Western blot of baculovirus-infected Sf9 cells labelled with anti-NS1. Lane 1: molecular marker (sizes in kDa). Lane 2: mock infected cells. Lane 3: wild type baculovirus infected cells. Lane 4: Bac-NS1 infected cells. Lane 5: Bac-NS1-eGFP infected cells.

A plaque purified Bac-VP3 strain was supplied by Shani Bekker and Gideon de Jager (Department of Genetics, University of Pretoria) and the expression of VP3 by the Bac-VP3 stock was confirmed by means of Western blot analysis using a polyclonal antibody against VP3 (GenScript), which clearly detected a unique band (Fig. 2.4). Recombinant baculovirus stocks expressing high levels of NS1, NS1-eGFP, VP3 and VP7 were therefore available for use during subsequent analyses.

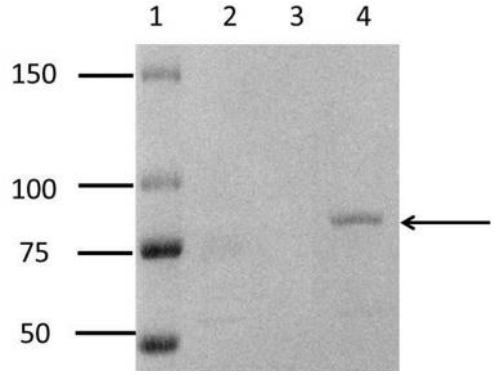

Figure 2.4. – Western blot analysis of Sf9 6-wells infected with Bac-VP3 labelled with anti-VP3. Lane 1: molecular marker (sizes in kDa). Lane 2: mock infected cells. Lane 3: wild type baculovirus infected cells. Lane 4: cells infected with the Bac-VP3 stock. The expected position of VP3 is indicated (arrow).

The co-expression efficiency of NS1, VP3 and VP7 in infected cells was also analysed, since this would be required during studies of the co-localisation of NS1 with VP3 and VP7. Sf9 cells seeded in 6-wells were co-infected with different combinations of Bac-NS1, Bac-VP3 and Bac-VP7 and analysed with SDS-PAGE. Bands of 100 kDa (VP3), 62 kDa (NS1) and 38 kDa (VP7) were seen in each corresponding infection and co-infection (Fig. 2.5), which confirmed that the three proteins could be expressed by cells in the same well.

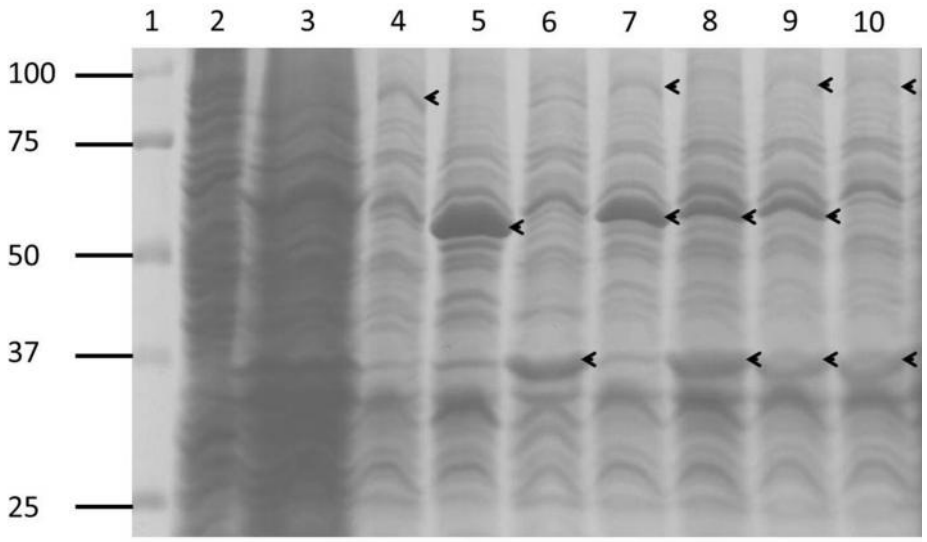

Figure 2.5. –SDS-PAGE analysis of Sf9 cells co-expressing NS1, VP3 and/or VP7 and stained with Coomassie brilliant blue. Lane 1: Molecular marker (kDa). Lane 2: mock infected cells. Lane 3: wild type baculovirus infected cells. Lane 4: cells expressing VP3. Lane 5: cells expressing NS1. Lane 6: cells expressing VP7. Lane 7: cells expressing NS1 and VP3. Lane 8: cells expressing NS1 and VP7. Lane 9: cells expressing NS1, VP3 and VP7. Lane 10: cells expressing VP3 and VP7. Arrowheads indicate the positions of NS1, VP7 and VP3.

2.3.1.2 Confocal microscopy of AHSV-infected BSR and KC cells

In order to define the localisation of NS1 in the context of AHSV infection in mammalian cells, BSR cells were infected with AHSV-3 and subjected to fixing and immunolabelling for confocal microscopy with anti-NS1 at 2, 4, 6, 18, 24 and 48 hours post infection (hpi) (Fig. 2.6). Nuclei were stained with DAPI (4',6-diamidino-2-phenylindole). Small foci could be seen from as early as 2 hpi. These foci became larger as infection progressed and were of variable shape, ranging from almost spherical to completely linear. Each focus was not always uniformly fluorescent, but appeared to consist of overlapping non-parallel striae in several instances. Fluorescence was more intense and occurred in most cells by 48 hpi, sometimes occupying a large part of the cytoplasm within an infected cell by 48 hpi. No fluorescence was observed in the nucleus or cell membrane. This distribution was consistent with that of NS1 tubule bundles.

To determine whether NS1 localises differently in AHSV-infected insect cells, KC cells were infected with AHSV-6 and subjected to immunolabelling with anti-NS1 at 1, 3, 5, 8 or 10 days post-infection (dpi) (Fig. 2.7). Both FITC (fluorescein isothiocyanate) and Alexa Fluor 488 conjugated IgG antibodies were tested for secondary labelling. It was possible to obtain well-resolved, clearly labelled images of single cells at 5 dpi, but not at 3 dpi or 1 dpi. At 8 dpi or 10 dpi, overgrowth of the cells often prohibited the resolution of single cells. At 5 dpi, elongated fluorescent foci occurred in the cytoplasm of most visualised cells (Fig. 2.7 B). These fluorescent foci could correspond to NS1 tubule bundles. Unfortunately, confocal microscopy with KC cells was poorly repeatable due to the tendency of these cells to rapidly overgrow. Infecting cells at various multiplicities of infection, fixing cells at different times, seeding cells at 50% rather than 90% density prior

to infection and immunolabelling with a range of primary and secondary antibody dilutions were of no avail. Alexa Fluor 488 yielded slightly better labelling quality compared to FITC (compare Fig. 2.7 C and F). In addition, the small size of these cells limits the detail with which the intracellular distribution of NS1 could be described.

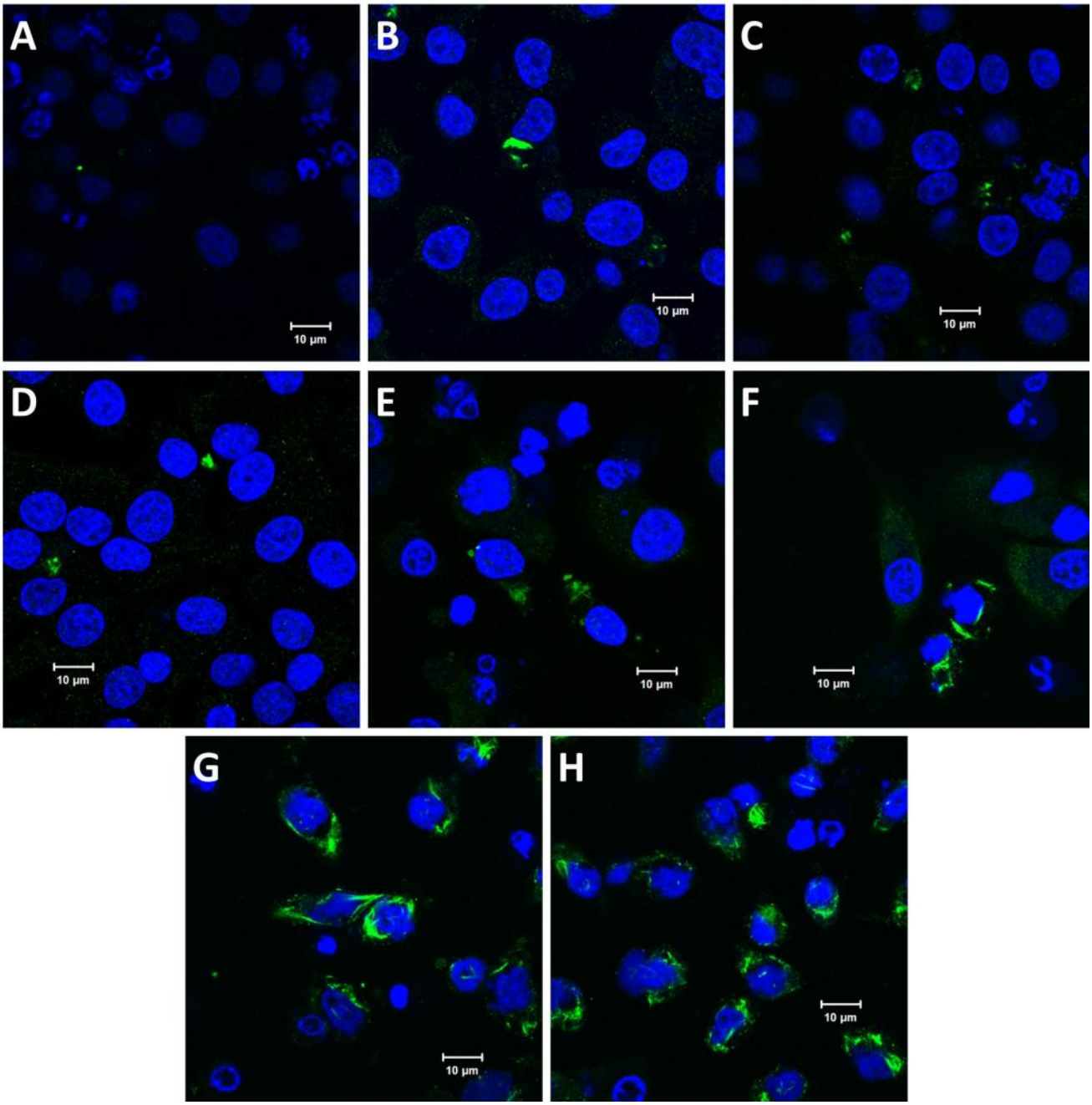

Figure 2.6. – BSR cells infected with AHSV-3 and immunolabelled with anti-NS1 at different times post infection. Alexa Fluor 488-conjugated IgG (green) was used for secondary labelling and nuclei were stained with DAPI (blue). A: mock infected cells. B: 2 hpi. C: 4 hpi. D: 6 hpi. E: 18 hpi. F: 24 hpi. G-H: 48 hpi.

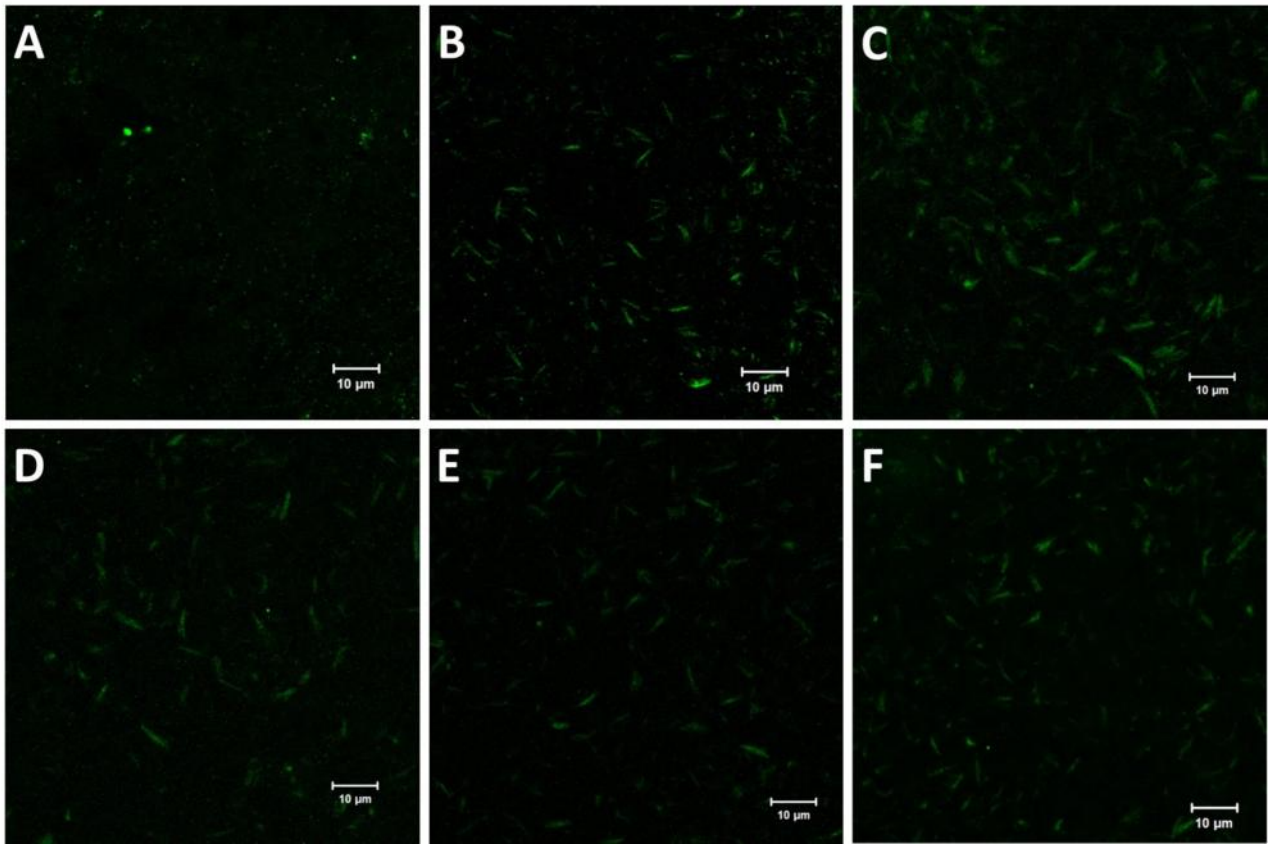

Figure 2.7. – KC cells infected with AHSV-6 and immunolabelled with anti-NS1 at different times post infection. Alexa Fluor 488 (A-E) or FITC-conjugated IgG (F) was used for secondary labelling. A: Mock infected cells. B: 5 dpi. C: 8 dpi D: 10 dpi and E: 10 dpi. F: 8 dpi.

2.3.1.3 Confocal microscopy comparing the distribution of NS1 and NS1-eGFP

The use of NS1-eGFP as a surrogate for wild type NS1 would have many benefits, including eliminating the need for immunolabelling of NS1 during confocal microscopy studies of interactions between NS1 and other viral proteins. Therefore, the intracellular distributions of NS1 and NS1-eGFP were compared to determine whether NS1-eGFP has a similar localisation to wild type NS1 at different times post infection, and also to study the localisation dynamics of NS1 when expressed in the absence of other viral proteins. Sf9 cells were infected with Bac-NS1 (Fig. 2.8) or Bac-NS1-eGFP (Fig. 2.9) and fixed at 18, 24, 30, 48 and 72 hpi. Cells infected with Bac-NS1 were labelled with anti-NS1 and either FITC- or Alexa Fluor- conjugated secondary antibody at a 1:100 or 1:250 dilution.

Initially, low levels of NS1 were seen throughout the cell, with small foci dotting the cytoplasm in some cells (Fig. 2.8 A, Fig. 2.9 A). The foci gradually became larger and fewer in number (Fig. 2.8 B-C, Fig. 2.9 B-D), eventually forming large fluorescent foci across the cytoplasm. By 72 hpi, a substantial part of the cytoplasm of infected cells was occupied by NS1-eGFP foci (Fig. 2.8 D-E, Fig. 2.9 E-F). The foci were roughly spherical, but not uniform in shape or size. Small spike-like protrusions were visible at the edges of some NS1-eGFP foci, and these thread-like striae could occasionally be seen alone (Fig. 2.9 D). These fluorescent foci could possibly correspond to NS1 tubule bundles or aggregates. Baculovirus expressed NS1 and NS1-

eGFP were far more abundant within Sf9 cells than NS1 in AHSV-infected cells, probably because of the high level of recombinant protein expression seen in the baculovirus expression system. NS1-eGFP was more intensely fluorescent than immunolabelled NS1 at the same times after infection, which could be the result of limitations on immunolabelling, or differences in protein expression between Bac-NS1 and Bac-NS1-eGFP. This is consistent with the lower levels of NS1 detected with Western blotting compared to NS1-eGFP and the difference in fluorescence intensity could therefore be due to differences in expression or a combination of both factors. Secondary immunolabelling with Alexa Fluor 633 conjugated antibodies appeared to be more sensitive than labelling with FITC-conjugated IgG (Fig. 2.8). Mock and wild-type baculovirus-infected cells exhibited acceptably low levels of background fluorescence (not shown). Z-stack analysis of infected cells confirmed that no fluorescence occurred in the nucleus (Fig. 2.10, sections 6-10).

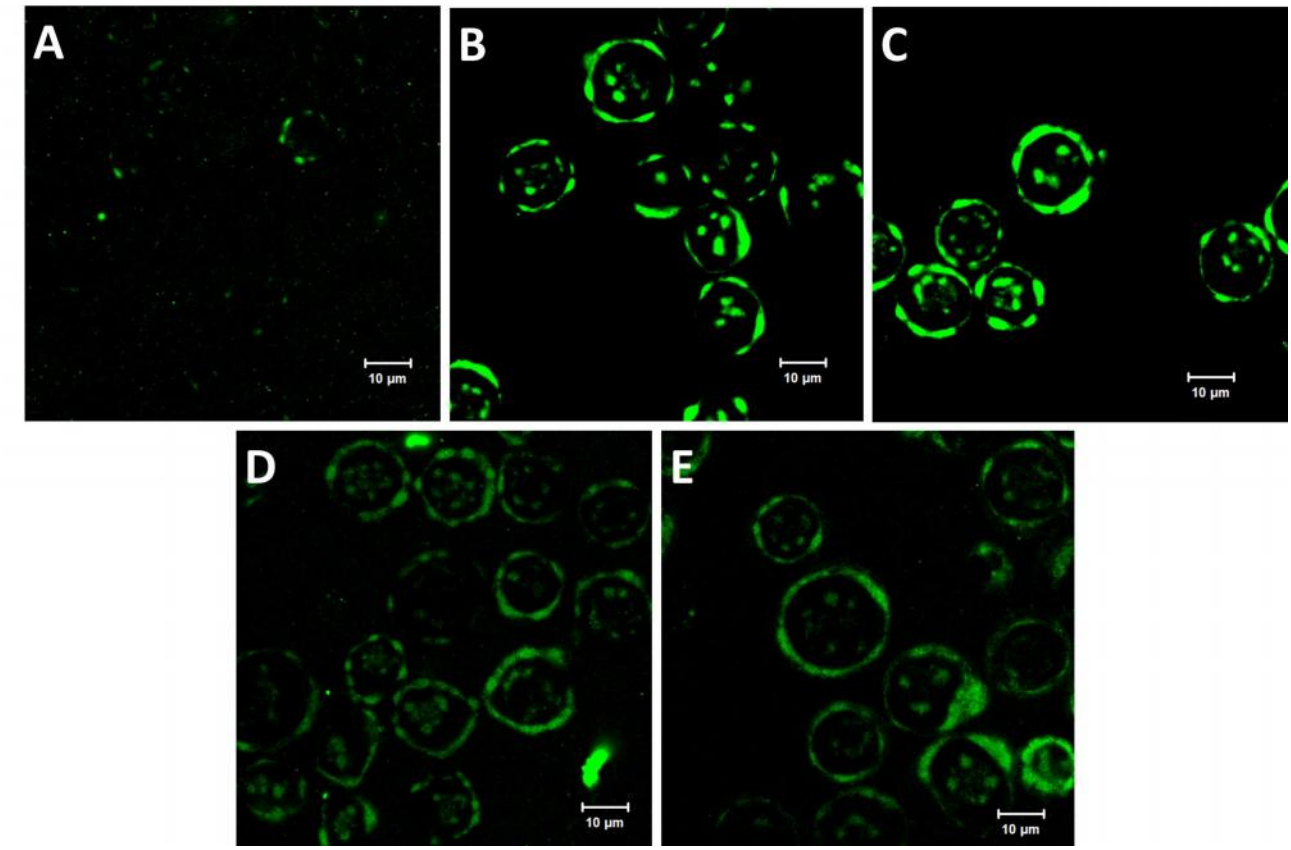

Figure 2.8. – Confocal laser scanning micrographs of Sf9 cells infected with Bac-NS1 and immunolabelled with anti-NS1 at different times after infection. Alexa Fluor 488 (A and D), Alexa Fluor 633 (B-C) or FITC-conjugated IgG (E) was used for secondary labelling. A: 30 hpi. B-C: 48 hpi. D-E: 72 hpi. The normally red fluorescence in B-C was coloured green for ease of comparison.

Overall, the data suggested that the distribution of NS1-eGFP mimics that of NS1 at all stages post infection and that NS1-eGFP can be used as a reliable surrogate for NS1 during confocal microscopic investigations of the interaction between NS1 with VP3 and VP7.

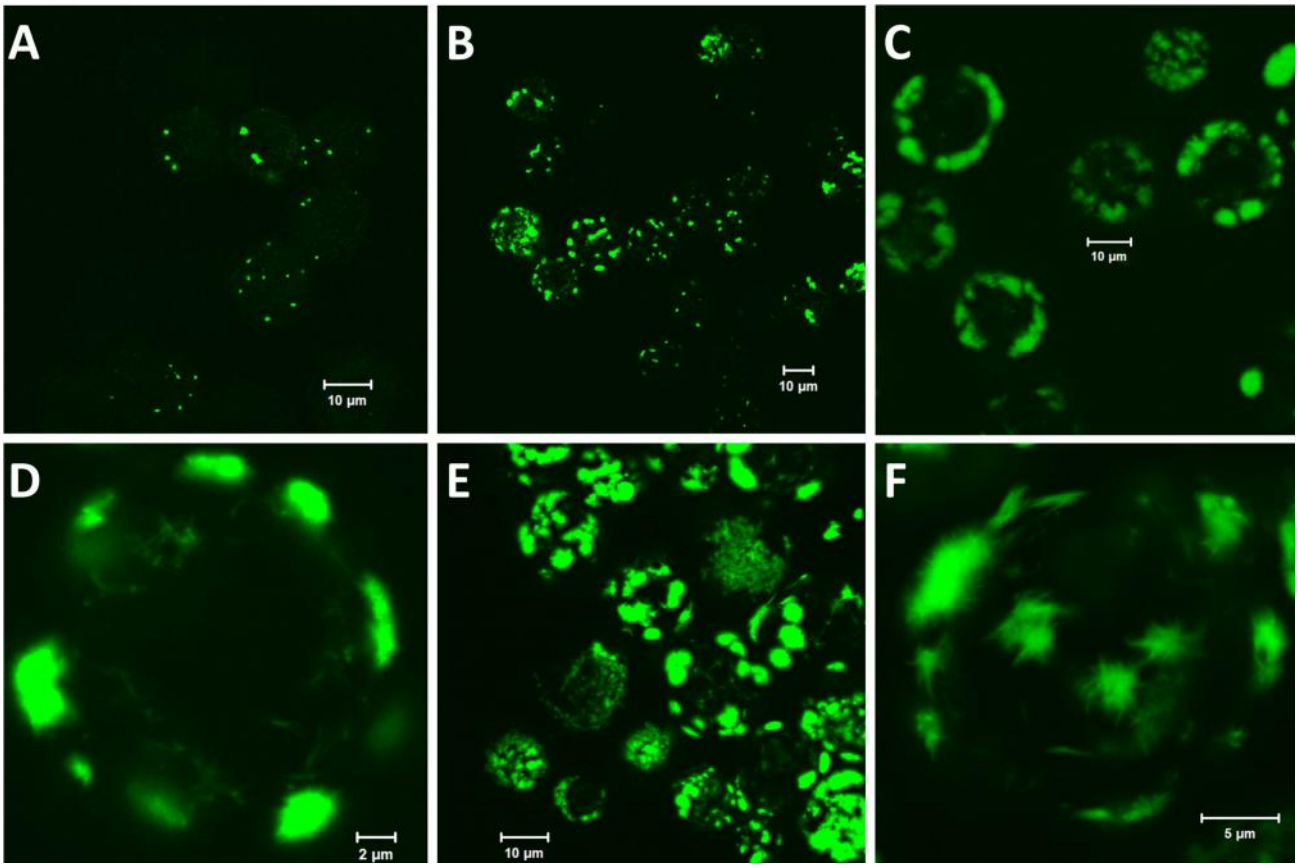

Figure 2.9. – Confocal scanning laser micrographs of Sf9 cells infected with Bac-NS1-eGFP and fixed at different times post-infection. A: 18 hpi. B: 24 hpi. C-D: 48 hpi. E-F: 72 hpi.

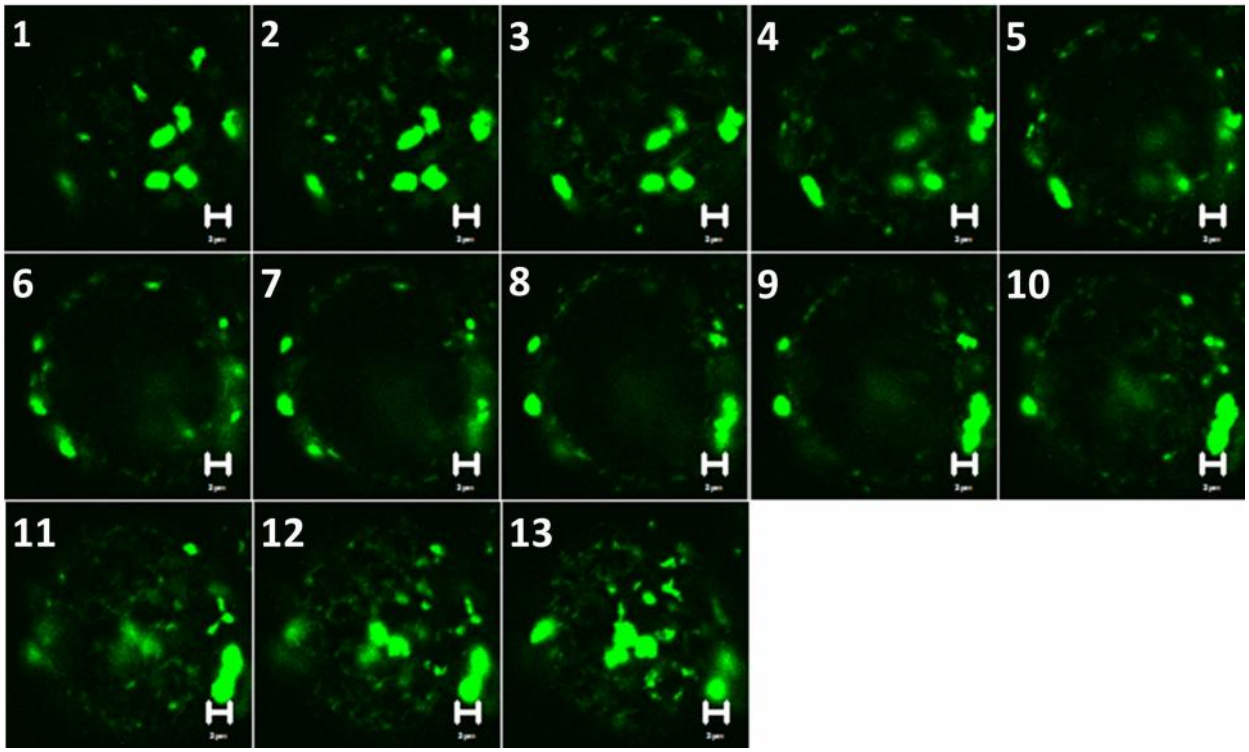

Figure 2.10. – Z-stack image series of a cell expressing NS1-eGFP visualised with confocal microscopy at 48 hpi. Scale bars represent 2 µm.

2.3.1.4 Examining the distribution of NS1 in AHSV-infected cells at a high resolution

In order to study the structure of native NS1 tubules at a high resolution, BSR and KC cells were infected with AHSV-3 and fixed for transmission electron microscopy (TEM) with high-pressure freezing and freeze substitution (HPF-FS) at 48 hpi and 10 dpi respectively. Following embedding in LR White resin, ultrathin sections of cells were immunogold labelled with anti-NS1 and visualised. Samples were stained with uranyl acetate and lead citrate in instances where higher contrast was required.

The previously described virus-specific structures (BURROUGHS *et al.* 1994; HUISMANS and ELS 1979; UITENWEERDE *et al.* 1995) could be seen in AHSV infected KC cells, including paracrystalline arrays (PCAs), VP7 crystalline particles, individual virus particles, viral inclusion bodies (VIBs) and NS1 tubules (Fig. 2.11). These structures were also seen in ASHV infected BSR cells (not shown). This confirmed that the cells had been infected. Virus-specific structures were occasionally seen within endosomal type structures in AHSV infected KC cells (Fig. 2.11 C and E).

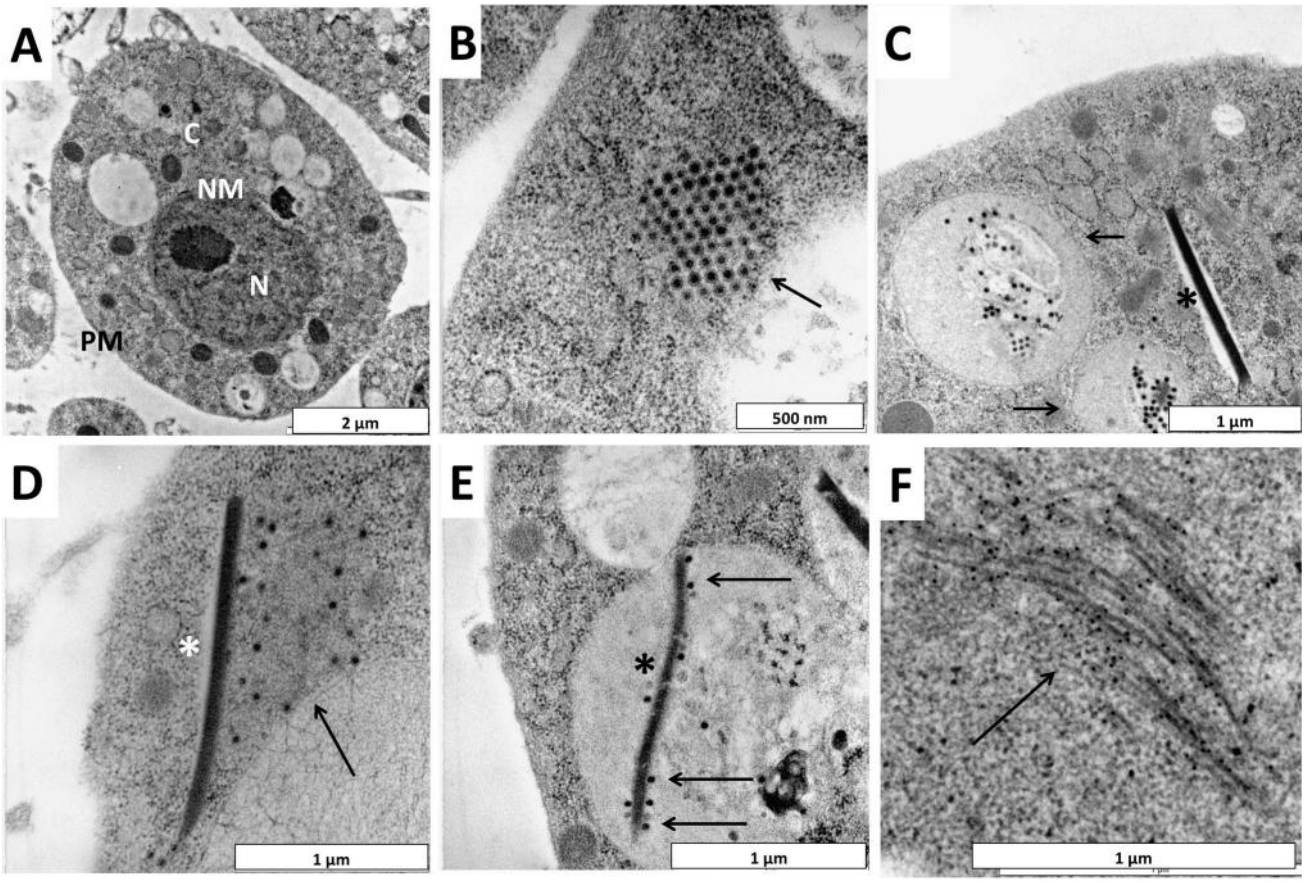

Figure 2.11. – TEM of KC cells infected with AHSV-3 showing AHSV infection-related structures. A: Mock infected cells. B-F: AHSV-3 infected cells. Arrows indicate B: a paracrystalline array of virus particles. C: endosomal type structures containing virions. D: a VIB. E: virus particles adjacent to a VP7 crystalline particle within an endosomal type structure. F: an NS1 tubule bundle immunogold labelled with anti-NS1. Asterisks indicate VP7 crystalline particles. N indicates the nucleus, NM the nuclear membrane, C the cytoplasm and PM the plasma membrane.

Uninfected cells had intact nuclear and plasma membranes and were devoid of background labelling and virus specific structures (Fig. 2.11 A, Fig. 2.12 A). Tubule bundles were labelled clearly and specifically and occurred abundantly in the cytoplasm of infected cells. Tubule bundles in KC (Fig. 2.11 F) and mammalian cells (Fig. 2.12 B) were morphologically similar, consisting of individual tubules arranged in parallel to each other. The tubule bundles had a similar distribution to the fluorescent foci seen in infected BSR and KC cells visualised with confocal microscopy. Tubule bundles often occupied a large part of the cytoplasm and were of variable length, ranging from a few hundred nanometres to nearly the length of the infected cell. The tubules each had a diameter of ± 21 nm and were occasionally observed individually.

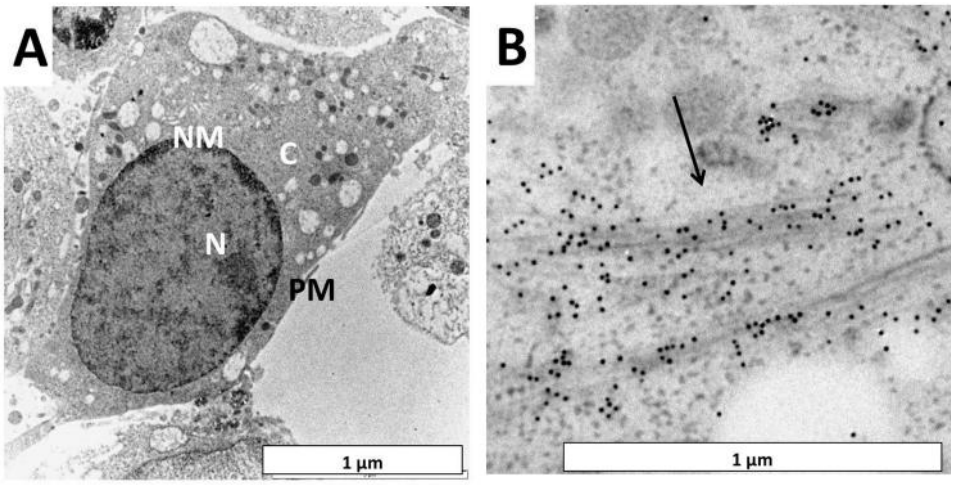

Figure 2.12. – TEM of AHSV-3 infected BSR cells immunogold labelled with anti-NS1 and 10 nm gold particle-conjugated secondary antibody. A: Mock infected cell. B: AHSV-3 infected cell. N indicates the nucleus, NM the nuclear membrane, C the cytoplasm and PM the plasma membrane. The arrow indicates an NS1 tubule bundle.

2.3.1.5 Comparison of wild type NS1 with NS1-eGFP at a high resolution

The distribution of recombinant NS1 in the absence of other viral proteins was next examined, including a comparison of the structure and distribution of NS1 and NS1-eGFP tubules. Sf9 cells were infected with recombinant baculoviruses expressing these proteins, subjected to HPF-FS at 48 hpi, embedded in LR White resin and sectioned. Ultrathin sections were immunogold labelled with anti-NS1 and gold particle-conjugated IgG and stained with uranyl acetate and lead citrate.

Sf9 cells are round or ovoid in shape and have large nuclei that are further enlarged upon infection with baculovirus, which replicates within the nucleus. The nucleus is surrounded by a narrow layer of cytoplasm. Mock infected cells did not show significant levels of background labelling (Fig. 2.13 A). Infected cells contained baculovirus specific structures such as fibrous structures formed by protein P10 (Fig. 2.13 B). Both NS1 and NS1-eGFP formed morphologically similar ± 21 nm diameter tubules within recombinant baculovirus infected cells that were immunogold labelled clearly (Fig. 2.13). These tubules converged with a random orientation with respect to each other to form loose aggregates. Approximately four to ten

aggregates could be seen within each section, which is consistent with observations made with confocal microscopy when taking into account the fact that only a small part of the cell can be visualised with TEM, whereas the entire cell can be seen with confocal microscopy. No significant amount of labelling was seen elsewhere within infected cells. In conjunction with the data obtained during confocal microscopic examination of cells expressing NS1 and NS1-eGFP, this shows that no NS1 protein could be detected in an untubulised form, which suggests that NS1 polymerises immediately after synthesis and could exist in an unpolymerised form only at quantities below the detection levels of these methods.

Although individual tubules resembled those seen in AHSV-infected cells, tubule bundle structure differed markedly from the neat tubule bundles seen in AHSV-infected KC and BSR cells. The distribution of NS1-eGFP resembled that of NS1 and the disorganised tubule bundles appeared to correspond to the fluorescent foci seen in Sf9 cells viewed with confocal microscopy. The addition of eGFP near the C-terminus of NS1 does not appear to interfere with NS1 tubulisation or trafficking *in vitro*. The data supported the use of NS1-eGFP as a surrogate for wild type NS1 for studying the co-localisation of NS1 with other AHSV proteins.

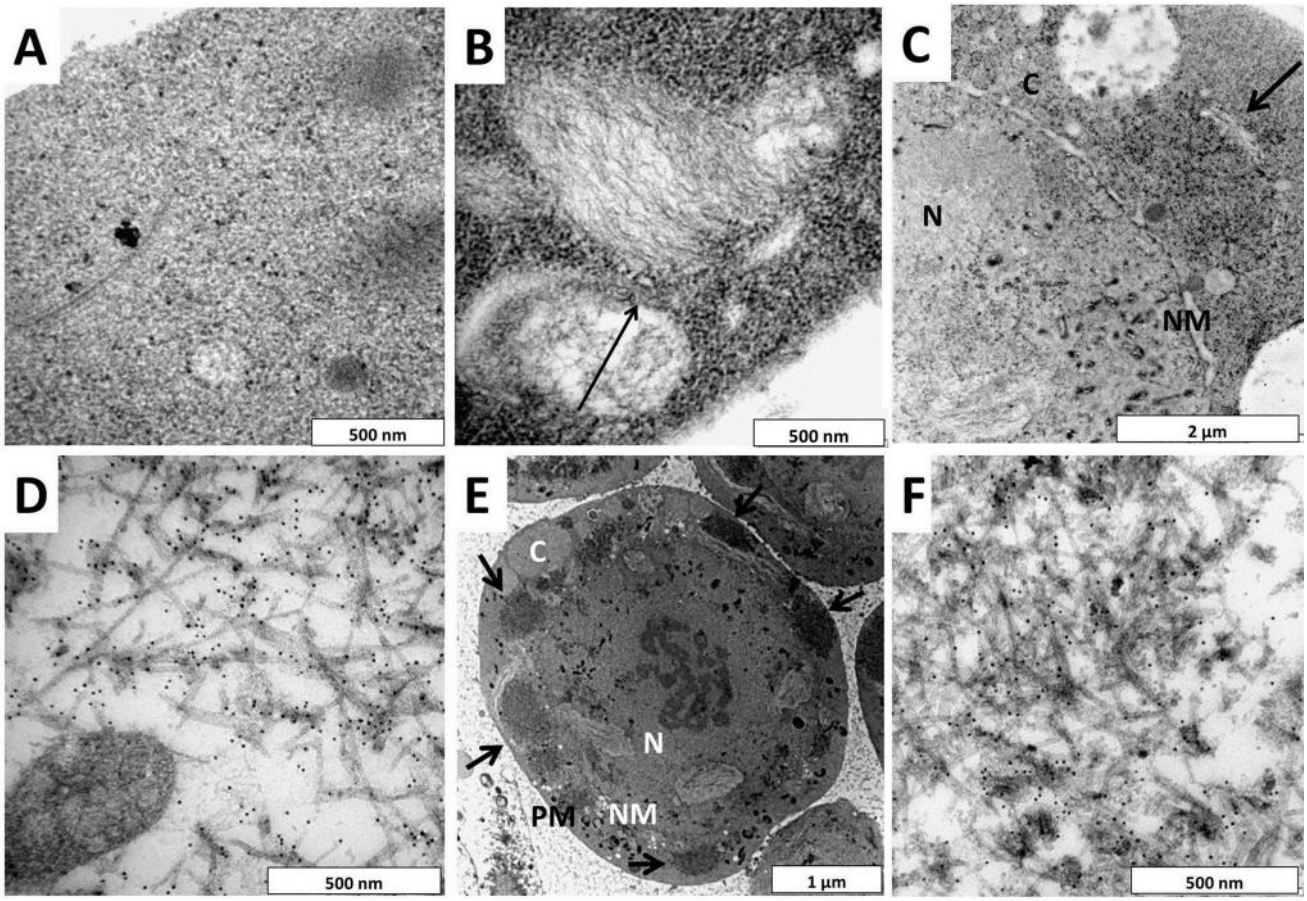

Figure 2.13. – Transmission electron micrographs comparing NS1 and NS1-eGFP in baculovirus infected Sf9 cells. Samples were immunogold labelled with anti-NS1 and gold conjugated IgG and stained with uranyl acetate and lead citrate. A: Mock infected cells. Cells were infected with B: Wild type baculovirus. C-D: Bac-

NS1. E-F: Bac-NS1-eGFP. Arrows indicate NS1 tubule bundles. N denotes the nucleus, NM the nuclear membrane, C the cytoplasm and PM the plasma membrane. The arrows indicate cytoplasmic NS1 tubule bundles.

2.3.2 Co-localisation of NS1 with other AHSV proteins

In order to investigate whether NS1 co-localises with other viral proteins, specifically VP3 and VP7, cells infected with AHSV were co-immunolabelled with anti-NS1, anti-VP3 or anti-VP7 and subjected to both confocal microscopy and TEM analysis. To determine whether NS1 co-localises with VP3 and VP7 in the absence of other AHSV proteins when overexpressed, Sf9 cells infected with recombinant baculoviruses co-expressing NS1 with VP3 or VP7 were also examined with confocal microscopy and TEM.

2.3.2.1 Confocal microscopy of the localisation of NS1, VP3 and VP7 in AHSV-infected cells

To determine whether NS1 and VP7 co-localise in AHSV-infected cells, BSR cells were infected with AHSV-3, fixed at 48 hpi and co-immunolabelled with anti-NS1 and anti-VP7. Alexa Fluor 488 (green) and Alexa Fluor 633 (red) conjugated IgG were used for secondary labelling of NS1 and VP7, respectively.

No red or green background fluorescence was detected in mock infected cells. The green fluorescence with a distribution characteristic of NS1 tubule bundles could be seen. Red fluorescent structures with hexagonal or rod-like shapes were seen in infected cells. This distribution is typical of AHSV VP7, which forms hexagonal crystalline particles within infected cells (BURROUGHS *et al.* 1994); rod-like shapes represent cross-sections through the flat hexagonal particles. NS1 and VP7 were often seen within the same cell, which would be expected during AHSV infection. However, co-localisation between NS1 and VP7 was extremely rare (Fig. 2.14). Therefore, NS1 and VP7 do not appear to co-localise within AHSV infected mammalian cells.

BSR cells were infected with AHSV-3 or AHSV-4 at a MOI of 1 and labelled with anti-VP3 at dilutions of 1:50 or 1:100 and Alexa Fluor 633 at a dilution of 1:100, but only very low levels of fluorescence could be detected (not shown). At a 1:100 dilution of anti-VP3, no fluorescence could be detected in AHSV-3 infected cells. VP3 could not be immunolabelled successfully. This is consistent with SDS-PAGE with Coomassie staining (not shown) and Western blot analyses of Sf9 cells expressing VP3 (Fig. 2.4, section 2.3.1.1); only small amounts of VP3 were detected with these methods, which suggests that VP3 is expressed at low levels in these cells. Low expression in combination with low antibody sensitivity could be responsible for the inability to label VP3 in recombinant baculovirus infected Sf9 cells. Because VP3 could not be immunolabelled for confocal microscopy, it is not clear whether NS1 and VP3 co-localise within infected mammalian cells.

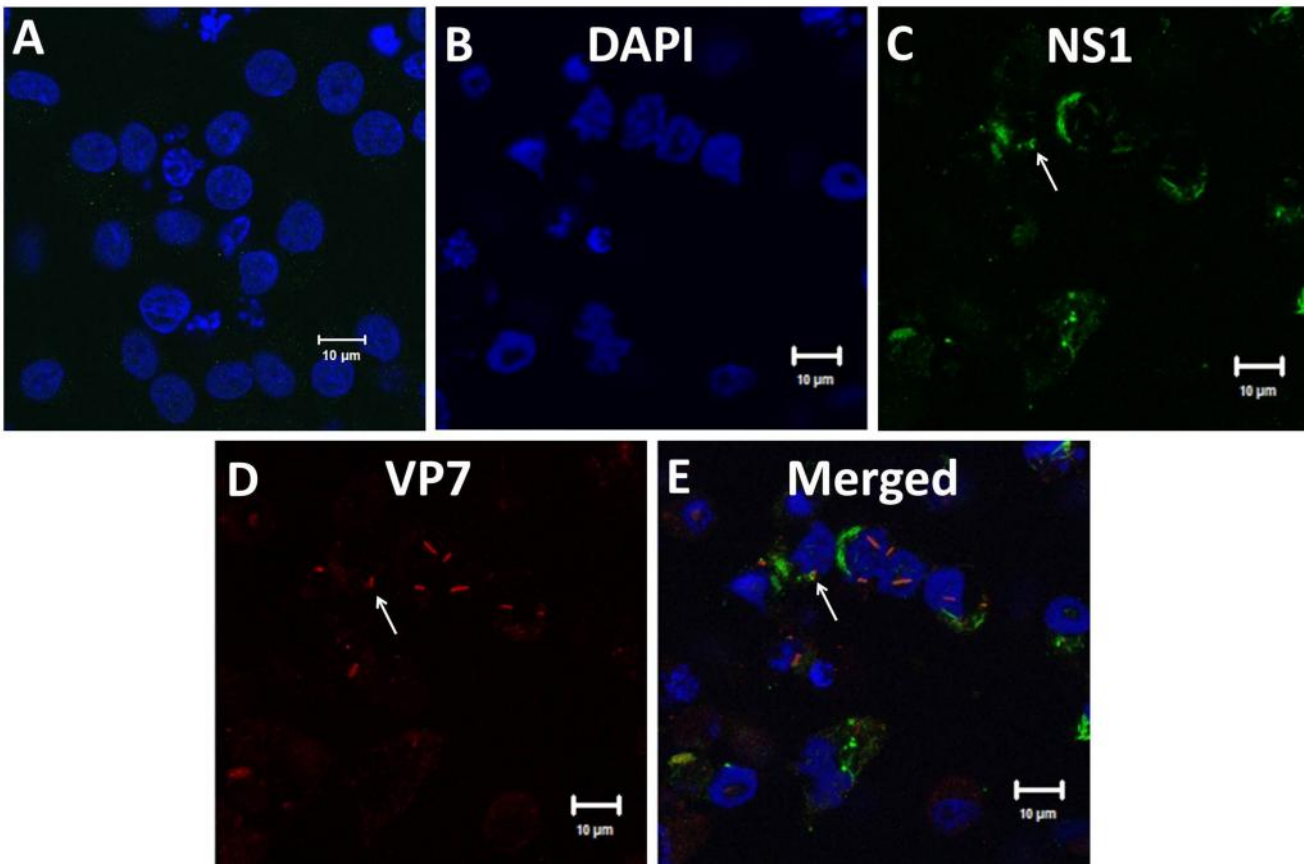

Figure 2.14. – Confocal microscopy of AHSV-3 infected BSR cells at 48 hpi. Cells were co-immunolabelled with anti-NS1 with Alexa Fluor 488 (green) and anti-VP7 with Alexa Fluor 633 (red). A: mock infected cells. B-E: AHSV-3 infected cells with fluorescence shown individually and merged. The arrow indicates a putative co-localisation between NS1 and VP7.

2.3.2.2 Confocal microscopy of Sf9 cells co-expressing NS1 and VP7

Confocal microscopy of Sf9 cells overexpressing NS1 and VP7 in the absence of other AHSV proteins was undertaken to determine whether a co-localisation could occur under these conditions. Sf9 cells were infected with Bac-NS1-eGFP and Bac-VP3 or Bac-VP7. Cells were fixed at 40 hpi or 48 hpi and immunolabelled with anti-VP3 or anti-VP7 antibody and Alexa Fluor 633 IgG as secondary antibody. The use of NS1-eGFP, which autofluoresces, would require single labelling of only VP3 or VP7 compared to using NS1, which would require double immunolabelling. This reduces the amount of optimisation required and could also enable more efficient co-immunolabelling of VP3 and VP7 if required.

During confocal microscopic analyses of the localisation of NS1-eGFP and VP3 (not shown), no fluorescence was observed in mock infected cells labelled with anti-VP3. However, the same red fluorescence pattern was initially observed in cells infected with wild type baculovirus and those expressing VP3. Only low levels of red fluorescence could be seen. Since at least some of this fluorescence appeared to be a cross-reaction of the anti-NS1 antibody with baculovirus proteins, the anti-VP3 serum was preabsorbed with a wild type baculovirus infected cell lysate. Following preabsorption, however, only negligible amounts of red

fluorescence could be detected in cells infected with Bac-VP3. Therefore, VP3 could not be reliably detected with confocal microscopy, probably due to the apparently low levels of VP3 expression which were also seen in AHSV-infected BSR cells. However, it is also possible that VP3 is expressed, but the antiserum does not detect it efficiently. This is supported by Western blot analysis of Bac-VP3 infected Sf9 cells (section 2.3.1.1), which showed that some VP3 is expressed in these cells. Therefore, although the expression of VP3 could not be verified, during co-localisation studies with NS1-eGFP and VP7, in addition to cells co-expressing the latter two proteins, some cells were infected with Bac-NS1-eGFP, Bac-VP7 and Bac-VP3 in order to determine whether the presence of VP3 might affect the localisation patterns of NS1-eGFP and VP7. This enabled an indirect preliminary investigation of a possible interaction between NS1 and VP3 despite the lack of a reliable serum against VP3.

During the investigation of the localisation patterns of NS1 and VP7, no red or green fluorescence was detected in mock-, Bac-VP3 or wild type baculovirus infected cells immunolabelled with anti-VP7 (Fig. 2.15 A-C). Only green fluorescence resembling the characteristic NS1-eGFP foci was detected in cells expressing NS1-eGFP alone (Fig. 2.15 D) or with VP3 (Fig. 2.15 E), and only red fluorescence, including hexagonal or rod-like shapes, was seen in cells expressing VP7 alone (Fig. 2.15 F). Therefore, the anti-VP7 serum with which the cells were labelled detected only VP7 and did not cross-react significantly with any baculovirus or other AHSV proteins. Immunolabelling of Sf9 cells expressing NS1-eGFP and VP7 with anti-VP7 revealed an interesting localisation pattern (Fig. 2.15 G-H). When cells co-expressed NS1-eGFP and VP7, both red and green fluorescence was observed. However, although the distribution of NS1-eGFP remained unchanged, the characteristic crystalline structures of VP7 were observed less frequently and VP7 more frequently appeared to co-localise with NS1 tubule bundle foci, forming a ring-like shape around each green fluorescent focus. This was observed in most co-infected cells. The addition of VP3 to these co-infected cells did not seem to affect the apparent co-localisation of NS1 and VP7, although the presence of VP3 could not be corroborated immunologically (not shown). Therefore, NS1-eGFP and VP7 appear to co-localise in the absence of other AHSV proteins when overexpressed in Sf9 cells.

Because of the unexpected co-localisation pattern between NS1-eGFP and VP7, experiments were also conducted where wild type NS1 was co-labelled with VP7 in cells co-expressing NS1 with VP3 and/or VP7 to determine whether this co-localisation pattern resulted from the addition of eGFP to the NS1 protein. Indeed, the co-localisation pattern seen in cells co-expressing NS1-eGFP and VP7 was not observed in cells co-expressing NS1 and VP7 (Fig. 2.16). NS1 formed the same fluorescent foci seen previously and VP7 formed hexagonal and rod-like shapes both when expressed individually and within the same cell. Co-localisations between NS1 tubule bundles and VP7 crystalline particles were only seen in a small subset of co-infected cells; although the two proteins often occurred within the same cell, they were only very rarely observed in close proximity (Fig. 2.16 G-J). This is consistent with confocal microscopy data of AHSV-infected BSR cells (section 2.3.2.1). Again, the co-expression of VP3 with NS1 or NS1-eGFP and VP7 did not

alter the distribution patterns of NS1 or VP7. Collectively, these results suggest that wild type NS1 does not interact with VP7, but that the insertion of eGFP near the C-terminus of NS1 induces a co-localisation between NS1-eGFP and VP7 that alters the distribution pattern of VP7 by an unknown mechanism.

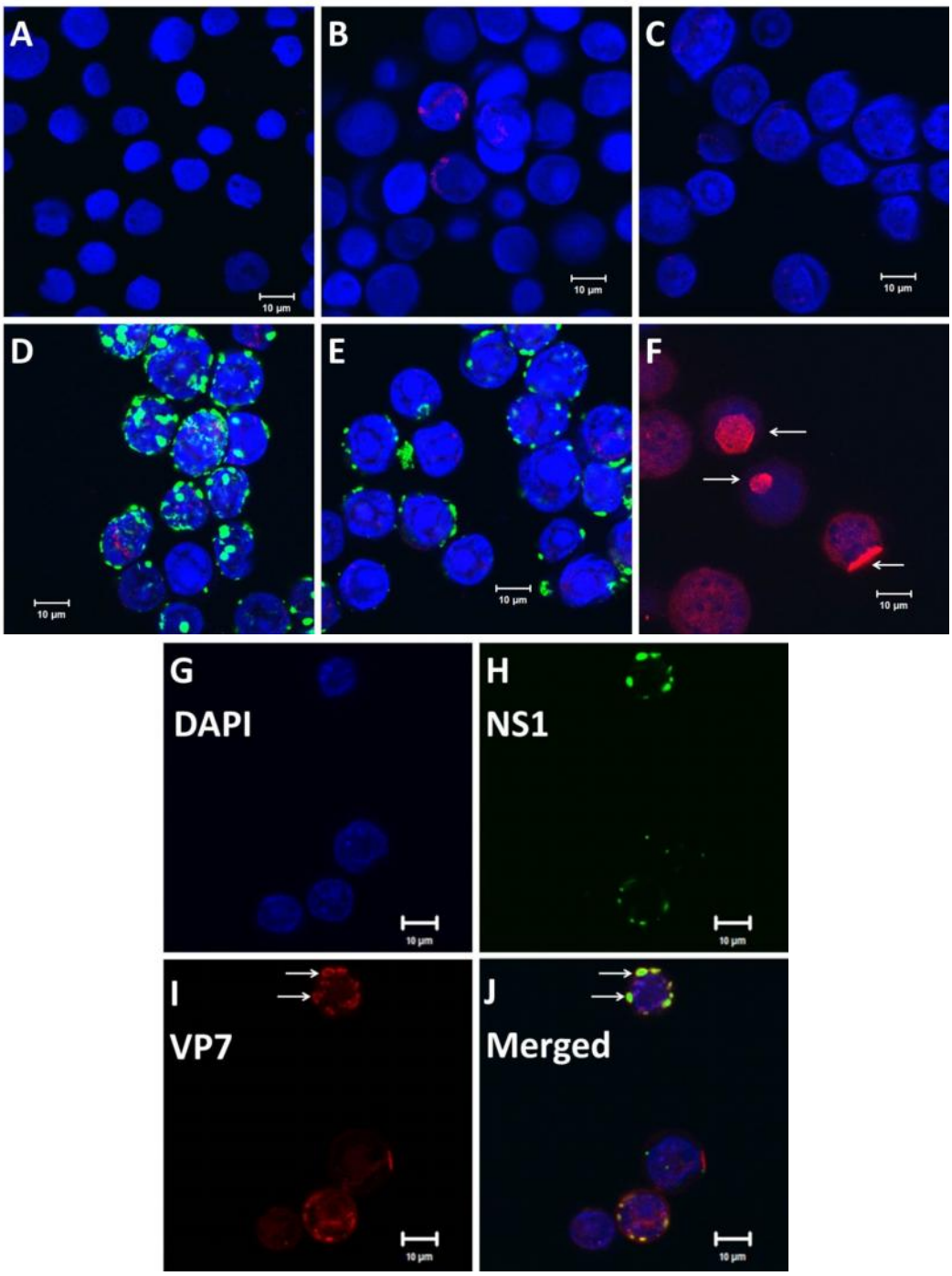

Figure 2.15. – Confocal microscopy of Sf9 cells expressing NS1-eGFP and VP7. Cells were labelled with anti-VP7 and Alexa Fluor 633 (red). A: mock infected cells. Cells were infected with B: wild type baculovirus. C: Bac-VP3. D: Bac-NS1-eGFP. E: Bac-NS1-eGFP and Bac-VP3. F: Bac-VP7. G-J: Bac-NS1-eGFP and Bac-VP7 with fluorescence shown individually and merged. I: Bac-NS1-eGFP, Bac-VP7 and Bac-VP3. The VP7 crystalline particles (F) and putative co-localisations (I-J) are indicated with arrows.

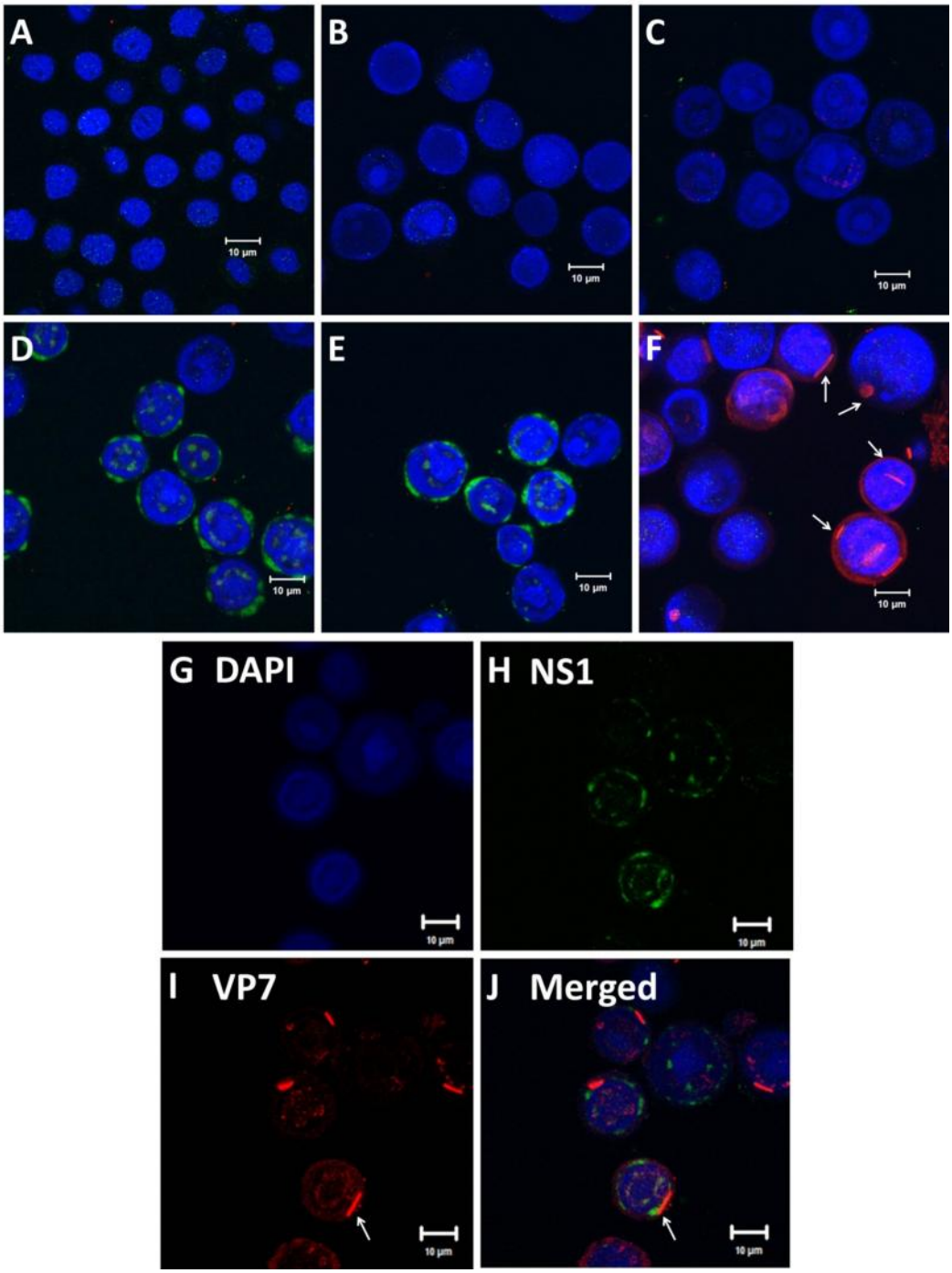

Figure 2.16. – Confocal microscopy of Sf9 cells co-expressing NS1 and VP7. Cells were immunolabelled with anti-NS1 with Alexa Fluor 488 (green) and anti-VP7 with Alexa Fluor 633 (red). A: mock infected cells. Cells were infected with B: wild type baculovirus. C: Bac-VP3. D: Bac-NS1. E: Bac-NS1 and Bac-VP3. F: Bac-VP7. G-J: Bac-NS1 and Bac-VP7. The VP7 crystalline particles (F) and a putative co-localisation (I-J) are indicated with arrows.

2.3.2.3 TEM analysis of the co-localisation of NS1 with VP3 and VP7 in AHSV-infected cells

In order to determine whether a co-localisation between NS1 and VP7 occurs at levels below the detection threshold of confocal microscopy in AHSV infected cells, BSR and KC cells were infected AHSV-3 and subjected to HPF-FS at 48 hpi and 10 dpi, respectively. The fixed samples were embedded in LR White resin

and sectioned. Ultrathin sections were immunogold labelled with anti-NS1, anti-VP7 or anti-AHSV (CLIFT and PENRITH 2010) and visualised with TEM.

In order to confirm the correct identification of putative VP7 crystalline particles, KC cells were labelled with anti-AHSV (Fig. 2.17) or anti-VP7 (not shown) antisera. No significant immunogold labelling could be seen in mock infected cells (not shown), and labelling localised to virus particles (not shown) as well as VP7 crystalline structures within infected cells (Fig. 2.17 A-B). This confirmed that the crystalline particles did in fact consist of VP7. The composition of NS1 tubules had already been confirmed (see section 2.3.1.4). Following confirmation of the composition of these viral structures, cells were screened for the presence of NS1 tubules and VP7 crystalline particles in close proximity. When NS1 tubules were observed in the vicinity of VP7 crystalline particles, no direct interaction was observed in the majority of cells (Fig. 2.17 A). Co-localisations were seen rarely (in less than about 5% of visualised cells), and in these cases, NS1 tubules were arranged in various orientations relative to the VP7 crystalline particles (Fig. 2.17 B-D). Interestingly, in one instance, anti-NS1 immunogold labelling was observed near a VP7 crystalline particle, but no tubules were visible (Fig. 2.17 E). In another instance, labelling of AHSV proteins (using the anti-AHSV serum) was seen near NS1 tubules without any evidence for the presence of a crystalline particle or virus particles (Fig. 2.17 F). This suggests that these proteins might exist in an unpolymerised form and occasionally co-localise in this state. These findings are similar to observations made by Hyatt and Eaton (1988), where immunogold labelling with anti-VP3 and anti-VP7 sera localised to BTV NS1 tubules.

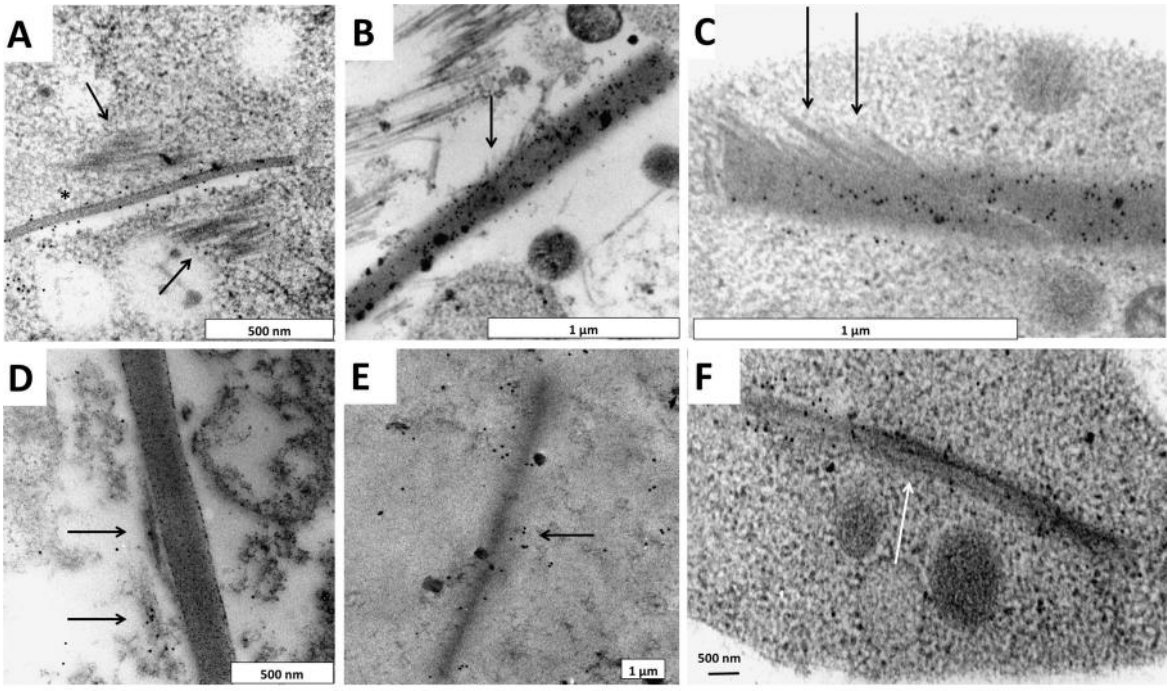

Figure 2.17. – TEM of KC cells infected with AHSV-3 and immunogold labelled with anti-AHSV (A-C and F) or anti-NS1 (D-E) sera. A: NS1 tubule bundles near a VP7 crystalline particle. B-D: NS1 tubule bundles in direct contact with VP7 crystalline particles. E: Immunolabelling with anti-NS1 near a VP7 crystalline particle. F: Immunolabelling with anti-AHSV near NS1 tubules. Arrows indicate NS1.

The co-localisation pattern of NS1 and VP7 was similar in AHSV-3 infected BSR cells (Fig. 2.18). No significant background labelling was seen in mock infected cells labelled with anti-VP7 (Fig. 2.18 A). The identity of VP7 crystalline particles was again confirmed with immunogold labelling (Fig. 2.18 B). Although NS1 tubules and VP7 crystalline particles were more often observed without interacting (Fig. 2.18 B-C), they were occasionally observed in very close proximity at approximately the same frequency (less than 5% of visualised cells) seen in infected KC cells (Fig. 2.18 C-E). These data suggest that no difference exists in the co-localisation pattern of NS1 and VP7 in AHSV-infected insect and mammalian cells and that the co-localisation is rare in the context of AHSV infection. Co-localisation studies of NS1 tubules with VP3 were not successful due to high levels of background labelling in all cell types at various dilutions of anti-VP3 antibody and secondary antibody (not shown). Therefore, it is still unclear whether NS1 and VP3 can interact. However, it appears that NS1 and VP7 can occasionally occur in direct contact, but that this co-localisation is rare in AHSV infected cells.

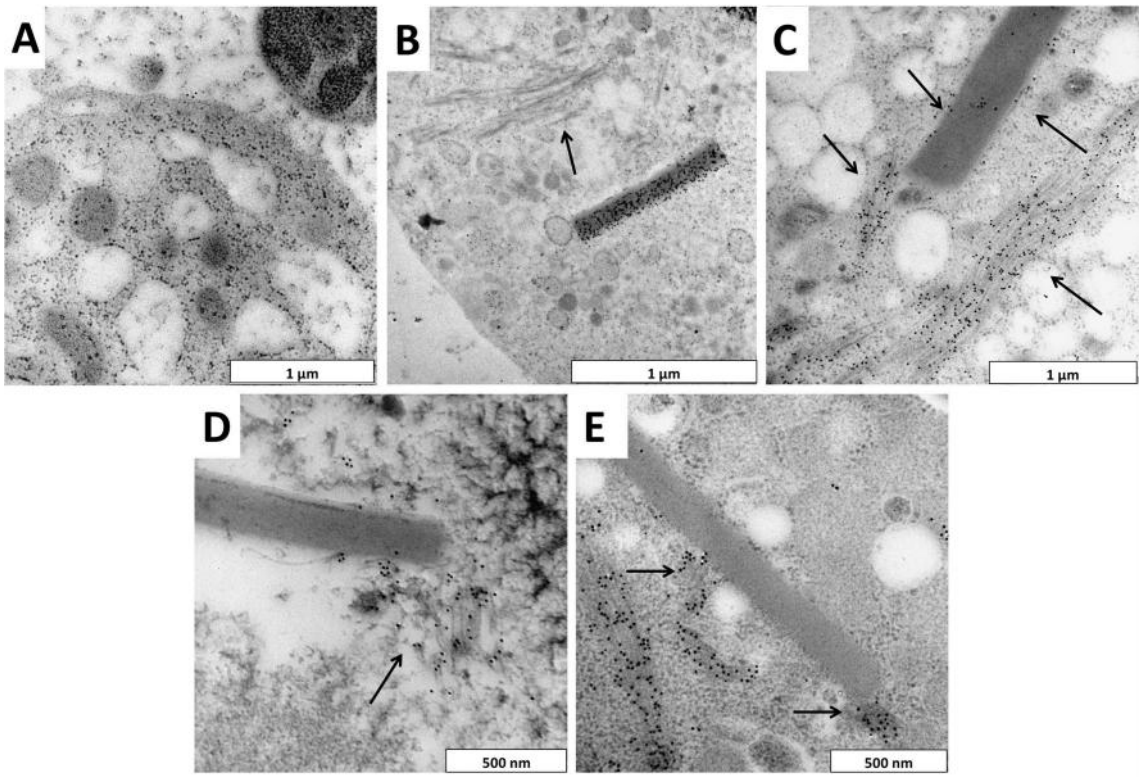

Figure 2.18. – TEM of BSR cells infected with AHSV-3 and immunogold labelled with anti-VP7 (A-B) or anti-NS1 (C-E). A: Mock infected cells. B: NS1 tubules near a VP7 crystalline particle. C: NS1 tubules near, and in direct contact with, a VP7 crystalline particle. D-E: NS1 tubules in direct contact with VP7 crystalline particles. Arrows indicate NS1 tubules.

2.3.2.4 TEM analysis of the co-localisation of NS1 with VP3 and VP7 in Sf9 insect cells

In order to determine whether NS1 can co-localise with VP3 or VP7 in the absence of other AHSV proteins, Sf9 cells expressing NS1 and VP7 or VP3 were subjected to high-pressure freezing, sectioning, immunogold labelling of NS1, VP3 or VP7 and visualised with TEM. Large amounts of background were observed in all

cells labelled with anti-VP3 at various dilutions of primary and secondary antibody (not shown). Therefore, the expression or distribution of VP3 could not be verified. This was also observed in BSR and KC cells, which suggests that the anti-VP3 serum is neither very specific nor very sensitive. No background labelling was observed in mock or wild type baculovirus infected cells labelled with anti-NS1 or anti-VP7 (not shown). Immunogold labelling with anti-VP7 showed that the putative crystalline particles were indeed composed of VP7 (Fig. 2.19 A). The co-localisation pattern in Sf9 cells resembled that seen in AHSV-infected cells; these proteins mostly failed to co-localise directly when they were observed within the same cell (Fig. 2.19 B) and the incidence of co-localisation between NS1 and VP7 (Fig. 2.19 C-E) was also observed in less than about 5% of visualised cells.

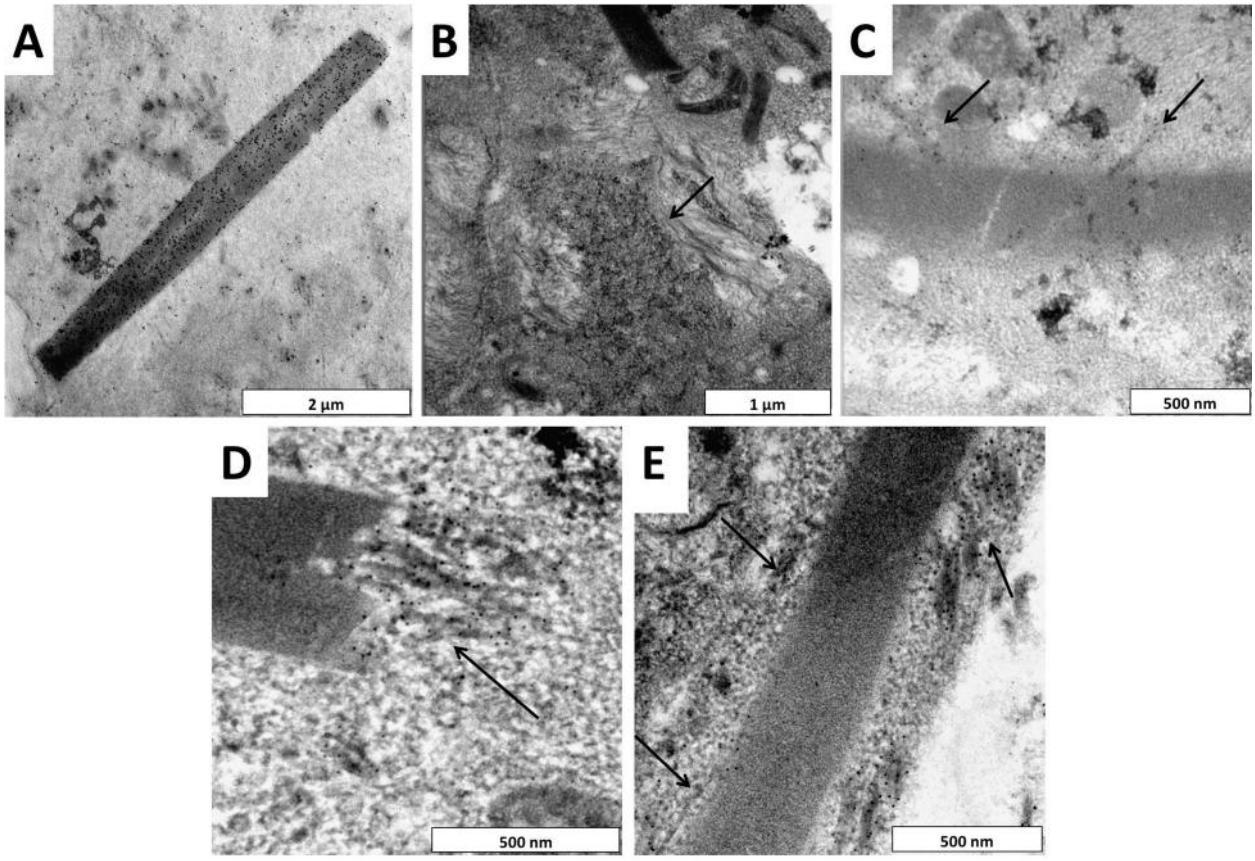

Figure 2.19. – Transmission electron micrographs of Sf9 cells co-expressing NS1 and VP7. Cells were labelled with anti-VP7 (A-C) or anti-NS1 (D-I). A: cells expressing VP7. B: Cells co-expressing NS1 and VP7 with an NS1 tubule bundle near a VP7 crystalline particle. C-E: cells co-expressing NS1 and VP7 with NS1 tubules in direct contact with VP7 crystalline particles. Arrows indicate NS1 tubules.

The localisation patterns of NS1 and VP7 in cells co-expressing NS1, VP7 and VP3 were indistinguishable from cells co-expressing only NS1 and VP7. This suggests that the co-localisation of NS1 tubules and VP7 crystalline particles is not affected by the presence of VP3, although it is possible that very few cells expressed significant amounts of VP3 and even fewer cells co-expressed all three AHSV proteins. Overall,

these data suggest that NS1 and VP7 interact at a very low rate when overexpressed in Sf9 insect cells and that their co-localisation is independent of other viral proteins.

2.4 Discussion

Several functions have been proposed for BTV NS1, including roles in virus morphogenesis, egress, pathogenesis and promoting viral protein synthesis during infection (BOYCE *et al.* 2012; BROOKES *et al.* 1993; EATON *et al.* 1988; OWENS *et al.* 2004). However, very little is known about the properties of AHSV NS1, including its distribution throughout infection and its interactions with other proteins. The identification of protein interaction partners can be useful for focusing the functional characterisation of proteins with unknown function. For example, an interaction of BTV NS1 with VP3 and VP7 has been reported that suggested a possible role for NS1 during virus morphogenesis (HYATT and EATON 1988). However, no similar studies have been undertaken to determine whether AHSV NS1 interacts with VP3 or VP7.

During this study, the intracellular distribution of NS1 and its co-localisation with AHSV VP3 and VP7 were investigated. The distribution and structure of NS1 within AHSV-infected cells was first defined by means of confocal- and transmission electron microscopy (TEM) and compared to that seen in Sf9 cells overexpressing NS1 and NS1-eGFP. NS1 and NS1-eGFP were also compared to determine whether NS1-eGFP could be used as a reliable substitute for wild type NS1 during confocal microscopic studies. Thereafter, confocal microscopy and TEM were used to determine whether NS1 could co-localise with VP3 or VP7, both within AHSV-infected cells and in Sf9 cells co-expressing NS1 with VP3 and/or VP7. Confocal microscopy was used to examine populations of cells simultaneously and to define the distribution of the viral proteins throughout the entire cell, whilst TEM was used to examine protein structures and co-localisations at a high resolution.

Confocal microscopy revealed that NS1 tubule bundles assemble gradually during infection, occurring first in small foci throughout the cytoplasm and later converging into larger foci both in AHSV infected cells and in Sf9 insect cells expressing the NS1 protein or an eGFP-tagged NS1 protein. Transmission electron microscopy with immunogold labelling of NS1 allowed an examination of tubule and tubule bundle structure at high resolution. Individual tubules had the characteristic ± 21 nm diameter and fine structure previously described (HUISMANS and ELS 1979; MAREE and HUISMANS 1997) and were indistinguishable between AHSV-infected cells and Sf9 cells expressing NS1 or NS1-eGFP. The similarity in tubule structures seen in Sf9 and BSR cells is consistent with the previously reported ability of NS1 to self-assemble into tubules (URAKAWA and ROY 1988; VAN STADEN *et al.* 1998).

Interestingly, the tubule bundles in AHSV-infected cells, which consisted of NS1 tubules in neat parallel arrays, were morphologically distinct from those seen in Sf9 cells overexpressing NS1. Tubule bundles consisting of NS1 or NS1-eGFP had highly similar morphology; tubules in bundles were orientated randomly with respect to each other to form nest-like aggregates throughout the cytoplasm. This difference could

suggest that the correct assembly of NS1 tubule bundles requires more careful regulation of the rate of NS1 expression which may be absent when the protein is expressed from the polyhedrin promoter of the Autographa californica nuclear polyhedrosis virus (AcNPV) within the Sf9 cell. Alternatively, the correct formation of NS1 tubule bundles could require the presence of other AHSV proteins or host cell specific factors. Therefore, although the intracellular localisation of NS1 within AHSV infected cells and recombinant baculovirus infected cells was generally similar (cytoplasmic foci consisting of NS1 tubule bundles), the baculovirus expression system may not be functionally analogous to AHSV infection, at least with regard to NS1.

NS1 modified via addition of eGFP retained the ability to assemble into tubule bundles *in vivo*. This was in accordance with previous electron microscopy studies of sucrose density gradient purified AHSV NS1-eGFP tubules, which were found to retain most of the characteristics of wild type tubules (LACHEINER 2006) as well as studies of BTV NS1 tubulisation where a range of C-terminal insertions was tolerated (GHOSH *et al.* 2002; LARKE *et al.* 2005; MIKHAILOV *et al.* 1996; MONASTYRSKAYA *et al.* 1995). The distribution of NS1-eGFP was very similar to that of wild type NS1 in recombinant baculovirus-infected Sf9 cells, which warranted its use as a surrogate for NS1 during confocal microscopy.

Confocal microscopy and TEM of AHSV-infected cells as well as Sf9 cells co-expressing NS1 with VP7 revealed an occasional co-localisation between NS1 tubules and VP7 crystalline particles. Confocal microscopy of Sf9 cells co-expressing NS1-eGFP with VP7 showed an interesting co-localisation pattern. VP7 appeared to form fewer crystalline particles in favour of forming ring-like structures around putative NS1-eGFP tubule bundles. This pattern was not seen in cells co-expressing wild type NS1 with VP7, which suggests that the addition of eGFP near the NS1 C-terminus is responsible for this enhanced co-localisation. The insertion of eGFP could induce a slight conformational change in the structure of NS1, or eGFP itself could be involved in the co-localisation with VP7. Due to an apparent lack of antiserum sensitivity, it was not possible to determine whether AHSV NS1 co-localises with VP3. Further studies will be required to determine the mechanism whereby the insertion of eGFP near the C-terminus of NS1 effects this co-localisation with VP7, and also to determine whether AHSV NS1 and VP3 interact.

The functional significance of the co-localisation between NS1 and VP7 is unclear. It is possible that the occasionally observed co-localisation is an artefact of host cell trafficking of foreign protein, whereby the insoluble NS1 tubule and VP7 crystalline structures are shuttled to a joint location within the cell, where they are perhaps too inaccessible or abundant for complete degradation by the host cell. The absence of VP7 crystalline structures in cells infected with BTV and other orbiviruses supports the notion that the association between the structures does not have any function. Alternatively, this observation could point to an inherent ability of NS1 and VP7 to co-localise during some aspect of viral replication. Perhaps NS1, in an untubulised form, is involved in virus morphogenesis and egress by interacting with VP7 in nascent virions and NS3, and that the ability to interact is not completely lost by the proteins once insoluble tubules

and crystalline particles are formed. A mechanism might exist whereby the amount of unpolymerised NS1 available for activity is controlled by its inclusion in inactive tubules. This is supported by rare observations of anti-NS1 labelling near a VP7 crystalline particle and anti-AHSV labelling near NS1 tubules, which suggests that these proteins might occur in an unpolymerised form, and also that other AHSV structural proteins, such as VP3, might co-localise with NS1 tubules. The processes of morphogenesis, egress and viral protein synthesis could in turn be governed by the amount of free NS1. It is also possible that NS1 forms tubules as an artifact of its amino acid composition, which is subject to selective constraints due to its true function during the viral replication cycle, which remains to be determined.

Chapter 3:
Characterisation of novel AHSV non-structural protein NS4.

3.1 Introduction

Recent bio-informatic analysis of genome segment 9 suggested that most orbiviruses may produce a fifth non-structural protein, which has been designated NS4. NS4 is expressed in BTV and Great Island virus (GIV) infected cells. NS4 in cells infected with these viruses localises to the nucleolus, cell membrane and cytoplasm at various stages of infection. GIV NS4 binds dsDNA and dsRNA, whereas BTV NS4 binds dsDNA only. BTV NS4 also appears to be involved in modulating host innate immunity during infection with some serotypes (BELHOUCHET *et al.* 2011; FIRTH 2008; RATINIER *et al.* 2011). The exact function of NS4 in the replication cycles of these viruses has not yet been determined, although its higher level of conservation compared to the overlapping VP6 gene is suggestive of functional significance.

Previous analysis of genome segment 9 sequences of AHSV-3 and AHSV-6 showed a 97% nucleotide identity and a 95% amino acid identity of the cognate VP6 protein (TURNBULL *et al.* 1996). The predicted AHSV NS4 protein has a size of approximately 17 or 20 kDa, contains three potential overlapping nuclear localisation signals (NLSs) which predict a dual cytoplasmic and nuclear localisation, and has putative nucleic acid binding or modifying domains (BELHOUCHET *et al.* 2011; FIRTH 2008). Whether the predicted NS4 gene is also expressed in AHSV-infected cells has not yet been established. The aim of this study was to characterise the putative AHSV NS4 protein with regard to its expression status in AHSV infected insect and mammalian cells as well as its intracellular distribution throughout infection and its putative nucleic acid binding activity. This was achieved by means of Western blot analysis, confocal laser scanning microscopy of AHSV-infected cells and nucleic acid protection assays using bacterially expressed purified recombinant NS4, respectively. This information could motivate further study of NS4 and assist in determining its precise function during viral replication.

3.2 Materials and methods

3.2.1 *In silico* analyses of AHSV genome segment sequence data

Open reading frames were identified using the open reading frame (ORF) Finder tool (http://www.ncbi.nlm.nih.gov/projects/gorf/). The molecular mass of proteins was predicted with the Compute pI/Mw tool in the Swiss Institute of Bioinformatics ExPASy resource portal (http://web.expasy.org/compute_pi/) using either average or monoisotopic resolution. Sequence alignments and Neighbour Joining analyses, as well as identity calculations, were performed with MAFFT (multiple alignment using fast Fourier transform) version 7 (http://mafft.cbrc.jp/alignment/server/). Default settings were used unless specified otherwise.

3.2.2 Cell culture and protein analysis

3.2.2.1 Antisera

Antisera used during this study are summarised in Table 3.1. A polyclonal antiserum against NS4 was produced by the company GenScript USA (Inc). Conserved peptides within each type of NS4 were identified amongst all nine AHSV serotypes and the mixture of the two peptides was used as an immunogen to generate an antiserum that would detect both types of AHSV NS4. The antibody was resuspended was in deionised water to the original concentration of the antiserum before lyophilisation and all antibodies were diluted in blocking buffer comprising 1% (w/v) milk powder in 1 x PBS (phosphate buffered saline).

Table 3.1. – A summary of the antisera used, describing the animal of origin and antigens used. The peptide antigens are shown in the N-terminal to C-terminal orientiation.

Name	Origin	Description	Antigen
Anti-NS4	Rabbit	Affinity purified IgG	QGAGLEGEEWAEWL, representing residues 2-15 or 17-30 (Clade I). MIEEWRARNLREAD, representing residues 33-46 (Clade II).
Anti-AHSV3	Guinea pig	¼ 27/09/99	Partially purified AHSV3
Anti-AHSV2	Guinea pig	GP anti-AHSV-2	Partially purified AHSV2
Anti-AHSV3	Equine	Onderstepoort 2004	Partially purified AHSV3
Anti-AHSV4	Equine	Onderstepoort 2004	Partially purified AHSV4
Anti-AHSV9	Sheep	Sheep 6971 7/60 Baton. 5/11/04	Partially purified AHSV9
Anti-AHSV (pooled)	Mixed	Combination of above 4 sera	Partially purified AHSV-2, AHSV-3, AHSV-4, AHSV-9

3.2.2.2 Protein expression with the baculovirus system

Bac-VP6 stock solutions were produced from recombinant bacmids containing the AHSV-3 or AHSV-6 genome segment 9 (DE WAAL 2005) according to the instructions in the Bac-to-Bac® Baculovirus Expression Systems manual (Life Technologies). Briefly, recombinant bacmid DNA with Cellfectin® reagent (Life Technologies) was used to transfect Sf9 cell monolayers in 6-well plates. The supernatant of transfected cells was titrated and single plaques were used to infect Sf9 cell monolayers in 6-well plates. The cells were harvested and analysed to identify plaques that express the recombinant protein. The supernatants of plaques expressing recombinant protein efficiently were used to infect Sf9 cell monolayers in 75cm^2 flasks. These cells were harvested at 7-10 days post infection and the supernatants used as recombinant baculovirus stocks. Sf9 cells were infected with virus stocks of Bac-AHSV3-VP6 at a MOI of 5 and with Bac-

AHSV6-VP6 at a MOI of 5 or 10. Protein expression was performed as described in Chapter 2 (section 2.2.1.4).

3.2.2.3 Infecting cells with AHSV

BSR cells and KC cells were infected as described in Chapter 2 (section 2.2.1.5) and Vero (epithelial cells from African green monkey kidney mammalian cells were infected with as described for BSR cells. The strains AHSV-1 (29/62), AHSV-2 (82/61), AHSV-3 (M322/97), AHSV-3 (13/63), AHSV-4 (Jane) #4, AHSV-4 (32/62) and AHSV-6 (93/63), obtained from the OIE Reference Laboratory (Onderstepoort Veterinary Institute, Onderstepoort, South Africa), were used during the study.

3.2.2.4 SDS-PAGE and Western blot analysis

SDS-PAGE and Western blotting were performed as described in Chapter 2 (section 2.2.1.6). Pre-cast Bolt™ 4-12% Bis-Tris Plus Protein Gels were also used for SDS-PAGE with the Novex® Bolt Mini Gel system (Life Technologies) with electrophoresis in MOPS (3-(N-morpholino)propanesulfonic acid buffer) for 30-40 minutes at 165 V.

3.2.3 DNA manipulation and analysis

3.2.3.1 Preparation and transformation of chemically competent cells

Escherichia coli (*E. coli*) JM109 or BL21(DE3) cells (Novagen) were streaked on Luria Bertani (LB) medium agar to obtain single colonies, which were cultured overnight with shaking in 3 mL LB medium at 37°C. A 100 mL volume of LB medium (1% w/v tryptone, 1% NaCl, 0.5% yeast extract, pH 7.4) was inoculated with 100-150 µL of the overnight culture and incubated with agitation until an OD_{600} of 0.4-1 was reached. The cells were centrifuged at 2000 rpm for 10 minutes at 4°C and resuspended in half of the original volume of filter sterilised 50 mM $CaCl_2$. The cells were centrifuged at 2000 rpm for 5 minutes at 4°C and resuspended in 1/20 of the original volume of 50 mM $CaCl_2$. The cells were incubated on ice for one hour before being transformed or aliquoted and stored at - 70°C in 15% glycerol.

Chemically competent cells were thawed on ice, 1-50 ng of plasmid DNA were added to 100-150 µL of competent cells and the mixture was incubated at on ice (4°C) for 30 minutes. Cells were subjected to heat shock at 42°C for 90 seconds and cooled on ice for two minutes. A volume of 400-600 µL of LB medium was added to the transformation mixture and incubated with agitation for one hour at 37°C. A volume of 10-150 µL of the transformation culture was spread onto LB medium agar plates, which were incubated inverted overnight at 37°C. If blue-white screening was required, 5% (w/v) X-Gal (5-bromo-4-chloro-3-indolyl-β-D-galactopyranoside) and 50 mM IPTG (isopropyl β-D-1-thiogalactopyranoside) were added to the agar plates.

3.2.3.2 Plasmid DNA isolation and analysis

Plasmid DNA (Table 3.2) was isolated with the High Pure Plasmid Isolation and Genopure Plasmid Maxi Kits (Roche) for small- and large-scale isolations, respectively. Samples were eluted in 1 x TE buffer (10 mM Tris, 1 mM EDTA, pH 7.4) and analysed with agarose gel electrophoresis at 100 V for 30-60 minutes in a gel containing 1% (w/v) agarose and 0.5 µg/mL ethidium bromide (EtBr) in 1 x TAE buffer (0.04 M Tris-acetate, 1 mM EDTA, pH 8.5). The gel was visualised with the GelDoc™ XR+ Imaging System (Bio-Rad). For a size standard, a quantity 0.75 µg of DNA Molecular Weight Marker II (Roche) was used per lane.

Table 3.2. – A summary of the vectors used during the study.

Name	Description
pUC57-NS4-I	Plasmid pUC57 containing the codon-optimised NS4-I gene based on the predicted NS4-I amino acid sequence of AHSV-4field (produced by GenScript).
pUC57-NS4-II	Plasmid pUC57 containing the codon-optimised NS4-II gene based on the predicted NS4-I amino acid sequence of AHSV-3field (produced by GenScript).
pStaby-VP7	pStaby1.2 vector containing an AHSV VP7 gene (provided by Dr. A.C. Potgieter).
pStaby-NS4-I	pStaby1.2 vector containing the codon-optimised NS4-I gene (constructed during this study).
pStaby-NS4-II	pStaby1.2 vector containing the codon-optimised NS4-II gene (constructed during this study).

3.2.3.3 Restriction digestion analysis

Plasmid DNA was digested with EcoRI, SalI, NdeI or XhoI (Roche). For small scale digestions with EcoRI and SalI, ± 1 µg of DNA was incubated with 5 units of each enzyme in 1 x Buffer H (Roche) in 10 µL reaction volumes for 1.5 h at 37°C. For small scale digestion with NdeI and XhoI, ± 0.8 µg of DNA was incubated with 5 units of NdeI or 2 units of XhoI in 1 x Buffer H with final reaction volumes of 15 µL for 3 hours at 37°C. Large scale digestions were performed overnight at 37°C with 2 µg DNA and 15 units of NdeI and 6 units of XhoI in 50 µL reaction volumes. The restriction digestion reactions were analysed with agarose gel electrophoresis in gels containing 1% (w/v) agarose and 0.5 µg/mL ethidium bromide in 1 x TAE buffer. For size standards, quantities of 0.75 µg DNA Molecular Weight Marker II (Roche) and 0.52 µg 100 bp DNA Ladder (Promega) were used per lane.

3.2.3.4 DNA purification

Digested fragments were purified using the High Pure PCR Product Purification Kit (Roche) following the protocol for isolation of DNA from agarose gel. DNA was digested at a large scale and separated on 0.8% agarose gels. The appropriate fragments were excised from the gel and purified. Samples were eluted in 1 x

TE buffer. For applications not involving fragments in agarose gel, DNA was purified or concentrated using the DNA Clean and Concentrator™ kit (Zymo Research).

3.2.3.5 Ligation

Purified vector and insert fragments in a 1:2 molar ratio were ligated overnight at 16°C using 1.8 units of T4 DNA ligase in DNA ligase buffer in a final volume of 18 µL.

3.2.3.6 Nucleic acid binding assays

Nucleic acid protection assays were based on the method described by Belhouchet *et al.* (2011). For the DNA protection assays, 1 µg of dsDNA (BenchTop pGEM DNA Marker, Promega) in DNaseI buffer was mixed with 500 ng of purified recombinant NS4 in a volume of 9 µL and incubated at room temperature for 20 minutes. Thereafter, 2 units of DNase I (New England Biolabs) were added to the reaction, which was incubated at 37°C for 30 minutes. The enzyme was inactivated by heating the reaction to 99°C for one minute. The reactions were analysed with agarose gel electrophoresis with agarose gels containing 2% (w/v) agarose 0.5 µg/mL EtBr. RNA protection assays were performed in the same manner with the same quantities of dsRNA (dsRNA Ladder, New England Biolabs), NS4 protein and RNase III (ShortCut® RNase III, New England Biolabs), but with the addition of 20 mM $MnCl_2$ to the reaction. After incubation, the enzyme was inactivated by the addition of 50 mM EDTA and the reactions were analysed with 3% agarose gel electrophoresis. Agarose gels were visualised with the GelDoc™ XR+ Imaging System (Bio-Rad).

3.2.4 Confocal microscopy

3.2.4.1 Fixing and immunolabelling cells

Confocal microscopy with immunolabelling was performed as described in Chapter 2 (section 2.2.3.1). Anti-fibrillarin [38F3] (Abcam®) primary antibody was used at dilutions of 1:100, 1:250 or 1:500.

3.2.5 Bacterial expression of NS4

BL21(DE3) *E. coli* cells transformed with recombinant pStaby-NS4 were used for small-scale recombinant protein expression as described in the StabyExpress™ T7 Kit Manual, version 1.7 (Delphi Genetics). Briefly, 10 mL of LB medium containing antibiotic were inoculated with a single transformed bacterial colony and incubated with shaking at 37°C until an OD_{600} of 0.6-0.8 was reached. Expression was induced by the addition of 1 mM IPTG and the cultures were again incubated. Cells were harvested at the appropriate time post induction.

For large-scale protein expression, 5 mL LB medium was inoculated either with single transformant colonies or with 100 µL of a transformant glycerol stock and incubated overnight with shaking at 37°C. The liquid culture was diluted 1:100 in the required volume of LB medium for large-scale protein expression and

incubated at 37°C until an OD_{600} of 0.6-0.8 was reached. Protein expression was induced by the addition of 1 mM IPTG and cultures were incubated at 37°C for one hour.

3.2.6 Purification of recombinant NS4 protein from bacterial cells

A cleared supernatant for column purification was prepared from bacterial cells expressing NS4. A volume of 200 mL LB medium was used to produce ± 1g of wet cell pellet required for protein purification; after induction with 1 mM IPTG for one hour, cells were harvested with centrifugation at 6100 x g for 40-60 minutes at 4°C. The cell pellet was resuspended in LEW buffer (Lysis-Equilibration-Wash buffer: 50 mM NaH_2PO_4, 300 mM NaCl, pH 8). DNaseI was not added during cell lysis and the cells were not sonicated, but lysed in the presence of 1 mg/mL lysozyme by passaging the suspension 20 times each through 22G and 27G needles. The lysate was centrifuged at 6100 x g for 40 minutes and the supernatant was cleared with a 0.2 µm filter.

The 6xHis-tagged NS4 proteins were purified with Protino® Ni-TED 1000 Packed Columns (Macherey-Nagel) according to the manufacturer's instructions for the purification of proteins under native conditions. Briefly, the columns were equilibrated with 2 mL of LEW buffer before the cleared supernatant was passed through the column. The column was washed twice with 2 mL of LEW buffer and proteins were eluted in three fractions of 1.5 mL each of Elution Buffer (50 mM NaH_2PO_4, 300 mM NaCl, 250 mM imidazole, pH 8). Eluted protein was aliquoted and stored in 15% glycerol at -70°C.

The concentration of recombinant NS4 protein in the first elution fraction of each sample was quantified with the Bicinchoninic Acid Protein Assay Kit (Sigma-Aldrich) and SDS-PAGE. The concentration of total protein in each sample was determined with the Bicinchoninic Acid (BCA) Assay Kit (Sigma-Aldrich). Briefly, eight parts of BCA Working Reagent (50 parts of Reagent A: bicinchoninic acid, sodium carbonate, sodium tartrate, and sodium bicarbonate in 0.1 N NaOH, pH 11.25, combined with 1 part of Reagent B: 4% (w/v) copper(II) sulfate pentahydrate) were added to one part of each protein sample. Bovine serum albumin (BSA) diluted in Elution Buffer was used as a concentration standard. The mixtures were incubated at 60°C for 15 minutes and the absorbance at 562 nm was measured with the NanoDrop® ND-1000 Spectrophotometer (Thermo Scientific). The concentration of protein in each sample was determined by comparison with the BSA standards.

SDS-PAGE was used to estimate the percentage of NS4 (or the percentage purity) in each protein sample. SDS-PAGE was performed with a 4-12% polyacrylamide gradient gel and electrophoresis with the Novex® Bolt Mini Gel system (Life Technologies) in MOPS (3-(N-morpholino)propanesulfonic acid) buffer for 30-40 minutes at 165 V. Gels were stained with Coomassie and visualised with the GelDoc™ XR+ Imaging System (Bio-Rad). Image Lab version 2.0.1 software (Bio-Rad) was used to analyse the purity composition of each sample. In order to calculate the concentration of NS4, the total protein concentration of each sample was multiplied by the percentage of NS4 within the sample.

3.3 Results

3.3.1 Analysis of AHSV genome segment 9 and NS4 sequences

In order to determine the relationships between the predicted AHSV NS4 proteins of different serotypes, the genome segment 9 nucleotide sequences of all nine serotypes obtained with pyrosequencing (provided by Dr. C.A. Potgieter, Deltamune) were compared with MAFFT (multiple alignment using fast Fourier transform) and subjected to Neighbour-Joining analysis. The serotypes diverged into two main groups with differences in genome segment length and nucleotide sequence (Fig. 3.1). These two groups were designated Clade I and Clade II, as indicated in Figure 3.1. Interestingly, the two types of AHSV-1 that were analysed occurred in different groups. The AHSV-1 reference strain NS4 occurred in Clade II and the field isolate in Clade I. This was also the case with the two AHSV-6 and AHSV-7 isolates (Fig. 3.1, Table 3.3, Appendix A) and could be evidence of reassortment.

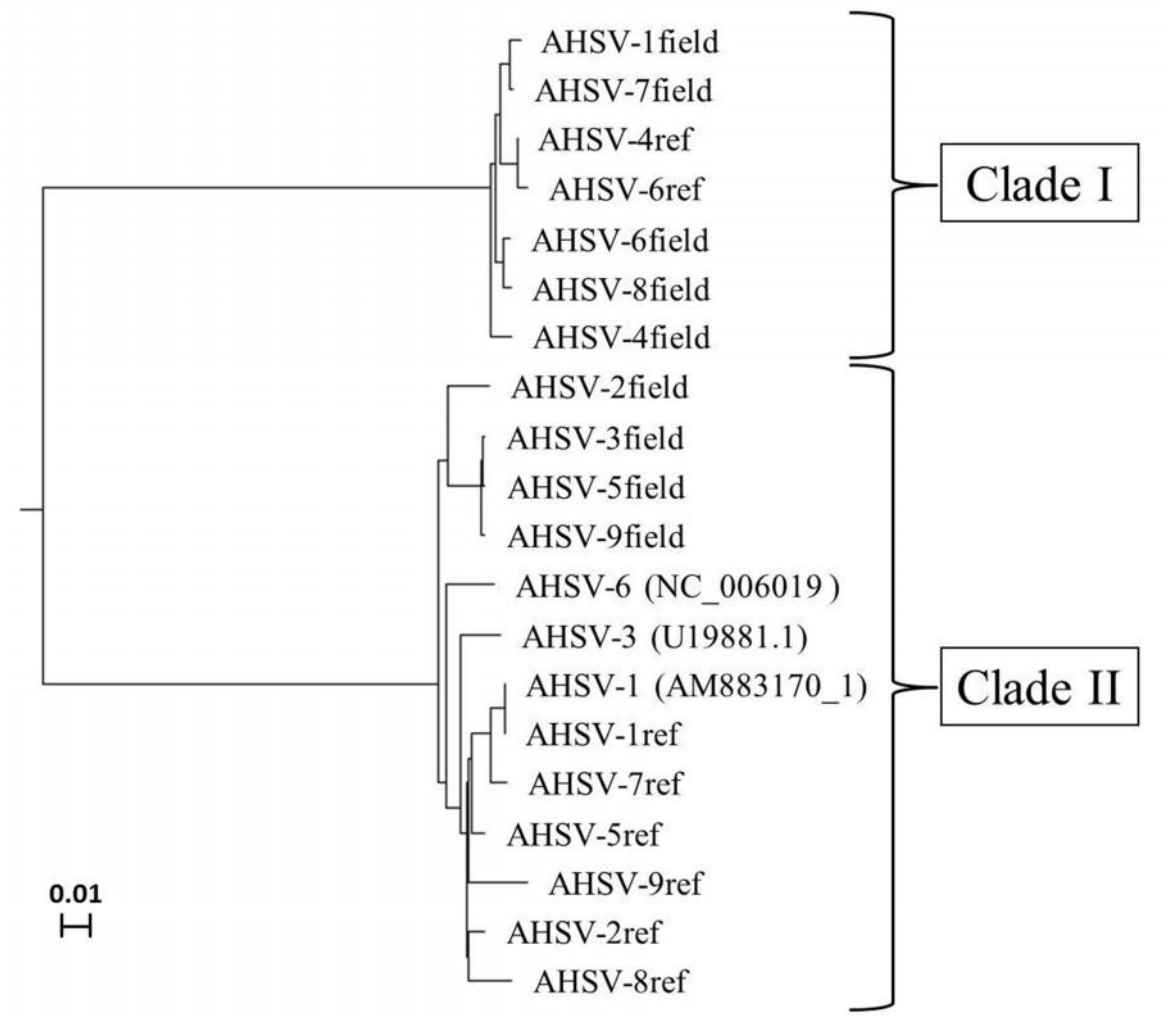

Figure 3.1. – Neighbour Joining tree showing the relationships between the full length genome segment 9 nucleotide sequences of all nine AHSV serotypes. The scale bar indicates the branch length corresponding to 0.01 nucleotide changes. The suffix "ref" denotes a reference strain and the suffix "field" denotes a field isolate. The Genbank accession numbers of the currently published sequences are shown in brackets.

In order to determine whether this grouping of the serotypes into two clades was also observed amongst the two segment 9 genes and their cognate proteins, the VP6 and NS4 open reading frames and amino acid sequences were identified and compared (Table 3.3, Appendix A). These sequences also separated the serotypes into two clades and each of these clades contained the same AHSV serotypes seen when comparing the full length segment 9 nucleotide sequences, with minor differences in grouping within clades (Table 3.3, Table 3.4, Appendix A). For all genome segment 9 sequences, the highest overall similarity (95-96%) was seen within Clade I, followed by sequences within Clade II (81-88%). The highest degree of divergence was seen between clades (56-65% identity). The difference in identity within clades could be partly due to the fact that more Clade II sequences were analysed and that the isolates in Clade I contained two isolates of some serotypes. The degree of similarity in each group appeared to be consistent regardless of the type of sequence analysed (Table 3.4). Collectively, this suggested that the existence of two distinct types of genome segment 9 nucleotide sequences underlies most of the differences between the VP6 and NS4 proteins encoded by the two clades.

Table 3.3. – A summary of the properties of the two open reading frames in AHSV genome segment 9. The suffix "ref" indicates a reference strain and the suffix "field" indicates a field isolate. "Nucleotide" is abbreviated "nt" and "amino acid" as "a/a". Genbank: NC_006019 encodes the NS4 sequence Genbank: YP_006491216.1 predicted by Belhouchet *et al.* (2011). AHSV-3 (Genbank: U19881.1) and AHSV-6 (NC_006019) were published by Turnbull *et al.* (1996). AHSV-1 (Genbank: AM883170.1) is the sequence published by Potgieter *et al.* (2009).

		Major ORF (VP6)				Minor ORF (NS4)			
	Isolate	Length (nt)	Position	Frame	Length (a/a)	Length (nt)	Position	Frame	Size in kDa (a/a)
Clade I, NS4-I	AHSV-1field	1101	18-1118	+3	366	435	214-648	+1	16.68 (144)
	AHSV-4field	1101	18-1118	+3	366	435	214-648	+1	16.77 (144)
	AHSV-6field	1101	18-1118	+3	366	435	214-648	+1	16.8 (144)
	AHSV-7field	1101	18-1118	+3	366	435	214-648	+1	16.78 (144)
	AHSV-8field	1101	18-1118	+3	366	435	214-648	+1	16.8 (144)
	AHSV-4ref	1101	18-1118	+3	366	435	214-648	+1	16.69 (144)
	AHSV-6ref	1101	18-1118	+3	366	435	214-648	+1	16.69 (144)
Clade II, NS4-II	AHSV-2field	1110	18-1127	+3	369	465	193-657	+1	18.19 (154)
	AHSV-3field	1110	18-1127	+3	369	465	193-657	+1	18.2 (154)
	AHSV-5field	1110	18-1127	+3	369	465	193-657	+1	18.2 (154)
	AHSV-9field	1110	18-1127	+3	369	465	193-657	+1	18.2 (154)
	AHSV-1ref	1110	17-1126	+2	369	465	192-656	+3	18.15 (154)
	AHSV-2ref	1110	18-1127	+3	369	465	193-657	+1	18.19 (154)
	AHSV-5ref	1110	18-1127	+3	369	465	193-657	+1	18.2 (154)
	AHSV-7ref	1110	18-1127	+3	369	465	193-657	+1	18.23 (154)
	AHSV-8ref	1110	18-1127	+3	369	465	193-657	+1	18.15 (154)
	AHSV-9ref	1110	18-1127	+3	369	465	193-657	+1	18.26 (154)
	AHSV-3 (U19881.1)	1110	18-1127	+3	369	510	148-657	+1	20.09 (169)
	AHSV-6 (NC_006019.1)	1110	18-1127	+3	369	432	148-579	+1	17.26 (143)
	AHSV-1 (AM883170.1)	1110	18-1127	+3	369	465	193-657	+1	18.14 (154)

Amongst the AHSV serotypes analysed, two types of VP6 were observed that differ in length and amino acid sequence (Table 3.3, Table 3.4, Appendix A). The nucleotide (65% identity) and amino acid (54% identity) sequence variation seen between genome segment 9 and VP6 of all AHSV isolates was greater than the previously predicted identities of 97% and 95%, respectively, where only AHSV-3 (U19881.1) and AHSV-6 (NC_006019.1) were compared (TURNBULL *et al.* 1996). The data obtained during the current study suggests that both of the latter isolates belong to Clade II, which would account for their high degree of similarity.

All of the predicted NS4 ORFs were in the +1 frame relative to the VP6 ORF. Most of the NS4 proteins within Clade I contained 144 amino acids (16 kDa) and those within Clade II contained 154 amino acids (18 kDa). A large amount of variation was seen in the NS4 proteins between AHSV serotypes (Appendix A). This variation was observed along the entire NS4 sequence, but was more pronounced near the N-terminus. Based on this information, the types of NS4 produced by members of each clade were designated NS4-I (144 amino acids, Clade I) and NS4-II (154 amino acids, Clade II), respectively (Table 1, Appendix A).

Table 3.4. – A summary of the sequence identity within and between clades. The genome segment 9 nucleotide sequences, as well as VP6 and NS4 ORFs and amino acid sequences, were compared. AHSV-6 (NC_006019.1) was omitted from the analyses on account of being an outlier.

		Sequence				
	Group	Segment 9 nucleotide	VP6 ORF	VP6 amino acid	NS4 ORF	NS4 amino acid
Identity	Between clades	65%	65%	54%	62%	56%
	Within Clade I	97%	96%	95%	96%	95%
	Within Clade II	88%	88%	81%	87%	86%

Two of the currently published (TURNBULL *et al.* 1996) sequences for AHSV-3 and AHSV-6 (Genbank: U19881.1 and Genbank: NC_006019, respectively) represent the genome segment 9 inserts within the recombinant baculoviruses used during this study. Sequence analysis showed that the NS4 amino acid sequences encoded by these two segments are highly similar to each other and to NS4-II, despite their different predicted sizes (Table 3.3). These sequences were almost identical, but the AHSV-3 NS4 ORF was 24 amino acids longer than that of AHSV-6. This was not seen in the sequences of the more recent AHSV-3 and AHSV-6 isolates, which were highly divergent (Appendix A). The similarity seen between the published AHSV-3 and AHSV-6 sequences suggested that these isolates might have been reassortant strains. The NS4 ORFs had a start site at a different position compared to those observed amongst the other AHSV serotypes, and AHSV-6 (NC_006019) appears to contain a premature stop site and encodes a shorter type of NS4-II compared to other members of Clade II (Appendix A). These baculoviruses were initially selected to represent the two types of NS4. However, due to the lack of availability of other recombinant baculoviruses, the two NS4-II variants were characterised instead. In addition to the difference in the position of the open reading frame compared to other members of Clade II, the predicted nuclear

localisation signals seen in Genbank: YP_006491216.1 were absent from all of the putative NS4 proteins identified during this study. Since the currently published (BELHOUCHET *et al.* 2011) NS4 sequence (Genbank: YP_006491216.1) was also based on AHSV-6 (NC_006019) (DE WAAL 2005), it is not fully representative of either of the two AHSV NS4 proteins predicted to occur amongst the nine serotypes.

Based on the information obtained during sequence analysis, two AHSV serotypes (AHSV-3 and AHSV-4 reference strains), representative of each type of segment 9 and predicted NS4 protein, were selected for use during subsequent analyses. These serotypes were expected to produce NS4-II (± 18 kDa) and NS4-I (± 16 kDa), respectively. The relationships of the genome segment 9 nucleotide sequences, VP6 ORFs and NS4 ORFs are shown in Figure 3.2. The predicted NS4 amino acid sequence data were also used during the development of a polyclonal antiserum specific for NS4, which was required during analyses of the expression status and intracellular distribution of NS4.

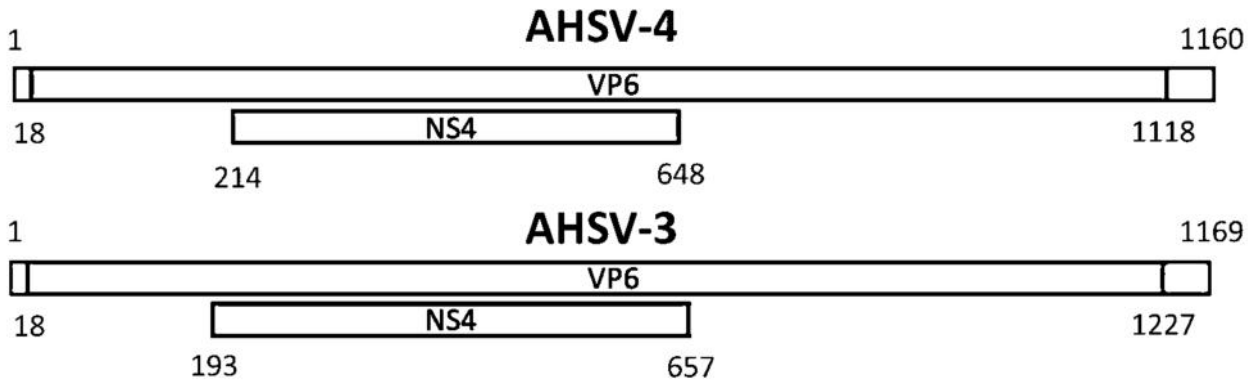

Figure 3.2 – A diagram depicting the relationships between the two open reading frames encoded by AHSV genome segment 9 of two serotypes, representing Clade I (AHSV-4) and Clade II (AHSV-3). The nucleotide positions of the VP6 and NS4 reading frames are indicated. The ORFs were predicted with the ORF Finder tool (NCBI).

3.3.2 Determining whether the putative AHSV NS4 protein is translated

3.3.2.1 Determining whether NS4 is expressed in AHSV infected cells

In order to determine whether the predicted NS4 protein is translated in infected cells, BSR, Vero and KC cells were infected with AHSV-3 or AHSV-4, harvested at 72 hpi or 9 days post infection (dpi), respectively, and analysed with SDS-PAGE or Western blotting with a number of primary antisera.

No unique band of the expected size of NS4 could be seen with SDS-PAGE analysis of Vero cells infected with AHSV-3, which suggested that NS4 was not expressed or expressed at levels below the detection threshold of PAGE with Coomassie staining (not shown). An antiserum that could detect NS4 was therefore required for Western blot analysis. Two antisera obtained from different animals exposed to various AHSV serotypes were used initially. Anti-AHSV-3 (guinea pig) was produced with purified AHSV-3 particles and

anti-AHSV (pooled) contained a mixture of four antisera produced with purified AHSV-2, AHSV-3, AHSV-4 and AHSV-9. Since a crude purification process was used to obtain the immunogenic AHSV particles, it was possible that some non-structural proteins could have been present during the production of these antisera, which might enable the detection of NS4. In Vero cells, anti-AHSV-3 (guinea pig) at a 1:50 dilution failed to detect a unique band of the expected size, but detected other AHSV-3 proteins (not shown). The other antiserum, anti-AHSV (pooled), detected a faint infection-specific band of 15-20 kDa in size, possibly corresponding to NS4 (not shown) at a 1:50 dilution of each constituent antiserum. No virus-specific proteins were detected in AHSV-3 infected KC cells with either antiserum, probably due to the low levels of viral protein expression in insect cells. Because these antisera might detect any viral proteins and not only NS4, these results, although promising, were inconclusive. Therefore, an antiserum specific for NS4 was required.

The predicted NS4 amino acid sequences (see section 3.3.1 and Appendix A) were subjected to *in silico* analysis to identify a antigenic peptide with the aid of the company GenScript USA (Inc). Although amino acid sequence alignment of the two serotypes showed regions of high conservation, it was not possible to design a single peptide antigen that could be expected to produce an antiserum that detects both types of NS4 protein reliably. Therefore, a mixed polyclonal antiserum was developed, using two separate peptides, targeting NS4-I and NS4-II, respectively, to inoculate the same animal. The antigenic peptide regions were conserved amongst the AHSV serotypes within each of the two genome segment 9 clades and both peptides were expected to generate antibodies that target regions near the N-terminus of NS4 (Appendix A). Once the antiserum was available, cells infected with AHSV could be analysed with Western blotting to determine whether NS4 is translated.

BSR, Vero and KC cells were infected with AHSV-3 or AHSV-4. Mammalian cells were harvested and subjected to Western blotting with the new anti-NS4 serum at 48 hpi and KC cells at 13 days post infection (dpi). Unique bands were detected in Vero (Fig. 3.3 A, lanes 2-4), BSR (Fig. 3.3 A, lanes 5-7) and KC cells (Fig. 3.3 B) infected with AHSV-3 but unique bands were only seen in Vero cells infected with AHSV-4 (Fig. 3.3 A, lane 4).

The AHSV-3 NS4 band was more intense than the AHSV-4 band, which could either reflect serotype-specific differences in expression levels or differences in antibody sensitivity for the two types of NS4. These bands appeared closer in size to 20 kDa than the predicted 16 kDa for NS4-I, and closer to 25 kDa than 18 kDa for NS4-II. This discrepancy could be the result of post-translational modification of NS4, the limitations of SDS-PAGE analysis for size determination or incorrect prediction of the NS4 reading frames. A slight difference in the predicted and observed size with Western blotting was also reported for BTV NS4 (BELHOUCHET *et al.* 2011). These results suggested that the putative NS4 protein of AHSV was translated in both insect and mammalian cells.

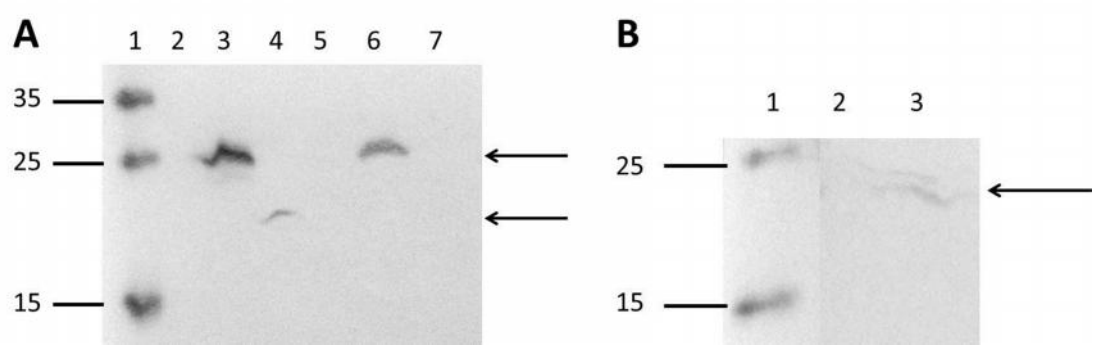

Figure 3.3. – Western blot with anti-NS4 demonstrating the presence of NS4 in AHSV-3 and AHSV-4 infected Vero cells and in AHSV-3 infected BSR and KC cells. **A.** Lane 1: molecular marker (sizes in kDa). Lane 2: mock infected Vero cells. Lane 3: Vero cells infected with AHSV-3. Lane 4: Vero cells infected with AHSV-4. Lane 5: mock infected BSR cells. Lane 6: BSR cells infected with AHSV-3. Lane 7: BSR cells infected with AHSV-4. **B.** Lane 1: molecular weight marker. Lane 2: mock infected KC cells. Lane 3: KC cells infected with AHSV-3. The putative positions of the two types of NS4 are indicated (arrows).

3.3.2.2 Determining whether NS4 is translated in Bac-VP6 infected cells

In order to determine whether NS4 can be translated *in vivo* from a full length segment 9 in the absence of other AHSV proteins, recombinant baculoviruses containing genome segment 9 were required. Recombinant bacmids containing the genome segment 9 of two serotypes (AHSV-3, Genbank: U19881 and AHSV-6, Genbank: NC_006019) were available for the production of recombinant baculoviruses (DE WAAL 2005). In order to produce recombinant baculoviruses, high molecular weight recombinant bacmid DNA was isolated from stored DH10Bac cells, and analysed with agarose gel electrophoresis. A band higher than the 23 130 bp fragment of the molecular marker DNA (Fig. 3.4) could be seen in DNA samples isolated from DH10Bac cells, which confirmed that recombinant bacmid DNA had been isolated.

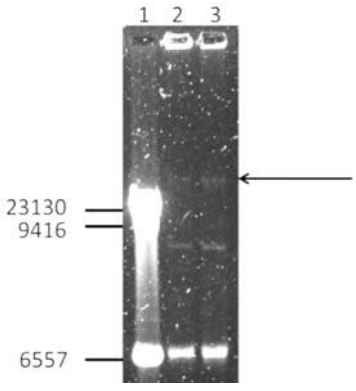

Figure 3.4. – An agarose gel depicting recombinant bacmid DNA isolated from transformed DH10Bac cells. Lane 1: molecular weight marker II (Roche, sizes in bp). Lane 2: DNA isolated from cells containing the AHSV-3 segment 9 bacmid. Lane 3: DNA isolated from cells containing the AHSV-6 segment 9 bacmid. The arrow indicates the position of recombinant bacmid DNA. The other two bands in lanes 2-3 represent the helper plasmid pMON7124.

The isolated recombinant bacmid DNA was used to transfect Sf9 cells. Filtered supernatants of transfected cells harvested were subjected to titration, and single plaques were selected and used to infect Sf9 cells. Infected Sf9 cell lysates were subjected to Western blotting with anti-AHSV (pooled) to identify plaques that express VP6 efficiently. Gels containing 12% polyacrylamide were used during Western blotting. Unique bands in slightly different positions could be seen in cells infected with both types of Bac-VP6 (Fig. 3.5). The apparent difference in size between the two types of VP6 has been reported for AHSV VP6 previously (DE WAAL 2005) and although the cause of the differences in migration rate is not clear, it is unlikely to represent an actual difference in size, because both types of VP6 have a predicted size of about 38.4 kDa. The plaque-derived viruses appeared to express VP6 with varying efficiency; Plaque 1 of both Bac-AHSV3-VP6 (Fig. 3.5, lane 4) and Bac-AHSV6-VP6 (Fig. 3.5, lane 7) expressed VP6 at lower levels than plaques 2 and 3 in each case. The third plaque of each AHSV-3 and AHSV-6 baculovirus titration was selected for amplification and use as virus stock solutions. The expression of VP6 by the two stock solutions was also confirmed by means of Western blotting (not shown). Recombinant baculoviruses expressing the main ORF (VP6) of genome segment 9 were therefore available to determine whether the minor ORF encoding NS4 could be translated, and to study the distribution of NS4 in the absence of all other AHSV proteins (excluding VP6) in Sf9 insect cells.

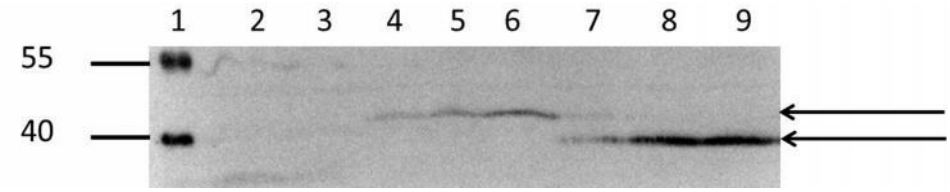

Figure 3.5. – Western blot of Sf9 cells infected with Bac-VP6 from single plaques using anti-AHSV (pooled). Lane 1: molecular size marker (kDa). Lane 2: mock infected Sf9 cell lysate. Cells were infected with Lane 3: wild type baculovirus. Lanes 4-6: Bac-AHSV3-VP6 plaques 1-3. Lanes 7-9: Bac-AHSV6-VP6 plaques 1-3. The positions of VP6 in the two respective AHSV serotypes are indicated (arrows).

In order to determine whether NS4 can be translated from genome segment 9, Sf9 cells were infected with Bac-AHSV3-VP6 or Bac-AHSV6-VP6 and analysed with Western blotting using anti-AHSV (pooled) and colorimetric detection as described in section 3.3.2.1. Gels containing 15% polyacrylamide were used to resolve proteins of the predicted size of NS4. Unique bands corresponding to VP6 were again seen in cells infected with both types of Bac-VP6 (Fig. 3.6). In addition, faint unique bands corresponding to the size of Bac-AHSV3-VP6 NS4 (± 20 kDa) could be discerned in cells infected with this virus (Fig. 3.6, lane 4). However, since the antiserum could potentially detect any AHSV protein, the detection of these bands was promising, but their identities were not certain. No unique band of the expected size of NS4 (± 17 kDa) could be detected in cells infected with Bac-AHSV6-VP6.

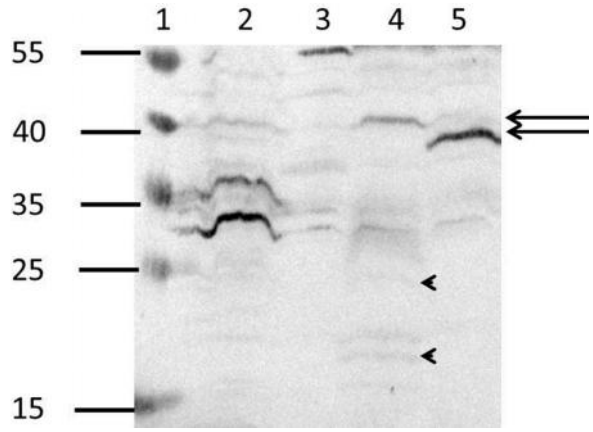

Figure 3.6. – Western blot of Sf9 cells infected with Bac-VP6 virus stocks using anti-AHSV (pooled). Lane 1: molecular size marker (kDa). Lane 2: mock infected Sf9 cells. Cells were infected with Lane 3: wild type baculovirus. Lane 4: Bac-AHSV3-VP6 stock. Lane 5: Bac-AHSV6-VP6 stock. Arrows indicate the positions of VP6 of the two serotypes and the arrowheads in Lane 4 show the unique bands corresponding to the predicted size of Bac-AHSV3-NS4 ± 20 kDa).

To determine the identity of these unique bands, the samples were also subjected to Western blotting using anti-NS4. Unique bands corresponding to the expected sizes of NS4 were observed in samples infected with either type of Bac-VP6 (Fig. 3.7). The signal was stronger in samples infected with Bac-AHSV3-VP6 compared to Bac-AHSV6-VP6, which is consistent with the difference observed in Vero cells infected with AHSV-3 compared to AHSV-4 and could be the result of a number of factors. NS4 could be translated more efficiently in Bac-AHSV3-VP6 infected cells compared to those infected with Bac-AHSV6-VP6. Alternatively, since the Bac-AHSV3-VP6 stock was harvested later than the Bac-AHSV6-VP6 stock, the cell lysate could have had a higher concentration of NS4 protein. Interestingly, multiple bands were apparent in the Bac-AHSV3-VP6 infected sample. The positions of these bands corresponded to those observed during Western blot analysis with anti-AHSV (pooled), which suggested that at least one of the bands detected previously (Fig. 3.6) consisted of NS4.

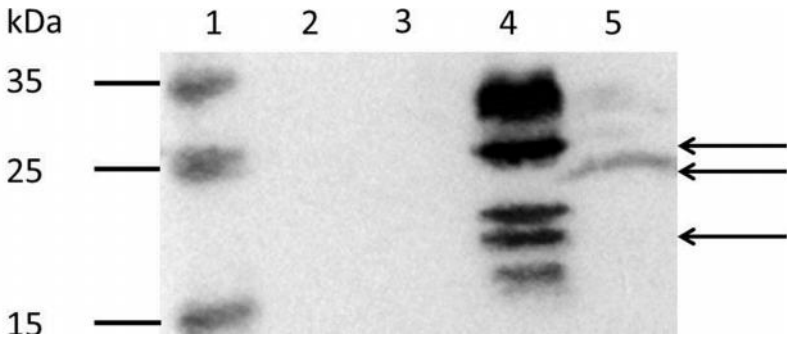

Figure 3.7. Western blot of Sf9 cells infected with Bac-VP6 and labelled with anti-NS4 (GenScript). Lane 1: molecular weight marker (kDa). Lane 2: mock infected Sf9 cells. Cells were infected with Lane 3: wild type baculovirus. Lane 4: Bac-AHSV3-VP6. Lane 5: Bac-AHSV6-VP6. Arrows indicate the putative positions of NS4.

The reason for the presence of multiple bands in cells infected with Bac-AHSV3-VP6 is unclear. Interestingly, the putative NS4 bands detected in Sf9 cells appeared to be larger than the expected sizes. This was also observed between the two types of AHSV VP6 encoded by the two Bac-VP6 baculoviruses as reported previously (DE WAAL 2005). The reason for this discrepancy is unknown. Collectively, these results showed that NS4 can be translated from AHSV genome segment 9 in the absence of other AHSV proteins.

3.3.3 Studying the intracellular distribution of AHSV NS4

3.3.3.1 Confocal microscopy to study the distribution of NS4 within AHSV infected cells

In order to study the intracellular localisation of NS4 within AHSV infected cells, BSR cells were infected with AHSV-3 (which produces NS4-II) or AHSV-4 (which produces NS4-I) and labelled with anti-NS4 (GenScript) for confocal microscopy at 2, 4, 6, 18, 24 and 48 hpi. Alexa Fluor 488 conjugated IgG (green) was used for secondary labelling and nuclei were stained blue with DAPI.

NS4 could be detected by 4 hpi in cells infected with AHSV-3 (Fig. 8). Initially, few small fluorescent foci were found mostly in the cytoplasm (Fig. 3.8 B-C), increasing significantly in size by 6 hpi (Fig. 3.8 D). By 18 hpi, fluorescent spots could be seen in the nucleus (Fig. 3.8 E). These nuclear foci became more intensely fluorescent and frequent as the cytoplasmic fluorescence decreased from 24 hpi to 48 hpi (Fig. 3.8 F-H). The distribution of NS4 varied within a population of visualised cells; multiple nuclear NS4 foci were observed in some cells, whilst other cells showed only cytoplasmic NS4 labelling and still others displayed a combination of cytoplasmic and nuclear NS4. This is consistent with the dual cytoplasmic and nuclear localisation predicted for AHSV NS4, and resembles the distribution of BTV NS4. It also confirms that NS4 is indeed expressed within AHSV infected mammalian cells, as suggested by the Western blot analyses of infected cell lysates. In addition, the fact that the NS4 proteins encoded by these viruses localise to the nucleus despite their lack of the predicted NLSs (BELHOUCHET *et al.* 2011) suggests that these signals might not be essential for nuclear localisation.

In cells infected with AHSV-4, much lower levels of NS4 were detected (Fig. 3.8 I). In these cells, NS4 was more prevalent in the cytoplasm and distinct fluorescent spots were not seen within the nucleus, although some diffuse nuclear fluorescence was occasionally observed. This could be due to differences between the two types of NS4 protein, or differences in the sensitivity of the anti-NS4 serum for the two types of NS4 during immunolabelling. This is consistent with the lower levels of NS4-I detected with Western blotting. The distribution also appeared to vary between different replicates of the same assays, which might suggest that NS4 shuttles between the nucleus and cytoplasm under the influence of unknown factors. No NS4 was observed at the plasma membrane in cells infected with AHSV-3 or AHSV-4.

Since the punctate distribution of AHSV NS4 in the nucleus resembled that of BTV NS4, which has a nucleolar localisation, AHSV infected BSR cells were subjected to co-immunolabelling of NS4 and the

nucleolar marker fibrillarin in order to determine whether AHSV NS4 also localises to the nucleolus. Cells were infected with five different serotypes of AHSV, fixed at 24 and 48 hpi and labelled with anti-NS4 with Alexa Fluor 488 and monoclonal anti-fibrillarin antibody with Alexa Fluor 594 (red), stained with DAPI and visualised with confocal microscopy.

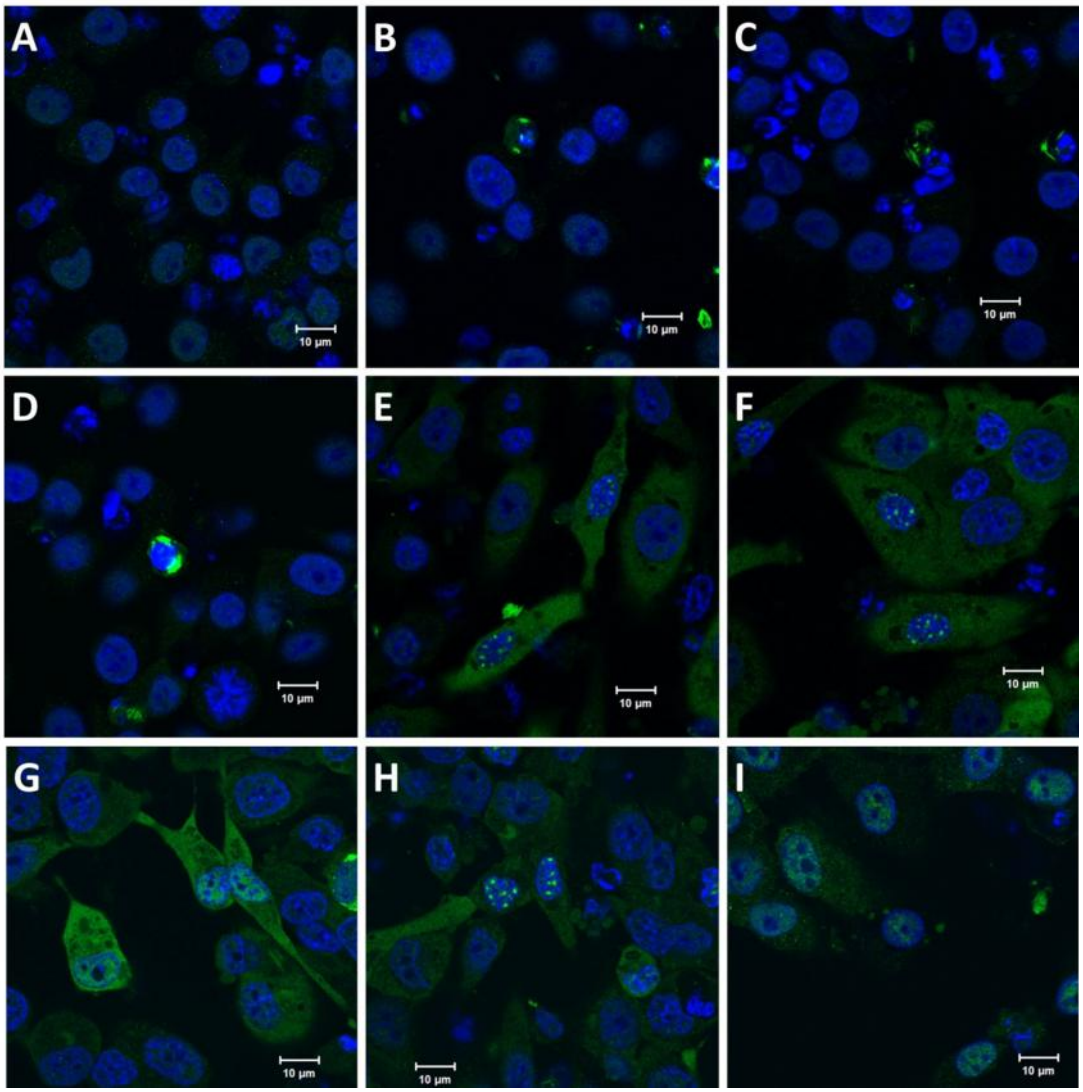

Figure 3.8. – Confocal microscopy of BSR cells infected with AHSV-3 (B-H) or AHSV-4 (I) immunolabelled with anti-NS4 and Alexa Fluor 488 (green) at different times post infection. Nuclei were stained with DAPI. A: mock infected cells. B: 2 hpi. C: 4 hpi. D: 6 hpi. E: 18 hpi. F: 24 hpi. G-H: 48 hpi. I: AHSV-4 infected cells at 48 hpi.

Cells labelled with anti-fibrillarin showed distinct fluorescent foci in the nucleus (Fig. 3.9) which were similar to those described by Belhouchet *et al.* (2011) and the antibody supplier (Abcam®). Labelling of fibrillarin resulted in weaker fluorescence at 48 hpi compared to 24 hpi. This was also reported for BTV, where it was proposed to result from cell death-related nuclear events induced by viral infection. The distribution of NS4 in AHSV infected cells was similar to that described above. Cells infected with AHSV-1 could not be visualised at 48 hpi due to the high level of CPE observed in cells infected with this serotype. At 24 hpi,

however, most NS4 was seen in the cytoplasm and nuclear NS4 had a diffuse rather than punctate distribution (Fig. 3.9 B). This NS4 distribution pattern was also observed in cells infected with AHSV-4 or AHSV-6 (field isolate) at both 24 hpi and 48 hpi (Fig. 3.9 C-E), all which belong to Clade I and are expected to produce NS4-I. Low levels of fluorescence were again detected in cells infected with AHSV-4. However, the fact that NS4 was detected at high levels in cells infected with AHSV-6, which produces the same type of NS4 as AHSV-4, suggests that the low fluorescence observed in cells infected with AHSV-4 is at least partly due to lower levels of NS4 expression in these cells. Cells infected with AHSV-2 or AHSV-3 had nuclear NS4 foci and some cytoplasmic NS4 (Fig. 3.9 F-H). Both of these AHSV serotypes belong to Clade II and are expected to produce NS4-II.

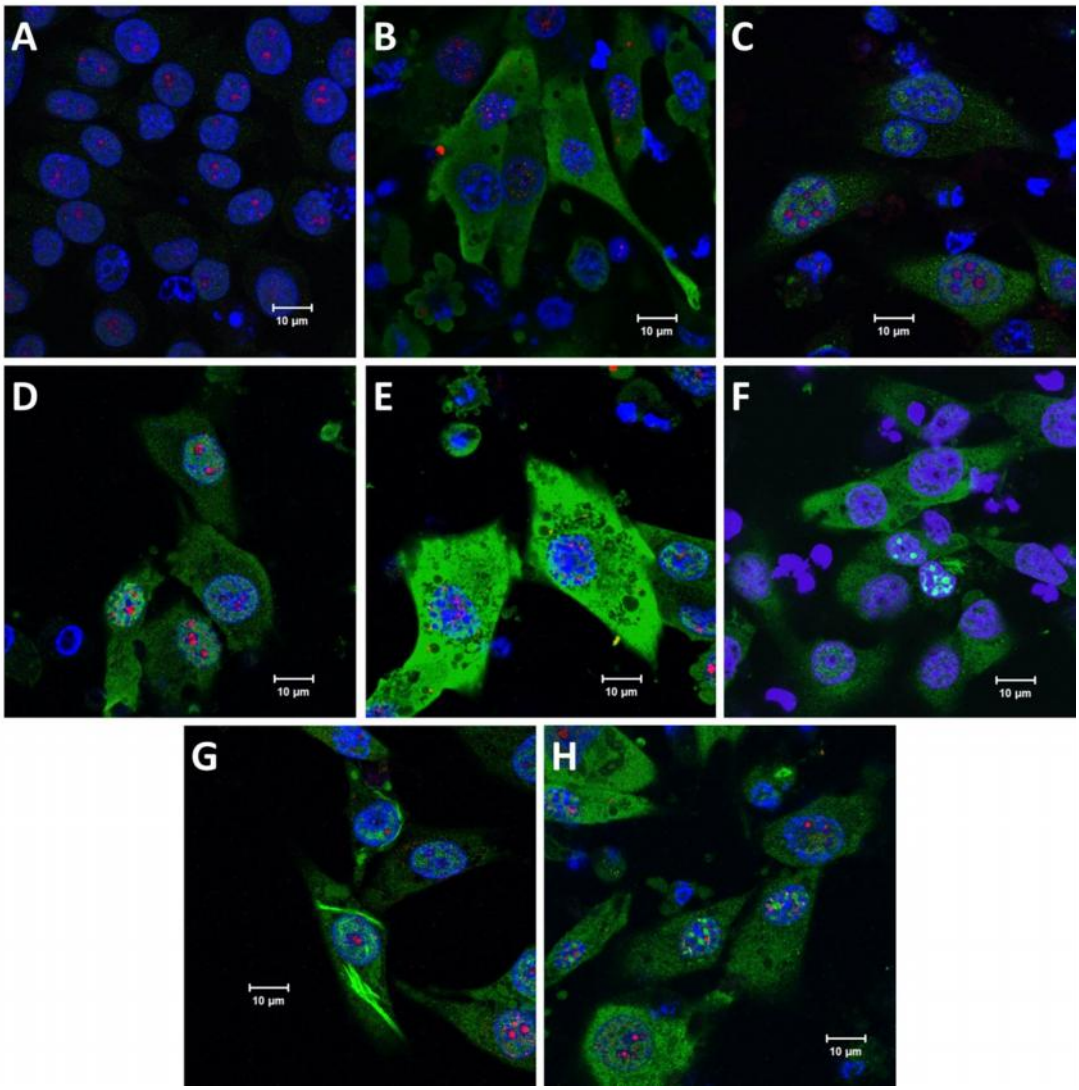

Figure 3.9. – Confocal micrographs of BSR cells infected with different serotypes of AHSV. Cells were labelled anti-NS4 with Alexa Fluor 488 anti-rabbit IgG and anti-fibrillarin with Alexa Fluor 594 at 48 hpi. Nuclei were stained with DAPI. A: mock infected cells. Cells were infected with B: AHSV-1. C: AHSV-4. D-E: AHSV-6. F-G: AHSV-2. H: AHSV-3.

The fact that the NS4 distribution in cells infected with different members of a particular clade was consistent supports the postulate that each clade encodes a different variant of NS4, and also suggests that the difference in NS4 amino acid sequence affects its intracellular distribution. Interestingly, fluorescent foci (morphologically resembling the NS1 tubule bundles observed with confocal microscopy, Chapter 2) often occurred in cells infected with AHSV-2 (Fig. 3.9 D). The significance of this observation is unclear; it could indicate a co-localisation between NS4 and NS1 or AHSV-2 NS4 could have a cytoplasmic distribution that resembles that of NS1 tubule bundles. Further analyses will be required to determine the significance of this localisation pattern. Overall, although both fibrillarin and NS4 could be detected simultaneously in the nucleus, they did not co-localise. This suggested that AHSV NS4 does not occur in the nucleolus at 24 hpi or 48 hpi. The intracellular distribution of NS4 in the absence of other AHSV proteins was next investigated.

3.3.3.2 Confocal microscopy to study the distribution of NS4 within cells infected with Bac-VP6

In order to study the intracellular distribution of two variants of NS4-II in the absence of other AHSV proteins, Sf9 cells were infected with Bac-AHSV3-VP6 or Bac-AHSV6-VP6 and immunolabelled for confocal microscopy with anti-NS4 (GenScript) at 24, 30, and 48 hpi. Alexa Fluor 488 was used for secondary labelling and nuclei were stained with DAPI.

In Bac-AHSV3-VP6 infected cells, NS4 was detected mainly in the cytoplasm of infected cells (Fig. 3.10). Small round foci occasionally occurred in the nucleus from 24 hpi (Fig. 3.10 C). Although these nuclear foci showed some similarity to those seen in AHSV-3 infected BSR cells, they often had the appearance of haloes rather than the solid fluorescent spots seen in BSR cells (Fig. 3.10 D-E). From 30 hpi, NS4 was abundant in the nucleus and cytoplasm (Fig. 3.10 D-E). Nuclear foci were occasionally seen within the nuclei of Bac-AHSV6-VP6 infected cells (Fig. 3.10 F), but NS4 occurred mostly in the cytoplasm of these cells and was detected at much lower levels than in Bac-AHSV3-VP6 infected cells (Fig. 3.10 G-H). This could be due to differences in expression levels of the proteins, or due to differences in their amino acid sequences. Notably, Bac-AHSV6-VP6 NS4 lacks the 24 C-terminal amino acids which most other types of NS4 contain. Both of the NS4-II variants encoded by these recombinant baculoviruses are predicted to contain the N-terminal NLSs identified by Belhouchet *et al.* (2011).

Although the frequency of the nuclear foci within infected cells appeared to vary between replicates of the same experiment, more NS4 was observed in the nucleus of Sf9 cells at 30 hpi compared to 48 hpi. The variability between replicates was similar to that seen in AHSV infected BSR cells. However, the distribution of NS4 in Sf9 cells at later stages of infection was reversed compared to that in BSR cells, where more NS4 appeared to enter the nucleus as infection progresses. This could mean that other viral proteins or host factors affect the trafficking or distribution of NS4. The cytoplasmic distribution of both types of NS4 was homogeneous, and no NS4 labelling was observed at the plasma membrane. This is consistent with the distribution of cytoplasmic NS4 in AHSV infected cells, and suggests that the distribution of NS4 is not

significantly affected by the presence of other AHSV proteins, except perhaps VP6, which is also produced in cells infected with these recombinant baculoviruses.

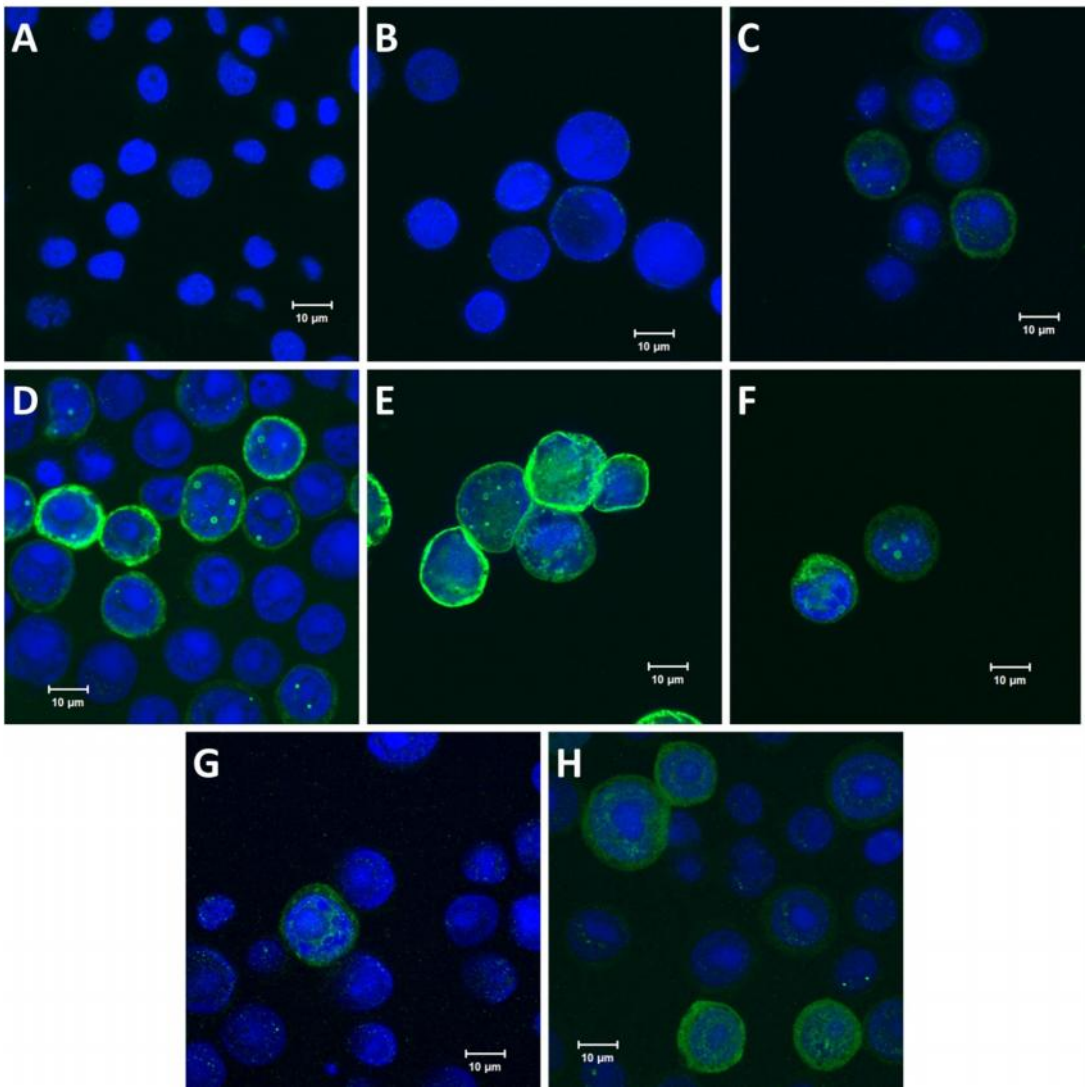

Figure 3.10. – Confocal micrographs of Sf9 cells infected with Bac-AHSV3-VP6 (C-E) or Bac-AHSV6-VP6 (F-H). Cells were labelled with anti-NS4 with Alexa Fluor 488 and stained with DAPI. A: mock infected cells. B: Wt-bac infected cells. C and G: 24 hpi. D and H: 30 hpi. E-F: 48 hpi.

Since baculovirus-expressed NS4 also occurred in the nucleus like BTV NS4, the possibility of a nucleolar NS4 localisation was also investigated in these cells. Sf9 cells infected with the two types of Bac-VP6 were co-immunolabelled with anti-NS4 and anti-fibrillarin at 30 and 48 hpi, using Alexa Fluor 488 and Alexa Fluor 594 for secondary labelling, respectively. Nuclei were stained with DAPI and cells were visualised with confocal microscopy.

Fibrillarin formed small nuclear spots that were more readily detected at 30 hpi (Fig. 3.11) compared to 48 hpi (not shown). This is consistent with the differences in labelling intensity observed in BSR cells reported previously. NS4 was occasionally observed in the nucleus. However, the two proteins did not co-localise (Fig. 3.11). This is consistent with the failure of NS4 to co-localise with fibrillarin in AHSV infected BSR cells.

These results suggest that AHSV NS4 does not localise to the nucleolus at the time points examined, and that this is not affected by the presence or absence of other AHSV proteins other than VP6. Overall, the expression and predicted dual cytoplasmic and nuclear localisation of NS4 was confirmed, and was shown to be independent of most other AHSV proteins.

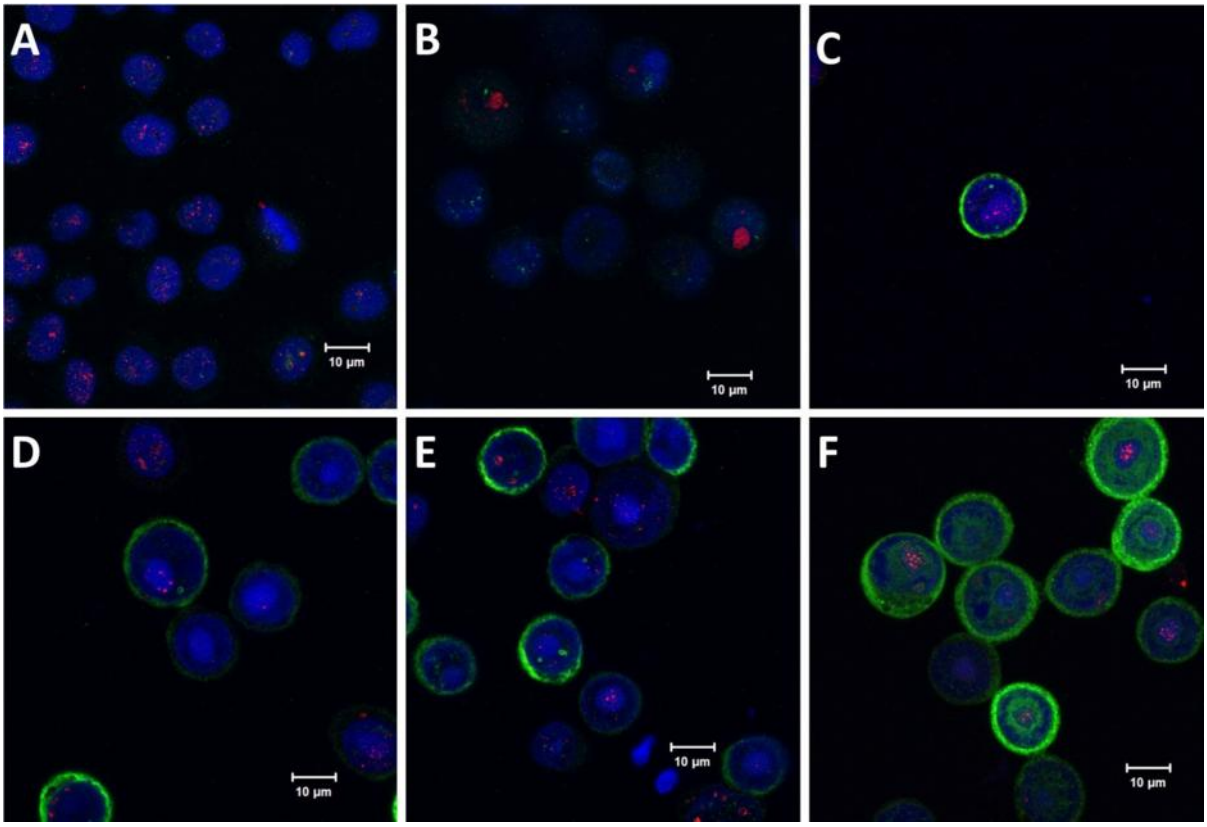

Figure 3.11. – Confocal micrographs of Sf9 cells infected with Bac-VP6. Cells were labelled with anti-NS4 with Alexa Fluor 488 anti-rabbit IgG and anti-fibrillarin with Alexa Fluor 594 at 30 hpi. Nuclei were stained with DAPI. A: mock infected cells. Cells were infected with B: wild type baculovirus. C-E: Bac-AHSV3-VP6. F: Bac-AHSV6-VP6.

3.3.4 Determining whether AHSV NS4 has the predicted nucleic acid binding activity

3.3.4.1 Subcloning codon optimised NS4 genes into bacterial expression vectors

In order to obtain pure recombinant NS4 to investigate its putative nucleic acid binding properties, bacterial expression vectors containing the NS4 coding regions were required. A set of plasmids containing the codon optimised predicted AHSV NS4 genes within pUC57 (Appendix B), representing each of the two types of NS4, were produced by the company Genscript USA (Inc). These genes were based on the sequences of AHSV-3field and AHSV-4field. The genes within the two recombinant plasmids will also be referred to as NS4-I (encoded by members of Clade I, e.g. AHSV-4) and NS4-II (encoded by members of Clade II, e.g. AHSV-3).

For bacterial expression, chemically competent *E. coli* JM109 cells were transformed with the recombinant pUC57-NS4 constructs. Plasmid DNA was extracted from these cultures, purified with the Roche High Pure PCR Purification kit and analysed with restriction enzyme digestion using EcoRI and SalI, which flank the gene insertion site, to confirm the presence of gene insert. Restriction digestion analysis of DNA isolated from the selected colonies was necessary because the ±500 bp difference in size between recombinant and non-recombinant pUC57 could not be discerned with conventional agarose gel electrophoresis of the undigested plasmid vectors. Bands of approximately 500 bp were visible in each of the restriction digestion reactions analysed with agarose gel electrophoresis, but absent from the undigested samples, which indicated that the DNA isolated from each of the selected transformants contained insert (Fig. 3.12). One transformant containing insert representing each pUC57-NS4 construct was subjected to large scale DNA isolation and purification, and the presence of insert was again confirmed with restriction digestion with EcoRI and SalI (not shown). Recombinant pUC57-NS4 had been successfully amplified.

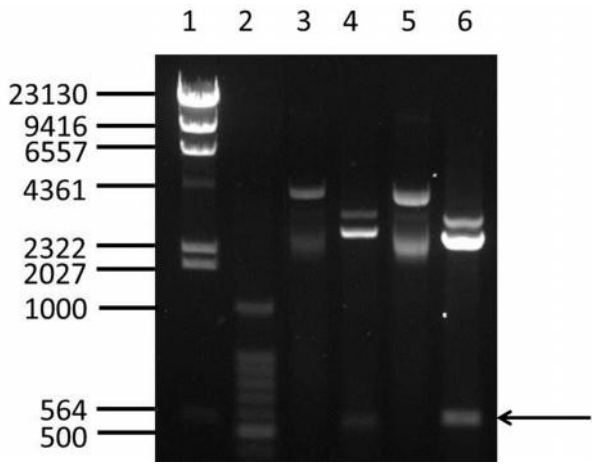

Figure 3.12. – Agarose gel containing isolated pUC57-NS4 DNA digested with EcoRI and SalI. Lane 1: molecular weight marker II (Roche, sizes in bp). Lane 2: 100 bp marker. Lane 3: pUC57-NS4-I DNA, undigested. Lane 4: pUC57-NS4-I DNA, digested. Lane 5: pUC57-NS4-II DNA, undigested. Lane 6: pUC57-NS4-II DNA, digested. The position of the ± 500 bp excised insert is indicated (arrows).

Following the purification of recombinant pUC57, the NS4 genes were subcloned into the modified bacterial expression vector pStaby1.2 (see map in Appendix B) using the NdeI and XhoI restriction sites for insertion. The NS4 genes were designed to contain an NdeI restriction site (5'-CA/TATG-3') at the start codon (underlined). The pStaby1.2 vector also contains an NdeI site. When the gene is inserted, the NdeI site and the start codon are restored. This subcloning strategy prevents the incorporation of fusion amino acids on the N-terminus of the protein, which would occur if a restriction site downstream from the NdeI site was used to insert the foreign gene. Finally, the pStaby1.2 vector encodes six C-terminal histidine residues for affinity purification of expressed recombinant protein.

Plasmid pStaby-VP7 and restriction digested was restriction digested with NdeI and XhoI to remove the AHSV VP7 gene, yielding an empty linear pStaby1.2 vector. pStaby-VP7 rather than non-recombinant pStaby1.2 was used for vector preparation, since complete digestion of the vector by both enzymes could be more easily confirmed by the presence of the excised VP7 gene insert (see Fig. 3.14, lanes 2-5 below). The pUC57-NS4 vectors containing the NS4 genes were digested with NdeI and XhoI to obtain insert, and the vector and insert fragments were purified from agarose using the Roche High Pure PCR Purification Kit (Fig. 3.13).

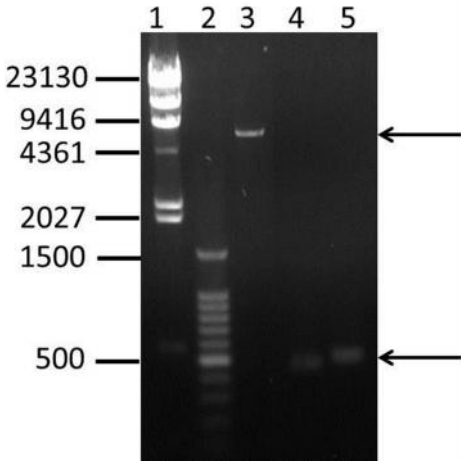

Figure 3.13. – AGE of purified linear pStaby1.2 vector and NS4-I and NS4-II gene inserts digested with NdeI and XhoI. Lane 1: molecular weight marker II (Roche). Lane 2: 100 bp ladder. Lane 3: purified pStaby1.2 vector. Lane 4: purified NS4-I gene insert. Lane 5: purified NS4-II gene insert. Arrows indicate the positions of the vector and inserts.

Purified vector and insert were ligated and used to transform Z competent *E. coli* cells (Zymo Research). Basal levels of expression of a foreign protein can reduce the recovery rate of transformed cells containing the recombinant vector due to the additional metabolic strain placed on the cell and/or potential toxic effects of the protein itself. Furthermore, transformation with supercoiled plasmid yields a higher transformation efficiency than transformation with a ligation reaction and should therefore result in more efficient protein expression. For these reasons, it was preferable to amplify recombinant pStaby1.2-NS4 in a non-expression host prior to transformation of the expression host. Plasmid DNA was isolated from single colonies and analysed with agarose gel electrophoresis. Bands corresponding to the size of pStaby1.2 were visible in all of the analysed samples (Fig. 3.14). Restriction digestion of the isolated plasmids resulted in the excision of ±500 bp bands (Fig. 3.14), which confirmed that the codon-optimised NS4 genes had been subcloned into pStaby 1.2. Bacterial expression vectors containing each type of NS4 gene were therefore available for recombinant protein expression. pStaby-NS4-I DNA isolated from colony 1 (Fig. 3.14, lane 9) and pStaby-NS4-II DNA isolated from colony 16 (Fig. 3.14, lane 15) was used for transformation into the expression host.

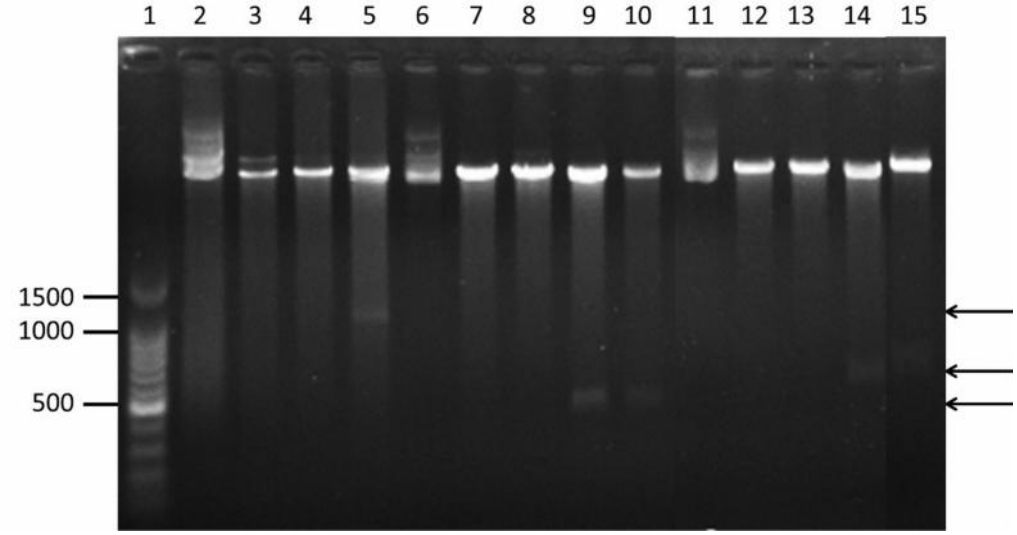

Figure 3.14. – An agarose gel depicting pStaby1.2 NS4 isolated from Z-competent *E. coli* cells and digested with NdeI and XhoI. Lane 1: 100 bp ladder. Lane 2: undigested pStaby-VP7. Lane 3: pStaby-VP7 digested with NdeI. Lane 4: pStaby-VP7 digested with XhoI. Lane 5: pStaby-VP7 digested with NdeI and XhoI. Lane 6: undigested pStaby-NS4-I. Lane 7: pStaby-NS4-I digested with NdeI. Lane 8: pStaby-NS4-I digested with XhoI. Lane 9: pStaby-NS4-I digested with NdeI and XhoI, colony 1. Lane 10: pStaby-NS4-I digested with NdeI and XhoI, colony 8. Lane 11: undigested pStaby-NS4-II. Lane 12: pStaby-NS4-II digested with NdeI. Lane 13: pStaby-NS4-II digested with XhoI. Lane 14: pStaby-NS4-II digested with NdeI and XhoI, colony 3. Lane 15: pStaby-NS4-II digested with NdeI and XhoI, colony 16.

3.3.4.2 Bacterial expression and purification of recombinant NS4

Genes inserted into the pStaby1.2 expression vector are under the control of a T7 promoter. Host cells therefore require a T7 RNA polymerase gene, which is controlled by an IPTG inducible *lacUV5* promoter. The expression of recombinant protein is therefore under the control of the *lac* repressor, which is expressed both from the host genome and the pStaby vector and inhibits the production of the T7 RNA polymerase. BL21(DE3) cells contain an IPTG inducible T7 RNA polymerase gene in the form of a phage λ-DE3 lysogen.

In order to express NS4, BL21(DE3) cells were transformed with the two isolated supercoiled recombinant pStaby-NS4 constructs. The transformants were subjected to small scale plasmid DNA isolation which was analysed with restriction digestion and agarose gel electrophoresis. All of the selected transformants contained plasmid DNA and all of the digested samples contained fragments of ± 500 bp (Fig. 3.15), which confirmed that the isolated plasmid DNA was recombinant. Liquid cultures of BL21(DE3) cells containing pStaby-NS4 were stored at -70°C in 15% glycerol.

Single colonies from BL21(DE3) cells transformed with the isolated pStaby-NS4 DNA were used for small scale protein expression. Cells were harvested at 1 hour post-induction (hpin), 2 hpin and 3 hpin, and

analysed with SDS-PAGE to determine the optimal harvesting time after induction of protein expression, and to compare the expression of NS4 when using fresh transformants or glycerol cultures.

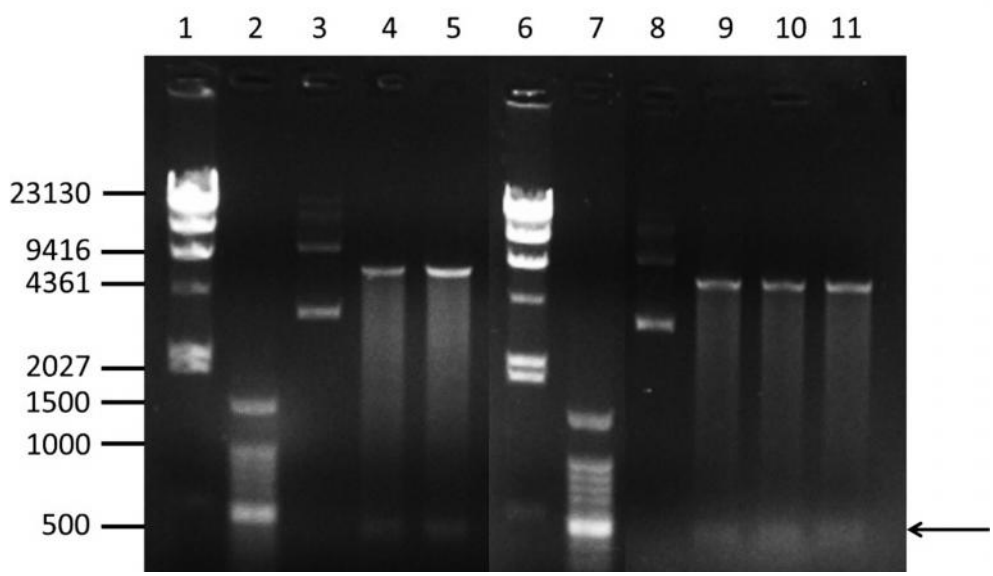

Figure 3.15. – AGE of pStaby-NS4 isolated from transformed BL21(DE3) cells digested with NdeI and XhoI. Lanes 1 and 6: molecular marker II (bp). Lanes 2 and 7: 100 bp ladder (bp). Lane 3: undigested pStaby-NS4-I, colony 1. Lane 4: digested pStaby-NS4-I, colony 1. Lane 5: digested pStaby-NS4-I, colony 2. Lane 8: undigested pStaby-NS4-II, colony 1. Lane 9: digested pStaby-NS4-II, colony 1. Lane 10: digested pStaby-NS4-II, colony 2. Lane 11: digested pStaby-NS4-II, colony 3.

SDS-PAGE of cells containing pStaby-NS4-I and pStaby-NS4-II revealed unique bands of approximately equal intensity for all induced samples in the expected position of each type of NS4 (Fig. 3.16 A and B), which confirmed the expression of NS4 by these cells. pStaby-VP7 was used as a positive expression control and cells transfected with this construct contained a ± 38 kDa band of equal intensity for all induced samples (Fig. 3.16 C), which confirmed the expression of AHSV VP7 by these cells. Uninduced samples also had bands of the corresponding sizes of NS4 or VP7, but at much lower intensities than in the induced samples. These bands probably represent the levels of recombinant protein produced due to leaky expression; the T7 promoter is not fully repressed within the chosen host strain, and some basal expression is expected. However, large amounts of NS4 protein could be expressed with relative ease and NS4 did not appear to have a pronounced toxic effect on BL21(DE3) cells.

The identities of the expressed proteins were confirmed with Western blotting (Fig. 3.17) using anti-NS4 or anti-VP7 with chemiluminescent detection. Unique bands of the expected sizes were again seen in samples containing cells transformed with recombinant pStaby. Therefore, the expressed proteins were indeed NS4 (Fig. 3.17 A) and VP7 (Fig. 3.17 B). These results showed that the NS4-I and NS4-II proteins were successfully expressed at high levels and that the same quantity of protein was present at all times post induction. No significant difference in protein yield was observed between samples obtained using fresh

transformants compared to using stored 15% glycerol cultures. Based on these data, 15% glycerol cultures were used to obtain single colonies and cells were harvested at one hour post induction during large scale protein expression for recombinant protein purification.

Slightly lower levels of NS4-I were detected with Western blotting of these cells compared to SDS-PAGE with Coomassie staining (Fig. 3.16, Fig. 3.17 A). During previous analyses of AHSV infected cells, lower levels of NS4-I were detected compared to NS4-II, but since NS4 could not be detected with SDS-PAGE and Coomassie staining, it was not clear whether the differences were due to differences in expression of the two proteins or differences in anti-NS4 sensitivity to the two types of NS4. The current data suggest that the difference in immunolabelling between the two types of NS4 results from a combination of different expression levels and antibody sensitivity.

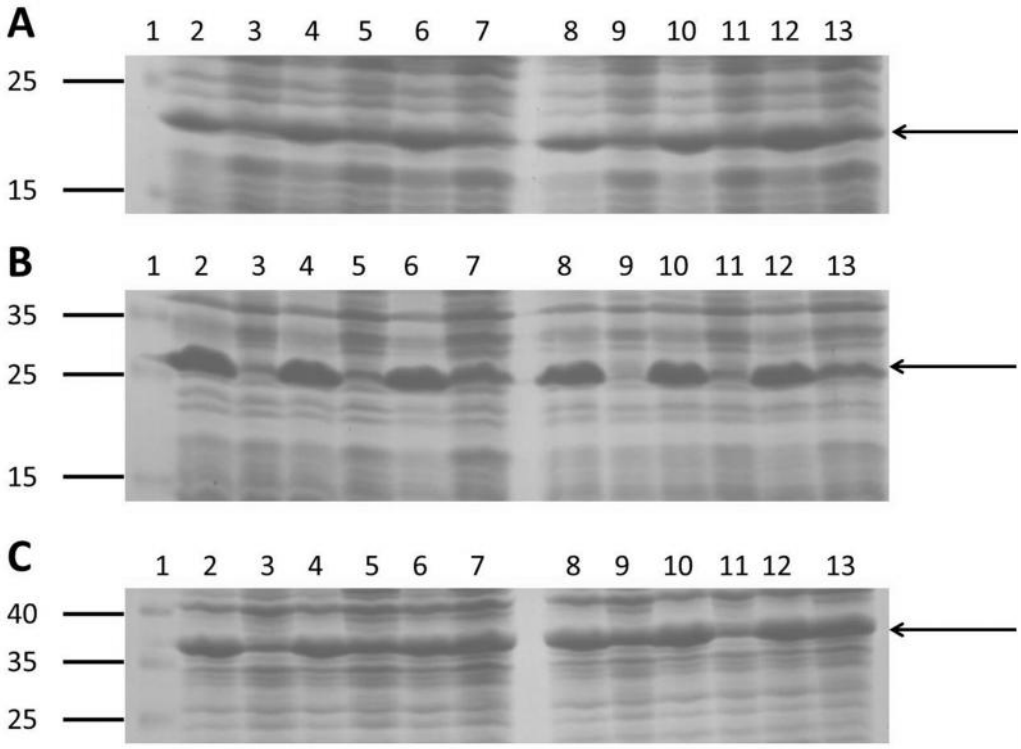

Figure 3.16. – SDS-PAGE of bacterial cells expressing NS4-I (A), NS4-II (B) and VP7 (C). Lane 1: molecular weight marker (kDa). Lanes 2-7 represent cells where fresh transformant colonies were used during expression and Lanes 8-13 represent those where 15% glycerol cultures were used to obtain colonies. Lane 2: 1 hpin, induced. Lane 3: 1 hpin, uninduced. Lane 4: 2 hpin, induced. Lane 5: 2 hpin, uninduced. Lane 6: 3 hpin, induced. Lane 7: 3 hpin, uninduced. Lanes 8-13 contain samples in the same order as in Lanes 2-7.

In order to purify large quantities of recombinant NS4 for use during DNA binding assays, NS4 was expressed in large scale cultures. Cells were harvested at one hour post induction and the wet cell pellet was lysed as per the Protino® Ni-TED affinity purification instructions for native protein purification

(Macherey-Nagel). However, since column purification does not guarantee the removal of all contaminating proteins, no DNaseI was added to prevent interference during the nucleic acid protection assays.

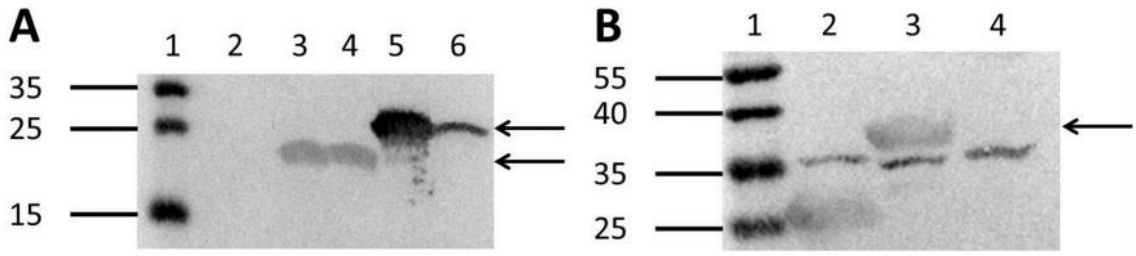

Figure 3.17. – Western blots of cells containing pStaby-NS4 (A) or pStaby-VP7 labelled with anti-NS4 or anti-VP7 at a 1:100 dilution and detected with chemiluminescence. **A.** Lane 1: molecular weight marker (kDa). The lysates of cells transformed with the following constructs were analysed. Lane 2: pStaby-VP7, induced. Lane 3: pStaby-NS4-I, induced. Lane 4: pStaby-NS4-I, uninduced. Lane 5: pStaby-NS4-II, induced. Lane 6: pStaby-NS4-II, uninduced. **B.** Lane 1: molecular weight marker (kDa). Lane 2: pStaby-NS4-II, induced. Lane 3: pStaby-VP7, induced. Lane 4: pStaby-VP7, uninduced. Arrows indicate the positions of NS4 and VP7.

The pellet and supernatant of lysed cells were analysed with SDS-PAGE and Western blotting with anti-NS4 antibody to determine whether NS4 occurs in soluble form in the supernatant. Although the majority of protein was present in the pellet in samples containing NS4 or VP7, unique bands were visible in both the pellet and supernatant of cells expressing NS4 (Fig. 3.18). The large quantities of NS4 seen in the cell pellets could be the result of incomplete cell lysis. These results showed that some soluble NS4 occurs in the supernatant, and that it would be possible to purify the histidine-tagged NS4 with the Ni-TED columns. The cleared supernatants were subjected to column purification and the purified protein in each of the three fractions was analysed with SDS-PAGE (Fig. 3.18 A) and Western blotting (Fig. 3.18 B) to determine which fraction contains the majority of purified protein and analyse the purity of the eluted protein samples. Most NS4 occurred in the first elution fraction (Fig. 3.18, lane 4) and very low levels of contaminating proteins were seen. The first fraction of each type of NS4 was aliquoted and stored at -70°C in 10% glycerol to preserve the native structure of the protein.

The concentration of the purified NS4 protein was next estimated by first determining the percentage purity of NS4 in the first fraction with 4-12% gradient SDS-PAGE and quantification with Image Lab software (Bio-Rad). NS4 constituted approximately 45% of total protein (Fig. 3.19). Thereafter, the total protein concentration in each sample was determined with the Bicinchoninic Acid Protein Assay Kit (BCA kit, Sigma). The concentration of NS4 in each sample was then determined using the percentage purity of the samples. The NS4-I and NS4-II samples had NS4 concentrations of 400 µg/ml and 300 µg/ml, respectively. Purified recombinant NS4 was therefore available for use during subsequent nucleic acid protection assays.

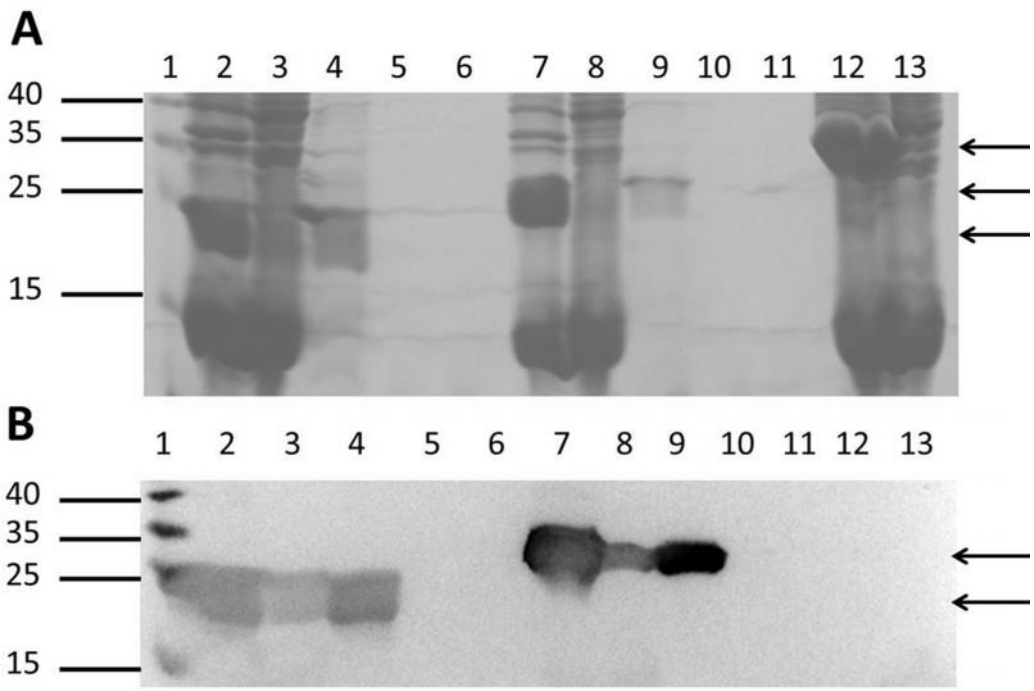

Figure 3.18. – A. SDS-PAGE and **B.** Western blot of the pellets, supernatants and elution fractions of cells expressing NS4. Lane 1: molecular weight marker (kDa). Lane 2: pellet of cells expressing NS4-I. Lane 3: supernatant of cells expressing NS4-I. Lanes 4-6: fractions 1-3 of purified NS4-I. Lane 7: pellet of cells expressing NS4-II. Lane 8: supernatant of cells expressing NS4-II. Lanes 9-11: fractions 1-3 of purified NS4-II. Lane 12: pellet of cells expressing VP7. Lane 13: supernatant of cells expressing VP7. The positions of NS4-I, NS4-II and VP7 are indicated (arrows).

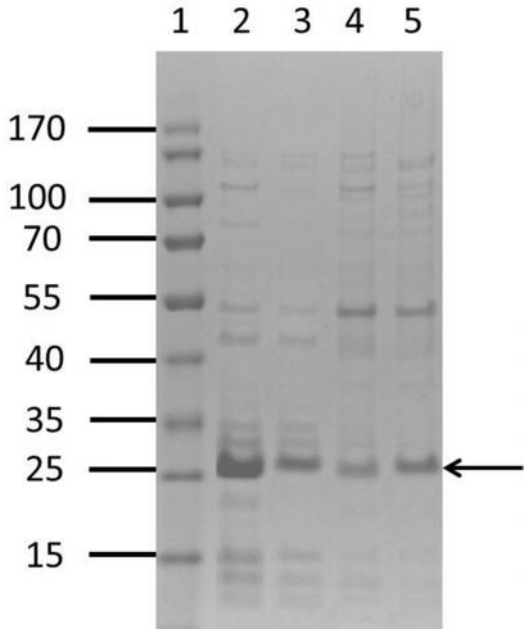

Figure 3.19. – SDS-PAGE of purified NS4. Lane 1: molecular weight marker (kDa). Lanes 2-3: fraction 1 of purified NS4-I. Lanes 4-5: fraction 1 of purified NS4-II.

3.3.4.3 Determining whether AHSV NS4 has nucleic acid binding activity

The bioinformatic analyses of Belhouchet *et al.* (2011) suggested that AHSV NS4 has nucleic acid binding or modifying activity. In order to investigate this property, bacterially expressed and purified NS4 protein was used to perform nucleic acid protection assays based on the approach described by Belhouchet *et al.* (2011).

To determine whether AHSV NS4 binds dsRNA, a dsRNA ladder was incubated with 500 ng of purified recombinant NS4-I or NS4-II prior to treatment with RNaseIII. RNase III digestion of dsRNA yields fragments of 18-21 bp. Incubation of dsRNA with RNase III resulted in degradation (Fig. 3.20, lane 2). Incubation of dsRNA with NS4 alone did not affect the integrity of the RNA (Fig. 20, lanes 3-4). Pre-incubation of dsRNA with NS4 prior to treatment with RNase III did not significantly reduce the amount of dsRNA degradation (Fig. 3.20, lanes 5-6). This suggested that NS4 does not bind dsRNA non-specifically.

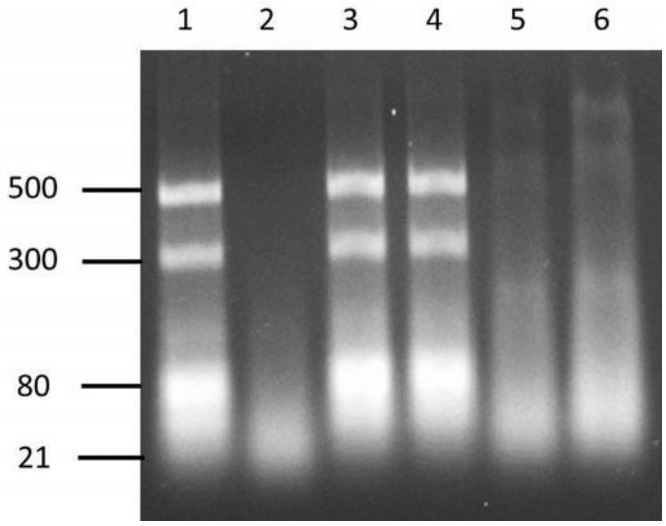

Figure 3.20. – Agarose gel (3% agarose) depicting the NS4 RNA protection assay. Lane 1: dsRNA ladder alone. Lane 2: dsRNA ladder incubated with RNase III. Lane 3: dsRNA ladder incubated with NS4-I. Lane 4: dsRNA ladder incubated with NS4-II. Lane 5: dsRNA ladder incubated with NS4-I and RNase III. Lane 6: dsRNA ladder incubated with NS4-II and RNase III.

To determine whether AHSV NS4 binds dsDNA, a dsDNA ladder was incubated with 500 ng of purified recombinant NS4-I or NS4-II before incubation with DNaseI. DNase I cuts DNA or DNA: RNA hybrids non-specifically to produce di-, tri-, and oligonucleotide fragments. During the dsDNA protection assay, incubation of dsDNA with DNase I resulted in degradation (Fig. 3.21 A, lane 2). Incubation with either type of NS4 alone did not affect DNA integrity (Fig. 3.21 A, lanes 3-4) and no degradation was observed when dsDNA was incubated with NS4 prior to DNase treatment (Fig. 3.21 A, lanes 5-6). This suggests that both types of NS4 can bind dsDNA *in vitro*. Interestingly, the dsDNA ladder appeared to have a different conformation following heat inactivation of the DNaseI enzyme at 99°C (Fig. 3.21 A, lane 1) compared to the native ladder (Fig. 3.21 B). This effect is less pronounced in samples pre-incubated with NS4 (Fig. 3.21 A,

lanes 3-4), suggesting that NS4 reduces DNA denaturation during heating, which is consistent with its ability to bind dsDNA. Reactions inactivated only with EDTA had electrophoresis profiles similar to the native ladder. These results confirm the predicted nucleic acid binding properties of AHSV NS4, which are similar to those of BTV NS4, which also binds dsDNA but not dsRNA. The implications of this DNA binding activity for the viral replication cycle remain to be determined.

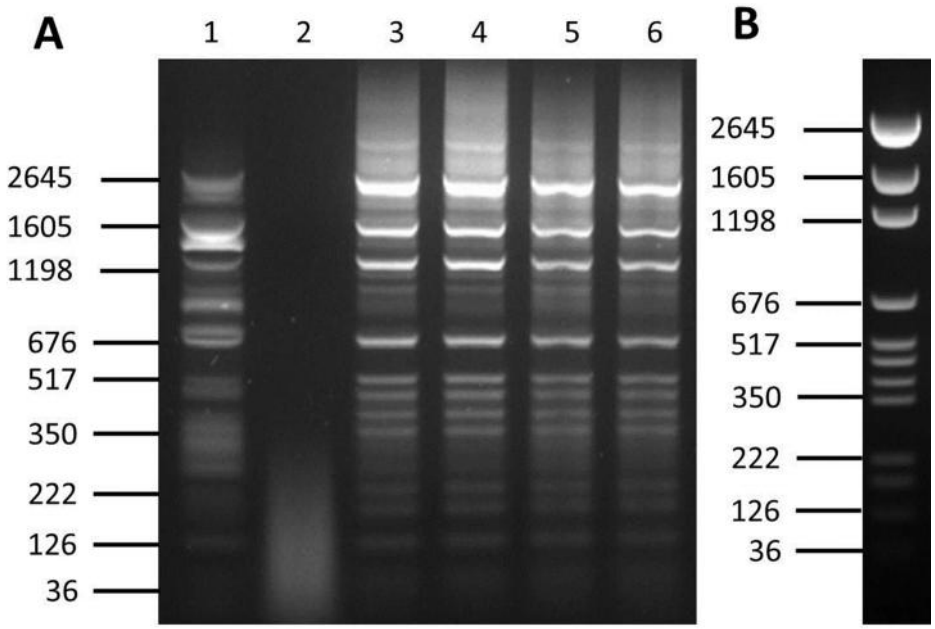

Figure 3.21. – Agarose gel (2% agarose) depicting the NS4 DNA protection assay. **A.** Lane 1: dsDNA ladder alone. Lane 2: dsDNA ladder incubated with DNase I. Lane 3: dsDNA ladder incubated with NS4-I. Lane 4: dsDNA ladder incubated with NS4-II. Lane 5: dsDNA ladder incubated with NS4-I and DNase I. Lane 6: dsDNA ladder incubated with NS4-II and DNase I. **B.** dsDNA ladder not subjected to heat treatment.

3.4 Discussion

A novel putative non-structural protein was recently identified in all orbivirus species but one (St Croix River virus). No homology was found between the putative NS4 protein and other known proteins (FIRTH 2008). The expression of this protein, designated NS4, has been confirmed in the two orbivirus species BTV and GIV (BELHOUCHET *et al.* 2011; RATINIER *et al.* 2011). These authors also studied the properties of NS4 and determined that it localises to the cytoplasm and nucleolus of infected cells, binds nucleic acid and in the case of BTV, confers a replication advantage to some strains and plays a role in pathogenicity within interferon-treated cells (RATINIER *et al.* 2011). The exact function of this novel protein has not yet been determined, and although a putative NS4 gene was proposed to exist within the AHSV genome, it has not yet been subjected to further investigation.

The aim of this part of the study was to determine whether AHSV NS4 is translated and whether it exhibits the predicted intracellular localisation and nucleic acid binding properties. Genome segment 9 sequences

were subjected to *in silico* analysis to compare the predicted NS4 ORF of all nine AHSV serotypes. The expression status of AHSV NS4 was then determined with Western blotting using an antiserum based on the predicted amino acid sequences of the two apparent types of NS4. Thereafter, the intracellular distribution of NS4 within AHSV infected insect and mammalian cells and in Sf9 cells infected with recombinant baculoviruses containing the entire genome segment 9 was investigated by means of confocal microscopy. Finally, the nucleic acid binding activity of NS4 was tested by means of nucleic acid protection assays using dsRNA and dsDNA ladders.

In silico analysis of the genome segment 9 nucleotide sequences of several AHSV isolates, including the currently published sequences AHSV-1 (Genbank: AM883170) (POTGIETER *et al.* 2009), AHSV-3 (Genbank: U19881) and AHSV-6 (Genbank: NC_006019) (TURNBULL *et al.* 1996), showed that the nine AHSV serotypes separate into two main clades, which were designated Clade I and Clade II. The genome segment 9 nucleotide sequences and lengths differ between members of the two clades. The same two clusters were observed when analysing the VP6 and NS4 ORFs and amino acid sequences.

The amount of variation in genome segment 9 nucleotide (65% identity) and VP6 amino acid (54% identity) sequences between serotypes was found to be greater the previously reported 97% and 95% identity, respectively (TURNBULL *et al.* 1996). The latter study compared only AHSV-3 (Genbank: U19881) and AHSV-6 (Genbank: NC_006019). Both of these sequences were most similar to members of Clade II, which could explain the high degree of similarity reported previously. Since the AHSV-6 field strain used during this study contained a genome segment 9 belonging to Clade I, it is possible that reassortment occurred in the more recent AHSV isolate or that the AHSV-6 (Genbank: NC_006019) strain was a laboratory reassortant.

A large amount of variation was also found in the NS4 amino acid sequences of different AHSV serotypes and strains, with most variation observed near the N-terminus. Two main types of NS4 protein appeared to exist that differ in size, ORF position and amino acid sequence, with a 56% amino acid identity between members of the two clades. Within each clade, the amino acid sequences were highly conserved, with a 95% identity between members of Clade I, and an 88% identity within Clade II. The two types of NS4 protein were designated NS4-I (Clade I) and NS4-II (Clade II). All three published nucleotide sequences that are currently available for AHSV genome segment 9 encoded variants of NS4-II. Although the NS4 sequence predicted by Belhouchet *et al.* (2011), which was derived from AHSV-6 (Genbank: NC_006019), encodes a type of NS4-II, it has different start and stop sites compared to the NS4 ORFs of other members within Clade II. The two Bac-VP6 constructs used during this study contained the genome segment 9 of AHSV-3 (Genbank: U19881) and AHSV-6 (Genbank: NC_006019), and therefore encoded variants of NS4-II, rather than NS4-I and NS4-II. Furthermore, since Belhouchet *et al.* (2011) used the sequence AHSV-6 (Genbank: NC_006019) to predict the currently published AHSV NS4 sequence (Genbank: YP_006491216), and since the ORF encoding this sequence occurs at a different position compared to all other members of Clade II, the currently published AHSV NS4 sequence may not be representative of most types of AHSV NS4.

The sequence data were used to produce an antiserum that should detect both types of NS4 across all recent AHSV isolates analysed during this study and to identify AHSV serotypes to use in order to characterise both types of NS4. AHSV-3 and AHSV-4 were selected to represent NS4-II and NS4-I, respectively.

SDS-PAGE and Western blotting of AHSV infected insect and mammalian cell lysates revealed that both types of putative NS4 are indeed translated during infection. The apparent levels of expression in different cell types were much higher in mammalian BSR and Vero cells compared to KC cells. NS4 was more readily detected during Western blotting and confocal microscopy of AHSV-3 infected cells compared to AHSV-4 infected cells. Indeed, NS4-I could not be detected with Western blotting of BSR or KC cells infected with AHSV-4. This was probably due to the generally lower levels of viral protein expression seen in insect cells as well as variation in NS4 expression amongst AHSV serotypes, but it is also possible that the anti-NS4 serum detects one type of NS4 more effectively than the other. This question could be addressed by means of S^{35}-methionine labelling assays, which will enable the quantification NS4 expression levels within infected cells more precisely and in more AHSV serotypes.

Confocal microscopy of AHSV infected mammalian cells confirmed the predicted localisation of AHSV NS4 to the cytoplasm and the nucleus. Although the distribution of NS4 varied somewhat between replicates of the same analysis and between isolates of the same serotype, a general distribution could be described. NS4-II was present from approximately 2 hours after infection and was visible in the nucleus by 18 hpi, whereafter it continued to occur in both the nucleus and cytoplasm. This suggests that NS4 starts to function at early stages of the replication cycle and possibly throughout infection. The distribution of AHSV-3 NS4-II resembled that of BTV NS4, but differed from that of AHSV-4 NS4-I. Although AHSV-4 NS4-I also had a dual cytoplasmic and nuclear distribution, the nuclear NS4 did not form distinct fluorescent foci but rather had a homogeneous appearance.

Furthermore, NS4 fluorescence was generally detected at much lower levels within AHSV-4 infected cells compared to AHSV-3 infected cells, which was consistent with observations made during Western blotting of infected cells. Whether this difference represents different levels of NS4 expression by different serotypes or whether it results from differences in antibody sensitivity to NS4-I and NS4-II, remains to be seen. The fact that recombinant NS4 was detected at lower levels during Western blot analysis with the anti-NS4 serum compared to SDS-PAGE with Coomassie staining suggests that both factors could be involved. The differences in amino acid sequence between the two types of NS4 could account for the slight difference in intracellular localisation. The localisation of NS4 within infected cells was not always consistent at the same times after infection, which could mean that the distribution of NS4 is influenced by factors other than time.

Similar intracellular distributions were seen in Sf9 cells expressing AHSV-3 or AHSV-6 NS4. In these cells, NS4 occurred within the cytoplasm and nucleus from 24 hpi (which corresponds to 6 hours after the strong baculovirus polyhedron promoter controlling the foreign gene becomes active) and this dual localisation was observed until 48 hpi. The distribution of AHSV-3 NS4 within the nucleus resembled that of AHSV-3 infected cells, where distinct round nuclear foci were formed. These foci were less frequently observed in Sf9 cells expressing AHSV-6 NS4, where the nuclear distribution was more often homogeneous. The overall amount of AHSV-6 NS4 fluorescence detected in Sf9 cells was also much lower than the amount of AHSV-3 NS4. Both of the recombinant Bac-VP6 viruses are expected to encode NS4-II variants that contain the same antigenic peptide sequence targeted by the anti-NS4 antibody. Collectively, these results suggest that differences in the levels of expression exist between the two NS4-II variants and that their intracellular distribution is unaffected by the presence of other AHSV proteins (apart from VP6).

Belhouchet *et al.* (2011) and Ratinier *et al.* (2011) showed that the NS4 encoded by BTV and GIV localises to the nucleolus of infected cells. It has been speculated that the nucleolar localisation of NS4 could be involved in the virus-host interaction, potentially allowing a virus with a cytoplasmic replication cycle to modulate the host innate immune response or translation. Since the punctate distribution of AHSV NS4 resembled that of BTV NS4 within the nucleus, the possibility that AHSV NS4 also localises to the nucleolus was investigated with confocal microscopy of AHSV infected BSR cells and Sf9 cells expressing VP6 and NS4. No co-localisation was observed between NS4 and fibrillarin in BSR cells infected with any of several AHSV serotypes, or in Sf9 cells expressing NS4. Rather, when both proteins were detected in the nucleus, they each formed multiple discrete, non-overlapping foci within the nucleus. In the case of AHSV-4 infected cells, where the nuclear fluorescence of NS4 has a more homogeneous appearance, it also failed to overlap with the nuclear fibrillarin foci. This suggests that AHSV NS4 performs a function unrelated to the nucleolus during viral replication and could explain some of the differences between the replication and properties of AHSV and the closely related BTV. The role of NS4 within the nucleus of AHSV infected cells is therefore still unclear, but is likely to differ from that of BTV or GIV NS4. Further investigations will be required to determine with which cellular structures AHSV NS4 co-localises.

Interestingly, the predicted nuclear localisation sequences were absent from all types of NS4 protein identified during this study apart from AHSV-3 (Genbank: U19881) and AHSV-6 (Genbank: NC_006019), which were used to construct the recombinant baculoviruses used during the study. This did not appear to affect the nuclear localisation of AHSV NS4, since nuclear foci were formed regardless of the presence or absence of the region predicted to contain the putative nuclear localisation signals. Further studies will be required to determine the mechanism by which AHSV NS4 localises to the nucleus.

Recombinant NS4 was expressed in bacteria and purified for use during nucleic acid protection assays. The StabyExpress™ T7 expression system was used with some modifications. Codon optimised NS4 genes based on the two main recent types of NS4 were subcloned into the expression host and purified by means of the

Protino® Ni-TED system for affinity purification His-tagged proteins. Recombinant NS4 could be expressed at sufficient levels and did not appear to have any significant toxic effect on the host cells, and since some soluble NS4 could be isolated from the cells, the native 6xHis-tagged proteins could be purified and remained stable in the presence of 15% glycerol in elution buffer at -70°C for at least two months.

The predicted nucleic acid binding or modifying properties of AHSV NS4 (BELHOUCHET *et al.* 2011) were investigated by means of dsDNA or dsRNA protection assays, which showed that both types of AHSV NS4 bind dsDNA, but not dsRNA. This is also the case for BTV NS4 (BELHOUCHET *et al.* 2011). Since AHSV NS4 occurs in the nucleus and binds dsDNA, but does not localise to the nucleolus, it seems possible that NS4 binds to host DNA within the nucleus. Further studies will be required to investigate this possibility.

Chapter 4:
Concluding remarks

Concluding remarks

The aims of this study were firstly to describe the intracellular distribution of AHSV NS1 throughout infection and to determine whether NS1 co-localises with other AHSV proteins, and secondly to characterise the properties of AHSV NS4 and to determine whether they coincide with those predicted by means of bioinformatic analysis. The distribution and co-localisation of NS1 with other AHSV proteins were investigated by means of confocal- and transmission electron microscopy of cells infected with AHSV and cells co-expressing NS1 or NS1-eGFP with VP3 or VP7. Western blotting of AHSV or Bac-VP6 infected cells was used to determine whether AHSV NS4 is translated. The distribution of NS4 was visualised with confocal microscopy of AHSV or Bac-VP6 infected cells. Finally, the nucleic acid binding properties of NS4 were investigated with DNA and RNA protection assays.

NS1-eGFP was proven to be an effective system for the study of NS1 localisation within the cell. In Sf9 cells visualised with confocal microscopy, NS1 formed small foci scattered throughout the cytoplasm which gradually converged into large fluorescent tubule bundles as infection progresses. In AHSV-infected cells, NS1 could be detected from as early as 2-4 hpi. Well-defined NS1 tubule bundles could be seen from 18-24 hpi and occupied a large proportion of the cytoplasm of infected cells by 48 hpi. Tubule bundle morphology differed between Sf9 cells and AHSV-infected BSR or KC cells. Tubule bundles were more neatly arranged in the latter, with individual tubules organised in parallel to each other. In Sf9 cells, tubules were arranged randomly within each bundle, forming nest-like aggregates within the cytoplasm. This suggests that tubule bundle formation requires the presence of other viral proteins during tubule bundle assembly or more stringent regulation of NS1 translation. Host cell factors could also play a role. Merely trafficking NS1 protein to a particular site within the cell might not be sufficient for the formation of the NS1 tubule bundles characteristic of orbivirus infection.

Confocal microscopy and TEM showed that NS1 and VP7 co-localised in a small subset of visualised cells infected with AHSV or co-expressing NS1 and VP7. However, confocal microscopy revealed that when NS1-eGFP was co-expressed with VP7 in Sf9 cells, significant amounts of VP7 co-localised with the large fluorescent NS1-eGFP tubule bundles throughout the cytoplasm, forming halo-like rings around each focus. The insertion of eGFP near the NS1 C-terminus appeared to induce a co-localisation between NS1 and VP7. This could suggest that NS1 has a latent ability to interact with VP7 that is abolished upon tubulisation and that the addition of eGFP to NS1 induces a conformational change in the protein that restores the ability of the tubulised NS1 to bind VP7. It is also possible that eGFP interacts with VP7. TEM analysis of cells co-expressing NS1-eGFP and VP7 will be required to visualise this co-localisation at a high resolution. It is not expected that the co-localisation of insoluble NS1 and VP7 is of functional significance, but rather that the observation of a co-localisation is an artifact of an interaction at another stage of viral replication. It is possible that unpolymerised NS1 interacts with VP7 during viral particle formation and free NS1 is inactivated by sequestration in tubules. The possibility of an interaction between AHSV NS1 and VP3 could

not be studied during this investigation due to low expression levels of VP3 or low sensitivity of the available anti-VP3 serum. This interaction could be investigated by more robust means, perhaps with a fluorescently tagged version of VP3 or a more sensitive antiserum. Further studies will be required to determine the exact role of NS1 during viral replication. The data obtained during this study could provide a valuable basis for functional analyses of NS1.

To characterise the NS4 proteins within the species, nucleotide sequences of all nine AHSV serotypes were subjected to *in silico* analysis. A large amount of variation was observed between the NS4 proteins encoded by the nine AHSV serotypes, which could be useful for identifying genetic differences that confer differences in pathogenicity and virulence amongst serotypes during future studies. Two main types of NS4 appeared to exist amongst AHSV serotypes that differed in length and amino acid sequence. These proteins were designated NS4-I and NS4-II.

Western blotting showed that AHSV-3 NS4-II is produced by mammalian and insect cells and that AHSV-4 NS4-I is present in mammalian cells. The generally low levels of NS4-I expression, coupled with the low overall levels of viral protein synthesis in insect cells, seemed to be responsible for the failure to detect NS4 in these cells. Future studies will be required to determine whether the NS4-I is produced in AHSV infected insect cells. Western blotting of Sf9 cells infected with Bac-AHSV3-VP6 or Bac-AHSV6-VP6 showed that the NS4-II variants encoded by these baculoviruses were expressed. These variants were predicted to encode variants of NS4-II, and to have different start and stop sites. These results confirmed that both types of NS4 are translated in AHSV infected cells and in the absence of most other AHSV proteins.

The intracellular distribution of NS4 was examined with confocal microscopy. The proteins localised to the nucleus and cytoplasm of AHSV infected cells as predicted. NS4 was detected in the cytoplasm from 4-6 hours post infection (hpi) and in both the cytoplasm and the nucleus from 18 hpi until 48 hpi. NS4-II produced in AHSV-3 infected cells formed punctate foci in the nuclei of infected cells, whereas NS4-I had a diffuse nuclear distribution in AHSV-4 infected cells. The distribution of the NS4-II variants produced by Bac-VP6 infected Sf9 cells was similar to that seen in AHSV infected cells, with a diffuse cytoplasmic distribution and occasional nuclear foci. A diffuse nuclear distribution was more frequently observed in Sf9 cells infected with Bac-AHSV6-VP6, which could reflect differences in localisation or levels of expression between the NS4-II variants. Further analyses will be necessary to quantify the differences in NS4 expression levels between AHSV serotypes. The predicted distribution of AHSV NS4 was confirmed and shown to be independent of other AHSV proteins apart from VP6. Furthermore, it was shown that cells infected with AHSV serotypes belonging to the same NS4 clade had a similar intracellular NS4 distribution. This suggested that the two types of NS4 predicted to be produced by members of the two clades had been correctly identified and that the amino acid sequence differences between the two types of NS4 altered their intracellular distribution.

Since the punctate distribution of AHSV NS4 within the nucleus resembled that of BTV NS4 (BELHOUCHET *et al.* 2011; RATINIER *et al.* 2011), which localised to the nucleolus, cells were subjected to confocal microscopy with co-immunolabelling of NS4 and the nucleolar marker fibrillarin in order to determine whether AHSV NS4 also localises to the nucleolus. Although fibrillarin and NS4 both formed punctate foci within the nuclei of infected cells, they did not co-localise in cells infected with AHSV or Bac-VP6. This showed that AHSV NS4 does not localise to the nucleolus.

Finally, nucleic acid protection assays showed that both types of NS4 bind dsDNA non-specifically, but not dsRNA. This is similar to BTV NS4, but different from GIV NS4, which binds both dsDNA and dsRNA. The functional significance of this interaction is not clear, although the fact that NS4 occurs in the nucleus suggests that an interaction with DNA, either directly or via other host proteins, could be of functional significance during the viral replication cycle. It is also possible that NS4 functions in the cytoplasm of infected cells. The fact that both types of NS4 can bind DNA suggests that the regions or secondary structures conserved between the two different proteins are involved in this binding activity. Future studies will be required to determine which regions are involved in the nucleic acid binding activity of NS4 and may also include more detailed analysis of the different NS4 sequences and the identification of additional interactions between NS4 and viral or host factors. The preliminary information regarding the properties of AHSV NS4 and the broad identification of regions involved in these properties in conjunction with the recently developed reverse genetics system for AHSV should provide a basis for the functional characterisation of AHSV NS4, particularly with regard to identifying genetic determinants of pathogenicity and virulence.

Viral proteins involved in pathogenesis include NS1, NS3 and NS4. The recent development of a reverse genetics system to study AHSV enables a more accurate analysis of the role of these proteins in viral pathogenesis and replication. The data regarding the properties of AHSV NS1 and NS4 obtained during this study provides an excellent basis for the functional characterisation of these proteins by means of a new reverse genetics system for AHSV (J. Theron, Department of Microbiology, University of Pretoria).

Acknowledgements

We would like to acknowledge Mr Flip Wege for his excellent cell culture and advice; Eudri Venter for his assistance, especially transmission electron microscopy (TEM); Orbivirus research group members for advice and support; Mr Alan Hall for his assistance with confocal microscopy and Mr Chris van der Merwe (Laboratory for Microscopy and Microanalysis, University of Pretoria) for his support, technical expertise and assistance with TEM; Prof Jacques Theron for his advice and assistance; and Prof Henk Huismans for his insight and discussions. This study was supported by funding from the National Research Foundation (NRF), the Poliomyelitis Research Foundation (PRF) and the University of Pretoria.

References

ALEXANDER, K. A., P. W. KAT, J. HOUSE, C. HOUSE, S. J. O'BRIEN *et al.*, 1995 African horse sickness and African carnivores. Veterinary Microbiology 47: 133-140.

ANDERSON, J., S. HAGGLUND, E. BREARD, L. COMTET, K. LOVGREN BENGTSSON *et al.*, 2013 Evaluation of the immunogenicity of an experimental subunit vaccine that allows differentiation between infected and vaccinated animals against bluetongue virus serotype 8 in cattle. Clin Vaccine Immunol 20: 1115-1122.

ANSARI, M. A., E. C. POPE, S. CARPENTER, E. J. SCHOLTE and T. M. BUTT, 2011 Entomopathogenic fungus as a biological control for an important vector of livestock disease: the Culicoides biting midge. PLoS One 6: e16108.

ATTOUI, H., S. MAAN, S. J. ANTHONY and P. P. C. MERTENS, 2009 Chapter 3 Bluetongue virus, other orbiviruses and other reoviruses: Their relationships and taxonomy, pp. 23-52 in *Bluetongue*

edited by R. NOAD and P. ROY.

BAETZA, H. J., 2013 Eradication of bluetongue disease in Germany by vaccination. Vet Immunol Immunopathol.

BARNARD, B. J., 1998 Epidemiology of African horse sickness and the role of the zebra in South Africa. Arch Virol Suppl 14: 13-19.

BAYLIS, M., H. PARKIN, K. KREPPEL, S. CARPENTER, P. S. MELLOR *et al.*, 2010 Evaluation of housing as a means to protect cattle from Culicoides biting midges, the vectors of bluetongue virus. Med Vet Entomol 24: 38-45.

BEATON, A. R., J. RODRIGUEZ, Y. K. REDDY and P. ROY, 2002 The membrane trafficking protein calpactin forms a complex with bluetongue virus protein NS3 and mediates virus release. Proc Natl Acad Sci U S A 99: 13154-13159.

BELHOUCHET, M., F. MOHD JAAFAR, A. E. FIRTH, J. M. GRIMES, P. P. MERTENS *et al.*, 2011 Detection of a fourth orbivirus non-structural protein. PLoS One 6: e25697.

BHATTACHARYA, B., R. J. NOAD and P. ROY, 2007 Interaction between Bluetongue virus outer capsid protein VP2 and vimentin is necessary for virus egress. Virol J 4: 7.

BHATTACHARYA, B., and P. ROY, 2008 Bluetongue Virus Outer Capsid Protein VP5 Interacts with Membrane Lipid Rafts via a SNARE Domain. J. Virol. 82: 10600-10612.

BHATTACHARYA, B., and P. ROY, 2013 Cellular phosphoinositides and the maturation of bluetongue virus, a non-enveloped capsid virus. Virol J 10: 73.

BINEPAL, V. S., B. N. WARIRU, F. G. DAVIES, R. SOI and R. OLUBAYO, 1992 An attempt to define the host range for African horse sickness virus (Orbivirus, reoviridae) in East Africa, by a serological survey in some equidae, camelidae, loxodontidae and carnivore. Veterinary Microbiology 31: 19-23.

BOONE, J. D., U. B. BALASURIYA, K. KARACA, J. C. AUDONNET, J. YAO *et al.*, 2007 Recombinant canarypox virus vaccine co-expressing genes encoding the VP2 and VP5 outer capsid proteins of bluetongue virus induces high level protection in sheep. Vaccine 25: 672-678.

BOUWKNEGT, C., P. A. VAN RIJN, J. J. SCHIPPER, D. HOLZEL, J. BOONSTRA *et al.*, 2010 Potential role of ticks as vectors of bluetongue virus. Exp Appl Acarol 52: 183-192.

BOYCE, M., C. C. CELMA and P. ROY, 2008 Development of reverse genetics systems for bluetongue virus: recovery of infectious virus from synthetic RNA transcripts. J Virol 82: 8339-8348.

BOYCE, M., C. C. CELMA and P. ROY, 2012 Bluetongue virus non-structural protein 1 is a positive regulator of viral protein synthesis. Virol J 9: 178.

BOYCE, M., and P. ROY, 2007 Recovery of infectious bluetongue virus from RNA. J Virol 81: 2179-2186.

BOYCE, M., J. WEHRFRITZ, R. NOAD and P. ROY, 2004 Purified recombinant bluetongue virus VP1 exhibits RNA replicase activity. J Virol 78: 3994-4002.

BRAVERMAN, Y., and A. CHIZOV-GINZBURG, 1996 Role of dogs (Canis domesticus) as hosts for African horse sickness virus. Veterinary Microbiology 51: 19-25.

BROOKES, S. M., A. D. HYATT and B. T. EATON, 1993 Characterization of virus inclusion bodies in bluetongue virus-infected cells. J Gen Virol 74 (Pt 3): 525-530.

BURROUGHS, J. N., R. S. O'HARA, C. J. SMALE, C. HAMBLIN, A. WALTON *et al.*, 1994 Purification and properties of virus particles, infectious subviral particles, cores and VP7 crystals of African horsesickness virus serotype 9. J Gen Virol 75 (Pt 8): 1849-1857.

CANTOR, G. H., 1996 A Potential Proline-Rich Motif Upstream of the Immunoreceptor Tyrosine-Based Activation Motif in Bovine Leukemia Virus gp30, Epstein-Barr Virus LMP2A, Herpesvirus Papio LMP2A, and African Horsesickness Virus VP7. Virology 220: 265-266.

CELMA, C. C., M. BOYCE, P. A. VAN RIJN, M. ESCHBAUMER, K. WERNIKE *et al.*, 2013 Rapid Generation of Replication-Deficient Monovalent and Multivalent Vaccines for Bluetongue Virus: Protection against Virulent Virus Challenge in Cattle and Sheep. J Virol 87: 9856-9864.

CELMA, C. C. P., and P. ROY, 2009 A Viral Nonstructural Protein Regulates Bluetongue Virus Trafficking and Release. J. Virol. 83: 6806-6816.

CELMA, C. C. P., and P. ROY, 2011 Interaction of calpactin light chain (S100A10/p11) and a viral NS protein is essential for intracellular trafficking of non-enveloped Bluetongue virus. J. Virol.: JVI.02352-02310.

CHAUVEAU, E., V. DOCEUL, E. LARA, E. BREARD, C. SAILLEAU *et al.*, 2013 NS3 of bluetongue virus interferes with the induction of type I interferon. J Virol 87: 8241-8246.

CLIFT, S. J., and M. L. PENRITH, 2010 Tissue and cell tropism of African horse sickness virus demonstrated by immunoperoxidase labeling in natural and experimental infection in horses in South Africa. Vet Pathol 47: 690-697.

DARPEL, K. E., K. F. LANGNER, M. NIMTZ, S. J. ANTHONY, J. BROWNLIE *et al.*, 2011 Saliva proteins of vector culicoides modify structure and infectivity of bluetongue virus particles. PLoS One 6: e17545.

DE WAAL, P. J., 2005 The characterization of inner core protein VP6 of African Horsesickness Virus, pp. 1-167 in *Department of Genetics*. University of Pretoria, Pretoria.

DE WAAL, P. J., and H. HUISMANS, 2005 Characterization of the nucleic acid binding activity of inner core protein VP6 of African horse sickness virus. Arch Virol.

DIPROSE, J. M., J. N. BURROUGHS, G. C. SUTTON, A. GOLDSMITH, P. GOUET *et al.*, 2001 Translocation portals for the substrates and products of a viral transcription complex: the bluetongue virus core. Embo J 20: 7229-7239.

DIPROSE, J. M., J. M. GRIMES, G. C. SUTTON, J. N. BURROUGHS, A. MEYER *et al.*, 2002 The core of bluetongue virus binds double-stranded RNA. J Virol 76: 9533-9536.

DU PLESSIS, M., M. CLOETE, H. AITCHISON and A. A. VAN DIJK, 1998 Protein aggregation complicates the development of baculovirus-expressed African horsesickness virus serotype 5 VP2 subunit vaccines. Onderstepoort J Vet Res 65: 321-329.

DU PLESSIS, M., and L. H. NEL, 1997 Comparative sequence analysis and expression of the M6 gene, encoding the outer capsid protein VP5, of African horsesickness virus serotype nine. Virus Res 47: 41-49.

DUNGU, B., C. POTGIETER, B. VON TEICHMAN and T. SMIT, 2004 Vaccination in the control of bluetongue in endemic regions: the South African experience. Dev Biol (Basel) 119: 463-472.

EATON, B. T., A. D. HYATT and J. R. WHITE, 1987a Association of bluetongue virus with the cytoskeleton. Virology 157: 107-116.

EATON, B. T., A. D. HYATT and J. R. WHITE, 1987b Association of bluetongue virus with the cytoskeleton. Virology 157: 107-116.

EATON, B. T., A. D. HYATT and J. R. WHITE, 1988 Localization of the nonstructural protein NS1 in bluetongue virus-infected cells and its presence in virus particles. Virology 163: 527-537.

FIRTH, A. E., 2008 Bioinformatic analysis suggests that the Orbivirus VP6 cistron encodes an overlapping gene. Virol J 5: 48.

FORZAN, M., M. MARSH and P. ROY, 2007 Bluetongue virus entry into cells. J Virol 81: 4819-4827.

FRENCH, T. J., J. J. MARSHALL and P. ROY, 1990 Assembly of double-shelled, viruslike particles of bluetongue virus by the simultaneous expression of four structural proteins. J Virol 64: 5695-5700.

FRENCH, T. J., and P. ROY, 1990 Synthesis of bluetongue virus (BTV) corelike particles by a recombinant baculovirus expressing the two major structural core proteins of BTV. J. Virol. 64: 1530-1536.

FUJIWARA, T., D. GIESMAN-COOKMEYER, B. DING, S. A. LOMMEL and W. J. LUCAS, 1993 Cell-to-Cell Trafficking of Macromolecules through Plasmodesmata Potentiated by the Red Clover Necrotic Mosaic Virus Movement Protein. Plant Cell 5: 1783-1794.

GHOSH, M. K., E. DERIAUD, M. F. SARON, R. LO-MAN, T. HENRY *et al.*, 2002 Induction of protective antiviral cytotoxic T cells by a tubular structure capable of carrying large foreign sequences. Vaccine 20: 1369-1377.

GOLD, S., P. MONAGHAN, P. MERTENS and T. JACKSON, 2010 A clathrin independent macropinocytosis-like entry mechanism used by bluetongue virus-1 during infection of BHK cells. PLoS One 5: e11360.

GOUET, P., J. M. DIPROSE, J. M. GRIMES, R. MALBY, J. N. BURROUGHS *et al.*, 1999 The highly ordered double-stranded RNA genome of bluetongue virus revealed by crystallography. Cell 97: 481-490.

GRIMES, J., A. K. BASAK, P. ROY and D. STUART, 1995 The crystal structure of bluetongue virus VP7. Nature 373: 167-170.

GRIMES, J. M., J. N. BURROUGHS, P. GOUET, J. M. DIPROSE, R. MALBY *et al.*, 1998 The atomic structure of the bluetongue virus core. Nature 395: 470-478.

GRUBMAN, M. J., 1990 Expression of bluetongue virus serotype 17 NS1 protein from a cloned gene. Virus Res 18: 21-28.

GU, L., V. MUSIIENKO, Z. BAI, A. QIN, S. W. SCHNELLER *et al.*, 2012 Novel virostatic agents against bluetongue virus. PLoS One 7: e43341.

GUIS, H., C. CAMINADE, C. CALVETE, A. P. MORSE, A. TRAN *et al.*, 2012 Modelling the effects of past and future climate on the risk of bluetongue emergence in Europe. J R Soc Interface 9: 339-350.

HAMBLIN, C., J. S. SALT, P. S. MELLOR, S. D. GRAHAM, P. R. SMITH *et al.*, 1998 Donkeys as reservoirs of African horse sickness virus. Arch Virol Suppl 14: 37-47.

HASSAN, S. H., C. WIRBLICH, M. FORZAN and P. ROY, 2001 Expression and functional characterization of bluetongue virus VP5 protein: role in cellular permeabilization. J Virol 75: 8356-8367.

HASSAN, S. S., and P. ROY, 1999 Expression and functional characterization of bluetongue virus VP2 protein: role in cell entry. J Virol 73: 9832-9842.

HEMATI, B., V. CONTRERAS, C. URIEN, M. BONNEAU, H. H. TAKAMATSU *et al.*, 2009 Bluetongue virus targets conventional dendritic cells in skin lymph. J Virol 83: 8789-8799.

HEWAT, E. A., T. F. BOOTH, R. H. WADE and P. ROY, 1992 3-D reconstruction of bluetongue virus tubules using cryoelectron microscopy. J Struct Biol 108: 35-48.

HOFFMANN, B., B. BAUER, C. BAUER, H. J. BATZA, M. BEER *et al.*, 2009 Monitoring of putative vectors of bluetongue virus serotype 8, Germany. Emerg Infect Dis 15: 1481-1484.

HOUSE, J. A., 1993 African horse sickness. Vet Clin North Am Equine Pract 9: 355-364.

HUANG, Z., Y. HAN and S. H. HOWELL, 2000 Formation of surface tubules and fluorescent foci in Arabidopsis thaliana protoplasts expressing a fusion between the green fluorescent protein and the cauliflower mosaic virus movement protein. Virology 271: 58-64.

HUISMANS, H., 1979 Protein synthesis in bluetongue virus-infected cells. Virology 92: 385-396.

HUISMANS, H., and H. J. ELS, 1979 Characterization of the tubules associated with the replication of three different orbiviruses. Virology 92: 397-406.

HYATT, A. D., and B. T. EATON, 1988 Ultrastructural distribution of the major capsid proteins within bluetongue virus and infected cells. J Gen Virol 69 (Pt 4): 805-815.

HYATT, A. D., Y. ZHAO and P. ROY, 1993 Release of bluetongue virus-like particles from insect cells is mediated by BTV nonstructural protein NS3/NS3A. Virology 193: 592-603.

IWATA, H., M. YAMAGAWA and P. ROY, 1992 Evolutionary relationships among the gnat-transmitted orbiviruses that cause African horse sickness, bluetongue, and epizootic hemorrhagic disease as evidenced by their capsid protein sequences. Virology 191: 251-261.

KAR, A. K., B. BHATTACHARYA and P. ROY, 2007 Bluetongue virus RNA binding protein NS2 is a modulator of viral replication and assembly. BMC Mol Biol 8: 4.

KAR, A. K., M. GHOSH and P. ROY, 2004 Mapping the assembly pathway of Bluetongue virus scaffolding protein VP3. Virology 324: 387-399.

KAR, A. K., and P. ROY, 2003 Defining the structure-function relationships of bluetongue virus helicase protein VP6. J Virol 77: 11347-11356.

KAWAKAMI, S., Y. WATANABE and R. N. BEACHY, 2004 Tobacco mosaic virus infection spreads cell to cell as intact replication complexes. Proc Natl Acad Sci U S A 101: 6291-6296.

LACHEINER, K., 2006 Tubules composed of non-structural protein NS1 of african horsesickness virus as a system for the immune display of foreign peptides., pp. 1-155 in *Department of Genetics*. University of Pretoria, Pretoria.

LAPORTE, C., G. VETTER, A. M. LOUDES, D. G. ROBINSON, S. HILLMER *et al.*, 2003 Involvement of the secretory pathway and the cytoskeleton in intracellular targeting and tubule assembly of Grapevine fanleaf virus movement protein in tobacco BY-2 cells. Plant Cell 15: 2058-2075.

LARKE, N., A. MURPHY, C. WIRBLICH, D. TEOH, M. J. ESTCOURT *et al.*, 2005 Induction of human immunodeficiency virus type 1-specific T cells by a bluetongue virus tubule-vectored vaccine prime-recombinant modified virus Ankara boost regimen. J Virol 79: 14822-14833.

LE BLOIS, H., and P. ROY, 1993 A single point mutation in the VP7 major core protein of bluetongue virus prevents the formation of core-like particles. J Virol 67: 353-359.

LI, Q., C. MADDOX, L. RASMUSSEN, J. V. HOBRATH and L. E. WHITE, 2009 Assay development and high-throughput antiviral drug screening against Bluetongue virus. Antiviral Res 83: 267-273.

LIEBISCH, G., and A. LIEBISCH, 2008 [Efficacy of Flectron-eartags (cypermethrin) for control of midges (Culicoides) the vectors of bluetongue virus in cattle: field studies and biossays]. Dtsch Tierarztl Wochenschr 115: 220-230.

LIMN, C. K., N. STAEUBER, K. MONASTYRSKAYA, P. GOUET and P. ROY, 2000 Functional dissection of the major structural protein of bluetongue virus: identification of key residues within VP7 essential for capsid assembly. J Virol 74: 8658-8669.

LORD, C. C., M. E. J. WOOLHOUSE and P. S. MELLOR, 1997 Simulation studies of vaccination strategies in African horse sickness. Vaccine 15: 519-524.

LOUDON, P. T., and P. ROY, 1991 Assembly of five bluetongue virus proteins expressed by recombinant baculoviruses: inclusion of the largest protein VP1 in the core and virus-like proteins. Virology 180: 798-802.

MACLACHLAN, N. J., U. B. BALASURIYA, N. L. DAVIS, M. COLLIER, R. E. JOHNSTON *et al.*, 2007 Experiences with new generation vaccines against equine viral arteritis, West Nile disease and African horse sickness. Vaccine 25: 5577-5582.

MACLACHLAN, N. J., and A. J. GUTHRIE, 2010 Re-emergence of bluetongue, African horse sickness, and other Orbivirus diseases. Vet Res 41: 35.

MACLACHLAN, N. J., and C. E. MAYO, 2013 Potential strategies for control of bluetongue, a globally emerging, Culicoides-transmitted viral disease of ruminant livestock and wildlife. Antiviral Res 99: 79-90.

MANOLE, V., P. LAURINMAKI, W. VAN WYNGAARDT, C. A. POTGIETER, I. M. WRIGHT *et al.*, 2012 Structural insight into African horsesickness virus infection. J Virol 86: 7858-7866.

MARCHI, P. R., P. RAWLINGS, J. N. BURROUGHS, M. WELLBY, P. P. MERTENS *et al.*, 1995 Proteolytic cleavage of VP2, an outer capsid protein of African horse sickness virus, by species-specific serum proteases enhances infectivity in Culicoides. J Gen Virol 76 (Pt 10): 2607-2611.

MAREE, F. F., and H. HUISMANS, 1997 Characterization of tubular structures composed of nonstructural protein NS1 of African horsesickness virus expressed in insect cells. J Gen Virol 78 (Pt 5): 1077-1082.

MAREE, S., S. DURBACH and H. HUISMANS, 1998 Intracellular production of African horsesickness virus core-like particles by expression of the two major core proteins, VP3 and VP7, in insect cells. J Gen Virol 79 (Pt 2): 333-337.

MARKOTTER, W., J. THERON and L. H. NEL, 2004 Segment specific inverted repeat sequences in bluetongue virus mRNA are required for interaction with the virus non structural protein NS2. Virus Research 105: 1-9.

MARTINEZ-COSTAS, J., G. SUTTON, N. RAMADEVI and P. ROY, 1998 Guanylyltransferase and RNA 5'-triphosphatase activities of the purified expressed VP4 protein of bluetongue virus. Journal of Molecular Biology 280: 859-866.

MATSUO, E., C. C. CELMA, M. BOYCE, C. VIAROUGE, C. SAILLEAU *et al.*, 2011 Generation of replication-defective virus-based vaccines that confer full protection in sheep against virulent bluetongue virus challenge. J Virol 85: 10213-10221.

MATSUO, E., C. C. CELMA and P. ROY, 2010 A reverse genetics system of African horse sickness virus reveals existence of primary replication. FEBS Lett 584: 3386-3391.

MATSUO, E., and P. ROY, 2009 Bluetongue virus VP6 acts early in the replication cycle and can form the basis of chimeric virus formation. J Virol 83: 8842-8848.

MATSUO, E., and P. ROY, 2011 Bluetongue virus VP1 polymerase activity in vitro: template dependency, dinucleotide priming and cap dependency. PLoS One 6: e27702.

MEHLHORN, H., V. WALLDORF, S. KLIMPEL, G. SCHAUB, E. KIEL *et al.*, 2009a Bluetongue disease in Germany (2007-2008): monitoring of entomological aspects. Parasitol Res 105: 313-319.

MEHLHORN, H., V. WALLDORF, S. KLIMPEL, G. SCHMAHL, S. AL-QURAISHY *et al.*, 2009b Entomological survey on vectors of Bluetongue virus in Northrhine-Westfalia (Germany) during 2007 and 2008. Parasitol Res 105: 321-329.

MEISWINKEL, R., M. BAYLIS and K. LABUSCHAGNE, 2000 Stabling and the protection of horses from Culicoides bolitinos (Diptera: Ceratopogonidae), a recently identified vector of African horse sickness. Bull Entomol Res 90: 509-515.

MEISWINKEL, R., and J. T. PAWESKA, 2003 Evidence for a new field Culicoides vector of African horse sickness in South Africa. Preventive Veterinary Medicine 60: 243-253.

MELLOR, P. S., 1994 Epizootiology and vectors of African horse sickness virus. Comp Immunol Microbiol Infect Dis 17: 287-296.

MELLOR, P. S., and J. BOORMAN, 1995 The transmission and geographical spread of African horse sickness and bluetongue viruses. Ann Trop Med Parasitol 89: 1-15.

MELLOR, P. S., J. BOORMAN and M. JENNINGS, 1975 The multiplication of African horse-sickness virus in two species of Culicoides (Diptera, Ceratopogonidae). Arch Virol 47: 351-356.

MERTENS, P. P., J. N. BURROUGHS, A. WALTON, M. P. WELLBY, H. FU *et al.*, 1996 Enhanced infectivity of modified bluetongue virus particles for two insect cell lines and for two Culicoides vector species. Virology 217: 582-593.

MERTENS, P. P., S. PEDLEY, J. COWLEY, J. N. BURROUGHS, A. H. CORTEYN *et al.*, 1989 Analysis of the roles of bluetongue virus outer capsid proteins VP2 and VP5 in determination of virus serotype. Virology 170: 561-565.

MERTENS, P. P. C., N. ROSS-SMITH, J. DIPROSE and H. ATTOUI, 2009 Chapter 6 The structure of bluetongue virus core and proteins, pp. 101-133 in *Bluetongue*, edited by R. NOAD and P. ROY.

METZ, S. W., and G. P. PIJLMAN, 2011 Arbovirus vaccines; opportunities for the baculovirus-insect cell expression system. J Invertebr Pathol 107 Suppl: S16-30.

MIKHAILOV, M., K. MONASTYRSKAYA, T. BAKKER and P. ROY, 1996 A New Form of Particulate Single and Multiple Immunogen Delivery System Based on Recombinant Bluetongue Virus-Derived Tubules. Virology 217: 323-331.

MIZUKOSHI, N., K. SAKAMOTO, A. IWATA, T. TSUCHIYA, S. UEDA *et al.*, 1993 The complete nucleotide sequence of African horsesickness virus serotype 4 (vaccine strain) segment 4, which encodes the minor core protein VP4. Virus Res 28: 299-306.

MODROF, J., K. LYMPEROPOULOS and P. ROY, 2005 Phosphorylation of bluetongue virus nonstructural protein 2 is essential for formation of viral inclusion bodies. J Virol 79: 10023-10031.

MONASTYRSKAYA, K., T. BOOTH, L. NEL and P. ROY, 1994 Mutation of either of two cysteine residues or deletion of the amino or carboxy terminus of nonstructural protein NS1 of bluetongue virus abrogates virus-specified tubule formation in insect cells. J Virol 68: 2169-2178.

MONASTYRSKAYA, K., E. A. GOULD and P. ROY, 1995 Characterization and modification of the carboxy-terminal sequences of bluetongue virus type 10 NS1 protein in relation to tubule formation and location of an antigenic epitope in the vicinity of the carboxy terminus of the protein. J Virol 69: 2831-2841.

MONASTYRSKAYA, K., N. STAEUBER, G. SUTTON and P. ROY, 1997 Effects of Domain-Switching and Site-Directed Mutagenesis on the Properties and Functions of the VP7 Proteins of Two Orbiviruses. Virology 237: 217-227.

MURPHY, A., and P. ROY, 2008 Manipulation of the bluetongue virus tubules for immunogen delivery. Future Microbiol 3: 351-359.

NASON, E. L., R. ROTHAGEL, S. K. MUKHERJEE, A. K. KAR, M. FORZAN *et al.*, 2004 Interactions between the inner and outer capsids of bluetongue virus. J Virol 78: 8059-8067.

NOAD, R., and P. ROY, 2009a Bluetongue vaccines. Vaccine 27 Suppl 4: D86-89.

NOAD, R., and P. ROY, 2009b Chapter 4 Bluetongue virus replication and assembly, pp. 53-76 in *Bluetongue*.

OLDFIELD, S., A. ADACHI, T. URAKAWA, T. HIRASAWA and P. ROY, 1990 Purification and characterization of the major group-specific core antigen VP7 of bluetongue virus synthesized by a recombinant baculovirus. J Gen Virol 71: 2649-2656.

OURA, C. A., and M. EL HARRAK, 2011 Midge-transmitted bluetongue in domestic dogs. Epidemiol Infect 139: 1396-1400.

OURA, C. A., P. A. IVENS, K. BACHANEK-BANKOWSKA, A. BIN-TARIF, D. B. JALLOW *et al.*, 2011 African horse sickness in The Gambia: circulation of a live-attenuated vaccine-derived strain. Epidemiol Infect: 1-4.

OWENS, R. J., C. LIMN and P. ROY, 2004 Role of an arbovirus nonstructural protein in cellular pathogenesis and virus release. J Virol 78: 6649-6656.

PAWESKA, J. T., S. PRINSLOO and G. J. VENTER, 2003 Oral susceptibility of South African Culicoides species to live-attenuated serotype-specific vaccine strains of African horse sickness virus (AHSV). Med Vet Entomol 17: 436-447.

POTGIETER, A. C., N. A. PAGE, J. LIEBENBERG, I. M. WRIGHT, O. LANDT *et al.*, 2009 Improved strategies for sequence-independent amplification and sequencing of viral double-stranded RNA genomes. J Gen Virol 90: 1423-1432.

PRASAD, B. V., S. YAMAGUCHI and P. ROY, 1992 Three-dimensional structure of single-shelled bluetongue virus. J Virol 66: 2135-2142.

RAMADEVI, N., N. J. BURROUGHS, P. P. MERTENS, I. M. JONES and P. ROY, 1998 Capping and methylation of mRNA by purified recombinant VP4 protein of bluetongue virus. Proc Natl Acad Sci U S A 95: 13537-13542.

RATINIER, M., M. CAPORALE, M. GOLDER, G. FRANZONI, K. ALLAN *et al.*, 2011 Identification and characterization of a novel non-structural protein of bluetongue virus. PLoS Pathog 7: e1002477.

REN, B., Y. GUO, F. GAO, P. ZHOU, F. WU *et al.*, 2010 Multiple functions of Rice dwarf phytoreovirus Pns10 in suppressing systemic RNA silencing. J Virol 84: 12914-12923.

ROSS-SMITH, N., K. E. DARPEL, P. MONAGHAN and P. P. C. MERTENS, 2009 Chapter 5 Bluetongue virus: cell biology, pp. 77-99 in *Bluetongue*, edited by R. NOAD and P. ROY.

ROY, P., 1996 Orbivirus structure and assembly. Virology 216: 1-11.

ROY, P., 2007 Orbiviruses, pp. 1-35 in *Fields' Virology*, edited by D. M. KNIPE, P.M. HOWLEY. Wolters Kluwer Health/Lippincott Williams & Wilkens, Philadelphia.

RUTKOWSKA, D. A., Q. C. MEYER, F. MAREE, W. VOSLOO, W. FICK *et al.*, 2011 The use of soluble African horse sickness viral protein 7 as an antigen delivery and presentation system. Virus Res 156: 35-48.

SCANLEN, M., J. T. PAWESKA, J. A. VERSCHOOR and A. A. VAN DIJK, 2002 The protective efficacy of a recombinant VP2-based African horsesickness subunit vaccine candidate is determined by adjuvant. Vaccine 20: 1079-1088.

SOLLAI, G., P. SOLARI, C. MASALA, R. CRNJAR and A. LISCIA, 2007 Effects of avermectins on olfactory responses of Culicoides imicola (Diptera: Ceratopogonidae). J Med Entomol 44: 656-659.

STASSEN, L., H. HUISMANS and J. THERON, 2011a African horse sickness virus induces apoptosis in cultured mammalian cells. Virus Res.

STASSEN, L., H. HUISMANS and J. THERON, 2011b Membrane permeabilization of the African horse sickness virus VP5 protein is mediated by two N-terminal amphipathic alpha-helices. Arch Virol 156: 711-715.

STAUBER, N., J. MARTINEZ-COSTAS, G. SUTTON, K. MONASTYRSKAYA and P. ROY, 1997 Bluetongue virus VP6 protein binds ATP and exhibits an RNA-dependent ATPase function and a helicase activity that catalyze the unwinding of double-stranded RNA substrates. J Virol 71: 7220-7226.

STOLTZ, M. A., C. F. VAN DER MERWE, J. COETZEE and H. HUISMANS, 1996 Subcellular localization of the nonstructural protein NS3 of African horsesickness virus. Onderstepoort J Vet Res 63: 57-61.

STUDER, D., W. GRABER, A. AL-AMOUDI and P. EGGLI, 2001 A new approach for cryofixation by high-pressure freezing. J Microsc 203: 285-294.

TAN, B. H., E. NASON, N. STAEUBER, W. JIANG, K. MONASTRYRSKAYA *et al.*, 2001 RGD tripeptide of bluetongue virus VP7 protein is responsible for core attachment to Culicoides cells. J Virol 75: 3937-3947.

TANAKA, S., and P. ROY, 1994 Identification of domains in bluetongue virus VP3 molecules essential for the assembly of virus cores. J Virol 68: 2795-2802.

THERON, J., J. M. UITENWEERDE, H. HUISMANS and L. H. NEL, 1994 Comparison of the expression and phosphorylation of the non-structural protein NS2 of three different orbiviruses: evidence for the involvement of an ubiquitous cellular kinase. J Gen Virol 75 (Pt 12): 3401-3411.

TURNBULL, P. J., S. B. CORMACK and H. HUISMANS, 1996 Characterization of the gene encoding core protein VP6 of two African horsesickness virus serotypes. J Gen Virol 77 (Pt 7): 1421-1423.

UITENWEERDE, J. M., J. THERON, M. A. STOLTZ and H. HUISMANS, 1995 The Multimeric Nonstructural NS2 Proteins of Bluetongue Virus, African Horsesickness Virus, and Epizootic Hemorrhagic Disease Virus Differ in Their Single-Stranded RNA-Binding Ability. Virology 209: 624-632.

URAKAWA, T., and P. ROY, 1988 Bluetongue virus tubules made in insect cells by recombinant baculoviruses: expression of the NS1 gene of bluetongue virus serotype 10. J. Virol. 62: 3919-3927.

VAN DIJK, A. A., and H. HUISMANS, 1988 In vitro transcription and translation of bluetongue virus mRNA. J Gen Virol 69 (Pt 3): 573-581.

VAN GENNIP, R. G., S. G. VAN DE WATER, M. MARIS-VELDHUIS and P. A. VAN RIJN, 2012a Bluetongue viruses based on modified-live vaccine serotype 6 with exchanged outer shell proteins confer full protection in sheep against virulent BTV8. PLoS One 7: e44619.

VAN GENNIP, R. G., S. G. VAN DE WATER, C. A. POTGIETER, I. M. WRIGHT, D. VELDMAN *et al.*, 2012b Rescue of recent virulent and avirulent field strains of bluetongue virus by reverse genetics. PLoS One 7: e30540.

VAN LENT, J., M. STORMS, F. VAN DER MEER, J. WELLINK and R. GOLDBACH, 1991 Tubular structures involved in movement of cowpea mosaic virus are also formed in infected cowpea protoplasts. J Gen Virol 72 (Pt 11): 2615-2623.

VAN NIEKERK, M., C. C. SMIT, W. C. FICK, V. VAN STADEN and H. HUISMANS, 2001 Membrane Association of African Horsesickness Virus Nonstructural Protein NS3 Determines Its Cytotoxicity. Virology 279: 499-508.

VAN RIJN, P. A., S. G. VAN DE WATER and H. G. VAN GENNIP, 2013 Bluetongue virus with mutated genome segment 10 to differentiate infected from vaccinated animals: A genetic DIVA approach. Vaccine.

VAN STADEN, V., and H. HUISMANS, 1991 A comparison of the genes which encode non-structural protein NS3 of different orbiviruses. J Gen Virol 72 (Pt 5): 1073-1079.

VAN STADEN, V., C. C. SMIT, M. A. STOLTZ, F. F. MAREE and H. HUISMANS, 1998 Characterization of two African horse sickness virus nonstructural proteins, NS1 and NS3. Arch Virol Suppl 14: 251-258.

VAN STADEN, V., M. A. STOLTZ and H. HUISMANS, 1995 Expression of nonstructural protein NS3 of African horsesickness virus (AHSV): evidence for a cytotoxic effect of NS3 in insect cells, and characterization of the gene products in AHSV infected Vero cells. Arch Virol 140: 289-306.

VAN STADEN, V., J. THERON, B. J. GREYLING, H. HUISMANS and L. H. NEL, 1991 A comparison of the nucleotide sequences of cognate NS2 genes of three different orbiviruses. Virology 185: 500-504.

VENAIL, R., B. MATHIEU, M. L. SETIER-RIO, C. BORBA, M. ALEXANDRE *et al.*, 2011 Laboratory and field-based tests of deltamethrin insecticides against adult Culicoides biting midges. J Med Entomol 48: 351-357.

VENTER, E., C. F. VAN DER MERWE and V. VAN STADEN, 2012 Utilization of cellulose microcapillary tubes as a model system for culturing and viral infection of mammalian cells. Microsc Res Tech 75: 1452-1459.

VENTER, G. J., I. M. WRIGHT, T. C. VAN DER LINDE and J. T. PAWESKA, 2009 The oral susceptibility of South African field populations of Culicoides to African horse sickness virus. Med Vet Entomol 23: 367-378.

VENTER, M., G. NAPIER and H. HUISMANS, 2000 Cloning, sequencing and expression of the gene that encodes the major neutralisation-specific antigen of African horsesickness virus serotype 9. Journal of Virological Methods 86: 41-53.

VREEDE, F. T., and H. HUISMANS, 1998 Sequence analysis of the RNA polymerase gene of African horse sickness virus. Arch Virol 143: 413-419.

WEHRFRITZ, J. M., M. BOYCE, S. MIRZA and P. ROY, 2007 Reconstitution of bluetongue virus polymerase activity from isolated domains based on a three-dimensional structural model. Biopolymers 86: 83-94.

WEI, T., A. KIKUCHI, Y. MORIYASU, N. SUZUKI, T. SHIMIZU *et al.*, 2006 The spread of Rice dwarf virus among cells of its insect vector exploits virus-induced tubular structures. J Virol 80: 8593-8602.

WEI, T., T. SHIMIZU and T. OMURA, 2008 Endomembranes and myosin mediate assembly into tubules of Pns10 of Rice dwarf virus and intercellular spreading of the virus in cultured insect vector cells. Virology 372: 349-356.

WEYER, C. T., M. QUAN, C. JOONE, C. W. LOURENS, N. J. MACLACHLAN *et al.*, 2013 African horse sickness in naturally infected, immunised horses. Equine Vet J 45: 117-119.

WHITE, D. M., W. C. WILSON, C. D. BLAIR and B. J. BEATY, 2005 Studies on overwintering of bluetongue viruses in insects. J Gen Virol 86: 453-462.

WILSON, A., P. S. MELLOR, C. SZMARAGD and P. P. MERTENS, 2009 Adaptive strategies of African horse sickness virus to facilitate vector transmission. Vet Res 40: 16.

WIRBLICH, C., B. BHATTACHARYA and P. ROY, 2006 Nonstructural protein 3 of bluetongue virus assists virus release by recruiting ESCRT-I protein Tsg101. J Virol 80: 460-473.

WOLF, S., C. M. DEOM, R. N. BEACHY and W. J. LUCAS, 1989 Movement protein of tobacco mosaic virus modifies plasmodesmatal size exclusion limit. Science 246: 377-379.

XU, G., W. WILSON, J. MECHAM, K. MURPHY, E. M. ZHOU *et al.*, 1997 VP7: an attachment protein of bluetongue virus for cellular receptors in Culicoides variipennis. J Gen Virol 78 (Pt 7): 1617-1623.

ZHANG, X., M. BOYCE, B. BHATTACHARYA, X. ZHANG, S. SCHEIN *et al.*, 2010 Bluetongue virus coat protein VP2 contains sialic acid-binding domains, and VP5 resembles enveloped virus fusion proteins. PNAS: 0913403107.

ZIENTARA, S., and J. M. SANCHEZ-VIZCAINO, 2013 Control of bluetongue in Europe. Vet Microbiol 165: 33-37.

Appendix A: Alignment of genome segment 9 sequences

```
AM883170.1      gttaaataagttgtctcatgtcttcggcattactccttgcacctggcgatctaatcgaaa
AHSV-1ref       gttaaataagttg-ctcatgtcttcggcattactccttgcacctggcgatctaatcgaaa
AHSV-7ref       gttaaataagttgtctcatgtcttcggcattactccttgcacctggcgatctaatcgaaa
AHSV-2ref       gttaaataagttgtctcatgtcttcggcattactccttgcacctggcgatctaatcgaaa
AHSV-5ref       gttaaataagttgtctcatgtcttcggcattactccttgcacctggcgatctaatcgaaa
AHSV-8ref       gttaaataagttgtctcatgtcttcggcattactccttgcacctggcgatctaatcgaaa
U19881.1        gttaaataagttgtctcatgtcttcggcattactccttgcacctggcgatctaatcgaaa
NC_006019.1     gttaaataagttgtctcatgtcttcggcattactccttgcacctggcgatctaatcgaaa
AHSV-9ref       gttaaataagttgtctcatgtcttcggcattactccttgcacctggcgatctaatcgaaa
AHSV-2field     gttaaataagttgtctcatgtcttcggcattactccttgcacctggcgatctaatcgaaa
AHSV-3field     gttaaataagttgtctcatgtcttcggcattactccttgcacctggcgatctaatcgaaa
AHSV-5field     gttaaataagttgtctcatgtcttcggcattactccttgcacctggcgatctaatcgaaa
AHSV-9field     gttaaataagttgtctcatgtcttcggcattactccttgcacctggcgatctaatcgaaa
AHSV-1field     gttaaataagttgtctcatgtcttcggcattactcctcgcacctggcgatctgatcgtta
AHSV-7field     gttaaataagttgtctcatgtcttcggcattactcctcgcacctggcgatctgatcgtta
AHSV-4ref       gttaaataagttgtctcatgtcttcggcattactcctcgcacctggcgatctgatcgtta
AHSV-6ref       gttaaataagttgtctcatgtcttcggcattactcctcgcacctggcgatctgatcgtta
AHSV-4field     gttaaataagttgtctcatgtcttcggcattactcctcgcacctggcgatctgatcgtta
AHSV-6field     gttaaataagttgtctcatgtcttcggcattactcctcgcacctggcgatctgatcgtta
AHSV-8field     gttaaataagttgtctcatgtcttcggcattactcctcgcacctggcgatctgatcgtta
                ************* ***********************.**************.****  *

AM883170.1      aagcaaagcgcgagctcgagcaacgctcgataactccgctattgcg--------------
AHSV-1ref       aagcaaagcgcgagctcgagcaacgctcgataactccgctattgcg--------------
AHSV-7ref       aagcaaagcgcgagctcgagcaacgctcgataactccgctcttgcg--------------
AHSV-2ref       aagcaaagcgcgagctcgagcaacgctcgataactccgctcttgcg--------------
AHSV-5ref       aagcaaagcgcgagctcgagcgacgctcgataactccgctcttgcg--------------
AHSV-8ref       aagcaaagcgagagctcgagcaacgctcgataactccgctcttgcg--------------
U19881.1        aagcaaagcgcgagctcgagcaacgctcgatagctccgctcttgcg--------------
NC_006019.1     aagcaaagcgcgagctcgagcaacgctcgataactccgcttttgcg--------------
AHSV-9ref       aagcaaagcgcgagctcgagcaacgctcgataactccgctcttgcg--------------
AHSV-2field     aagcaaagcgcgagctcgagcaacgctcgataactccgctcttgcg--------------
AHSV-3field     aagcaaagcgcgagctcgagcaacgctcgataactccgctcttgcg--------------
AHSV-5field     aagcaaagcgcgagctcgagcaacgctcgataactccgctcttgcg--------------
AHSV-9field     aagcaaagcgcgagctcgagcaacgctcgataactccgctcttgcg--------------
AHSV-1field     aagcaaagcgtgagctcgagcagcgctcgattagctcattgctgcgctctacgagcggag
AHSV-7field     aagcaaagcgtgagctcgagcagcgctcgattagctcattgctgcgctctacgagcggag
AHSV-4ref       aagcaaagcgtgagctcgagcagcgctcgattagctcattgctgcgctctacgagcggag
AHSV-6ref       aagcaaagcgtgagctcgagcagcgctcgattagctcattgctgcgctctacgagcggag
AHSV-4field     aagcaaagcgtgagctcgagcagcgctcgattagctcattgctgcgctctacgagcggag
AHSV-6field     aagcaaagcgtgagctcgagcaacgctcgattagctcattgctgcgctctacgagtggag
AHSV-8field     aagcaaagcgtgagctcgagcagcgctcgattagctcattgctgcgctctacgagtggag
                ********** **********..******** . ..*..* .****
```

```
AM883170.1      -ggagaaagattcgaaagaagccaaatctaaattaaaagaagacggggagaagaagaaca
AHSV-1ref       -ggagaaagattcgaaagaagccaaatctaaattaaaagaagacggggagaagaagaaca
AHSV-7ref       -ggagaaagattcgaaagaagccaaatctaaatttaaagaagacggggagaagaagaaca
AHSV-2ref       -ggagaaagattcgaaggaagccaaatctaaattaaaagaagacggggagaagaagaaca
AHSV-5ref       -ggagaaagattcgaaagaagccaaatctaaattaaaagaagacggggagaagaagaaca
AHSV-8ref       -agagaaagattcgaaagaagccaaatctaaattaaaagaagacggggagaagaagaaca
U19881.1        -ggagaaaaactcgacagaagccaaatctaaactaaaagaggatggggagaagaagaaca
NC_006019.1     -ggagaaaggctcgacagaagccaaatctaaactaaaagaggatggggagaagaagaaca
AHSV-9ref       -ggaaaaagattcgaaagaagccaaatctaaatcaagagaagacggggagaagaagaaca
AHSV-2field     -ggagaaagattcgaaagaagccaaacctaaattaaaagaagacggggagaagaagaaca
AHSV-3field     -ggagaaagattctaaagaagccaaatctaaattaaaagaagacggggaggagaagaaca
AHSV-5field     -ggagaaagattctaaagaagccaaatctaaattaaaagaagacggggaggagaagaaca
AHSV-9field     -ggagaaagattctaaagaagccaaatctaaattaaaagaagacggggaggagaagaaca
AHSV-1field     aaccgagggaagagaggaaagaaaagcagaacaaccaaaaagacggggaaaaggaggaca
AHSV-7field     aaccgaaggaagagaggaaagaaaagcaaaacaaccaaaaagacggggaaaaggaggaca
AHSV-4ref       aaccgaaggaagagaggaaagaaaagcagaacaaccaaaaagacggggaaaaggaggaca
AHSV-6ref       aaccgaaggaagagaggaaagaaaagcagaacaaccaaaaagacggggaaaaggaggaca
AHSV-4field     aaccgaaggaagagaggaaagaaaagcaaaacaatcaaaaagacggggaaaaggaggaca
AHSV-6field     aaccgaaggaagagagggaagaaaagcaaaacaatcaaaaagacggggaaaaggaggaca
AHSV-8field     aaccgaaggaagagaggaaagaaaagcaaaacaatcaaaaagacggggaaaaggaggaca
                 .  .*....    * ..***  **..  **     .*.*.**.*****..**.**.***

AM883170.1      agagtgaaaaagaagagaacaaaatacatgatgatcgaagagtggagagccagaaatctg
AHSV-1ref       agagtgaaaaagaagagaacaaaatacatgatgatcgaagagtggagagccagaaatctg
AHSV-7ref       agggcgaaaaagaagagaacaaaatacatgatgatcgaagagtggagagccagaaatctg
AHSV-2ref       agagtgaaaaggaagagaacaaaatacatgatgatcgaagagtggagagccagaaatctg
AHSV-5ref       agagtgaaaaggaagagaacaaaatacatgatgatcgaagagtggagagccagaaatctg
AHSV-8ref       agagtgaaaaggaagagaacaaaatacatgatgatcgaagagtggagagccagagatccg
U19881.1        agagtgaaaaggaagagaacaaaatacatgatgatcgaagagtggagagccaggaatctg
NC_006019.1     agagtgaaaaggaagagaacaaaatacatgatgatcgaagagtggagagccagaaatctg
AHSV-9ref       agagtgaaaaggaagagaacaaaatacatgatgatcgaagagtggagagccagaaatctg
AHSV-2field     agagtgaaaaggaagagaacaaaatacatgatgatcgaggagtggagagccaggaatctg
AHSV-3field     agagtgaaaaggaagagaacaaaatacatgatgatcgaagagtggagagccagaaatctg
AHSV-5field     agagtgaaaaggaagagaacaaaatacatgatgatcgaagagtggagagccagaaatctg
AHSV-9field     agagtgaaaaggaagagaacaaaatacatgatgatcgaagagtggagagccagaaatctg
AHSV-1field     aggcggaaaagggtgaggaaaagataccaaaagatggaggattgggatcagcaaaatcag
AHSV-7field     aggcggaaaagggtgaggaaaagataccaaaagatggaggattgggatcagcaaaatcag
AHSV-4ref       aggcggaaaagggtgaggaaaagataccaaaagatggaggattgggatcagcaaaatcag
AHSV-6ref       aggcggaaaagggtgaggaaaagataccaaaagatggaggattgggatcagcaaaatcag
AHSV-4field     aggcgaaaaggggtgaggaaaagataccaaaagatggaggattgggatcagcaaaatcag
AHSV-6field     aggcgaaaaagggtgaggaaaagataccaaaagatggaggattgggatcagcaaaatcag
AHSV-8field     aggcgaaaaagggtgaggaaaagataccaaaagatggaggattgggatcagcaaaatcag
                **.  .***..*. ***.* **.****  .* *** **.** ***..     ...*** *
```

```
AM883170.1      agggaagcggatcagccgattgtcaacgcggcgcaggaagcgcaggagcagattgcgcaa
AHSV-1ref       agggaagcggatcagccgattgtcaacgcggcgcaggaagcgcaggagcagattgcgcaa
AHSV-7ref       agggaagcggatcagccgatcgtcgaagcggcgcaggaagcgcaggagcagattgtgcaa
AHSV-2ref       agggaagcggatcagccgattgtcgacgcggcgcaggaagcgcaggagcagattgcgcaa
AHSV-5ref       agggaggcggatcagccgattgtcaacgcggcgcaggaagcgcaggagcagattgcgcaa
AHSV-8ref       agggaggcggatcagccgattgtcaacgcagcgcaggaagcgcaggagcagattgcgcaa
U19881.1        agggaagcggatcagccgattgtcaacgcggcgcaggaagccgaggagcagattgcgcaa
NC_006019.1     agggaggcggaccagccgattgtcaacgtggcgcaggaagccgaggagcaaattgtgcaa
AHSV-9ref       agggaggcggatcagccgattgtcaacgcggcgcaggaagcacaggatcagattgcgcaa
AHSV-2field     agggaggcggaccagccgattgccaacgcggcgcaggaagcgcaggagcaaatcgtgcaa
AHSV-3field     agggaggcggaccagccgattgtcaacgcggcgcaggaggcgcaggagcagattgtgcaa
AHSV-5field     agggaggcggaccagccgattgtcaacgcggcgcaggaggcgcaggagcagattgtgcaa
AHSV-9field     agggaggcggaccagccgattgtcaacgcggcgcaggaggcgcaggagcagattgtgcaa
AHSV-1field     cagaaccagaaccagcggat----------------------ggatcaggagaatcag
AHSV-7field     cagaaccagaaccagcggat----------------------ggatcaggagaatcag
AHSV-4ref       cagaaccagaaccagcggat----------------------ggatcaggagaatcag
AHSV-6ref       cagaaccagaaccagcggat----------------------ggatcaggagaatcag
AHSV-4field     cagaaccagaaccagcggat----------------------ggatcaggagaatcag
AHSV-6field     cagaaccagaaccagcggat----------------------ggatcaggagaatcag
AHSV-8field     cagaaccagaaccagcggat----------------------ggatcaggagaatcag
                 .*.*   *.*.**** ***                      *** **..  .  **.

AM883170.1      catcagcaggaggaggagatggaggtgcaggagcaaggaccgggattggaggggaggag
AHSV-1ref       catcagcaggaggaggagatggaggtgcaggagcaaggaccgggattggaggggaggag
AHSV-7ref       catcagcaggaggaggagatggaggtgcaggagcaaggaccgggattggaggggaggag
AHSV-2ref       catcaacaggaggaggagatggaggtgcaggagcaaggaccgggattggaggggaggag
AHSV-5ref       catcagcaggaggaggagatggaggtgcaggagcaaggaccgggattggaggggaggag
AHSV-8ref       catcaacaggaggaggagatggagstgcaggagcaaggaccgggattggaggggaggag
U19881.1        catcaacaggaggaggagatggaggtgcaggagcaaggaccgggattggaggggaggag
NC_006019.1     catcaacaggaggaggagatggaagtgcaggagcaaggaccgggattggaggggaggag
AHSV-9ref       catcaacaggaggaggagatggaggtgcaggagcaaggaccgggattggaggggaggag
AHSV-2field     catcaacaggaggaggagatggaagtgcaggagcaaggaccgggattggaggggaggag
AHSV-3field     catcaacaggaggaggagatggaagtgcaggagcaaggaccgggattggaggggaggag
AHSV-5field     catcaacaggaggaggagatggaagtgcaggagcaaggaccgggattggaggggaggag
AHSV-9field     catcaacaggaggaggagatggaagtgcaggagcaaggaccgggattggaggggaggag
AHSV-1field     caaaatcgacaggaggagatggaggtggaggagcagggcgcggggctggagggagaggag
AHSV-7field     caaaatcgacaggaggagatggaggtggaggagcagggcgcggggttggagggagaggag
AHSV-4ref       caaaatcgacaggaggagatggaggtggaggagcagggcgcggggctggagggagaggag
AHSV-6ref       caaaatcgacaggaggagatggaggtggaggagcagggcgcggggctggagggagaggag
AHSV-4field     cgaaatcgacaggaggaaatggaggtggaggagcagggcgcggggctggagggagaggag
AHSV-6field     caaaatcgacaggaggagatggaggtggaggagcagggcgcggggctggagggagaggag
AHSV-8field     caaaatcgacaggaggagatggaggtggaggagcagggcgcggggctggagggagaggag
                *.  * *.. *******.*****. ** *******.**  ****..*******.******

AM883170.1      tgggaggagtggattcgagacctggaggacatggaggacagggtgcagcctcggatggaa
```

```
AHSV-1ref       tgggaggagtggattcgagacctggaggacatggaggacagggtgcagcctcggatggaa
AHSV-7ref       tgggaggagtggattcgagacctggaggatatggaggacagggtgcagcctcggatggaa
AHSV-2ref       tgggaggagtggattcgagatctggaggatatggaggacagggtgcagcctcggatggaa
AHSV-5ref       tgggaggagtggattcgagatctggaggacatggaggacagggtgcagcctcggatggaa
AHSV-8ref       tgggaggagtggattcgagatctggaggacatggaggacagggtgcagcctcggatggaa
U19881.1        tgggaagagtggattcgagatctggaggacgtggaggacagggtgcagcctcggatggaa
NC_006019.1     tgggaagagtggattcgagatctggaggacgtggaggacagggtgcagcctcggatggaa
AHSV-9ref       tgggaggagtggattcgagatatggaggacatggaggacaggatgcagcctcggctggaa
AHSV-2field     tgggaggagtggattcgagatctggaggacatggaggacagggtgcagcctcggatggaa
AHSV-3field     tgggaggagtggattcgagatctggaggacatggaggagagggtgcagcctcggttggaa
AHSV-5field     tgggaggagtggattcgagatctggaggacatggaggagagggtgcagcctcggttggaa
AHSV-9field     tgggaggagtggattcgagatctggaggacatggaggagagggtgcagcctcggttggaa
AHSV-1field     tgggcggagtggctggagggactggaggacgtggaggatcacttcgtgggggacgagatg
AHSV-7field     tgggcggagtggctggagggactggaggacgtggaggatcacttcgtgggggacgagatg
AHSV-4ref       tgggcggagtggctggaggggctggacgacgtggaggatcacttcgtgggggacgggatg
AHSV-6ref       tgggcggagtggctggaggggctggacgacgtggaggatcacttcgtgggggacgggatg
AHSV-4field     tgggcggagtggctggaggggctggaggacgtggaggatcacttcgtgggggacgaggtg
AHSV-6field     tgggcggagtggctggaggggctggaggacgtggaggatcacttcgtgggggacgagatg
AHSV-8field     tgggcggagtggctggaggggctggaggacgtggaggatcacttcgtgggggacgagatg
                **** .****** *  ..*.  **** **..*******  .  *   *    .   *. .


AM883170.1      agggagtgggtaaatctaagaccggagcagatcgtgtcgctaatgatggtgcaacacgcg
AHSV-1ref       agggagtgggtaaatctaagaccggagcagatcgtgtcgctaatgatggtgcaacacgcg
AHSV-7ref       agggagtgggtaaatctaagaccggagcagatcgtgtcgctaatgatgatgcaacacgcg
AHSV-2ref       agggagtgggtaaatctaagaccggagcagatcgtgtcgctaatgatggtgcaacacgcg
AHSV-5ref       agggagtgggtaaatctaagaccggagcagatcgtgtcgctaatgatgatgcaacacgcg
AHSV-8ref       agggagtgggtaaatctaagaccggagcagatcgtgtcgctgatgatggtgcaacacgcg
U19881.1        agggagtgggtaaatctaagaccggagcagatcgtgtcgctaatgatggtgcaacacgcg
NC_006019.1     agggagtgggtaaatctaagaccggagcagatcgtgtcgctaatgatgatgcaacacgca
AHSV-9ref       agggagtgggtaaatctaagaccggagcagatcgtgtcgctaatgatgatgcaacacgca
AHSV-2field     agggattgggtaaatctaagaccggagcagatcgtgtcgctaatgatgatgcaacacgca
AHSV-3field     agggagtgggcaaatctaagaccggagcaaatcgtgtcgctaatgatgatgcagcacgca
AHSV-5field     agggagtgggcaaatctaagaccggagcaaatcgtgtcgctaatgatgatgcaacacgca
AHSV-9field     agggagtgggcaaatctaagaccggagcaaatcgtgtcgctaatgatgatgcaacacgca
AHSV-1field     caggattgggcgaatctacgtccggagcaaatcatatcactaatgatgatgcaacacgca
AHSV-7field     caggattgggcgaatctacgtccggagcaaatcatatcactaatgatgatgcaacacgca
AHSV-4ref       caggattgggcgaatctacgtccggaacaaatcatatcactaatgatgatgcaacacgca
AHSV-6ref       caggattgggcgaatctacgtccggaacaaatcatatcactaatgatgatgcagcacgca
AHSV-4field     caggattgggcgaatctacgtccggagcaaatcatatcactaatgatgatgcaacacgca
AHSV-6field     caggattgggcgaatctacgtccggagcaaatcatatcactaatgatgatgcaacacgca
AHSV-8field     caggattgggcgaatctacgtccggagcaaatcatatcactaatgatgatgcaacacgca
                 .*** ****..****** * *****.**.***.*.**.**.******.****.*****.


AM883170.1      atgctggttccagtgaggtaccatctggtggaatcacttcaggaggtcttcaaggccgag
AHSV-1ref       atgctggttccagtgaggtaccatctggtggaatcacttcaggaggtcttcaaggccgag
```

```
AHSV-7ref       atgttggttccagtgaggtaccatctggtggaatcacttcaggaggtcttcaaggccgag
AHSV-2ref       aggttggttccagtgagatatcatctggtggaatcacttcaggaggtcttcaaggccgag
AHSV-5ref       atgttggttccagtgaggtatcatctggtggaatcacttcaggaggtcttcaaggccgag
AHSV-8ref       atgttagttccagtgaggtatcatctggtggaatcacttcaggaggtcttcaaggccgag
U19881.1        atgttggtaccagtgaggtatcatctagtggaatcacttcaggaggtcttcaaggccgag
NC_006019.1     atgttggttccagtgaggtatcacctggtggaatcacttcaggaggtcttcaaggccgag
AHSV-9ref       atgttggttccagtgaggtatcatctggtggaatcgcttcaggaggtcttcaaggccgag
AHSV-2field     atgttggttccagtgaggtatcatctggtggaatcacttcaggaggtcttcaaggccgag
AHSV-3field     atgttggttccagtgaggtatcatctggtggaatcacttcaggaggtcttcaaggccgag
AHSV-5field     atgttggttccagtgaggtatcatctggtggaatcacttcaggaggtcttcaaggccgag
AHSV-9field     atgttggttccagtgaggtatcatctggtggaatcacttcaggaggtcttcaaggccgag
AHSV-1field     atgctggttccggtgaggtaccatctggtggagtcacttcaggaagttctcaaggcggag
AHSV-7field     atgctggttccggtgaggtaccatctggtggagtcacttcaggaagttctcaaggcggag
AHSV-4ref       atgctggttccggtgaggtaccatctggtggagtcacttcaggaagttctcaaggcggag
AHSV-6ref       atgctggttccggtgaggtaccatctggtggagtcacttcaggaagttctcaaggcggag
AHSV-4field     atgctggttccggtgaggtaccatctggtggaatcacttcaggaagttctcaaggcggag
AHSV-6field     atgctggttccggtgaggtaccatctggtggagtcacttcaggaagttctcagggcggag
AHSV-8field     atgctggttccggtgaggtaccatctggtggagtcacttcaggaagttctcagggcggag
                * *.*.** **.*****.**.**.**.*****.**.********.**..***.*** ***


AM883170.1      gaggactcgttgctaagagtagtgaatgtggcggggaaccattggataggacaggcggct
AHSV-1ref       gaggactcgttgctaagagtagtgaatgtggcggggaaccattggataggacaggcggct
AHSV-7ref       gaggactcgttgctaagagtagtgaatgtggcggggaaccattggataggacaggcggct
AHSV-2ref       gaggactcgttgcaaagagtagtgaatgtggcggggaaccattggataggacaggcggct
AHSV-5ref       gaggactcgttgcaaagagtagtgaatgtggcggggaatcattggataggacaggcggct
AHSV-8ref       gaggactcgttacaaagagtagtgaatgtggcggggaaccattggatagggcaggcggct
U19881.1        gaggactcgttgcaaagagtagtgaatgtggcggggaaccattggataggacaggcggct
NC_006019.1     gaggactcgttgcaaagagtggtgaatgtggcggggaatcattggataggataggcggct
AHSV-9ref       gaggactcgttgcaaagagtagtgaatctggcagggaaccattggataggacaggcggct
AHSV-2field     gaggactcgttgcaaagagtggcaaatgtggcggggaaccattggataggacaggcggct
AHSV-3field     gaggactcgttgcaaagagtggtgaatgtggcggggaaccattggataggacaggcggct
AHSV-5field     gaggactcgttgcaaagagtggtgaatgtggcggggaaccattggataggacaggcggct
AHSV-9field     gaggactcgttgcaaagagtggtgaatgtggcggggaaccattggataggacaggcggct
AHSV-1field     gaggggcgctacaacgagtggtgaatctggcgggcaaccactrgatcggaagagcggcg
AHSV-7field     gaggggcgctacaacgagtggtgaatctggcgggcgaccattggatcggaagagcggcg
AHSV-4ref       gaggggcgctacaacgagtggtgaatctggcgggcaaccactggatcggaagagcggcg
AHSV-6ref       gaggggcgctacaacgagtggtgaatctggcgggcaaccactggatcggaagagcggcg
AHSV-4field     gaggggcgctacaacgagtggtgaatctggcgggcaaccactggatcggaagagcggcg
AHSV-6field     gaggggcgctgcagcgagtggtgaatctggcgggcaaccactggatcggaagagcggcg
AHSV-8field     gaggggcgctacaacgagtggtgaatctggcgggcaaccactggatcggaagagcggcg
                ****.  **.*.* . ****.*..*** ****.** .*.**.* *** **. ..*****


AM883170.1      gcagcggaaattcaaaaactgagggagaggaggcaaaggttggagggagcgatagacgga
AHSV-1ref       gcagcggaaattcaaaaactgagggagaggaggcaaaggttggagggagcgatagacgga
AHSV-7ref       gcagcggaaattcaaaaactgagggagaggaggcaaaggttggagggggcgatagacgga
```

```
AHSV-2ref       gcagcggaaattcaaaaactgagggagaggaggcaaaggttggaggggcgatagacgga
AHSV-5ref       gcagcggaaattcaaaaactgagggagaggaggcaaaggttggaggggcgatagacgga
AHSV-8ref       gcagcggaaattcaaaaactgagggagaggaggcaaaggttggaggggcgatagacgga
U19881.1        gcagcggaaattcaaaaactgagggagaggaggcaaaggttggaggggcgatagacgga
NC_006019.1     gcagcggaaattcaaaaactgagggagaggaggcgaaggctggaggggcgatagacgga
AHSV-9ref       gcagcggaaattcaaaaactgagagagaggaggcgaaggttggaggggcgatagacgga
AHSV-2field     gcagcggaaattcaaaaactgagggagaggaggcgaaggctggaggggcgatagacgga
AHSV-3field     gcagcggaaattcaaaagctgagggagaggaggcaaaggctggaggggcgatagacgga
AHSV-5field     gcagcggaaattcaaaagctgagggagaggaggcaaaggctggaggggcgatagacgga
AHSV-9field     gcagcggaaattcaaaagctaagggagaggaggcaaaggctggaggggcgatagacgga
AHSV-1field     caagcggagatacaagatctccaggcgagaagacaaaggttgatgggggcgatcgacggg
AHSV-7field     caagcggagatacaagatctccaggcgagaagacaaaggttgatgggggcgatcgacggg
AHSV-4ref       caagcggagatacaagatctccaagcgagaagacaaaggttgatgggggcgatcgacggg
AHSV-6ref       caagcggagatacaagatctccaagcgagaagacaaaggttgatgggggcgatcgacggg
AHSV-4field     caagcggagatacaagatctccaggcgagaagacaaaggttgatgggggcgatcgacggg
AHSV-6field     caagcggagatacaagatctccaggcgagaagacaaaggttgatgggggcgatcgacggg
AHSV-8field     caagcggagatacaagatctccaggcgagaagacaaaggttgatgggggcgatcgacggg
                 ******.** ***.* **  ..* ***.**.*.****.**. ***.***** *****.

AM883170.1      ttggaggattagcaacgcaggagattgccgactttgtgaagaagaagatcggagttgaag
AHSV-1ref       ttggaggattagcaacgcaggagattgccgactttgtgaagaagaagatcggagttgaag
AHSV-7ref       ttggaggattagcaacgcaggagattgccgactttgtgaagaagaagatcggagttgaag
AHSV-2ref       ttggaggattagcaacgcaggagattgccgactttgtgaagaagaagatcggagttgaag
AHSV-5ref       ttggaggattagcaacgcaggagattgccgactttgtgaagaagaagatcggagttgaag
AHSV-8ref       ttggaggattagcaacgcaggagattgccgactttgtgaaaaagaaaatcggagttgaag
U19881.1        ttggaggattagcaacgcaggggattgccgactttgtgaagaagaagatcggagttgaag
NC_006019.1     ttggaggattagcaacgcaggagattgcagactttgtgaagaagaagatcggagttgaag
AHSV-9ref       ttggaggactagcaacgcaggagattgccgactttgtgaagaagaagatcggagttgaag
AHSV-2field     ttggaggattagcaacgcaggagattgcggattttgtgaagaagaagatcggagttgaag
AHSV-3field     ttggaggactagcgacgcaggagattgcagattttgtgaagaagaagatcggagttgaag
AHSV-5field     ttggaggactagcgacgcaggagattgcagattttgtgaagaagaagatcggagttgaag
AHSV-9field     ttggaggactagcgacgcaggagattgcagattttgtgaagaagaagatcggagttgaag
AHSV-1field     atgggggattagctactcaagagatagtcgattatgtcagaaggaaagttggagttgaag
AHSV-7field     atgggggattagctactcaagagatagtcgattatgtcagaaggaaagttggagttgaag
AHSV-4ref       atgggggattagctactcaagagatagtcgattatgtcagaaagaaggttggagttgaag
AHSV-6ref       atgggggattagctactcaagagatagtcgattatgtcagaaagaaggttggagttgaag
AHSV-4field     atgggggattagctactcaagagatagtcgattatgtcagaaagaaagttggagttgaag
AHSV-6field     atgggggattagctactcaagagatagtcgattatgtcagaaagaaagttggagttgaag
AHSV-8field     atgggggattagctactcaagagatagtcgattatgtcagaaagaaagttggagttgaag
                 ***.***.**** ** **.*.*** *. **.* *** *..*.***..*.**********

AM883170.1      ttcaggtgttttccaaaggaatgagcaacttatttactgtagataaatcattgcttgagc
AHSV-1ref       ttcaggtgttttccaaaggaatgagcaacttatttactgtagataaatcattgcttgagc
AHSV-7ref       ttcaggtgttttccaaaggaatgagcaacttatttactgtagataaatcattgcttgagc
AHSV-2ref       ttcaggtgttttctaaaggaatgagcaacttatttactgtagataaatcattgcttgagc
```

```
AHSV-5ref       ttcaggtgttttctaaaggaatgagcaacttatttactgtagataaatcattgcttgagc
AHSV-8ref       ttcaggtgttttccaaaggaatgagcaacttatttactgtagataaatcattgcttgagc
U19881.1        ttcaggtgttttctaaaggaatgagtaacttttttactgtagataaatcattgcttaagc
NC_006019.1     ttcaggtgttttctaaaggaatgagcaacttatttactgtagataaatcattgcttaagc
AHSV-9ref       ttcaggtgttttccaaagggatgagcaacttatttactgtagataaatcattgcttgagc
AHSV-2field     ttcaggtgttttctaaaggaatgagcagcttatttactgtagataagtcattgcttgagc
AHSV-3field     ttcaggtgttttctaaaggaatgagcaacttatttactgtagataagtcattgcttgagc
AHSV-5field     ttcaggtgttttctaaaggaatgagcaacttatttactgtagataagtcattgcttgagc
AHSV-9field     ttcaggtgttttctaaaggaatgagcaacttatttactgtagataagtcattgcttgagc
AHSV-1field     ttccgatttatcagaagggaatgagcaacttatttactgtagataggggcttgcttgagc
AHSV-7field     ttccgatttatcagaagggaatgagcaacttatttactgtagataggggcttgcttgagc
AHSV-4ref       ttccgatttatcagaagggaatgagcaacttatttactgtagataggggcttgcttgagc
AHSV-6ref       ttccgatttatcagaagggaatgagcaacttatttactgtagataggggcctgcttgagc
AHSV-4field     ttccgatttatcagaagggaatgagcaacttatttactgtagataggggcttgcttgagc
AHSV-6field     ttccgatttatcagaagggaatgagcaacttatttactgtagataggggcttgcttgagc
AHSV-8field     ttccgatttatcagaagggaatgagcaacttatttactgtagataggggcttgcttgagc
                *** *.* * *.  **.**.*****.*.*** **********..   .*****.***

AM883170.1      ggggtgggttagggagggaagacattctacatcaatcagatattgtaaaagagattagag
AHSV-1ref       ggggtgggttagggagggaagacattctacatcaatcagatattgtaaaagagattagag
AHSV-7ref       ggggtgggttagggagggaagacattctacatcaatcagatattgtaaaagagattagag
AHSV-2ref       ggggtgggttagggagggaagacattctacatcaatcagatattgtaaaagagattagag
AHSV-5ref       ggggtgggttagggagggaagacattctacatcaatcagatattgtaaaagagattagag
AHSV-8ref       ggggtgggttagggagggaggacattctacatcaatcagatattgtaaaagagattagag
U19881.1        ggggtgggttagggagggaagacattctacatcaatcagatattgtaaaagagattagag
NC_006019.1     ggggtgggttagggagggaagacattctacatcaatcagatattgtaaaagagattagag
AHSV-9ref       ggggtgggttagggagggaagacattctacatcaatcagatattgcaaaagaaattagag
AHSV-2field     ggggtgggttagggagggaggacattctacatcaatcagatattgtaaaagagattagag
AHSV-3field     ggggtgggttagggagggaggacattctacatcaatcagatattgtaaaagagattagag
AHSV-5field     ggggtgggttagggagggaggacattctacatcaatcagatattgtaaaagagattagag
AHSV-9field     ggggtgggttagggagggaggacattctacatcaatcagatattgtaaaagagattagag
AHSV-1field     gggggggtttatctaaagatgatctgctacatcaatctgatatcgtaaaagaggcgaagg
AHSV-7field     gggggggtttatctaaagatgatctgctacatcaatctgatatcgtaaaagaggcgaagg
AHSV-4ref       gggggggtttatctaaagatgatctgctacatcaatctgatatcgtaaaagaggcgaagg
AHSV-6ref       gggggggtttatctaaagatgatctgctacatcaatctgatatcgtaaaagaggcgaagg
AHSV-4field     gggggggtttatctaaagatgatctgctacatcaatctgatatcgtaaaagaggcgaagg
AHSV-6field     gggggggtttatctaaagatgatctgctacatcaatctgatatcgtaaaagaggcgaagg
AHSV-8field     gggggggtttatctaaagatgatctgctacatcaatctgatatcgtaaaagaggcgaagg
                **** ** ***   *..** **. * ********** *****.*.******... *..*

AM883170.1      caagtgataaaagagtcaaaattattcctctttctacagtgaagagaatgatagcggaat
AHSV-1ref       caagtgataaaagagtcaaaattattcctctttctacagtgaagagaatgatagcggaat
AHSV-7ref       caagtgataaaagagtcaaaattattcctctttctacagtgaagagaatgatagcggaat
AHSV-2ref       caagtgataaaaaagtcaagattattcctctttctacagtgaagagaatgatggcggaat
AHSV-5ref       caagtgataaaaaagtcaaaattattcctctttctacagtgaagagaatgatagcggaat
```

```
AHSV-8ref       caagtgataaaaaagtcaagattattccccttttctacggtgaagaggatgatagcggaat
U19881.1        caagcgataaaaaagtcaagattattcctctttctacagtgaagagaatgatagcggaat
NC_006019.1     caagcgataaaaaagtcaagattattcctctttccacagtaaagagaatgatagcggaat
AHSV-9ref       caagtgataaaaaagtcaagattattcctctttctacagtgaagagaatgatagcggaat
AHSV-2field     taagtgataaaaaagtcaagattattcctctttctacagtaaagagaatgatagcggagt
AHSV-3field     taagtgataaaaaagtcaaaattattcctctttccacagtaaagagaatgatagcggaat
AHSV-5field     taagtgatagaaaagtcaaaattattcctctttccacagtaaagagaatgatagcggaat
AHSV-9field     taagtgataaaaaagtcaaaattattcctctttccacagtaaagagaatgatagcggaat
AHSV-1field     ccaatgataaaaagttgaaagtggttccactctcaacggtcaaaagaattattgcggaat
AHSV-7field     ccaatgataaaaagttgaaagtggttccactctcaacggtcaaaagaattattgcggaat
AHSV-4ref       ccaatgataaaaaattgaaagtggttccactctcaacagtcaaaagaattattgcggaat
AHSV-6ref       ccaatgataaaaaattgaaagtggttccactctcaacagtcaaaagaattactgcggaat
AHSV-4field     ctaatgataaaaaattgaaggtggttccactctcaacggtcaaaagaattattgcggaat
AHSV-6field     ctaatgataaaaaattgaaagtggttccactctcaacggtcaaaagaattattgcggaat
AHSV-8field     ctaatgataaaaaattgaaagtggttccactctcaacggtcaaaagaattattgcggaat
                . *..****.**.. * **..* .**** **.** **.** **.**.** *. *****.*

AM883170.1      tcggagggacagaggaggatgaaatcaaagctgttcaaactcaaagctcttctatcaggt
AHSV-1ref       tcggagggacagaggaggatgaaatcaaagctgttcaaactcaaagctcttctatcaggt
AHSV-7ref       tcggaggaacagaggaggatgaaatcaaagctgttcaaactcaaagctcttctatcaggt
AHSV-2ref       tcggaggaacagaggaggatgaaatcaaagctgttcaaactcaaagctcttctatcaggt
AHSV-5ref       tcggaggaacagaggaggatgaaatcaaagctrttcaaattcaaagctcttctatcaggt
AHSV-8ref       tcggaggaacagaggaggatgaaatcaaagctgttcaaactcaaagctcttctatcaggt
U19881.1        tcggaggaacagaggaggatgaaatcaaagctgttcaaactcaaagctcttctatcaggt
NC_006019.1     tcggaggaacagaggaggatgaaatcaaagctgttcaaactcaaagttcttctatcaggt
AHSV-9ref       tcggaggaacagaggaggatgaaatcaaagctgttcaaactcaaagctcttctatcaggt
AHSV-2field     tcggaggaacagaggaggatgagatcaaagctgttcaaactcaaagttcttctatcaggt
AHSV-3field     tcggaggaacagaggaggatgaaatcaaagctgttcaaactcaaagttcttctatcaggt
AHSV-5field     tcggaggaacagaggaggatgaaatcaaagctgttcaaactcaaagttcttctatcaggt
AHSV-9field     tcggaggaacagaggaggatgaaatcaaagctgttcaaactcaaagttcttctatcaggt
AHSV-1field     ttggagggtcggaagaagaagatgtaaagggaatgcagacacaaagttcttccataagat
AHSV-7field     ttggagggtcggaagaagaagatgtaaagggaatgcagacacaaagttcttccataagat
AHSV-4ref       ttggagggtcggaagaagaagatgtaaagggaatgcagacacaaagttcttccataagat
AHSV-6ref       ttggagggtcggaagaagaagatgtaaagggaatgcagacacaaagttcttccataagat
AHSV-4field     ttggagggtcggaagaagaagatgtgaagggaatgcagacacaaagttcttccataagat
AHSV-6field     ttggaggatcggaagaagaagatgtaaagggaatgcagacacaaagttcttccataagat
AHSV-8field     ttggaggatcggaagaagaagatgtaaagggaatgcagacacaaagttcttccataagat
                *.*****. *.**.**.** ** .* **.*   * **.*. *****.*****.** **.*

AM883170.1      atattagtaatagaatggaagatgtttcaagagcgaaggcgatgttcacagcgccgacag
AHSV-1ref       atattagtaatagaatggaagatgtttcaagagcgaaggcgatgttcacagcgccgacag
AHSV-7ref       atattagtaatagaatggaagatgtttcaagagcgaaggcgatgttcacagcgccgacag
AHSV-2ref       atattagtaatagaatggaagatgtttcaagagcgaaggcgatgttcacagcgccgacag
AHSV-5ref       atattagtaatagaatggaagatgtttcaagagcgaaggcgatgttcacagcgccgacag
AHSV-8ref       atattagtaatagaatggaggatgtttcaagagcaaaggcgatgttcacagcgccgacag
```

```
U19881.1        atattagtaatagaatggaagatgtttcaagagcgaaggcgatgttcacagcgccgacag
NC_006019.1     atattagtaatagaatggaagatgtttcaagagcgaaggcgatgttcacagcgccgacgg
AHSV-9ref       atattagtaatagaatggaagacgtttcaagagcgaaggcgatgttcacagcgccgacag
AHSV-2field     atattagtaatagaatggaggatgtttcaagagcgaaggcgatgttcacagcgccgacag
AHSV-3field     atattagtaatagaatcgaagatgtttcaagagcgaaggcgatgttcacagcgccgacag
AHSV-5field     atattagtaatagaatcgaagatgtttcaagagcgaaggcgatgttcacagcgccgacag
AHSV-9field     atattagtaatagaatcgaagatgtttcaagagcgaaggcgatgttcacagcgccgacag
AHSV-1field     acataagcaatagaatggaagatgttcctaaagcgaaggccatgttcacggcgccgactg
AHSV-7field     acataagcaatagaatggaagatgttcctaaagcgaaggccatgttcacggcgccgactg
AHSV-4ref       acataagcaatagaatggaagatgttcctaaagcgaaggccatgttcacggcgccgactg
AHSV-6ref       acataagcaatagaatggaagatgttcctaaagcgaaggccatgttcacggcgccgactg
AHSV-4field     atataagcaatagaatggaagatgttcctaaagcgaaggccatgttcacggcgccgactg
AHSV-6field     acataagcaatagaatggaagatgttcctaaagcgaaggccatgttcacggcgccgactg
AHSV-8field     acataagcaatagaatggaagatgttcctaaagcgaaggccatgttcacggcgccgactg
                *.** **.******** **.**.***.* *.***.***** ********.******** *


AM883170.1      gtgacgaggggtggaaagaggttgctaaagcagcaactcagcgtcctaacatcatggcgt
AHSV-1ref       gtgacgaggggtggaaagaggttgctaaagcagcaactcagcgtcctaacatcatggcgt
AHSV-7ref       gtgacgaggggtggaaagaggttgctaaagcagcaactcagcgtcctaacatcatggcgt
AHSV-2ref       gtgatgaggggtggaaagaggttgctaaagcagcaactcagcgtcctaacatcatggcgt
AHSV-5ref       gtgatgaggggtggaaagaggttgctaaagcagcaactcagcgtcctaacatcatggcgt
AHSV-8ref       gtgatgaggggtggaaagaggttgctaaagcagcaactcagcgtcctaacatcatggcgt
U19881.1        gtgatgaggggtggaaagaggttgctaaagcagcaactcagcgtcctaacatcatggcgt
NC_006019.1     gtgatgaggggtggaaagaggtcgctaaagcagcaactcagcgtcctaacatcatggcgt
AHSV-9ref       gtgatgaggggtggaaagaggttgctaaagcagcgactcagcgtcctaacatcatggcgt
AHSV-2field     gtgatgaggggtggaaagaggtcgctaaagcagcaactcaacgtcctaacgtcatggcgt
AHSV-3field     gtgatgaggggtggaaagaggtcgctaaagcagcaactcagcgccctaacatcatggcgt
AHSV-5field     gtgatgaggggtggaaagaggtcgctaaagcagcaactcagcgccctaacatcatggcgt
AHSV-9field     gtgatgaggggtggaaagaggtcgctaaagcagcaactcagcgccctaacatcatggcgt
AHSV-1field     gagatgaagggtggaaggaggtcgcaaaagcggcgacgttgaggccaaatatcatggctt
AHSV-7field     gagatgaagggtggaaggaggtcgcaaaagcggcgacgttgaggccaaatatcatggctt
AHSV-4ref       gagatgaagggtggaaggaggtcgcaaaagcggcgacgttgaggccaaatatcatggctt
AHSV-6ref       gagatgaagggtggaaggaggtcgcaaaagcggcgacgttgaggccaaatatcatggctt
AHSV-4field     gagatgaagggtggaaggaggtcgcaaaagcagcgacgttgaggccaaatatcatggctt
AHSV-6field     gagatgaagggtggaaggaggtcgcaaaagcggcgacgttgaggccaaatatcatggctt
AHSV-8field     gagatgaagggtggaaggaggtcgcaaaagcggcgacgttgaggccaaatatcatggcgt
                * **.**.********.*****.** *****.**.** . . * ** **..******* *


AM883170.1      atgtacacgaaggggaaggtgatggattgaaagagcttttacatctgattgatcatatct
AHSV-1ref       atgtacacgaaggggaaggtgatggattgaaagagcttttacatctgattgatcatatct
AHSV-7ref       atgtacacgaaggggaaggtgatggattgaaagaacttttacatctgattgatcatatct
AHSV-2ref       atgtgcacgaaggggaaggcgatggattgaaagagcttttacatctgattgatcatatct
AHSV-5ref       atgtgcacgaaggggaaggtgatggattgaaagagcttttacatctgattgatcatatct
AHSV-8ref       atgtgcacgaaggggaaggcgatggattgaaagagcttttacatctgattgatcatatct
U19881.1        atgtgcacgaaggggaaggcgatggattgaaagagcttttacatctgattgatcatatct
```

```
NC_006019.1     atgtgcacgaaggggaaggtgatggattgaaagagcttttacatctgattgatcatatct
AHSV-9ref       atgtatacgaaggggaaggcgacggattgaaagagcttttacatctgattgatcatatct
AHSV-2field     atgtgcacgaaggagaaggtgatggattgaaagagcttttacatctgattgatcatatct
AHSV-3field     atgtgcacgaaggagaaggtgatggattgaaagagcttttacatctgattgatcatatct
AHSV-5field     atgtgcacgaaggagaaggtgatggattgaaagagcttttacatctgattgatcatatct
AHSV-9field     atgtgcacgaaggagaaggcgatggattgaaagagcttttacatctgattgatcatatct
AHSV-1field     acgttcacgaaggggagggggatggactgaaggagcttttacatttaatagatcatatct
AHSV-7field     acgttcacgaaggggaaggggatggactgaaggagcttttacatttaatagatcatatct
AHSV-4ref       acgttcatgaaggggaaggggatggactgaaggagcttttacatttaatagatcatatct
AHSV-6ref       acgttcatgaaggggaaggggatggactgaaggagcttttacatttaatagatcatatct
AHSV-4field     acgttcatgaaggggaaggggatggactgaaggagcttttacatttaatagatcatatct
AHSV-6field     acgttcatgaaggggaaggggatggactgaaggagcttttacatttaatagatcatatct
AHSV-8field     acgttcatgaaggggaaggggatggactgaaggagcttttacatttaatagatcatatct
                *.** .*.*****.*.*** **.***.****.**.*********.*.** **********


AM883170.1      aggtccaggggtaaacggcagcttgagggcaacttaaaacttac----------------
AHSV-1ref       aggtccaggggtaaacggcagcttgagggcaacttaaaacttacggcaacttaaaactta
AHSV-7ref       aggtccaggggtaaacggcagcttgagggcaacttaaaacttac----------------
AHSV-2ref       aggtccaggggtaaacggcagcttgagggcaacttaaaacttac----------------
AHSV-5ref       aggtccaggggtaaacggcagcttgagggcaacttaaaacttac----------------
AHSV-8ref       aggtccaggggtaaacggcagcttgagggcaacttaaaacttac----------------
U19881.1        aggtccaggggtaaacggcagcttgagggcaacttaaaacttac----------------
NC_006019.1     aggtccaggggtaaacggcagcttgagggcaacttaaaacttac----------------
AHSV-9ref       aggtccaggggtaaacggcagcttgagggcaacttaaaacttac----------------
AHSV-2field     aggtccaggggtaaacggcagcttgagggcaacttaaaacttac----------------
AHSV-3field     aggtccaggggtaaacggcagcttgagggcaacttaaaacttac----------------
AHSV-5field     aggtccaggggtaaacggcagcttgagggcaacttaaaacttac----------------
AHSV-9field     aggtccaggggtaaacggcagcttgagggcaacttaaaacttac----------------
AHSV-1field     aggtccaggggtaaacggcagcttgcaggcaacttaaaacttac----------------
AHSV-7field     aggtccaggggtaaacggcagcttgcaggcaacttaaaacttac----------------
AHSV-4ref       aggtccaggggtaaacggcagcttgcaggcaacttaaaacttac----------------
AHSV-6ref       aggtccaggggtaaacggcagcttgcaggcaacttaaaacttac----------------
AHSV-4field     aggtccaggggtaaacggcagcttgcaggcaacttaaaacttac----------------
AHSV-6field     aggtccaggggtaaacggcagcttgcaggcaacttaaaacttac----------------
AHSV-8field     aggtccaggggtaaacggcagcttgcaggcaacttaaaacttac----------------
                ************************** .*****************

AM883170.1      -
AHSV-1ref       c
AHSV-7ref       -
AHSV-2ref       -
AHSV-5ref       -
AHSV-8ref       -
U19881.1        -
NC_006019.1     -
AHSV-9ref       -
```

```
AHSV-2field     -
AHSV-3field     -
AHSV-5field     -
AHSV-9field     -
AHSV-1field     -
AHSV-7field     -
AHSV-4ref       -
AHSV-6ref       -
AHSV-4field     -
AHSV-6field     -

AHSV-8field     -
```

Figure A.1. – CLUSTAL format alignment by MAFFT (v7.127b) of genome segment 9 nucleotide sequences of several AHSV isolates. Genbank: U19881.1 and NC_006019 are the sequences corresponding ASHV-3 and AHSV-6, respectively (TURNBULL *et al.* 1996). Genbank: AM883170.1 was published by Potgieter *et al.* (2009) and corresponds to AHSV-1. The NS4 open reading frames are underlined and the VP6 ORFs are indicated in bold print and italicised. Asterisks (*) indicate identical residues.

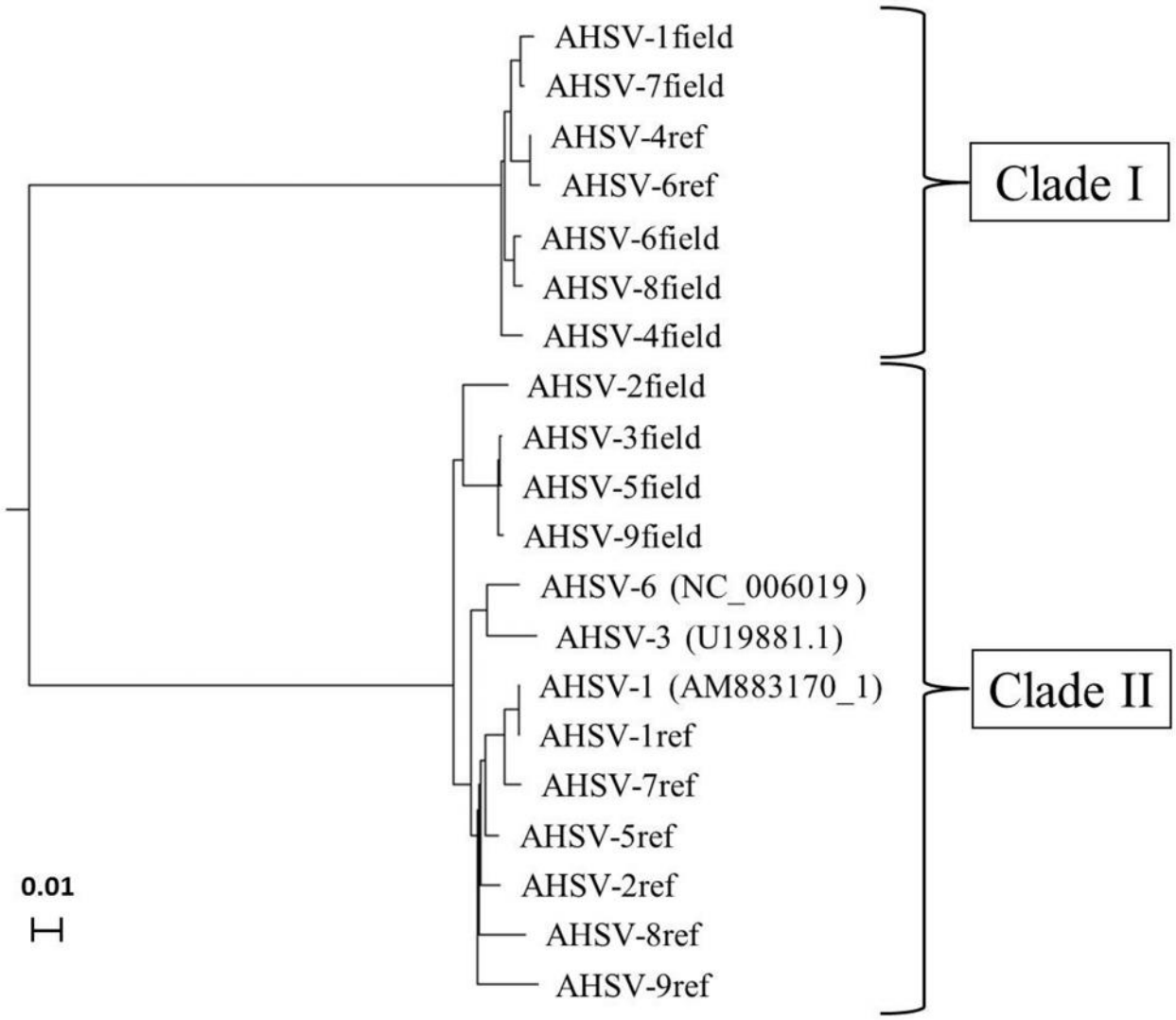

Figure A.2. – Neighbour Joining tree using only the region of the genome segment 9 nucleotide sequences corresponding to the predicted VP6 open reading frames of all nine AHSV serotypes. The Genbank accession numbers of the three currently published sequences are shown in brackets.

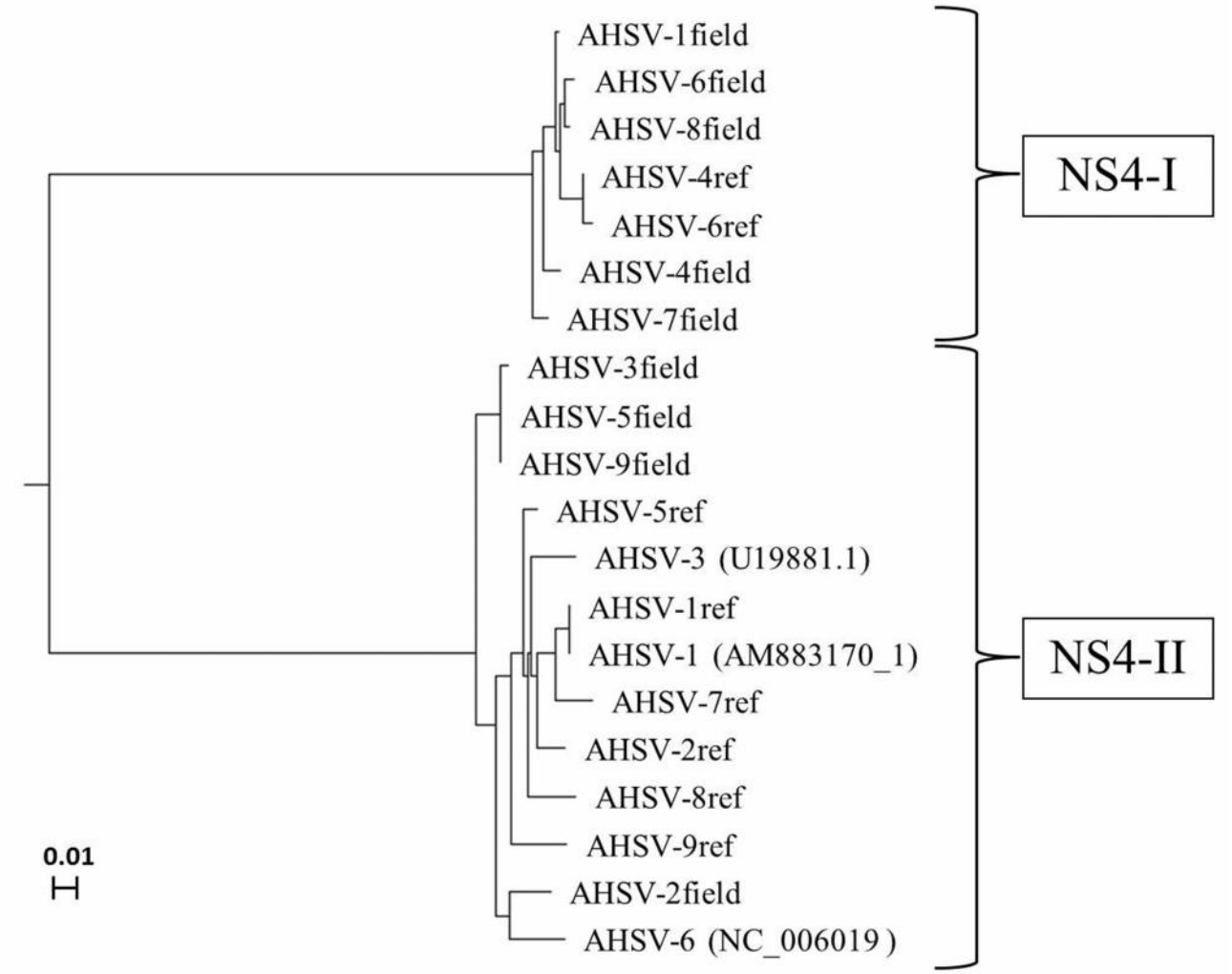

Figure A.3. – Neighbour Joining tree using only the genome segment 9 nucleotide sequences corresponding to the predicted NS4 open reading frames of all nine AHSV serotypes. The suffix “ref” denotes a reference strain and “field” indicates a field isolate.

```
U19881.1        MSSALLLAPGDLIEKAKRELEQRSIAPLLRE-----KNSTEAKSKLKEDGEKKNKSEKEE
AHSV-1ref       MSSALLLAPGDLIEKAKRELEQRSITPLLRE-----KDSKEAKSKLKEDGEKKNKSEKEE
AM883170.1      MSSALLLAPGDLIEKAKRELEQRSITPLLRE-----KDSKEAKSKLKEDGEKKNKSEKEE
AHSV-2ref       MSSALLLAPGDLIEKAKRELEQRSITPLLRE-----KDSKEAKSKLKEDGEKKNKSEKEE
AHSV-7ref       MSSALLLAPGDLIEKAKRELEQRSITPLLRE-----KDSKEAKSKFKEDGEKKNKGEKEE
AHSV-5ref       MSSALLLAPGDLIEKAKRELERRSITPLLRE-----KDSKEAKSKLKEDGEKKNKSEKEE
AHSV-8ref       MSSALLLAPGDLIEKAKRELEQRSITPLLRE-----KDSKEAKSKLKEDGEKKNKSEKEE
NC_006019       MSSALLLAPGDLIEKAKRELEQRSITPLLRE-----KGSTEAKSKLKEDGEKKNKSEKEE
AHSV-2field     MSSALLLAPGDLIEKAKRELEQRSITPLLRE-----KDSKEAKPKLKEDGEKKNKSEKEE
AHSV-3field     MSSALLLAPGDLIEKAKRELEQRSITPLLRE-----KDSKEAKSKLKEDGEEKNKSEKEE
AHSV-5field     MSSALLLAPGDLIEKAKRELEQRSITPLLRE-----KDSKEAKSKLKEDGEEKNKSEKEE
AHSV-9field     MSSALLLAPGDLIEKAKRELEQRSITPLLRE-----KDSKEAKSKLKEDGEEKNKSEKEE
AHSV-9ref       MSSALLLAPGDLIEKAKRELEQRSITPLLRE-----KDSKEAKSKSREDGEKKNKSEKEE
AHSV-1field     MSSALLLAPGDLIVKAKRELEQRSISSLLRSTSGEPREERKEKQNNQKDGEKEDKAEKGE
AHSV-7field     MSSALLLAPGDLIVKAKRELEQRSISSLLRSTSGEPKEERKEKQNNQKDGEKEDKAEKGE
AHSV-4field     MSSALLLAPGDLIVKAKRELEQRSISSLLRSTSGEPKEERKEKQNNQKDGEKEDKAKRGE
AHSV-6field     MSSALLLAPGDLIVKAKRELEQRSISSLLRSTSGEPKEEREEKQNNQKDGEKEDKAKKGE
AHSV-8field     MSSALLLAPGDLIVKAKRELEQRSISSLLRSTSGEPKEERKEKQNNQKDGEKEDKAKKGE
AHSV-4ref       MSSALLLAPGDLIVKAKRELEQRSISSLLRSTSGEPKEERKEKQNNQKDGEKEDKAEKGE
AHSV-6ref       MSSALLLAPGDLIVKAKRELEQRSISSLLRSTSGEPKEERKEKQNNQKDGEKEDKAEKGE
                ************* *******:***:.***.     : . : * : ::***:::*.:: *


U19881.1        NKIHDDRRVESQESEGSGSADCQRGAGSRGADCATSTGGGDGGAGARTGIGGGGVGRVDS
AHSV-1ref       NKIHDDRRVESQKSEGSGSADCQRGAGSAGADCATSAGGGDGGAGARTGIGGGGVGGVDS
AM883170.1      NKIHDDRRVESQKSEGSGSADCQRGAGSAGADCATSAGGGDGGAGARTGIGGGGVGGVDS
AHSV-2ref       NKIHDDRRVESQKSEGSGSADCRRGAGSAGADCATSTGGGDGGAGARTGIGGGGVGGVDS
AHSV-7ref       NKIHDDRRVESQKSEGSGSADRRSGAGSAGADCATSAGGGDGGAGARTGIGGGGVGGVDS
AHSV-5ref       NKIHDDRRVESQKSEGGGSADCQRGAGSAGADCATSAGGGDGGAGARTGIGGGGVGGVDS
AHSV-8ref       NKIHDDRRVESQRSEGGGSADCQRSAGSAGADCATSTGGGDGXAGARTGIGGGGVGGVDS
NC_006019       NKIHDDRRVESQKSEGGGPADCQRGAGSRGANCATSTGGGDGSAGARTGIGGGGVGRVDS
AHSV-2field     NKIHDDRGVESQESEGGGPADCQRGAGSAGANRATSTGGGDGSAGARTGIGGGGVGGVDS
AHSV-3field     NKIHDDRRVESQKSEGGGPADCQRGAGGAGADCATSTGGGDGSAGARTGIGGGGVGGVDS
AHSV-5field     NKIHDDRRVESQKSEGGGPADCQRGAGGAGADCATSTGGGDGSAGARTGIGGGGVGGVDS
AHSV-9field     NKIHDDRRVESQKSEGGGPADCQRGAGGAGADCATSTGGGDGSAGARTGIGGGGVGGVDS
AHSV-9ref       NKIHDDRRVESQKSEGGGSADCQRGAGSTGSDCATSTGGGDGGAGARTGIGGGGVGGVDS
AHSV-1field     EKIPKDGGLGSAKSAEPEPAD--------GSGESAKSTGGDGGGGAGRGAGGRGVGGVAG
AHSV-7field     EKIPKDGGLGSAKSAEPEPAD--------GSGESAKSTGGDGGGGAGRGVGGRGVGGVAG
AHSV-4field     EKIPKDGGLGSAKSAEPEPAD--------GSGESAKSTGGNGGGGAGRGAGGRGVGGVAG
AHSV-6field     EKIPKDGGLGSAKSAEPEPAD--------GSGESAKSTGGDGGGGAGRGAGGRGVGGVAG
AHSV-8field     EKIPKDGGLGSAKSAEPEPAD--------GSGESAKSTGGDGGGGAGRGAGGRGVGGVAG
AHSV-4ref       EKIPKDGGLGSAKSAEPEPAD--------GSGESAKSTGGDGGGGAGRGAGGRGVGGVAG
AHSV-6ref       EKIPKDGGLGSAKSAEPEPAD--------GSGESAKSTGGDGGGGAGRGAGGRGVGGVAG
                :** .*  : * .*    .**        *:. ::.: **:* .**  * ** *** * .
```

```
U19881.1        RSGGRGGQGAASDGKGVGKSKTGADRVANDGATRDVGTSEVSSSGITSGGLQGRGGLVAK
AHSV-1ref       RPGGHGGQGAASDGKGVGKSKTGADRVANDGATRDAGSSEVPSGGITSGGLQGRGGLVAK
AM883170.1      RPGGHGGQGAASDGKGVGKSKTGADRVANDGATRDAGSSEVPSGGITSGGLQGRGGLVAK
AHSV-2ref       RSGGYGGQGAASDGKGVGKSKTGADRVANDGATREVGSSEISSGGITSGGLQGRGGLVAK
AHSV-7ref       RPGGYGGQGAASDGKGVGKSKTGADRVANDDATRDVGSSEVPSGGITSGGLQGRGGLVAK
AHSV-5ref       RSGGHGGQGAASDGKGVGKSKTGADRVANDDATRDVGSSEVSSGGITSGGLQGRGGLVAK
AHSV-8ref       RSGGHGGQGAASDGKGVGKSKTGADRVADDGATRDVSSSEVSSGGITSGGLQGRGGLVTK
NC_006019       RSGGRGGQGAASDGKGVGKSKTGADRVANDDATRNVGSSEVSPGGITSGGLQGRGGLVAK
AHSV-2field     RSGGHGGQGAASDGKGLGKSKTGADRVANDDATRNVGSSEVSSGGITSGGLQGRGGLVAK
AHSV-3field     RSGGHGGEGAASVGKGVGKSKTGANRVANDDAARNVGSSEVSSGGITSGGLQGRGGLVAK
AHSV-5field     RSGGHGGEGAASVGKGVGKSKTGANRVANDDATRNVGSSEVSSGGITSGGLQGRGGLVAK
AHSV-9field     RSGGHGGEGAASVGKGVGKSKTGANRVANDDATRNVGSSEVSSGGITSGGLQGRGGLVAK
AHSV-9ref       RYGGHGGQDAASAGKGVGKSKTGADRVANDDATRNVGSSEVSSGGIASGGLQGRGGLVAK
AHSV-1field     GTGGRGGSLRGGRDAGLGESTSGANHITNDDATRNAGSGEVPSGGVTSGSSQGGGGGATT
AHSV-7field     GTGGRGGSLRGGRDAGLGESTSGANHITNDDATRNAGSGEVPSGGVTSGSSQGGGGGATT
AHSV-4field     GAGGRGGSLRGGRGAGLGESTSGANHITNDDATRNAGSGEVPSGGITSGSSQGGGGGATT
AHSV-6field     GAGGRGGSLRGGRDAGLGESTSGANHITNDDATRNAGSGEVPSGGVTSGSSQGGGGGAAA
AHSV-8field     GAGGRGGSLRGGRDAGLGESTSGANHITNDDATRNAGSGEVPSGGVTSGSSQGGGGGATT
AHSV-4ref       GAGRRGGSLRGGRDAGLGESTSGTNHITNDDATRNAGSGEVPSGGVTSGSSQGGGGGATT
AHSV-6ref       GAGRRGGSLRGGRDAGLGESTSGTNHITNDDAARNAGSGEVPSGGVTSGSSQGGGGGATT
                  *  **.  .. . *:*:*.:*:::::::*.*:*:..:.*:...*::**. ** ** .:


U19881.1        SSECGGEPLDRTGGCSGNSKTEGEEAKVGGGDRRIGGLATQGIADFVKKKIGVEVQVFSK
AHSV-1ref       SSECGGEPLDRTGGCSGNSKTEGEEAKVGGSDRRIGGLATQEIADFVKKKIGVEVQVFSK
AM883170.1      SSECGGEPLDRTGGCSGNSKTEGEEAKVGGSDRRIGGLATQEIADFVKKKIGVEVQVFSK
AHSV-2ref       SSECGGEPLDRTGGCSGNSKTEGEEAKVGGGDRRIGGLATQEIADFVKKKIGVEVQVFSK
AHSV-7ref       SSECGGEPLDRTGGCSGNSKTEGEEAKVGGGDRRIGGLATQEIADFVKKKIGVEVQVFSK
AHSV-5ref       SSECGGESLDRTGGCSGNSKTEGEEAKVGGGDRRIGGLATQEIADFVKKKIGVEVQVFSK
AHSV-8ref       SSECGGEPLDRAGGCSGNSKTEGEEAKVGGGDRRIGGLATQEIADFVKKKIGVEVQVFSK
NC_006019       SGECGGESLDRIGGCSGNSKTEGEEAKAGGGDRRIGGLATQEIADFVKKKIGVEVQVFSK
AHSV-2field     SGKCGGEPLDRTGGCSGNSKTEGEEAKAGGGDRRIGGLATQEIADFVKKKIGVEVQVFSK
AHSV-3field     SGECGGEPLDRTGGCSGNSKAEGEEAKAGGGDRRIGGLATQEIADFVKKKIGVEVQVFSK
AHSV-5field     SGECGGEPLDRTGGCSGNSKAEGEEAKAGGGDRRIGGLATQEIADFVKKKIGVEVQVFSK
AHSV-9field     SGECGGEPLDRTGGCSGNSKAKGEEAKAGGGDRRIGGLATQEIADFVKKKIGVEVQVFSK
AHSV-9ref       SSESGREPLDRTGGCSGNSKTEREEAKVGGGDRRIGGLATQEIADFVKKKIGVEVQVFSK
AHSV-1field     SGESGGQPLDRKSGASGDTRSPGEKTKVDGGDRRDGGLATQEIVDYVRRKVGVEVPIYQK
AHSV-7field     SGESGGRPLDRKSGASGDTRSPGEKTKVDGGDRRDGGLATQEIVDYVRRKVGVEVPIYQK
AHSV-4field     SGESGGQPLDRKSGASGDTRSPGEKTKVDGGDRRDGGLATQEIVDYVRRKVGVEVPIYQK
AHSV-6field     SGESGGQPLDRKSGASGDTRSPGEKTKVDGGDRRDGGLATQEIVDYVRRKVGVEVPIYQK
AHSV-8field     SGESGGQPLDRKSGASGDTRSPGEKTKVDGGDRRDGGLATQEIVDYVRRKVGVEVPIYQK
AHSV-4ref       SGESGGQPLDRKSGASGDTRSPSEKTKVDGGDRRDGGLATQEIVDYVRRKVGVEVPIYQK
AHSV-6ref       SGESGGQPLDRKSGASGDTRSPSEKTKVDGGDRRDGGLATQEIVDYVRRKVGVEVPIYQK
                *.:.* ..*** .*.**:::: *::*..*.*** ****** *.*:*::*:**** ::.*
```

```
U19881.1        GMSNFFTVDKSLLKRGGLGREDILHQSDIVKEIRASDKKVKIIPLSTVKRMIAEFGGTEE
AHSV-1ref       GMSNLFTVDKSLLERGGLGREDILHQSDIVKEIRASDKRVKIIPLSTVKRMIAEFGGTEE
AM883170.1      GMSNLFTVDKSLLERGGLGREDILHQSDIVKEIRASDKRVKIIPLSTVKRMIAEFGGTEE
AHSV-2ref       GMSNLFTVDKSLLERGGLGREDILHQSDIVKEIRASDKKVKIIPLSTVKRMMAEFGGTEE
AHSV-7ref       GMSNLFTVDKSLLERGGLGREDILHQSDIVKEIRASDKRVKIIPLSTVKRMIAEFGGTEE
AHSV-5ref       GMSNLFTVDKSLLERGGLGREDILHQSDIVKEIRASDKKVKIIPLSTVKRMIAEFGGTEE
AHSV-8ref       GMSNLFTVDKSLLERGGLGREDILHQSDIVKEIRASDKKVKIIPLSTVKRMIAEFGGTEE
NC_006019       GMSNLFTVDKSLLKRGGLGREDILHQSDIVKEIRASDKKVKIIPLSTVKRMIAEFGGTEE
AHSV-2field     GMSSLFTVDKSLLERGGLGREDILHQSDIVKEIRVSDKKVKIIPLSTVKRMIAEFGGTEE
AHSV-3field     GMSNLFTVDKSLLERGGLGREDILHQSDIVKEIRVSDKKVKIIPLSTVKRMIAEFGGTEE
AHSV-5field     GMSNLFTVDKSLLERGGLGREDILHQSDIVKEIRVSDRKVKIIPLSTVKRMIAEFGGTEE
AHSV-9field     GMSNLFTVDKSLLERGGLGREDILHQSDIVKEIRVSDKKVKIIPLSTVKRMIAEFGGTEE
AHSV-9ref       GMSNLFTVDKSLLERGGLGREDILHQSDIAKEIRASDKKVKIIPLSTVKRMIAEFGGTEE
AHSV-1field     GMSNLFTVDRGLLERGGLSKDDLLHQSDIVKEAKANDKKLKVVPLSTVKRIIAEFGGSEE
AHSV-7field     GMSNLFTVDRGLLERGGLSKDDLLHQSDIVKEAKANDKKLKVVPLSTVKRIIAEFGGSEE
AHSV-4field     GMSNLFTVDRGLLERGGLSKDDLLHQSDIVKEAKANDKKLKVVPLSTVKRIIAEFGGSEE
AHSV-6field     GMSNLFTVDRGLLERGGLSKDDLLHQSDIVKEAKANDKKLKVVPLSTVKRIIAEFGGSEE
AHSV-8field     GMSNLFTVDRGLLERGGLSKDDLLHQSDIVKEAKANDKKLKVVPLSTVKRIIAEFGGSEE
AHSV-4ref       GMSNLFTVDRGLLERGGLSKDDLLHQSDIVKEAKANDKKLKVVPLSTVKRIIAEFGGSEE
AHSV-6ref       GMSNLFTVDRGLLERGGLSKDDLLHQSDIVKEAKANDKKLKVVPLSTVKRITAEFGGSEE
                ***.:****:.**:****.::*:******.** :..*:::*::*******: *****:**

U19881.1        DEIKAVQTQSSSIRYISNRMEDVSRAKAMFTAPTGDEGWKEVAKAATQRPNIMAYVHEGE
AHSV-1ref       DEIKAVQTQSSSIRYISNRMEDVSRAKAMFTAPTGDEGWKEVAKAATQRPNIMAYVHEGE
AM883170.1      DEIKAVQTQSSSIRYISNRMEDVSRAKAMFTAPTGDEGWKEVAKAATQRPNIMAYVHEGE
AHSV-2ref       DEIKAVQTQSSSIRYISNRMEDVSRAKAMFTAPTGDEGWKEVAKAATQRPNIMAYVHEGE
AHSV-7ref       DEIKAVQTQSSSIRYISNRMEDVSRAKAMFTAPTGDEGWKEVAKAATQRPNIMAYVHEGE
AHSV-5ref       DEIKAXQIQSSSIRYISNRMEDVSRAKAMFTAPTGDEGWKEVAKAATQRPNIMAYVHEGE
AHSV-8ref       DEIKAVQTQSSSIRYISNRMEDVSRAKAMFTAPTGDEGWKEVAKAATQRPNIMAYVHEGE
NC_006019       DEIKAVQTQSSSIRYISNRMEDVSRAKAMFTAPTGDEGWKEVAKAATQRPNIMAYVHEGE
AHSV-2field     DEIKAVQTQSSSIRYISNRMEDVSRAKAMFTAPTGDEGWKEVAKAATQRPNVMAYVHEGE
AHSV-3field     DEIKAVQTQSSSIRYISNRIEDVSRAKAMFTAPTGDEGWKEVAKAATQRPNIMAYVHEGE
AHSV-5field     DEIKAVQTQSSSIRYISNRIEDVSRAKAMFTAPTGDEGWKEVAKAATQRPNIMAYVHEGE
AHSV-9field     DEIKAVQTQSSSIRYISNRIEDVSRAKAMFTAPTGDEGWKEVAKAATQRPNIMAYVHEGE
AHSV-9ref       DEIKAVQTQSSSIRYISNRMEDVSRAKAMFTAPTGDEGWKEVAKAATQRPNIMAYVYEGE
AHSV-1field     EDVKGMQTQSSSIRYISNRMEDVPKAKAMFTAPTGDEGWKEVAKAATLRPNIMAYVHEGG
AHSV-7field     EDVKGMQTQSSSIRYISNRMEDVPKAKAMFTAPTGDEGWKEVAKAATLRPNIMAYVHEGE
AHSV-4field     EDVKGMQTQSSSIRYISNRMEDVPKAKAMFTAPTGDEGWKEVAKAATLRPNIMAYVHEGE
AHSV-6field     EDVKGMQTQSSSIRYISNRMEDVPKAKAMFTAPTGDEGWKEVAKAATLRPNIMAYVHEGE
AHSV-8field     EDVKGMQTQSSSIRYISNRMEDVPKAKAMFTAPTGDEGWKEVAKAATLRPNIMAYVHEGE
AHSV-4ref       EDVKGMQTQSSSIRYISNRMEDVPKAKAMFTAPTGDEGWKEVAKAATLRPNIMAYVHEGE
AHSV-6ref       EDVKGMQTQSSSIRYISNRMEDVPKAKAMFTAPTGDEGWKEVAKAATLRPNIMAYVHEGE
                :::*. * ***********:***.:********************** ***:****:**

U19881.1        GDGLKELLHLIDHI
```

```
AHSV-1ref       GDGLKELLHLIDHI
AM883170.1      GDGLKELLHLIDHI
AHSV-2ref       GDGLKELLHLIDHI
AHSV-7ref       GDGLKELLHLIDHI
AHSV-5ref       GDGLKELLHLIDHI
AHSV-8ref       GDGLKELLHLIDHI
NC_006019       GDGLKELLHLIDHI
AHSV-2field     GDGLKELLHLIDHI
AHSV-3field     GDGLKELLHLIDHI
AHSV-5field     GDGLKELLHLIDHI
AHSV-9field     GDGLKELLHLIDHI
AHSV-9ref       GDGLKELLHLIDHI
AHSV-1field     GDGLKELLHLIDHI
AHSV-7field     GDGLKELLHLIDHI
AHSV-4field     GDGLKELLHLIDHI
AHSV-6field     GDGLKELLHLIDHI
AHSV-8field     GDGLKELLHLIDHI
AHSV-4ref       GDGLKELLHLIDHI
AHSV-6ref       GDGLKELLHLIDHI
                **************
```

Figure A.4. – CLUSTAL format alignment by MAFFT (v7.127b) of the predicted VP6 amino acid sequences of all nine AHSV serotypes.

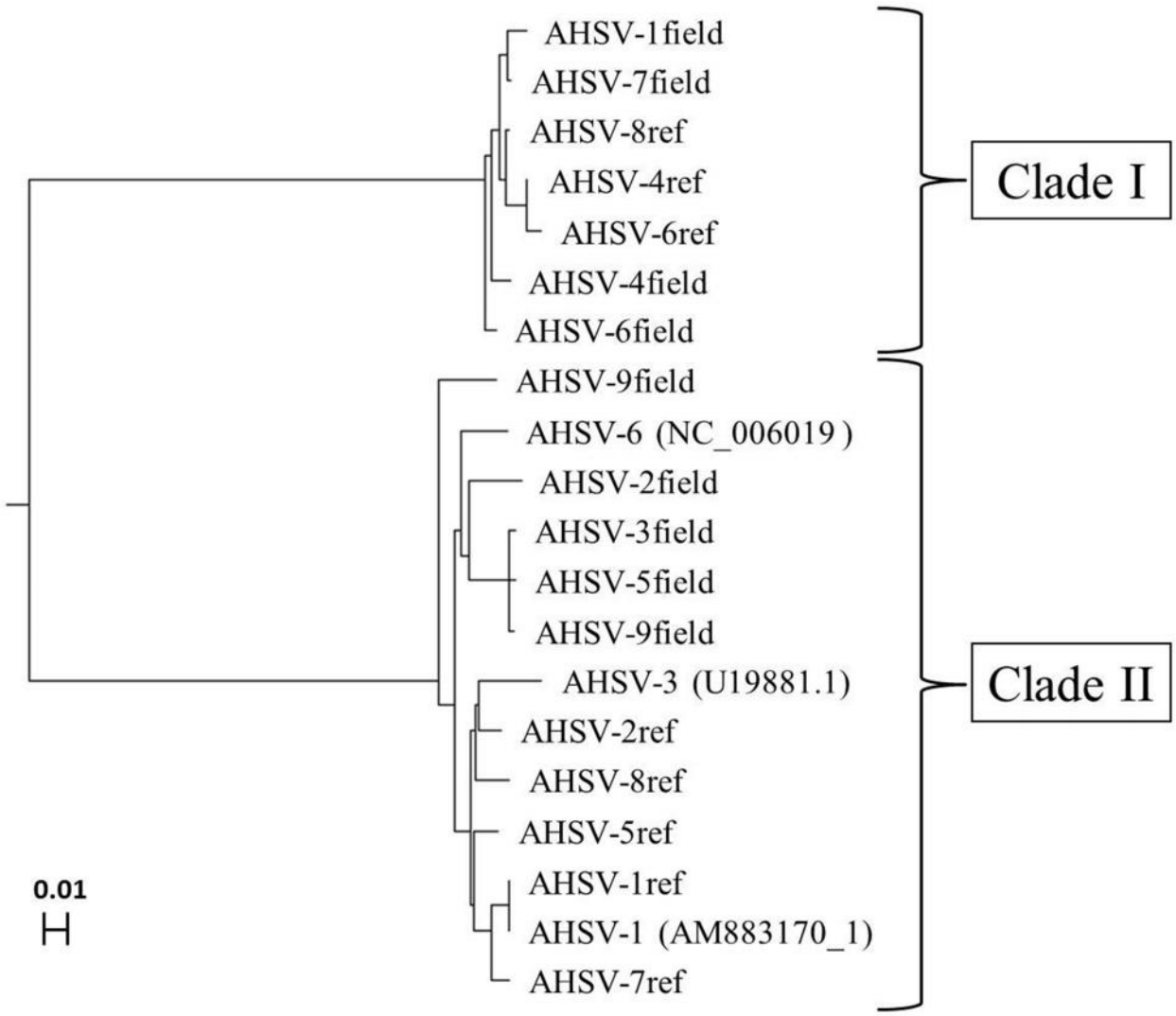

Figure A.5. – Neighbour Joining tree using the predicted VP6 amino acid sequences of all nine AHSV serotypes.

```
AM883170.1      ---------------MMIEEWRARNLREADQPIVNAAQEAQEQIAQHQQEEEMEVQEQGP
AHSV-1ref       ---------------MMIEEWRARNLREADQPIVNAAQEAQEQIAQHQQEEEMEVQEQGP
AHSV-5ref       ---------------MMIEEWRARNLREADQPIVNAAQEAQEQIAQHQQEEEMEVQEQGP
U19881.1        MGRRRTRVKRKRTKYMMIEEWRARNLREADQPIVNAAQEAEEQIAQHQQEEEMEVQEQGP
AHSV-7ref       ---------------MMIEEWRARNLREADQPIVEAAQEAQEQIVQHQQEEEMEVQEQGP
AHSV-5field     ---------------MMIEEWRARNLREADQPIVNAAQEAQEQIVQHQQEEEMEVQEQGP
AHSV-9field     ---------------MMIEEWRARNLREADQPIVNAAQEAQEQIVQHQQEEEMEVQEQGP
AHSV-3field     ---------------MMIEEWRARNLREADQPIVNAAQEAQEQIVQHQQEEEMEVQEQGP
pUC57-NS4-II    ---------------MMIEEWRARNLREADQPIVNAAQEAQEQIVQHQQEEEMEVQEQGP
AHSV-2ref       ---------------MMIEEWRARNLREADQPIVDAAQEAQEQIAQHQQEEEMEVQEQGP
AHSV-2field     ---------------MMIEEWRARNLREADQPIANAAQEAQEQIVQHQQEEEMEVQEQGP
AHSV-9ref       ---------------MMIEEWRARNLREADQPIVNAAQEAQDQIAQHQQEEEMEVQEQGP
AHSV-8ref       ---------------MMIEEWRARDPREADQPIVNAAQEAQEQIAQHQQEEEMEXQEQGP
NC_006019       MGRRRTRVKRKRTKYMMIEEWRARNLREADQPIVNVAQEAEEQIVQHQQEEEMEVQEQGP
AHSV-1field     -----------------MEDWDQQNQQNQNQRM--------DQENQQNRQEEMEVEEQGA
AHSV-4ref       -----------------MEDWDQQNQQNQNQRM--------DQENQQNRQEEMEVEEQGA
AHSV-6          -----------------MEDWDQQNQQNQNQRM--------DQENQQNRQEEMEVEEQGA
AHSV-8field     -----------------MEDWDQQNQQNQNQRM--------DQENQQNRQEEMEVEEQGA
AHSV-6field     -----------------MEDWDQQNQQNQNQRM--------DQENQQNRQEEMEVEEQGA
pUC57-NS4-I     -----------------MEDWDQQNQQNQNQRM--------DQENQQNRQEEMEVEEQGA
AHSV-7field     -----------------MEDWDQQNQQNQNQRM--------DQENQQNRQEEMEVEEQGA
AHSV-4field     -----------------MEDWDQQNQQNQNQRM--------DQENQRNRQEEMEVEEQGA
                              :*:*  :: :: :* :        :*  *::::**** :***.

AM883170.1      GLEGEEWEEWIRDLEDMEDRVQPRMEREWVNLRPEQIVSLMMVQHAMLVPVRYHLVESLQ
AHSV-1ref       GLEGEEWEEWIRDLEDMEDRVQPRMEREWVNLRPEQIVSLMMVQHAMLVPVRYHLVESLQ
AHSV-5ref       GLEGEEWEEWIRDLEDMEDRVQPRMEREWVNLRPEQIVSLMMMQHAMLVPVRYHLVESLQ
U19881.1        GLEGEEWEEWIRDLEDVEDRVQPRMEREWVNLRPEQIVSLMMVQHAMLVPVRYHLVESLQ
AHSV-7ref       GLEGEEWEEWIRDLEDMEDRVQPRMEREWVNLRPEQIVSLMMMQHAMLVPVRYHLVESLQ
AHSV-5field     GLEGEEWEEWIRDLEDMEERVQPRLEREWANLRPEQIVSLMMMQHAMLVPVRYHLVESLQ
AHSV-9field     GLEGEEWEEWIRDLEDMEERVQPRLEREWANLRPEQIVSLMMMQHAMLVPVRYHLVESLQ
AHSV-3field     GLEGEEWEEWIRDLEDMEERVQPRLEREWANLRPEQIVSLMMMQHAMLVPVRYHLVESLQ
pUC57-NS4-II    GLEGEEWEEWIRDLEDMEERVQPRLEREWANLRPEQIVSLMMMQHAMLVPVRYHLVESLQ
AHSV-2ref       GLEGEEWEEWIRDLEDMEDRVQPRMEREWVNLRPEQIVSLMMVQHARLVPVRYHLVESLQ
AHSV-2field     GLEGEEWEEWIRDLEDMEDRVQPRMERDWVNLRPEQIVSLMMMQHAMLVPVRYHLVESLQ
AHSV-9ref       GLEGEEWEEWIRDMEDMEDRMQPRLEREWVNLRPEQIVSLMMMQHAMLVPVRYHLVESLQ
AHSV-8ref       GLEGEEWEEWIRDLEDMEDRVQPRMEREWVNLRPEQIVSLMMVQHAMLVPVRYHLVESLQ
NC_006019       GLEGEEWEEWIRDLEDVEDRVQPRMEREWVNLRPEQIVSLMMMQHAMLVPVRYHLVESLQ
AHSV-1field     GLEGEEWAEWLEGLEDVEDHFVGDEMQDWANLRPEQIISLMMMQHAMLVPVRYHLVESLQ
AHSV-4ref       GLEGEEWAEWLEGLDDVEDHFVGDGMQDWANLRPEQIISLMMMQHAMLVPVRYHLVESLQ
AHSV-6          GLEGEEWAEWLEGLDDVEDHFVGDGMQDWANLRPEQIISLMMMQHAMLVPVRYHLVESLQ
AHSV-8field     GLEGEEWAEWLEGLEDVEDHFVGDEMQDWANLRPEQIISLMMMQHAMLVPVRYHLVESLQ
AHSV-6field     GLEGEEWAEWLEGLEDVEDHFVGDEMQDWANLRPEQIISLMMMQHAMLVPVRYHLVESLQ
pUC57-NS4-I     GLEGEEWAEWLEGLEDVEDHFVGDEMQDWANLRPEQIISLMMMQHAMLVPVRYHLVESLQ
AHSV-7field     GLEGEEWAEWLEGLEDVEDHFVGDEMQDWANLRPEQIISLMMMQHAMLVPVRYHLVESLQ
AHSV-4field     GLEGEEWAEWLEGLEDVEDHFVGDEVQDWANLRPEQIISLMMMQHAMLVPVRYHLVESLQ
                ******* **:..::*:*::.     ::*.*******:****:*** ************
```

```
AM883170.1      EVFKAEEDSLLRVVNVAGNHWIGQAAAAEIQKLRERRQRLEGAIDGLED--
AHSV-1ref       EVFKAEEDSLLRVVNVAGNHWIGQAAAAEIQKLRERRQRLEGAIDGLED--
AHSV-5ref       EVFKAEEDSLQRVVNVAGNHWIGQAAAAEIQKLRERRQRLEGAIDGLED--
U19881.1        EVFKAEEDSLQRVVNVAGNHWIGQAAAAEIQKLRERRQRLEGAIDGLED--
AHSV-7ref       EVFKAEEDSLLRVVNVAGNHWIGQAAAAEIQKLRERRQRLEGAIDGLED--
AHSV-5field     EVFKAEEDSLQRVVNVAGNHWIGQAAAAEIQKLRERRQRLEGAIDGLED--
AHSV-9field     EVFKAEEDSLQRVVNVAGNHWIGQAAAAEIQKLRERRQRLEGAIDGLED--
AHSV-3field     EVFKAEEDSLQRVVNVAGNHWIGQAAAAEIQKLRERRQRLEGAIDGLED--
pUC57-NS4-II    EVFKAEEDSLQRVVNVAGNHWIGQAAAAEIQKLRERRQRLEGAIDGLEDLE
AHSV-2ref       EVFKAEEDSLQRVVNVAGNHWIGQAAAAEIQKLRERRQRLEGAIDGLED--
AHSV-2field     EVFKAEEDSLQRVANVAGNHWIGQAAAAEIQKLRERRRRLEGAIDGLED--
AHSV-9ref       EVFKAEEDSLQRVVNLAGNHWIGQAAAAEIQKLRERRRRLEGAIDGLED--
AHSV-8ref       EVFKAEEDSLQRVVNVAGNHWIGQAAAAEIQKLRERRQRLEGAIDGLED--
NC_006019       EVFKAEEDSLQRVVNVAGNHWIG--------------------------
AHSV-1field     EVLKAEEGALQRVVNLAGNHXIGRAAQAEIQDLQARRQRLMGAIDGMGD--
AHSV-4ref       EVLKAEEGALQRVVNLAGNHWIGRAAQAEIQDLQARRQRLMGAIDGMGD--
AHSV-6          EVLKAEEGALQRVVNLAGNHWIGRAAQAEIQDLQARRQRLMGAIDGMGD--
AHSV-8field     EVLRAEEGALQRVVNLAGNHWIGRAAQAEIQDLQARRQRLMGAIDGMGD--
AHSV-6field     EVLRAEEGALQRVVNLAGNHWIGRAAQAEIQDLQARRQRLMGAIDGMGD--
pUC57-NS4-I     EVLKAEEGALQRVVNLAGNHWIGRAAQAEIQDLQARRQRLMGAIDGMGDLE
AHSV-7field     EVLKAEEGALQRVVNLAGDHWIGRAAQAEIQDLQARRQRLMGAIDGMGD--
AHSV-4field     EVLKAEEGALQRVVNLAGNHWIGRAAQAEIQDLQARRQRLMGAIDGMGD--
                **::***.:* **.*:**:* **
```

Figure A.6. – CLUSTAL format alignment by MAFFT (v7.127b) of several predicted AHSV NS4 amino acid sequences. The sequence derived from Genbank: NC_006019 (TURNBULL *et al.* 1996) is identical to the sequence (Genbank: YP_006491216.1) predicted by Belhouchet *et. al* (2011) and is the sequence within the Bac-AHSV6-VP6 recombinant baculovirus. AM883170.1 was derived from the Genbank sequence published by Potgieter *et al.* (2009) and U19881.1 was derived from the AHSV-3 Genbank sequence published by Turnbull *et al.* (1996) which was used to construct Bac-AHSV3-VP6. The region in which the three predicted overlapping canonical nuclear localisation sequences occur (BELHOUCHET *et al.* 2011) are in indicated in bold print within the "NC_006019" sequence. The peptide sequences used as immunogens during the development of an antiserum specific for NS4 are underlined in AHSV-3field and AHSV-4field. The pUC57-NS4 sequences are the amino acid sequences encoded by the codon-optimised genes used for bacterial expression and purification of NS4.

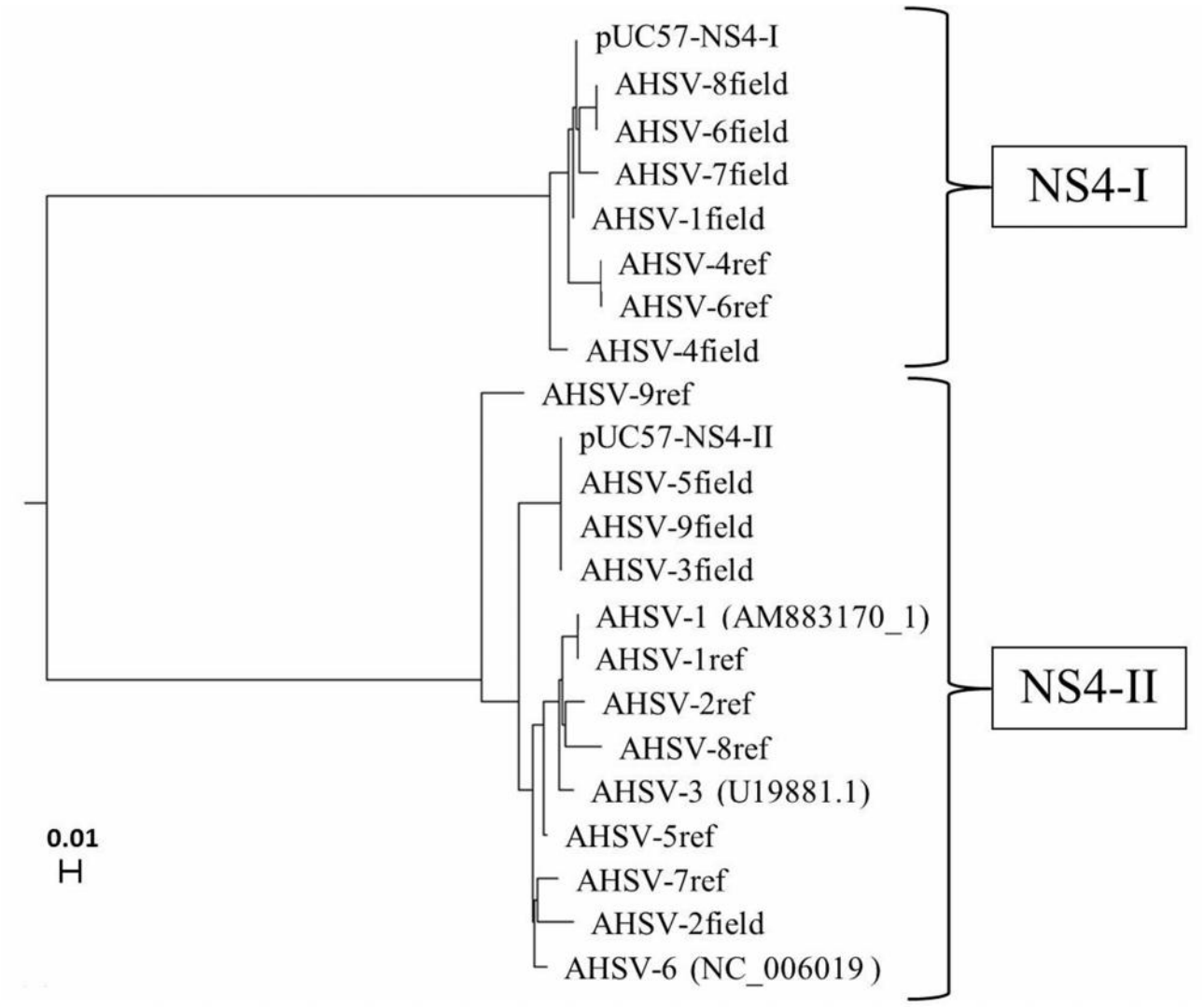

Figure A.7. – Neighbour Joining tree using the predicted NS4 amino acid sequences of all nine AHSV serotypes. The suffix "ref" denotes a reference strain and "field" denotes a field isolate. The pUC57-NS4 sequences are the amino acid sequences of the bacterially expressed codon-optimised NS4 genes used during this study.

Appendix B: Plasmid maps and gene insert sequences

The NdeI and XhoI restriction sites are highlighted in bold type with the cut site indicated with a "/" symbol. The start codons are underlined.

Codon-optimised NS4-I nucleotide sequence:

CA/T<u>ATG</u>GAAGACTGGGACCAACAAAATCAACAAAATCAGAACCAACGCATGGACCAAGAAAATCAACAGAATCGCC
AAGAAGAAATGGAAGTGGAAGAACAGGGCGCGGGTCTGGAAGGCGAAGAATGGGCCGAATGGCTGGAAGGTCTG
GAAGATGTTGAAGACCATTTTGTCGGCGATGAAATGCAAGACTGGGCAAACCTGCGTCCGGAACAGATTATCAGCCT
GATGATGATGCAACATGCCATGCTGGTCCCGGTGCGCTATCACCTGGTGGAATCTCTGCAAGAAGTGCTGAAAGCAG
AAGAAGGTGCTCTGCAACGTGTGGTTAACCTGGCAGGCAATCACTGGATTGGTCGCGCGGCCCAGGCTGAAATCCAA
GACCTGCAAGCCCGCCGCCAACGCCTGATGGGTGCTATTGATGGTATGGGTGAC**C/TCGAG**

Codon-optimised NS4-I amino acid sequence (based on AHSV-4field):

MEDWDQQNQQNQNQRMDQENQQNRQEEMEVEEQGAGLEGEEWAEWLEGLEDVEDHFVGDEMQDWANLRPEQII
SLMMMQHAMLVPVRYHLVESLQEVLKAEEGALQRVVNLAGNHWIGRAAQAEIQDLQARRQRLMGAIDGMGDLE

Codon-optimised NS4-II nucleotide sequence:

CA/T<u>ATG</u>ATGATTGAAGAATGGCGTGCCCGTAACCTGCGTGAAGCCGACCAACCGATTGTGAATGCCGCTCAGGAAG
CCCAAGAACAGATTGTCCAGCATCAGCAGGAAGAAGAAATGGAAGTCCAGGAACAAGGCCCGGGTCTGGAAGGCGA
AGAATGGGAAGAATGGATTCGTGATCTGGAAGACATGGAAGAACGCGTGCAGCCGCGTCTGGAACGCGAATGGGCA
AACCTGCGTCCGGAACAGATCGTTAGTCTGATGATGATGCAACATGCCATGCTGGTCCCGGTGCGCTATCACCTGGTT
GAAAGCCTGCAAGAAGTGTTTAAAGCGGAAGAAGATTCTCTGCAACGTGTGGTTAACGTTGCCGGCAATCACTGGAT
TGGTCAGGCGGCCGCAGCTGAAATTCAGAAACTGCGTGAACGTCGTCAGCGCCTGGAAGGTGCGATTGATGGCCTG
GAAGAT**C/TCGAG**

Codon-optimised NS4-II amino acid sequence (based on AHSV-3field):

MMIEEWRARNLREADQPIVNAAQEAQEQIVQHQQEEEMEVQEQGPGLEGEEWEEWIRDLEDMEERVQPRLEREWAN
LRPEQIVSLMMMQHAMLVPVRYHLVESLQEVFKAEEDSLQRVVNVAGNHWIGQAAAAEIQKLRERRQRLEGAIDGLEDL
E

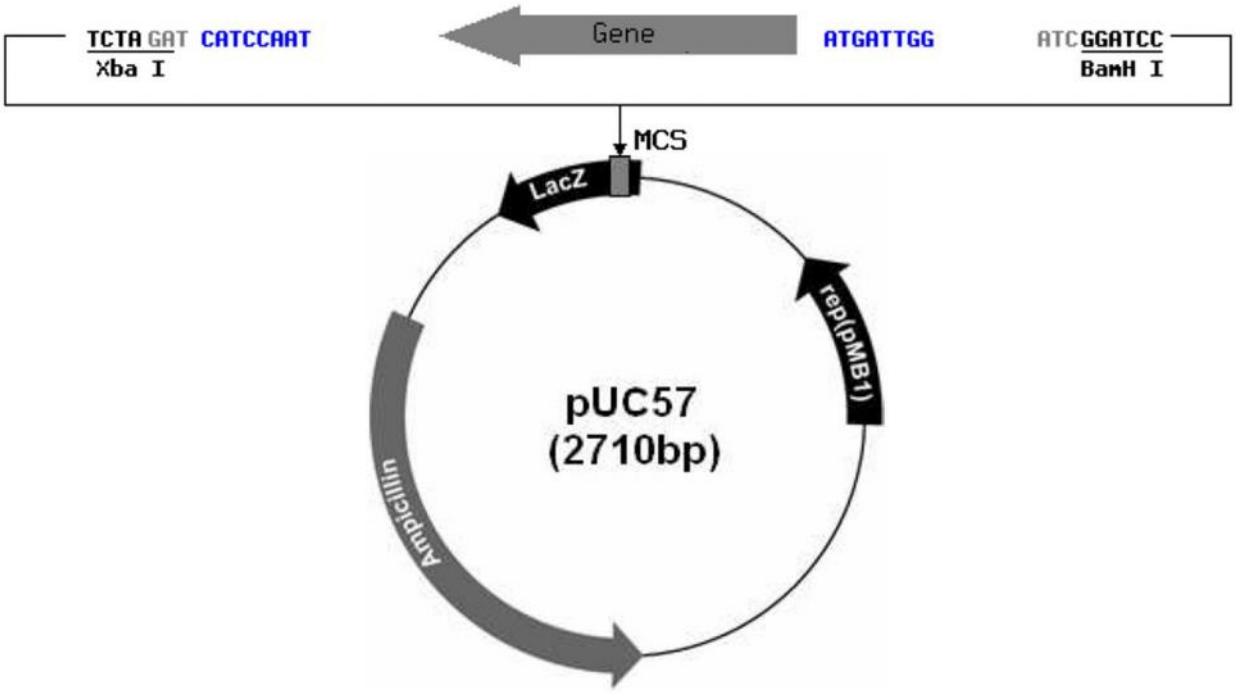

Figure B.1. – A map of the pUC-57-NS4 vector which contained the codon optimised AHSV NS4 genes. The image was provided by the company GenScript USA (Inc).

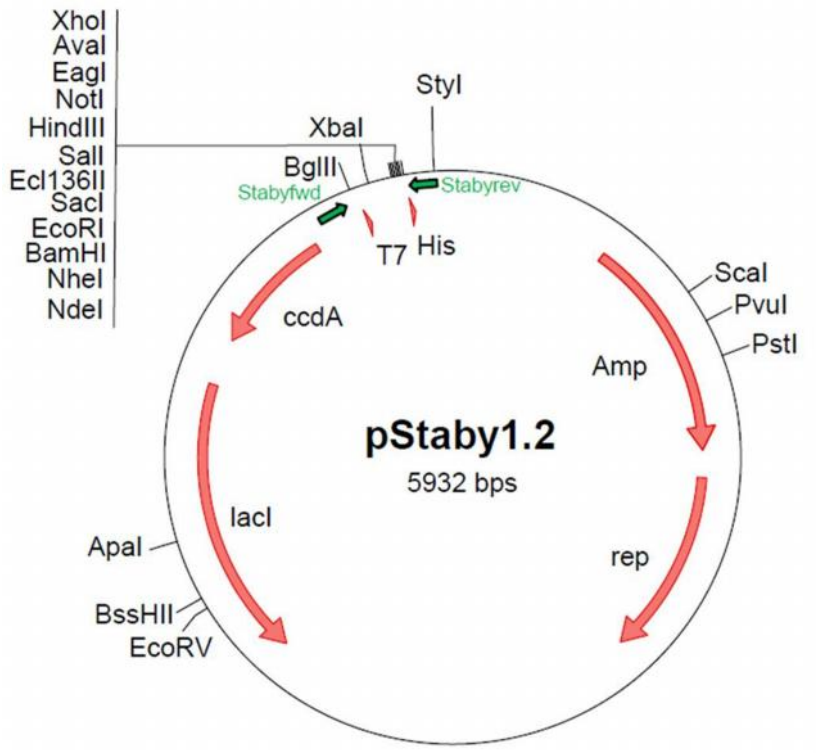

Figure B.2. – A map of the modified pStaby expression vector which contains the 6 histidine tag codons at the end of the inserted gene (adapted from the StabyExpress™ T7 Kit Manual, version 1.7).